

**CHEMICAL AND ENZYMATIC SYNTHESIS OF SUGAR NUCLEOTIDES  
FOR GLYCOSYLATION ENGINEERING**

by

Shannon C. Timmons

Submitted in partial fulfillment of the requirements  
for the degree of Doctor of Philosophy

at

Dalhousie University  
Halifax, Nova Scotia  
May 2007

© Copyright by Shannon C. Timmons, 2007



Library and  
Archives Canada

Bibliothèque et  
Archives Canada

Published Heritage  
Branch

Direction du  
Patrimoine de l'édition

395 Wellington Street  
Ottawa ON K1A 0N4  
Canada

395, rue Wellington  
Ottawa ON K1A 0N4  
Canada

*Your file    Votre référence*

*ISBN: 978-0-494-27169-8*

*Our file    Notre référence*

*ISBN: 978-0-494-27169-8*

#### NOTICE:

The author has granted a non-exclusive license allowing Library and Archives Canada to reproduce, publish, archive, preserve, conserve, communicate to the public by telecommunication or on the Internet, loan, distribute and sell theses worldwide, for commercial or non-commercial purposes, in microform, paper, electronic and/or any other formats.

The author retains copyright ownership and moral rights in this thesis. Neither the thesis nor substantial extracts from it may be printed or otherwise reproduced without the author's permission.

#### AVIS:

L'auteur a accordé une licence non exclusive permettant à la Bibliothèque et Archives Canada de reproduire, publier, archiver, sauvegarder, conserver, transmettre au public par télécommunication ou par l'Internet, prêter, distribuer et vendre des thèses partout dans le monde, à des fins commerciales ou autres, sur support microforme, papier, électronique et/ou autres formats.

L'auteur conserve la propriété du droit d'auteur et des droits moraux qui protègent cette thèse. Ni la thèse ni des extraits substantiels de celle-ci ne doivent être imprimés ou autrement reproduits sans son autorisation.

---

In compliance with the Canadian Privacy Act some supporting forms may have been removed from this thesis.

Conformément à la loi canadienne sur la protection de la vie privée, quelques formulaires secondaires ont été enlevés de cette thèse.

While these forms may be included in the document page count, their removal does not represent any loss of content from the thesis.

Bien que ces formulaires aient inclus dans la pagination, il n'y aura aucun contenu manquant.

  
**Canada**

DALHOUSIE UNIVERSITY

To comply with the Canadian Privacy Act the National Library of Canada has requested that the following pages be removed from this copy of the thesis:

Preliminary Pages

Examiners Signature Page (pii)

Dalhousie Library Copyright Agreement (piii)

Appendices

Copyright Releases (if applicable)

# Table of Contents

---

<b>List of Tables .....</b>	<b>vii</b>
<b>List of Figures.....</b>	<b>viii</b>
<b>Abstract.....</b>	<b>xiv</b>
<b>List of Abbreviations and Symbols Used .....</b>	<b>xv</b>
<b>Acknowledgements .....</b>	<b>xx</b>
<b>Chapter 1. Introduction .....</b>	<b>1</b>
1.1. Natural Products and Drug Discovery .....	1
1.1.1. Angucycline Antibiotics .....	3
1.1.1.1. Jadomycins.....	6
1.2. Medicinal Role of Carbohydrate Functionalities.....	8
1.2.1. Effect of Adding or Removing a Monosaccharide .....	9
1.2.2. Effect of Modifying an Existing Monosaccharide.....	11
1.2.3. Effect of Glycosylating a Previously Non-Glycosylated Natural Product .....	13
1.3. Natural Product Glycosylation Engineering .....	15
1.3.1. Chemical Synthesis and Semi-Synthesis Strategies .....	15
1.3.2. <i>In Vivo</i> Biosynthetic Pathway Engineering Strategies.....	18
1.3.3. <i>In Vitro</i> Glycorandomization Strategies .....	20
1.4. Glycosyltransferase Enzymes .....	23
1.4.1. Classification.....	24
1.4.2. Structural Superfamilies.....	26



1.4.3. Enzymatic Mechanisms .....	30
1.4.3.1. Inverting Glycosyltransferases.....	30
1.4.3.2. Retaining Glycosyltransferases.....	32
1.4.4. Substrate Promiscuity of Glycosyltransferases Involved in Natural Product Biosynthesis .....	36
1.4.5. JadS Glycosyltransferase .....	39
1.5. Preparation of Sugar Nucleotides .....	41
1.5.1. Chemical Synthesis.....	41
1.5.2. Enzymatic Synthesis .....	43
1.6. Project Objectives .....	46
<b>Chapter 2. Results and Discussion .....</b>	<b>48</b>
2.1. Synthesis of L-Digitoxose .....	48
2.1.1. Method A .....	49
2.1.2. Method B .....	64
2.2. Monosaccharide Analogues Prepared from a Synthetic Intermediate.....	70
2.2.1. Fluorinated 6-Deoxysugar Analogues .....	70
2.2.2. 2,6-Dideoxysugar Analogue .....	74
2.3. Chemical Synthesis of Sugar Nucleotides .....	75
2.3.1. Preparation of a 2,6-Dideoxysugar Nucleotide.....	75
2.3.2. Preparation of Analogue Sugar Nucleotides via an Indirect Coupling Methodology .....	85
2.3.2.1. Synthesis of Sugar-1-Phosphates.....	87
2.3.2.2. Coupling of Sugar-1-Phosphates with <i>N</i> -Methylimidazolidine Nucleoside 5'-Monophosphate Donors .....	95

2.3.3. Preparation of Analogue Sugar Nucleotides via Direct Coupling Methodologies.....	100
2.3.3.1. Nucleoside 5'-Diphosphate- <i>N</i> -Methylimidazolidone Donors .....	100
2.3.3.2. Glycosyl Iodide Donors .....	101
2.3.3.3. Glycosyl Bromide Donors .....	105
2.4. Enzymatic Synthesis of Sugar Nucleotides .....	113
2.4.1. Substrate Promiscuity of Three Nucleotidyltransferases.....	114
<b>Chapter 3. Experimental.....</b>	<b>123</b>
3.1. General Methods.....	123
3.2. Synthesis and Characterization of Compounds .....	125
3.3. Nucleotidyltransferase Assay Conditions.....	183
3.4. Characterization of Enzymatically Prepared Sugar Nucleotides .....	184
<b>Chapter 4. Conclusions.....</b>	<b>190</b>
<b>References.....</b>	<b>192</b>
<b>Appendix 1. NMR Spectra of Representative Compounds.....</b>	<b>208</b>

## List of Tables

---

<b>Table 1.</b> Selected results from varying conditions of Klemmer-Rodemeyer elimination reaction with <b>58</b> , <b>59</b> , and <b>62</b> .....	54
<b>Table 2.</b> Selected Klemmer-Rodemeyer elimination reaction results with different bases .....	62
<b>Table 3.</b> Yields of sugar nucleotides prepared via coupling of sugar-1-phosphates with NMP- <i>N</i> -methylimidazolides .....	99
<b>Table 4.</b> Effect of variables on the percentage conversion of UDP to UDP- $\alpha/\beta$ -L-rhamnose ( <b>153b</b> ) on coupling with 2,3,4-tri- <i>O</i> -trimethylsilyl- $\alpha$ -L-rhamnopyranosyl iodide ( <b>157</b> ) .....	104
<b>Table 5.</b> Effect of variables on the $\alpha:\beta$ ratio of UDP- $\alpha/\beta$ -L-rhamnose ( <b>153b</b> ) when prepared via coupling of 2,3,4-tri- <i>O</i> -trimethylsilyl- $\alpha$ -L-rhamnopyranosyl iodide ( <b>157</b> ) with UDP .....	105
<b>Table 6.</b> Effect of variables on the yield of UDP- $\alpha$ -L-rhamnose ( <b>153a</b> ) when prepared via direct coupling of 2,3,4-tri- <i>O</i> -acetyl- $\alpha$ -L-rhamnopyranosyl bromide ( <b>131</b> ) and UDP .....	106
<b>Table 7.</b> Characterization of D-manno- and L-fuco-linked sugar nucleotides .....	112
<b>Table 8.</b> Percentage conversions to sugar nucleotide products after 30 min incubations .....	184
<b>Table 9.</b> HPLC retention times of NTP and NDP standards .....	187
<b>Table 10.</b> Comparison of percentage conversions to sugar nucleotide products after 30 min and 24 h incubations .....	188
<b>Table 11.</b> Sugar nucleotide ESI-MS/MS data .....	189

## List of Figures

---

<b>Figure 1.</b> Structures of chloramphenicol (1), erythromycin A (2), and vancomycin (3) .....	2
<b>Figure 2.</b> Structures of tetrangomycin (4) and tetrangulol (5) .....	3
<b>Figure 3.</b> Characteristic tetracyclic benz[ <i>a</i> ]anthracene framework of angucyclines .....	4
<b>Figure 4.</b> Structure of urdamycin B (6) .....	5
<b>Figure 5.</b> Structures of jadomycin (7) and jadomycin B (8) .....	6
<b>Figure 6.</b> Structures of erythromycin A (2) and megalomicin (9) .....	10
<b>Figure 7.</b> Structure of calicheamicin $\gamma_1^I$ (10) .....	11
<b>Figure 8.</b> Structures of doxorubicin (11) and epirubicin (12) .....	12
<b>Figure 9.</b> Structures of daunorubicin (13) and 2'- $\beta$ -fluorodaunorubicin (14) .....	13
<b>Figure 10.</b> Structure of colchicine (15) and glycosylated derivatives 16-19 .....	14
<b>Figure 11.</b> General [3 + 2] cycloaddition reaction used to prepare a glycopeptide library based on a tyrocidine scaffold (circles represent amino acids) .....	16
<b>Figure 12.</b> General neoglycorandomization strategy .....	17
<b>Figure 13.</b> Structure of digitoxin (20) and neoglycoside derivatives 21-22 .....	18
<b>Figure 14.</b> Structures of rebeccamycin (23) and staurosporine (24) .....	19
<b>Figure 15.</b> Structures of jadomycin B (8) and ILEVS1080 (25) .....	20
<b>Figure 16.</b> Representative Huisgen 1,3-dipolar cycloaddition reaction used to diversify the vancomycin scaffold, producing derivative 26 .....	22
<b>Figure 17.</b> Summary of <i>in vitro</i> glycorandomization approaches possible via glycosyltransferase catalysis .....	23
<b>Figure 18.</b> Representative mechanism of a GT-B inverting glycosyltransferase .....	31
<b>Figure 19.</b> Proposed double displacement mechanism of a retaining glycosyltransferase .....	33

<b>Figure 20.</b> Proposed S <sub>N</sub> i-like mechanism of a retaining glycosyltransferase .....	34
<b>Figure 21.</b> Structures of 8-demethyltetracenomycin C (27), L-rhamnosyltetracenomycin C (28), and glycosylated derivatives 29-33.....	37
<b>Figure 22.</b> Structures of α-L-noviose (34), desmethyldescarbamoyl novobiocin (35) and derivatives 36-40 .....	38
<b>Figure 23.</b> Structures of β-D-vicenisamine (41), vicienistatin (42), and representative derivatives 43-45 .....	39
<b>Figure 24.</b> One of the last steps in the biosynthesis of jadomycin B (8) .....	40
<b>Figure 25.</b> Two strategies for preparing sugar nucleotides using dTDP-β-L-digitoxose (46) as an example.....	42
<b>Figure 26.</b> Representative mechanism of nucleotidyltransferase catalysis.....	44
<b>Figure 27.</b> Structures of dTDP-β-L-digitoxose (46), L-digitoxose (50) and proposed monosaccharide analogues 51-56.....	47
<b>Figure 28.</b> Structures of L-digitoxose (50) and D-digitoxose (57) enantiomers.....	48
<b>Figure 29.</b> Klemmer-Rodemeyer elimination reaction results reported by Brimacombe and Clode.....	50
<b>Figure 30.</b> Klemmer-Rodemeyer elimination reaction protecting group strategies.....	50
<b>Figure 31.</b> Mechanism of the Klemmer-Rodemeyer elimination reaction .....	52
<b>Figure 32.</b> Synthesis of methyl 4,6- <i>O</i> -benzylidene-α-D- <i>erythro</i> - hexopyranosid-3-ulose (69) by Klemmer and Rodemeyer .....	52
<b>Figure 33.</b> Possible Klemmer-Rodemeyer reaction proton abstractions and corresponding products.....	53
<b>Figure 34.</b> Base-induced elimination of ethylene (72) from 2-phenyl- 1,3-dioxolane (71).....	54
<b>Figure 35.</b> Regioselectivity of the Klemmer-Rodemeyer reaction with 4- <i>O</i> -TBDMS-protected α-L-rhamnopyranoside 73 as demonstrated by Morin .....	55
<b>Figure 36.</b> <i>Exo</i> and <i>endo</i> diastereomers of methyl 2,3- <i>O</i> -benzylidene-4- <i>O</i> - methyl-α-L-rhamnopyranoside (62) (arrows indicate strong 1D NOE interactions).....	56
<b>Figure 37.</b> Several identified Klemmer-Rodemeyer elimination reaction byproducts .....	58

<b>Figure 38.</b> Synthesis of methyl 2,3- <i>O</i> -isopropylidene-4- <i>O</i> -methyl- $\alpha$ -L-rhamnopyranoside ( <b>79</b> ) from methyl $\alpha$ -L-rhamnopyranoside ( <b>66</b> ).....	59
<b>Figure 39.</b> Proposed synthesis of methyl 2,6-dideoxy-4- <i>O</i> -methyl- $\alpha$ -L- <i>erythro</i> -hexopyranosid-3-ulose ( <b>63</b> ) from methyl 2,3- <i>O</i> -isopropylidene-4- <i>O</i> -methyl- $\alpha$ -L-rhamnopyranoside ( <b>79</b> ) .....	59
<b>Figure 40.</b> Synthesis of methyl 2,6-dideoxy-4- <i>O</i> -(tetrahydropyran-2-yl)- $\alpha$ -L- <i>erythro</i> -hexopyranosid-3-ulose ( <b>81</b> ) from methyl 2,3- <i>O</i> -benzylidene-4- <i>O</i> -(tetrahydropyran-2-yl)- $\alpha$ -L-rhamnopyranoside ( <b>80</b> ) by Klemer and Balkau.....	61
<b>Figure 41.</b> Sodium borohydride reduction of methyl 2,6-dideoxy-4- <i>O</i> -(2-methoxyethoxymethyl)- $\alpha$ -L- <i>erythro</i> -hexopyranosid-3-ulose ( <b>60</b> ) to methyl 2,6-dideoxy-4- <i>O</i> -(2-methoxyethoxymethyl)- $\alpha$ -L- <i>ribo</i> -hexopyranoside ( <b>82</b> ) .....	62
<b>Figure 42.</b> Method used by Brimacombe to deprotect methyl 2,6-dideoxy-4- <i>O</i> -(2-methoxyethoxymethyl)- $\alpha$ -L- <i>ribo</i> -hexopyranoside ( <b>82</b> ), affording L-digitoxose ( <b>50</b> ) .....	63
<b>Figure 43.</b> Five isomeric possibilities for L-digitoxose ( <b>50</b> ) after deprotection.....	64
<b>Figure 44.</b> Novel synthesis of protected L-digitoxose derivative <b>90</b> via Method B.....	65
<b>Figure 45.</b> Reduction of 1,5-anhydro-2,6-dideoxy-L- <i>erythro</i> -hex-1-en-3-ulose ( <b>85</b> ) under various reduction conditions .....	67
<b>Figure 46.</b> Structure of nucleocidin ( <b>91</b> ) .....	70
<b>Figure 47.</b> Structure of Selectfluor® (1-chloromethyl-4-fluoro-1,4-diazoniabicyclo[2.2.2]octane bis(tetrafluoroborate)).....	72
<b>Figure 48.</b> Synthesis of 1,3,4-tri- <i>O</i> -acetyl-2-deoxy-2-fluoro- $\alpha$ / $\beta$ -L-rhamnopyranose ( <b>94</b> ) and 1,3,4-tri- <i>O</i> -acetyl-2,6-dideoxy-2-fluoro- $\alpha$ / $\beta$ -L-glucopyranose ( <b>95</b> ) from 3,4-di- <i>O</i> -acetyl-L-rhamnal ( <b>83</b> ) using Selectfluor® .....	73
<b>Figure 49.</b> Reaction of 3,4-di- <i>O</i> -acetyl-L-rhamnal ( <b>83</b> ) with CF <sub>3</sub> OF by Butchard and Kent, producing <b>96-99</b> .....	74
<b>Figure 50.</b> Structures of L-digitoxose ( <b>50</b> ) and L-olivose ( <b>100</b> ).....	74
<b>Figure 51.</b> Synthesis of 1,3,4-tri- <i>O</i> -acetyl- $\alpha$ / $\beta$ -L-olivopyranose ( <b>101</b> ) from 3,4-di- <i>O</i> -acetyl-L-rhamnal ( <b>83</b> ).....	75
<b>Figure 52.</b> Proposed retrosynthetic strategy to access dTDP- $\beta$ -L-digitoxose from protected L-digitoxose derivative <b>90</b> .....	77

<b>Figure 53.</b> Synthesis of 2,3,4,6-tetra- <i>O</i> -acetyl- $\alpha$ -D-galactopyranosyl iodide (105) from methyl glycoside 106 by Thiem and Meyer .....	78
<b>Figure 54.</b> Synthesis of UDP-2-deoxy- $\alpha$ -D-galactose (109) via 2-deoxyglycosyl iodide 107 by Uchiyama and Hindsgaul .....	79
<b>Figure 55.</b> Synthesis of 2,6-dideoxyglycosyl bromide 111 from $\beta$ -configured methyl 2,6-dideoxyglycoside 110 by Monneret and coworkers .....	81
<b>Figure 56.</b> Synthesis of 2,6-dideoxyglycosyl bromides 115 and 116 from methyl 2,6-dideoxyglycosides 113 and 114, respectively, by Thiem and Meyer .....	82
<b>Figure 57.</b> Synthesis of 2,6-dideoxyglycosyl bromide 103 from methyl 2,6-dideoxyglycoside 90 using 2 equiv of TMS-Br in toluene and DCM .....	83
<b>Figure 58.</b> Synthesis of UDP- $\alpha/\beta$ -L-digitoxose (119) via 2,6-dideoxyglycosyl bromide 103, produced using 1 equiv of TMS-Br from methyl 2,6-dideoxyglycoside 90 .....	83
<b>Figure 59.</b> Synthesis of UDP- $\alpha$ -D-galactofuranose (120) via coupling of UMP- <i>N</i> -methylimidazolidine (121) with $\alpha$ -D-galactofuranose-1-phosphate (122) by Marlow and Kiessling .....	86
<b>Figure 60.</b> Influence of neighbouring group participation on the trajectory of dibenzyl phosphate attack in the case of 2,3,4-tri- <i>O</i> -benzoyl- $\alpha$ -L-fucopyranosyl bromide (124) .....	87
<b>Figure 61.</b> Synthesis of $\beta$ -L-fucose-1-phosphate (123) .....	89
<b>Figure 62.</b> Structures and $^1J_{C-1,H-1}$ values of $\alpha$ -D-glucose-1-phosphate (128) and $\alpha$ -D-mannose-1-phosphate (129) .....	90
<b>Figure 63.</b> NMR characterization data supporting the preparation of $\beta$ -L-fucose-1-phosphate (123), $\alpha$ -L-rhamnose-1-phosphate (134), and $\alpha$ -L-arabinose-1-phosphate (135) (arrows indicate strong 1D NOE interactions) .....	90
<b>Figure 64.</b> Synthesis of $\alpha$ -L-rhamnose-1-phosphate (134) .....	91
<b>Figure 65.</b> Synthesis of $\alpha$ -L-arabinose-1-phosphate (135) .....	94
<b>Figure 66.</b> NMR characterization data supporting the preparation of 2-deoxy-2-fluoro- $\alpha$ -L-rhamnose-1-phosphate (140), 2,6-dideoxy-2-fluoro- $\beta$ -L-glucose-1-phosphate (141), and 2-deoxy-2-fluoro- $\beta$ -L-fucose-1-phosphate (142) (arrows indicate strong 1D NOE interactions) .....	95

<b>Figure 67.</b> Preparation of AMP- ( <b>145</b> ) and UMP- <i>N</i> -methylimidazolides ( <b>121</b> ).....	96
<b>Figure 68.</b> Reaction of sugar-1-phosphates with NMP- <i>N</i> -methylimidazolides to prepare sugar nucleotides <b>146-153a</b> .....	98
<b>Figure 69.</b> Reaction attempt to generate a UDP- <i>N</i> -methylimidazolid electrophile for coupling with a selectively deprotected monosaccharide .....	101
<b>Figure 70.</b> Synthesis of UDP- $\alpha/\beta$ -L-rhamnose ( <b>153b</b> ) via coupling of 2,3,4-tri- <i>O</i> -trimethylsilyl- $\alpha$ -L-rhamnopyranosyl iodide ( <b>157</b> ) with UDP .....	103
<b>Figure 71.</b> Stereoselective synthesis of UDP- $\alpha$ -L-rhamnose ( <b>153a</b> ) via coupling of 2,3,4-tri- <i>O</i> -acetyl- $\alpha$ -L-rhamnopyranosyl bromide ( <b>131</b> ) with UDP .....	106
<b>Figure 72.</b> NMR characterization data supporting the preparation of UDP- $\alpha$ -L-rhamnose ( <b>153a</b> ) via direct coupling of 2,3,4-tri- <i>O</i> -acetyl- $\alpha$ -L-rhamnopyranosyl bromide ( <b>131</b> ) with UDP (arrow indicates a strong NOE interaction) .....	107
<b>Figure 73.</b> Influence of neighbouring group participation on the trajectory of NDP attack for acylated glycosyl bromides derived from L-rhamnose ( <b>55</b> ), D-mannose ( <b>158</b> ), and L-fucose ( <b>54</b> ) .....	108
<b>Figure 74.</b> Stereoselective synthesis of UDP- $\alpha$ -D-mannose ( <b>163</b> ) and GDP- $\alpha$ -D-mannose ( <b>159</b> ) via direct displacement of acetylated D-mannosyl bromide ( <b>161</b> ) with NDPs .....	110
<b>Figure 75.</b> Stereoselective synthesis of UDP- $\beta$ -L-fucose ( <b>151</b> ) and GDP- $\beta$ -L-fucose ( <b>160</b> ) via direct displacement of benzoylated L-fucosyl bromide ( <b>124</b> ) with NDPs .....	112
<b>Figure 76.</b> Reaction catalyzed by Cps2L, RmlA, and RmlA3 $\alpha$ -D-glucose-1-phosphate thymidyltransferases .....	115
<b>Figure 77.</b> Structures of sugar-1-phosphates used in thymidyltransferase substrate promiscuity studies .....	116
<b>Figure 78.</b> Structures of NTPs used in thymidyltransferase substrate promiscuity studies .....	117
<b>Figure 79.</b> Substrate promiscuity of Cps2L, RmlA, and RmlA3 thymidyltransferases after 30 min and 24 h incubations at 37 °C .....	119
<b>Figure 80.</b> NMR spectra of (6 <i>R</i> )-6-hydroxy-3-methoxy-dec-2-en-4-one ( <b>77</b> ) .....	208
<b>Figure 81.</b> NMR spectra of methyl 4- <i>O</i> -( <i>tert</i> -butyldimethylsilyl)-2,6-dideoxy-3- <i>O</i> -(trimethylsilyl)- $\alpha$ -L-ribo-hexopyranoside ( <b>90</b> ) .....	214



<b>Figure 82.</b> NMR spectra of GDP- $\alpha$ -D-mannose ( <b>159</b> ).....	217
---	-----

## Abstract

---

In Nature, GT-B glycosyltransferase enzymes catalyze the transfer of carbohydrates from sugar nucleotide donors to natural product acceptors with exquisite chemo-, regio-, and stereoselectivity, invoking interest in using these biocatalysts in glycosylation engineering. One major limitation to investigating the scope and synthetic utility of these enzymes remains poor access to sugar nucleotide substrates, as these compounds are notoriously difficult to chemically synthesize and purify.

In this thesis, an improved synthetic route to the 2,6-dideoxysugar L-digitoxose and its conversion to UDP- $\alpha/\beta$ -L-digitoxose are described. Furthermore, the chemical synthesis and purification of eleven non-deoxy- and 6-deoxysugar nucleotides via the indirect coupling of sugar-1-phosphates with *N*-methylimidazole-activated nucleoside 5'-monophosphates, as well as the direct coupling of glycosyl iodides and bromides with nucleoside 5'-diphosphates, is discussed. Of particular importance is the development of the first stereoselective chemical synthesis of the biologically relevant sugar nucleotides GDP- $\alpha$ -D-mannose and GDP- $\beta$ -L-fucose via coupling of nucleoside 5'-diphosphates and acylated glycosyl bromides using neighbouring group participation. In addition, the enzymatic synthesis of sugar nucleotides is investigated using three wild-type thymidyltransferase enzymes, resulting in the preparation of fifteen sugar nucleotides. The broad substrate flexibility demonstrated by these biocatalysts in initial assays provides impetus to further examine their synthetic potential.

## List of Abbreviations and Symbols Used

---

Å	Angstrom
Ac	acetyl
ADP	adenosine 5'-diphosphate
AMP	adenosine 5'-monophosphate
Ara	arabinose
ATP	adenosine 5'-triphosphate
ax	axial
BCE	before the common era
Bn	benzyl
br	broad
Bu	butyl
BuLi	butyllithium
Bz	benzoyl
calcd	calculated
CAZy	Carbohydrate-Active enZYmes
CDP	cytidine 5'-diphosphate
CE	common era
COSY	correlation spectroscopy
CTP	cytidine 5'-triphosphate
CV	column volume(s)

d	doublet
D	dimensional
DCM	dichloromethane
DMA	<i>N,N</i> -dimethylaniline
DMF	<i>N,N</i> -dimethylformamide
DNA	deoxyribonucleic acid
dTDP	deoxythymidine 5'-diphosphate
dTTP	deoxythymidine 5'-triphosphate
$\epsilon$	molar extinction coefficient
EC	Enzyme Commission
EI	electron impact
eq	equatorial
equiv	molar equivalent(s)
ESI	electrospray ionization
Et	ethyl
EtOAc	ethyl acetate
EtOH	ethanol
EU	enzyme unit
Fuc	fucose
Gal	galactose
GDP	guanosine 5'-diphosphate
Glc	glucose

GlcNAc	<i>N</i> -acetyl-glucosamine
GlcNH <sub>2</sub>	glucosamine
GT	glycosyltransferase
GTP	guanosine 5'-triphosphate
HMBC	heteronuclear multiple bond correlation
HPLC	high-performance liquid chromatography
HRMS	high-resolution mass spectrometry
HSQC	heteronuclear single quantum correlation
<sup>i</sup> Pr	isopropyl
IC <sub>50</sub>	dose that is lethal in 50% of test subjects
IUBMB	International Union of Biochemistry and Molecular Biology
<i>J</i>	coupling constant
LC	liquid chromatography
LDA	lithium diisopropylamide
lit.	literature value
LRMS	low-resolution mass spectrometry
m	multiplet
Man	mannose
max	maximum
MeCN	acetonitrile
MEM	2-methoxyethoxymethyl
MeOH	methanol

MOM	methoxymethyl
MOP	2-(1,2- <i>trans</i> -glycopyranosyloxy)-3-methoxypyridine
mp	melting point
MS	mass spectrometry
NDP	nucleoside 5'-diphosphate
NMP	nucleoside 5'-monophosphate
NMR	nuclear magnetic resonance
n/o	not observed
NOE	nuclear Overhauser effect
NOESY	nuclear Overhauser effect spectroscopy
NppN	dinucleoside diphosphate
NT	nucleotidyltransferase
NTP	nucleoside 5'-triphosphate
P	phosphate
PDC	pyridinium dichromate
Ph	phenyl
q	quartet
$R_f$	retention factor
Rha	rhamnose
RNA	ribonucleic acid
rt	room temperature
s	singlet

Selectfluor®	1-chloromethyl-4-fluoro-1,4-diazoniabicyclo[2.2.2]octane bis(tetrafluoroborate)
$S_Ni$	internal nucleophilic substitution
$S_N2$	bimolecular nucleophilic substitution
t	triplet
TBDMS	<i>tert</i> -butyldimethylsilyl
Tf	trifluoromethanesulfonyl
TFAA	trifluoroacetic anhydride
THF	tetrahydrofuran
THP	tetrahydropyran-2-yl
TLC	thin-layer chromatography
TMS	trimethylsilyl
$t_R$	retention time
TsOH	toluenesulfonic acid
UDP	uridine 5'-diphosphate
UMP	uridine 5'-monophosphate
UTP	uridine 5'-triphosphate
UV	ultraviolet
v/v	volume per unit volume
w/v	weight per unit volume
$\delta$	chemical shift in parts per million
$\lambda$	wavelength

## Acknowledgements

---

I am first and foremost indebted to my supervisor, Dr. David Jakeman, for the guidance and encouragement he has provided throughout the course of this work. Many thanks are also extended to past and present members of the Jakeman laboratory, especially Dr. Ray Syvitski, Dr. Charles Borissow, and Samy Mohamady for helpful discussions, as well as Dr. Roy Mosher and Sheryl Knowles for purifying nucleotidyltransferases, and Stephanie Lucas for synthesizing 2-deoxy-2-fluorosugar-1-phosphates.

I also wish to acknowledge the support of my supervisory committee, Dr. Stephen Bearne, Dr. T. Bruce Grindley, and Dr. Norman Schepp, all of who kindly taught me graduate courses in their respective fields. Thanks are extended to Dr. Mike Lumsden, Dr. Bob Berno, and Dr. Kathy Robertson in the Atlantic Region Magnetic Resonance Centre for training and advice as well as Xiao Feng, Elden Rowland, Joseph Hui, and Dr. Evelyn Soo for mass spectrometry services. Many thanks also to the College of Pharmacy for housing my research laboratory and the Department of Chemistry for providing me with a stimulating graduate program.

I am also indebted to my extraordinary parents for their multifaceted and unconditional love and support throughout my life. Lastly, my husband Adam has been and continues to be my best friend and my greatest source of inspiration, as well as a pillar of support and encouragement, and for this I am eternally grateful.



# Chapter 1. Introduction

---

## 1.1. Natural Products and Drug Discovery

Nature has long served as a plentiful source of therapeutic agents. Pharmaceutical records dating as far back as *ca.* 2600 BCE document the use of approximately 1000 plant-derived natural products in ancient Mesopotamia to treat everything from coughs and colds to inflammation and infections.<sup>1</sup> Interestingly, many of these compounds, including oils extracted from cedar, cypress, and myrrh, are still in use today. On a more recent reflection of the implications of natural products over the last century, the discovery of penicillin, first reported by Fleming in 1929,<sup>2</sup> remains one of the most important achievements. By the early 1940s, the problems associated with producing and purifying large amounts of this antibiotic had been solved thanks to the efforts of Chain and colleagues,<sup>3</sup> in collaboration with several pharmaceutical companies in the United States. The success of penicillin sparked the golden age of antibiotic discovery as many pharmaceutical companies and academic research groups quickly moved to assemble large inventories of microorganisms in hopes of discovering new bioactive secondary metabolites.<sup>4</sup> This surge in interest resulted in the discovery of many important antibiotics still in use today including chloramphenicol (**1**), erythromycin A (**2**), and vancomycin (**3**) (Figure 1).<sup>5</sup>

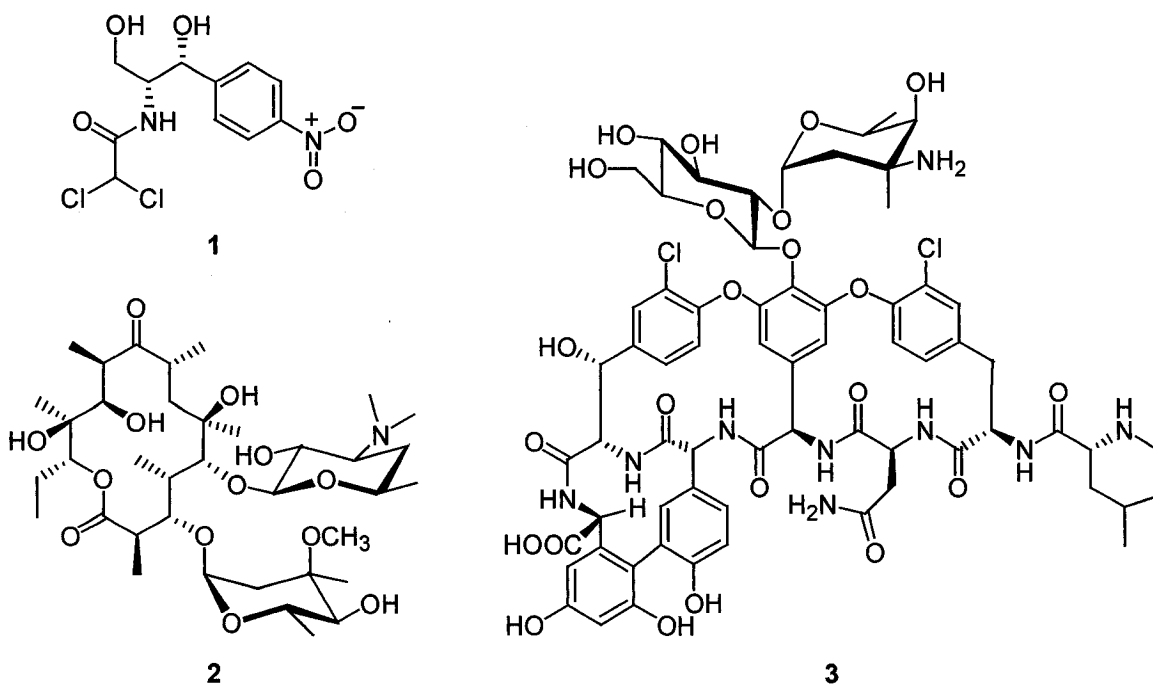


**Figure 1.** Structures of chloramphenicol (1), erythromycin A (2), and vancomycin (3)

Despite advances in modern drug discovery, the majority of pharmaceuticals continue to be derived from natural product scaffolds. A survey of new chemical entities approved by regulatory agencies between 1981 and 2002 revealed that approximately half were natural products, semi-synthetic derivatives of natural products, or synthetic compounds whose pharmacophore was derived from a natural product.<sup>6</sup> Of particular note are the areas of cancer and infectious diseases, where over 60% and 75% of therapeutic agents, respectively, were shown to be of natural product origin.

The natural products of interest in our laboratory are microbial secondary metabolites. These compounds are produced by bacteria in response to physiological or environmental stress and are not essential for an organism to grow and multiply.<sup>7</sup> Microbial secondary metabolites comprise a vast group of compounds that are both chemically diverse and structurally complex. It has been estimated that each cubic centimetre of the earth's surface contains more than 1000 species of microbes and greater

than 99% of all microbial flora have yet to be identified.<sup>8</sup> Although more than 20,000 microbial secondary metabolites have been described, only a very small proportion of these have been systematically screened for use as therapeutic agents.<sup>9</sup> Recent improvements in instrumentation, robotics, and screening technologies have significantly increased the speed of isolation and structural elucidation of secondary metabolites, thereby increasing the viability of studying this largely untapped resource.<sup>5</sup>

### 1.1.1. Angucycline Antibiotics

The term antibiotic was defined by Waksman in 1942 as a chemical substance produced by a microorganism capable of inhibiting the growth of other microorganisms.<sup>10</sup> Angucycline antibiotics, a relatively new and emerging group of bioactive natural products with over one hundred members,<sup>11,12</sup> are of particular interest in our laboratory. The founding members of this group, tetrangomycin (**4**) and tetrangulol (**5**) (Figure 2), were isolated in 1965 in a New York laboratory conducting an antibiotic screening program.<sup>13,14</sup> They were the first microbial natural products found to contain unsymmetrically assembled tetracyclic ring frames.

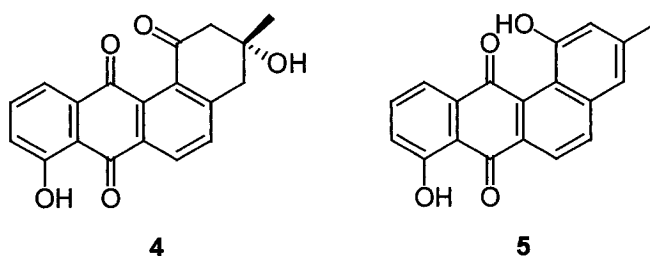


**Figure 2.** Structures of tetrangomycin (**4**) and tetrangulol (**5**)

The terms ‘angucycline’ and ‘angucyclinone’ were first introduced in 1984 during a renaissance of the angucycline group, which had remained a discrete group of antibiotics throughout the 1970s.<sup>12</sup> The name angucyclin-e/-one is derived from the Latin

word ‘angus’ (angle), referring to the angular tetracyclic (benz[*a*]anthracene) backbone, the most characteristic feature of this group of antibiotics (Figure 3).

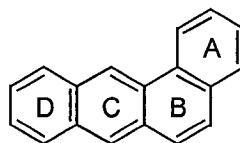


**Figure 3.** Characteristic tetracyclic benz[*a*]anthracene framework of angucyclines

By 1984, more than a dozen angucycline antibiotics had been discovered, but a variety of terms had been used to describe their similar structures. In 1992, Rohr and Thiericke proposed a consolidation of all former expressions into practical terminology.<sup>12</sup> Under their recommendations, the term ‘angucyclinone’ includes natural products consisting of, or derived from, an angular tetracyclic benz[*a*]anthracene ring system (Figure 3) formed via a polyketide biosynthetic pathway. The term ‘angucycline’ is used to describe members of this group of antibiotics containing hydrolyzable carbohydrate groups, while the term ‘angucyclinone’ refers to members with no carbohydrate appendages attached to their respective aglycons. Although the term ‘aglycon’ is commonly defined as a chemical structure without hydrolyzable carbohydrates, some angucyclinones still contain *C*-glycosidic linked carbohydrate functionalities, and are therefore sometimes referred to as ‘pseudoaglyca’. One example of an angucyclinone with a *C*-glycosidic linked sugar ligand is urdamycin B (**6**),<sup>15</sup> which contains an oligosaccharide appendage composed of both D-olivose and L-rhodinose building blocks (Figure 4). The biosynthetic formation of this unique glycosidic linkage is an intriguing topic of current study.<sup>16,17,18,19,20</sup>

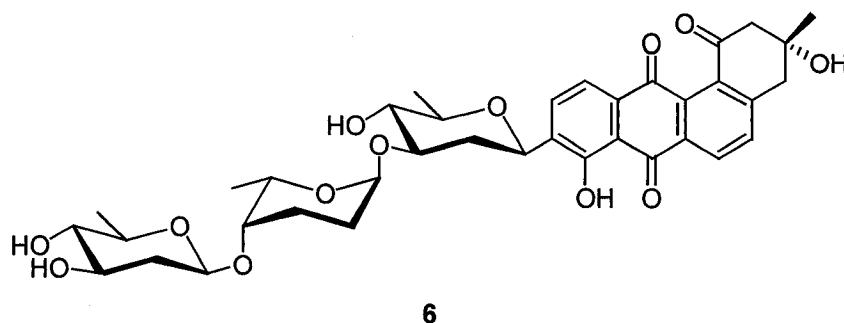


**Figure 4.** Structure of urdamycin B (6)

The majority of members of the angucycline group of antibiotics are secondary metabolites of microorganisms isolated from soil samples,<sup>12</sup> although at least one member has been isolated from shallow sea mud.<sup>21</sup> Taxonomic investigations have revealed that all producing organisms of angucycline antibiotics belong exclusively to the *Actinomycetes* group of bacteria.<sup>12</sup> The *Actinomycetes* are Gram-positive bacteria with DNA rich in guanine plus cytosine and usually exhibit branched filaments.<sup>22</sup> They are a very successful widely distributed group of bacteria best known for their economic importance as producers of antibiotics, vitamins, and enzymes.<sup>22</sup> Interestingly, this group of bacteria has produced more than two-thirds of naturally occurring antibiotics discovered to date.<sup>23</sup> The majority of microorganisms that produce angucycline antibiotics are from various species of the genus *Streptomyces*.<sup>12</sup>

In terms of therapeutic utility, the angucyclines display a broad range of biological activities and do not appear to be restricted to any specific mode of action.<sup>12</sup> Some angucyclines have been shown to act as potent inhibitors of blood platelet aggregation or hydrolase and/or mono-oxygenase inhibitors. Others exhibit antibacterial activity against mainly Gram-positive bacteria or display antiviral activity. Perhaps the most promising discovery is the cytostatic and cytotoxic activities demonstrated by numerous angucyclines against various cancer cell lines.<sup>11,12,24</sup>

#### 1.1.1.1. Jadomycins

The jadomycins are a subgroup of angucycline antibiotics of particular interest in our laboratory. The first member of this unique class of angucyclines, jadomycin (7), was isolated and structurally characterized in 1991 (Figure 5).<sup>25</sup> Interestingly, through the discovery of jadomycin, it was found that secondary metabolite production could be induced by a change in bacterial culture incubation temperature. While incubation of bacterial cultures of *Streptomyces venezuelae* ISP5230 at 28 °C produced the common antibiotic chloramphenicol (1) (Figure 1), incubation of the same bacterial cultures at 37 °C produced the novel antibiotic jadomycin (7), demonstrating the capability of a heat shock response.<sup>25</sup> In 1993, a glycosylated form of jadomycin (7), jadomycin B (8), was isolated and structurally characterized from *Streptomyces venezuelae* ISP5230 bacterial cultures (Figure 5).<sup>26</sup>

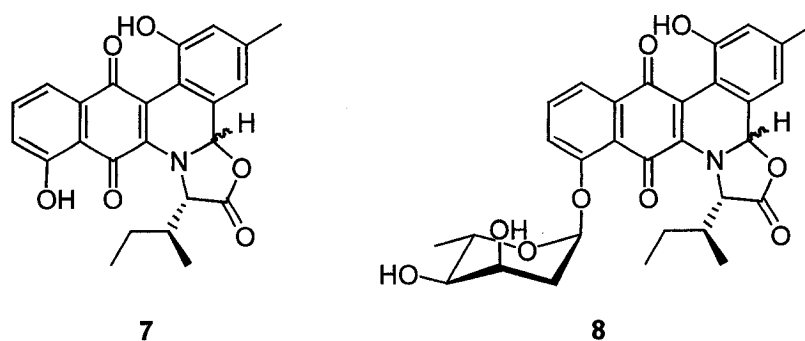


**Figure 5.** Structures of jadomycin (7) and jadomycin B (8)

The jadomycins are structurally composed of a unique polyketide-derived pentacyclic angucyclinone aglycon containing nitrogen and oxygen heteroatoms. The additional fifth ring is a distinguishing feature of all jadomycins and is believed to be the result of the direct incorporation of an amino acid (L-isoleucine in the case of 7 and 8) from the bacterial growth medium where the amino acid serves as the sole bacterial

nitrogen source.<sup>27</sup> A non-enzymatic mechanism has been proposed for amino acid incorporation into the aglycon<sup>28</sup> and recent studies have shown that a dynamic equilibrium exists between two jadomycin diastereomeric forms.<sup>29</sup> In contrast to jadomycin (7), jadomycin B (8) also contains a carbohydrate appendage, the 2,6-dideoxysugar L-digitoxose. An interesting physical characteristic of secondary metabolites 7 and 8 is their intense colours as jadomycin (7) is dark green, while the glycosylated jadomycin B (8) is crimson.

The observation that an intact L-isoleucine amino acid appeared to be incorporated into the angucyclinone aglycon of jadomycin B stimulated interest regarding the possibility of directed biosynthesis through providing alternative amino acid nitrogen sources to the bacterial growth medium. When Doull and coworkers replaced L-isoleucine with other L-amino acids in the bacterial growth medium, a series of differentially coloured secondary metabolites were observed, suggesting that modified jadomycin B analogues had been produced.<sup>27</sup> Both Rohr<sup>28</sup> and Jakeman<sup>30,31</sup> have built upon this initial work and, as a result, many jadomycins with various L-, D-, and synthetically modified amino acids have been isolated and characterized, creating a structurally diverse library of jadomycins.

Preliminary biological testing of jadomycin (7) and jadomycin B (8) against various cancer cell lines through a collaborative study with Dr. Jonathan Blay (Department of Pharmacology, Dalhousie University) revealed that jadomycin B (8) is approximately an order of magnitude more active than its non-glycosylated counterpart.<sup>32</sup> It was also concluded that jadomycin B is approximately an order of magnitude less active than the glycosylated anthracycline chemotherapy drug doxorubicin. These results

provide impetus to investigate the potential biological role of the carbohydrate appendage of jadomycin B (**8**) via glycosylation engineering.

## **1.2. Medicinal Role of Carbohydrate Functionalities**

Many therapeutic agents derived from secondary metabolites are glycosylated, and it is widely acknowledged that natural product sugar ligands are frequently critical in conferring biological activity.<sup>33,34,35,36</sup> The precise medicinal role of carbohydrate residues varies greatly, due in part to the diverse expanse of chemical space readily accessed by glycosides.<sup>37</sup> In general, glycosylated natural products are more hydrophilic than their aglycon counterparts, influencing pharmacokinetic properties of drugs such as absorption, distribution, metabolism, and excretion.<sup>33</sup> Traditionally, carbohydrates were believed to play exclusively this pharmacokinetic role and thus research into the biological implications of secondary metabolite glycosylation has lagged behind that of proteins and nucleic acids. It has more recently been established that glycosylation plays a wide variety of important mechanistic roles as sugars have been shown to impart specific interactions with biological targets.<sup>33,35,36</sup> Although the precise roles of carbohydrates in bioactive compounds are still unclear in many cases, research into this area is expanding as the potential of carbohydrate-based drugs remains largely underexplored.<sup>33</sup> Several examples illustrating a number of currently identified roles of sugar residues in biologically relevant natural products are discussed below.



### 1.2.1. Effect of Adding or Removing a Monosaccharide

The macrolides are a clinically important group of secondary metabolites that demonstrate excellent activity against Gram-positive bacteria.<sup>35,36</sup> In general, macrolides function by binding with the bacterial 50S ribosomal subunit, inhibiting protein biosynthesis.<sup>38,39</sup> Most macrolides are glycosylated, and early work established that these carbohydrate appendages are critical for bioactivity.<sup>40,41,42</sup> Although the precise role of many macrolide sugar ligands remains elusive, their carbohydrate appendages have been linked with many of the pharmacological properties of this class of therapeutic agents.<sup>35,36</sup> In particular, the basicity of aminosugar nitrogen atoms have been shown to improve the active transport of macrolides into cells<sup>33</sup> and, consequently, a trend exists demonstrating that more basic macrolides have increased bioactivity.<sup>43</sup> The first member of the macrolide family of antibiotics, erythromycin A (**2**), was isolated in 1952.<sup>44</sup> This novel antibiotic, possibly the most famous macrolide, rapidly gained widespread clinical use and continues to be prescribed today as an antibacterial agent. The isolation of megalomicin (**9**), a glycosylated derivative of **2**, has also been reported.<sup>45,46</sup> An analysis of their structures reveals that erythromycin A (**2**) is converted to megalomicin (**9**) by the addition of a single monosaccharide, 2,3,4,6-tetradeoxy-3-dimethylamino- $\beta$ -D-*threo*-hexopyranose (Figure 6).<sup>35</sup> Interestingly, this change in glycosylation results in a compound with significantly different bioactivity as an antiviral and antiparasitic agent.<sup>47</sup>

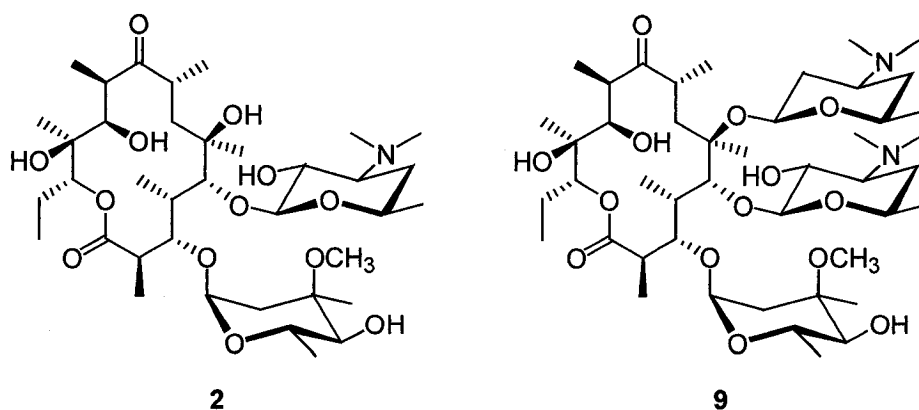


**Figure 6.** Structures of erythromycin A (**2**) and megalomicin (**9**)

One of the best-studied glycosylated secondary metabolites with respect to the role of sugar ligands is calicheamicin  $\gamma_1^I$  (**10**), a member of the enediyne family of potent antitumour agents (Figure 7).<sup>48,49</sup> The enediynes function by cleaving DNA via a diradical species generated by a Bergman-type cycloaromatization of the aglycon.<sup>50</sup> In the presence of oxygen, the diradical species is responsible for the concerted cleavage of double-stranded DNA.<sup>51</sup> The biological role of the aryltetrasaccharide unit has been assessed using **10** as well as several analogues. While functional studies have demonstrated that only monosaccharides A and B are necessary for positioning calicheamicin  $\gamma_1^I$  (**10**) for double-stranded DNA scission, the complete aryltetrasaccharide was required for tumour specificity, illustrating the importance of the oligosaccharide appendage.<sup>35,36</sup> Moreover, NMR studies on the calicheamicin  $\gamma_1^I$  (**10**)-DNA complex have revealed that the bound aryltetrasaccharide is critical for properly aligning the enediyne ring in the minor groove of DNA so the pro-radical centres of the ring will be properly positioned for proton abstraction.<sup>52,53</sup>



composed of a linearly aligned tetracyclic aglycon and the trideoxyaminosugar L-daunosamine (Figure 8). A synthetic analogue of **11**, epirubicin (**12**), has also been described, which differs from **11** only in the stereochemistry of the hydroxyl group positioned at C-4 in the monosaccharide ring (Figure 8). Interestingly, epirubicin (**12**) has been shown to be significantly less toxic than doxorubicin (**11**) and is also used clinically.<sup>56</sup> Although doxorubicin (**11**) and epirubicin (**12**) were found to be equally active, patients taking the same dosage of **12** compared to **11** experienced less neutropenia, alopecia, nausea, and vomiting. In addition, fewer patients receiving **12** suffered congestive heart failure or other cardiotoxic effects as compared to patients receiving **11**, illustrating a significant difference between these two epimeric drugs.

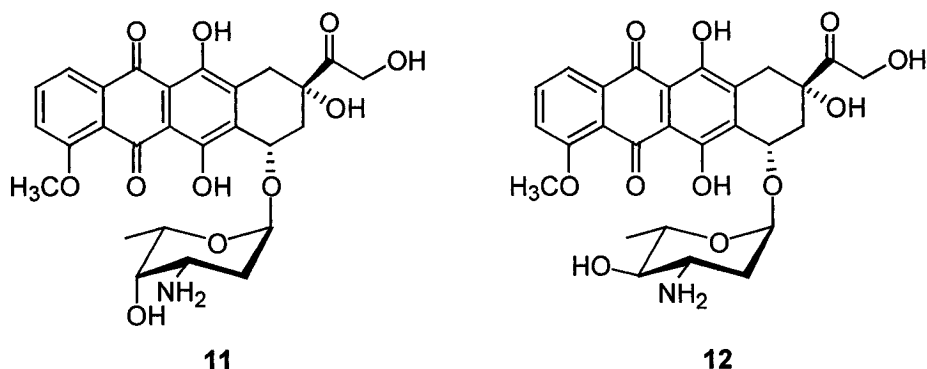


**Figure 8.** Structures of doxorubicin (**11**) and epirubicin (**12**)

As evidenced by the examples described thus far, many glycosylated secondary metabolite-derived drugs contain 2,6-dideoxysugars. In many cases, cleavage of the glycosidic bond is believed to be one of the main causes of drug toxicity.<sup>36</sup> For this reason, numerous natural product analogues containing 2,6-dideoxy-2-fluorosugar appendages have been prepared.<sup>57,58</sup> The introduction of a 2,6-dideoxy-2-fluorosugar in lieu of a 2,6-dideoxysugar strengthens the glycosidic bond between the sugar and the aglycon due to the electron-withdrawing influence of the fluoro- substituent. In addition,

because of the similar sizes of fluorine atoms and hydroxyl groups, this substitution results in only a minimal steric effect. This strategy is exemplified in the case of daunorubicin (**13**), an antitumour anthracycline used to treat acute leukaemia, and 2'- $\beta$ -fluorodaunorubicin (**14**) (Figure 9).<sup>58</sup> Although fluorinated analogue **14** is slightly less active than parent compound **13**, it was found to be less toxic and had a higher dose range compared to **13**, illustrating the advantage of this approach.

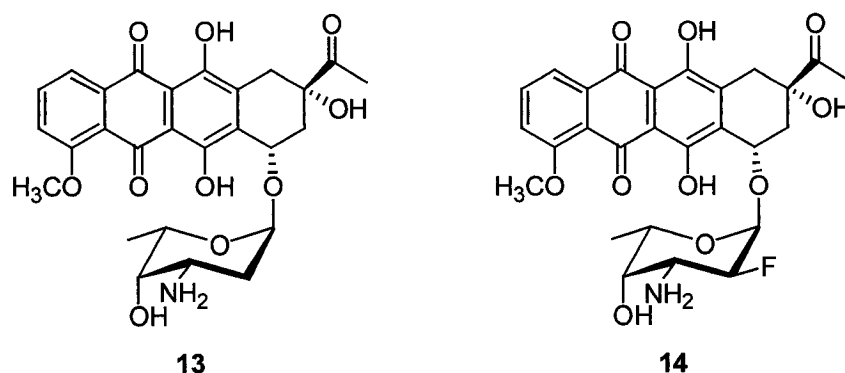


**Figure 9.** Structures of daunorubicin (**13**) and 2'- $\beta$ -fluorodaunorubicin (**14**)

### 1.2.3. Effect of Glycosylating a Previously Non-Glycosylated Natural Product

Recent successes associated with modifying the carbohydrate components of secondary metabolites to lower toxicity and/or improve bioactivity has led to interest in the effect of glycosylating previously non-glycosylated natural products.

The potential of this approach is exemplified by the generation of a structurally diverse 58-member library of glycosylated colchicine derivatives by Thorson and coworkers.<sup>59</sup> Colchicine (**15**) is a highly potent plant-derived alkaloid first described as a treatment for gout by the ancient Greek physician Dioscorides in the first century CE (Figure 10).<sup>60</sup> It was isolated in 1820 by French chemists Pelletier and Caventou<sup>61</sup> and is

still occasionally prescribed for its pain-relieving and anti-inflammatory effects to treat gout, familial Mediterranean fever, and Behcet's disease, although toxicity limits its widespread clinical use.<sup>59</sup> Colchicine (**15**) functions by suppressing microtubule polymerization by binding to tubulin, which inhibits mitosis and suppresses cell division.<sup>59</sup> Upon library screening against numerous human cancer cell lines, fifteen derivatives displayed IC<sub>50</sub> values of less than 1  $\mu$ M compared with an IC<sub>50</sub> of 3  $\mu$ M for parent compound **15** in at least one cell line. On probing the mechanism of glycosylated colchicine derivatives, several library members (**16**, **17**) demonstrated no apparent effect on microtubule polymerization while other derivatives (**18**, **19**) actually stabilized microtubule polymerization (Figure 10). This interesting discovery is a rare example of a mechanistic interconversion mediated by the addition of a monosaccharide residue to a previously non-glycosylated natural product.

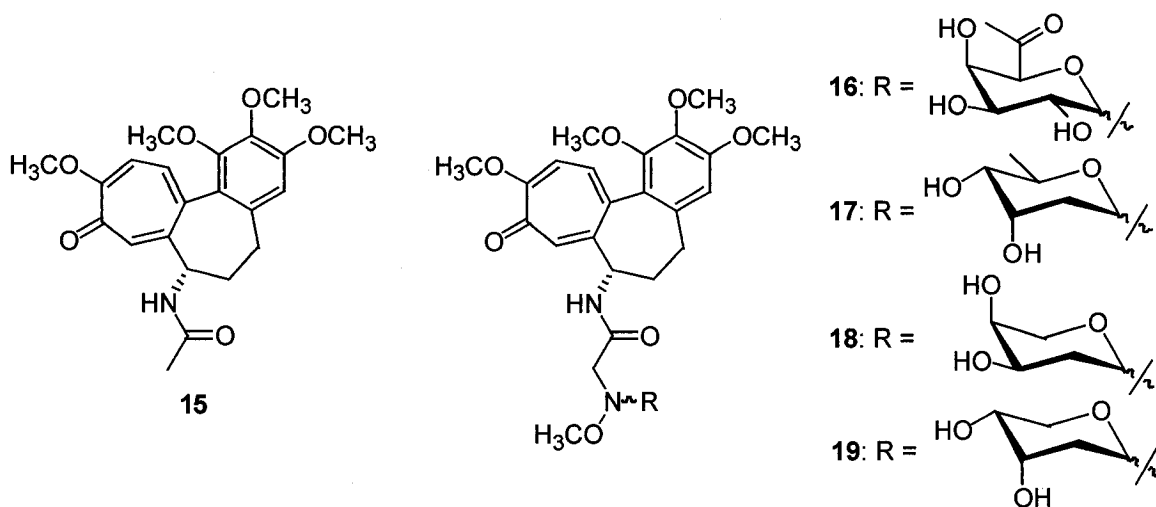


**Figure 10.** Structure of colchicine (**15**) and glycosylated derivatives **16-19**

### **1.3. Natural Product Glycosylation Engineering**

Glycosylated natural products are increasingly being recognized as reliable scaffolds for drug discovery and development. In order to facilitate an improved understanding of the relationship between sugar ligands and biological activity, the development of efficient glycosylation engineering strategies is of paramount importance. In the following sections, three approaches used to modify the glycosylation patterns of natural products will be discussed.

#### **1.3.1. Chemical Synthesis and Semi-Synthesis Strategies**

The classical method of glycosylation engineering relies upon the total synthesis of glycosylated analogues or the synthetic modification of intermediates typically produced by fermentation or hydrolysis of the parent natural product. One advantage of this approach is unparalleled access to chemical diversity limited only by synthetic expertise and reagents. Nevertheless, a significant disadvantage of this strategy is the tremendous structural complexity of many bioactive natural products. In addition to requiring access to the necessary aglycon, chemical methods typically involve tedious aglycon protection steps prior to glycosylation followed by additional deprotection steps. Depending on the aglycon, it can be difficult to find suitable conditions for these protection and deprotection steps as some aglycons are chemically unstable. In the case of the angucycline antibiotic aquayamycin, for example, skeletal rearrangements of the aglycon were observed under acidic, basic, thermal, and photochemical conditions.<sup>62,63</sup> Even if suitable protection and deprotection conditions are achieved, stereocontrol is often poor, the exception being 1,2-*trans* glycosidic linkages where neighbouring group

participation can be exploited, although improvements in this area have recently been reported.<sup>64</sup> Solubility can also be an issue since protected aglycons must be soluble in organic solvents suitable for chemical glycosylation and synthetic routes are often long, frequently resulting in low yields.

Using click chemistry, Lin and Walsh have overcome some of the limitations described above in the preparation of a 247-member glycopeptide library based on a tyrocidine scaffold.<sup>65</sup> This cyclic decapeptide is a nonribosomal peptide antibiotic that is believed to function via generating pores in the lipid bilayer of bacteria.<sup>65</sup> To facilitate this approach, linear tyrocidine peptides containing propargylglycine were first synthesized on a solid support and subsequently cyclized using a substrate flexible thioesterase. The resulting cyclic peptides were then conjugated to 21 different azido sugars in a combinatorial strategy employing a copper(I)-catalyzed [3 + 2] cycloaddition reaction previously described by Sharpless and coworkers (Figure 11).<sup>66</sup>

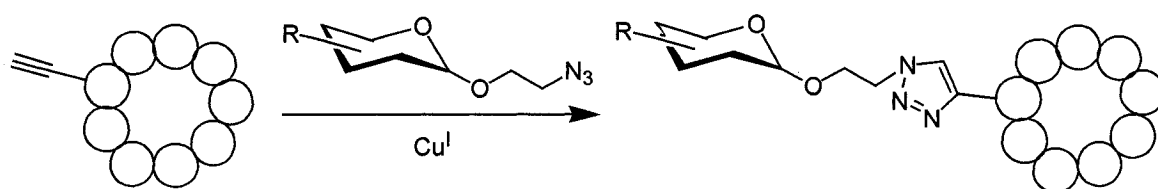


**Figure 11.** General [3 + 2] cycloaddition reaction used to prepare a glycopeptide library based on a tyrocidine scaffold (circles represent amino acids)<sup>65</sup>

Of the 247-member glycopeptide library prepared using this chemoselective ligation approach, numerous derivatives with improved therapeutic indices<sup>a</sup> over the parent compound were identified, which also maintained tyrocidine's antibacterial activity.<sup>65</sup> The most promising derivatives were those containing sugars with lipophilic side chains, which are known to enhance membrane affinity.<sup>65</sup> Interestingly, small

<sup>a</sup> defined as the ratio of the minimal hemolytic concentration to the minimal inhibitory concentration of bacterial growth



configurational changes within certain lipophilic carbohydrate appendages significantly impacted observed therapeutic indices, demonstrating the importance of generating a combinatorial library in this type of study.

A second chemoselective ligation strategy used to prepare libraries of novel glycosylated natural products is neoglycorandomization, first described by Thorson and coworkers in 2005.<sup>67,68,69</sup> The term neoglycorandomization refers to a synthetic procedure involving the chemoselective formation of a neoglycosidic bond between a reducing sugar and an aglycon containing a secondary alkoxyamine acceptor (Figure 12). The notable difference between this approach and traditional chemical glycosylation reactions is the use of unprotected and non-activated reducing sugars as glycosyl donors under mild reaction conditions.

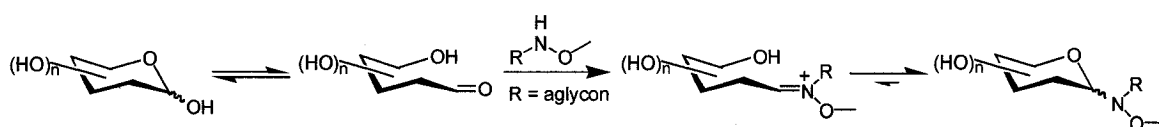


**Figure 12.** General neoglycorandomization strategy<sup>67</sup>

To test the practicality of this concept, Thorson and coworkers selected digitoxin (**20**), a plant-derived cardiac glycoside, as a model scaffold (Figure 14).<sup>67</sup> This compound had previously shown promise in numerous areas of cancer research, but the impact of varying sugar ligands had not been explored, making **20** a good candidate for neoglycorandomization. Using this approach, a library of 78 glycosylated derivatives of digitoxin (**20**) were synthesized and purified in parallel from 39 structurally diverse reducing sugars, which included L-sugars, deoxysugars, dideoxysugars, disaccharides, uronic acids, and monosaccharides containing functional handles such as acetyl and azido groups.<sup>67</sup> An aglycon of **20** containing a secondary alkoxyamine functionality was easily

obtained from the parent natural product in three chemical steps.<sup>67</sup> High-throughput screening of this 78-member neoglycoside library revealed several analogues (**21**, **22**) with improved activity and selectivity over **20** in numerous human cancer cell lines (Figure 13).

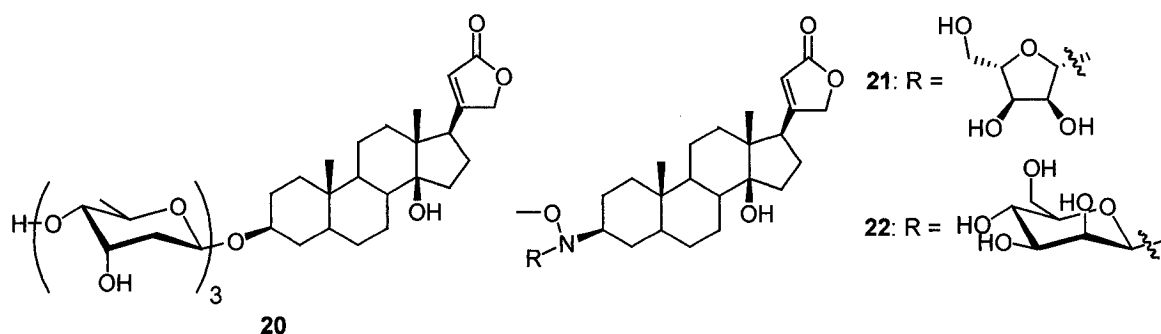


**Figure 13.** Structure of digitoxin (**20**) and neoglycoside derivatives **21-22**

### 1.3.2. *In Vivo* Biosynthetic Pathway Engineering Strategies

The second approach increasingly being used to generate natural products with diversified sugar ligands is *in vivo* biosynthetic pathway engineering, which includes the disruption of genes in sugar ligand biosynthetic pathways as well as the feeding of aglycons to bacterial strains containing sugar ligand biosynthetic pathways.<sup>70</sup> A compelling advantage of this strategy is the ability to access novel glycosides via fermentation, although purification of interesting analogues from bacterial culture broths can prove difficult. It should also be noted that this approach generally suffers from a lack of chemical diversity with the number and type of possible analogues defined by each biosynthetic pathway. In addition, it has been suggested that analogues possessing antibacterial activity may kill the producing organism before they can be isolated from the bacterial culture broth.<sup>70</sup> This means that, in the case of antibacterial agents, *in vivo* methods may actually encourage the isolation of only inactive compounds.

Nonetheless, this strategy has found success as a complementary approach to chemical synthesis. In particular, Salas and coworkers recently reported the preparation of more than 30 rebeccamycin (**23**) and staurosporine (**24**) analogues using several recombinant bacterial strains (Figure 14).<sup>71</sup> These natural products are members of the indolocarbazole alkaloid family, which has attracted attention because of its antitumour and neuroprotective properties. Eight representative analogues were tested against numerous cancer cell lines and the most active compounds were all glycosylated, illustrating the importance of the carbohydrate appendage in yet another class of natural products.

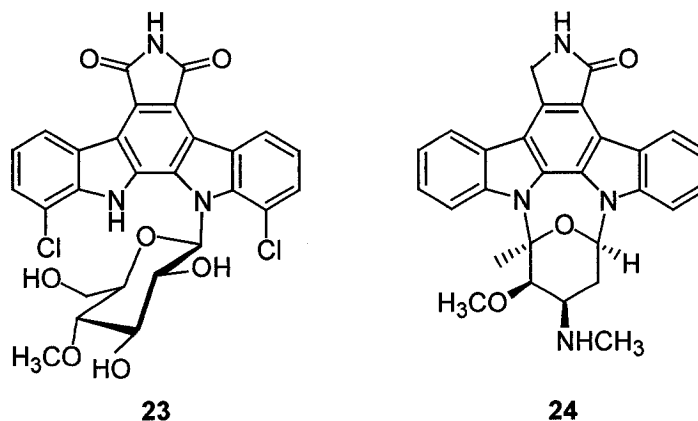


**Figure 14.** Structures of rebeccamycin (**23**) and staurosporine (**24**)

A similar genetic engineering approach has been used to produce an analogue of jadomycin B (**8**) in the Jakeman laboratory. Upon disruption of *jadO*, a putative NDP-hexose 2,3-dehydratase in the dideoxysugar biosynthetic pathway of jadomycin B, a novel analogue, ILEVS1080 (**25**), was isolated and characterized using NMR spectroscopy and mass spectrometry (Figure 15).<sup>72</sup> A structural comparison of jadomycin B (**8**) and ILEVS1080 (**25**) reveals that **25** contains a 6-deoxysugar, 6-deoxy-L-altrose, in contrast to **8**, which contains the 2,6-dideoxysugar L-digitoxose. This

example confirms the function of *jadO* in the dideoxysugar biosynthetic gene assembly and illustrates the substrate promiscuity of downstream genes in the L-digitoxose biosynthetic pathway.

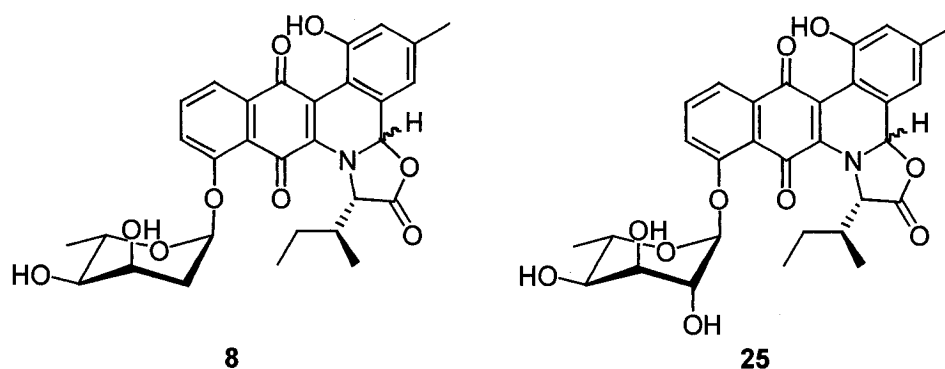


**Figure 15.** Structures of jadomycin B (**8**) and ILEVS1080 (**25**)

### 1.3.3. *In Vitro* Glycorandomization Strategies

A third natural product glycosylation engineering strategy that has shown promise in recent years is *in vitro* glycorandomization, a term coined by Nikolov and coworkers in 2001.<sup>73</sup> This chemo-enzymatic approach combines the benefit of the diversity available through chemical synthesis of unique carbohydrate precursors with the inherent or engineered substrate promiscuity of several classes of enzymes to efficiently activate and attach an array of sugar ligands to natural products. *In vitro* glycorandomization involves the initial preparation of a sugar-1-phosphate, traditionally prepared via chemical synthesis, but more recently sometimes available through enzymatic means via engineered anomeric kinases.<sup>74,75,76,77</sup> These precursors are subsequently attached to natural products via a one-pot two-enzyme (nucleotidyltransferase/glycosyltransferase) protocol.<sup>68,69,78</sup> A significant advantage of this approach is the exquisite chemo-, regio-, and stereospecificity generally observed using these multienzyme systems. The mild

reaction conditions that accompany enzymatic reactions are also amenable to the glycosylation of structurally complex natural products as no intricate protection and deprotection steps are required. One main reason for past reluctance to embrace enzymatic synthesis has been the widespread view that enzymes are substrate specific. Recent successes with carbohydrate-active enzymes has shown otherwise (*vide infra*) and, although some stringent substrate specificity has been reported, many enzymes have demonstrated remarkable inherent or engineered promiscuity with respect to both donor and acceptor substrates.<sup>79</sup> This concept will be further discussed in Section 1.4.4.

One of the most notable success stories of *in vitro* glycorandomization involves vancomycin (**3**), a potent glycopeptide antibiotic clinically used against Gram-positive bacteria.<sup>80</sup> Of 33 enzymatically prepared sugar nucleotide donors, 31 were efficiently transferred to the vancomycin aglycon by a second enzyme responsible for glycosyltransfer, producing a library of novel vancomycin analogues.<sup>80</sup> To add another level of diversity, this initial library included monosaccharides armed with functional handles amenable for use in further chemoselective ligation reactions. Huisgen 1,3-dipolar cycloaddition reactions with enzymatically installed glycosyl azides and various alkynes afforded 1,2,3-triazoles ligated to carbohydrate functionalities decorating the vancomycin scaffold (Figure 16).<sup>80,81</sup> Interestingly, these variants were among the most active compounds isolated, with derivative **26** displaying both enhanced antibacterial activity and specificity over parent compound **3** (Figure 16).

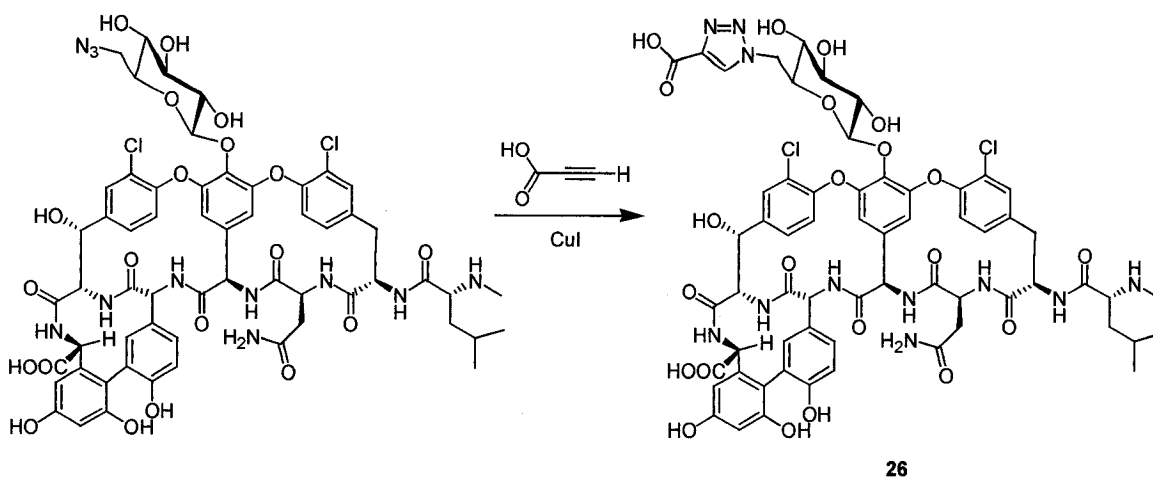


**Figure 16.** Representative Huisgen 1,3-dipolar cycloaddition reaction used to diversify the vancomycin scaffold, producing derivative **26**<sup>80</sup>

Another recent *in vitro* glycorandomization advance involves the exploitation of the reversibility of enzymes involved in glycosyltransfer. Using four enzymes from two natural product biosynthetic pathways, Thorson and coworkers recently revealed that the reversibility of these biocatalysts could be harnessed to exchange sugar ligands and aglycons with ease.<sup>82</sup> Although early examples of glycosyltransferase reversibility were described using chitin synthetase<sup>83</sup> and sucrose synthetase,<sup>84</sup> natural product glycosyltransferases have traditionally been perceived as unidirectional catalysts.<sup>82</sup> The aforementioned glycosyltransferases, GtfD and GtfE from vancomycin (**3**) and CalG1 and CalG4 from calicheamicin  $\gamma_1^I$  (**10**), specifically demonstrated their ability to catalyze three new reactions: (i) the biosynthesis of synthetically challenging deoxysugar donors from glycosylated natural products, (ii) the exchange of parent molecule carbohydrate ligands with exogenous sugar donors, and (iii) the transfer of a carbohydrate from one natural product scaffold to a second structurally distinct aglycon (Figure 17).<sup>82</sup>

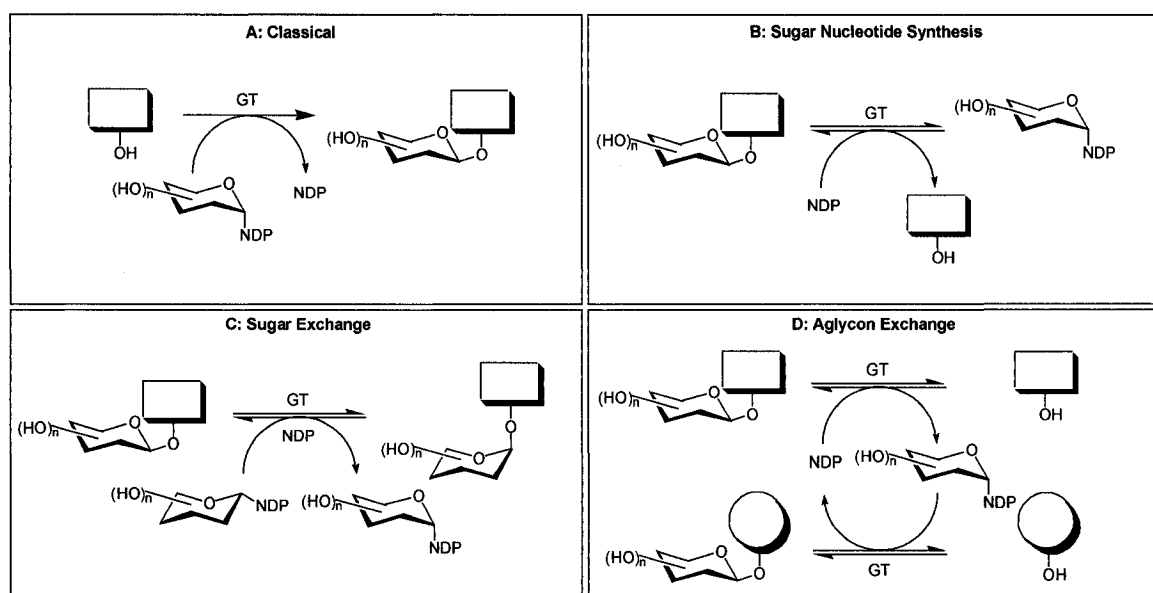


**Figure 17.** Summary of *in vitro* glycorandomization approaches possible via glycosyltransferase catalysis<sup>82</sup>

Using this strategy, more than 70 structurally diverse analogues of **3** and **10** were efficiently prepared, illustrating the tremendous potential of this approach in natural product glycosylation engineering.<sup>82</sup> This discovery will prove useful in overcoming challenges related to preparing unstable deoxysugar nucleotide donors and provides another useful route to introducing carbohydrate diversity in natural products. The reversibility of VinC, a glycosyltransferase involved in vicienistatin biosynthesis,<sup>85</sup> and AveBI, an iterative glycosyltransferase involved in avermectin biosynthesis,<sup>86</sup> have also recently been reported, illustrating that glycosyltransferase reversibility appears to be a general trend.

#### 1.4. Glycosyltransferase Enzymes

Glycosyltransferases are a ubiquitous group of enzymes responsible for transferring carbohydrates from electrophilic donors to a wide variety of acceptor molecules including oligosaccharides, proteins, nucleic acids, lipids, and many classes of

natural products.<sup>87</sup> Glycosyl donors are hexoses or pentoses and may possess either a D- or L-configuration depending on the glycosyltransferase. The leaving groups of electrophilic sugar donors include mono- and diphosphonucleosides as well as various mono- and diphospholipids. The vast majority of glycosyltransferases utilize nucleoside diphosphate leaving groups with uridine and deoxythymidine diphosphates being the most common.<sup>87</sup> Enzymes catalyzing reactions involving this category of glycosyl donor are sometimes referred to as Leloir-type glycosyltransferases based on Leloir's 1949 description of the biosynthesis of glycosidic bonds, for which he was awarded the 1970 Nobel Prize in Chemistry.<sup>88,89</sup>

Examples of the *in vitro* use of glycosyltransferases first appeared in the early 1980s when a  $\beta$ -(1 $\rightarrow$ 4)-galactosyltransferase was isolated from bovine colostrum and used to prepare both the disaccharide  $\beta$ -Gal(1 $\rightarrow$ 4)GlcNAc and the trisaccharide  $\beta$ -Gal(1 $\rightarrow$ 4)GlcNAc- $\beta$ -(1 $\rightarrow$ 6/3)Gal on a millimolar scale using immobilized enzymes and sugar nucleotide regeneration systems.<sup>90,91</sup> This enzyme has since become the best-characterized glycosyltransferase to date and is commercially available.

#### **1.4.1. Classification**

The sequencing of genomes has revealed a vast number of putative glycosyltransferase gene sequences. Recent estimates suggest that approximately 1% of the open reading frames of each genome are dedicated to the biosynthesis of glycosidic bonds.<sup>92</sup> Despite the prevalence of these anabolic enzymes, glycosyltransferase research has lagged behind that of other carbohydrate-active enzymes, such as glycosidases, due to difficulties associated with overexpression, purification, and crystallization.<sup>93</sup> These



obstacles have resulted in a significant gap between the few characterized glycosyltransferases and the thousands of putative sequences available in databanks.

Traditionally, the International Union of Biochemistry and Molecular Biology (IUBMB) have classified enzymes based on their donor, acceptor, and product specificity.<sup>b</sup> This classification system is not practical for glycosyltransferases because full characterization of an enzyme's donor(s), acceptor(s), and product(s) are required before an Enzyme Commission (EC) number is assigned. In addition, EC numbers are not designed to accommodate enzymes capable of accepting numerous substrates, thereby producing a variety of products, which poses a problem for the many promiscuous glycosyltransferases.<sup>94</sup> Furthermore, EC numbers do not reflect the intrinsic structural and mechanistic features of enzymes, making it difficult to gain a broader understanding of the relatedness of various glycosyltransferases.

In an attempt to overcome the limitations of the IUBMB system, Henrissat and coworkers proposed a classification system based on amino acid sequence homology in 1997.<sup>95</sup> This new classification scheme allows correlation between the structural features of glycosyltransferases and their observed biochemical functions. It was inspired by the widely accepted classification system of the mechanistically related glycosidases, metabolic carbohydrate-active enzymes generally responsible for glycosidic bond hydrolysis.<sup>96</sup> When this classification scheme was first published, 27 families were described based on an analysis of 600 glycosyltransferase sequences available at the time.<sup>95,97</sup> Since this first analysis, the number of available glycosyltransferase sequences has increased dramatically to more than 12,000 as of 2006.<sup>93</sup> To accommodate the

---

<sup>b</sup> Nomenclature Committee of the International Union of Biochemistry and Molecular Biology (NC-IUBMB), <http://www.chem.qmul.ac.uk/iubmb/enzyme/rules.html> (Accessed: 26/03/07)

growing number of sequences encoding putative glycosyltransferases, Henrissat and coworkers established an online database<sup>c</sup> where families are continuously updated.<sup>98</sup> The current classification system is discriminatory with respect to molecular mechanism since this feature is conserved within a given family. The resultant grouping of glycosyltransferases with different donor, acceptor, and product specificities into the same families provides meaningful insight into the divergent evolution of glycosyltransferase families.

#### 1.4.2. Structural Superfamilies

Given the structural and functional diversity of products prepared via glycosyltransferase catalysis, combined with their divergent evolutionary history, it is not surprising that significant diversity is displayed in terms of sequence.<sup>92,95,97</sup> In light of the large number of enzyme folds identified for glycosidases, it was hypothesized that glycosyltransferases adopt a similarly extensive number of different folds.<sup>87</sup> However, until recently, only two different fold superfamilies, named GT-A and GT-B, had been identified from glycosyltransferase crystal structures.<sup>99,100</sup> In 2004, a third superfamily emerged based on the analysis of the crystal structure of a bacterial sialyltransferase in complex with a substrate analogue.<sup>101</sup> This enzyme has a similar fold to proteins in the GT-A superfamily, but displays some unique structural features (*vide infra*), thereby constituting a new fold. Very recently, a fourth superfamily has also been discovered as the crystal structure of PBP2, a bifunctional bacterial cell wall cross-linking enzyme consisting of both transpeptidase and glycosyltransferase domains, was elucidated.<sup>102</sup> Interestingly, the overall fold of PBP2 revealed no similarity to that of either GT-A or

---

<sup>c</sup> Carbohydrate-Active Enzymes Database, <http://afmb.cnrs-mrs.fr/CAZY/> (Accessed: 26/03/07)

GT-B superfamily folds.<sup>102</sup> Henrissat and coworkers have suggested that the small number of glycosyltransferase folds identified thus far is a reflection of both the constraints of the sugar nucleotide binding motif and the potential evolutionary origin of these biocatalysts from a small number of precursor sequences.<sup>92</sup>

The GT-A superfamily fold consists of two tightly associated, adjoining  $\beta/\alpha/\beta$  domains that favour the formation of a continuous central sheet of at least eight  $\beta$ -strands, which is sometimes referred to as a single domain fold or a Rossmann fold.<sup>92</sup> Common features of all GT-A enzymes include the presence of a two coordinating aspartate residues, often called a DXD motif, as well as the requirement of a divalent cation, which is essential for enzyme activity.<sup>93</sup> In all GT-A crystal structures solved thus far, the DXD motif has been shown to associate with the phosphate groups of the nucleotide donor via coordination with a divalent cation, which is usually  $Mn^{2+}$ . The variable amino acid of the DXD motif, typically an aliphatic or polar residue of moderate size, has been shown to aid in the binding of the ribose portion of the sugar nucleotide donor.<sup>93</sup> In addition, some GT-A members contain a conserved aspartate residue that coordinates with N-3 of the uridine base.<sup>92</sup> Interestingly, the DXD motif, as well as several other structural elements, is well conserved throughout the entire GT-A superfamily regardless of catalytic mechanism, which dictates the stereochemical outcome of the reaction, indicating the widespread importance of these regions in glycosyltransfer.<sup>93</sup>

The third suggested structural superfamily is composed thus far of CstII, a sialyltransferase from *Campylobacter jejuni*.<sup>101</sup> This enzyme is similar to other GT-A glycosyltransferases in that it adopts a single domain Rossmann-type fold, but also deviates from GT-A enzymes with respect to other structural features. Significant

differences exist in the connectivity of secondary structural components. In addition, CstII contains no DXD motif, in contrast to all other GT-A enzymes, and is thus considered a new fold.<sup>93</sup>

The GT-B superfamily fold also consists of two  $\beta/\alpha/\beta$  domains, but these are not as tightly associated as in GT-A enzymes and are said to “face each other” with conformational changes in relative orientation accompanying substrate binding.<sup>92</sup> Wrabl and Grishin have described several distinctive sequence motifs of GT-B superfamily members.<sup>103</sup> Included in their observations is a prominent ribose-coordinating glutamate residue in addition to several phosphate-coordinating loops rich in glycine residues. Thus far, however, no strictly conserved residues have been observed within the GT-B superfamily.<sup>87</sup> In contrast to GT-A enzymes, no bound divalent cations have been associated with GT-B catalysis to date, although they may be required for full enzyme activity.<sup>93</sup> Additional correlations require the characterization of additional enzyme-substrate complexes from this glycosyltransferase superfamily.

The most recently uncovered fold belonging to the glycosyltransferase domain of PBP2, a bifunctional enzyme involved in bacterial cell wall peptidoglycan biosynthesis, is predominantly  $\alpha$ -helical and demonstrates virtually no structural similarity to previously described GT-A and GT-B folds.<sup>102</sup> Both the apoenzyme structure and the structure of PBP2 in complex with the antibiotic substrate analogue moenomycin were found to consist of two principal regions: a larger segment composed of seven  $\alpha$  helices and a small region of  $\beta$  sheets as well as a smaller segment composed of three  $\alpha$  helices.<sup>102</sup> In addition, two putative catalytic glutamic acid residues (one on each segment) have been identified.<sup>102</sup> The structural elucidation of PBP2 provides a basis for

the design and development of new antibacterial agents to combat the rise of antibiotic-resistant bacteria.

With respect to substrate binding, nucleotide binding has currently been observed on the N-terminal domain of GT-A enzymes and the C-terminal domain of GT-B enzymes, with acceptors binding on the opposite domains in both cases. Given the inherent “symmetry” of both GT-A and GT-B folds, it remains possible that some glycosyltransferases yet to be discovered may bind the nucleotide donor and acceptor in “reversed” domains.<sup>92</sup> Of notable importance is the observation that these two folds are not mechanistically correlated and thus do not determine the stereochemical outcome of catalysis.

By analogy to glycosidases, Henrissat and coworkers have also proposed the grouping on glycosyltransferase families into clans based on similarities in fold, catalytic machinery, and molecular mechanism.<sup>92</sup> Two clans representing the inverting and retaining mechanisms of glycosyltransferases (*vide infra*) have been identified for each structural superfamily.

The terms superfamily (or fold), clan, family, and subfamily are frequently used to assign increasingly convergent levels of relatedness between glycosyltransferase enzymes. A complete explanation of this hierarchical classification system has been published,<sup>92</sup> and the CAZy database is continuously updated to reflect the superfamily, clan, and family of each enzyme as more information becomes available.<sup>d</sup>

---

<sup>d</sup> Carbohydrate-Active Enzymes Database, <http://afmb.cnrs-mrs.fr/CAZY/> (Accessed: 26/03/07)

### **1.4.3. Enzymatic Mechanisms**

Although a significant body of information is available describing mechanistic strategies used in glycosidase catalysis,<sup>104,105,106</sup> investigations into the catalytic mechanisms of glycosyltransferases have lagged far behind. This is mainly attributed to technical difficulties involved in obtaining catalytically active forms of these elusive, often membrane-associated, enzymes in sufficient quantities for structural and mechanistic investigations. Recent advances in recombinant DNA technologies have largely overcome these problems, and, as a result, more than 100 crystal structures have been described for proteins corresponding to more than two dozen glycosyltransferases, many of them in the last 2-3 years.<sup>93</sup>

From a mechanistic standpoint, glycosyltransferases can be classified according to the relative stereochemistries of reaction substrates and products as either inverting or retaining enzymes. The catalytic machinery of these two mechanistic classes of glycosyltransferases will be described in Sections 1.4.3.1 and 1.4.3.2.

#### **1.4.3.1. Inverting Glycosyltransferases**

Inverting glycosyltransferases are enzymes that catalyze glycosidic bond formation with net inversion of stereochemical configuration at the anomeric carbon of the product, as compared to the donor substrate. This mechanistic class of glycosyltransferase is most common in secondary metabolite biosynthesis.<sup>107</sup> Inverting glycosyltransferases are believed to catalyze reactions in a similar fashion to inverting glycosidases wherein catalysis involves two carboxylate residues.<sup>93,108</sup> One acidic residue acts as a general acid, providing leaving group assistance, while the other

carboxylate residue acts as a general base, facilitating nucleophilic attack via deprotonation of the incoming acceptor molecule. Structural and mechanistic studies clearly support an  $S_N2$  mechanism, which was originally proposed by Wong and coworkers in 1996.<sup>109</sup> In addition, a recent computational study by Kozmon and Tvaroška also supports an  $S_N2$  mechanism for inverting glycosyltransferases.<sup>110</sup> Inverting GT-A enzymes rely on divalent cations, typically  $Mn^{2+}$ , to play the role of acid catalyst, while inverting GT-B enzymes have significantly different active sites where no divalent cation appears to be involved and an acidic amino acid serves as the acid catalyst.<sup>93</sup> A representative example of a mechanism consistent with a GT-B inverting glycosyltransferase is shown in Figure 18.

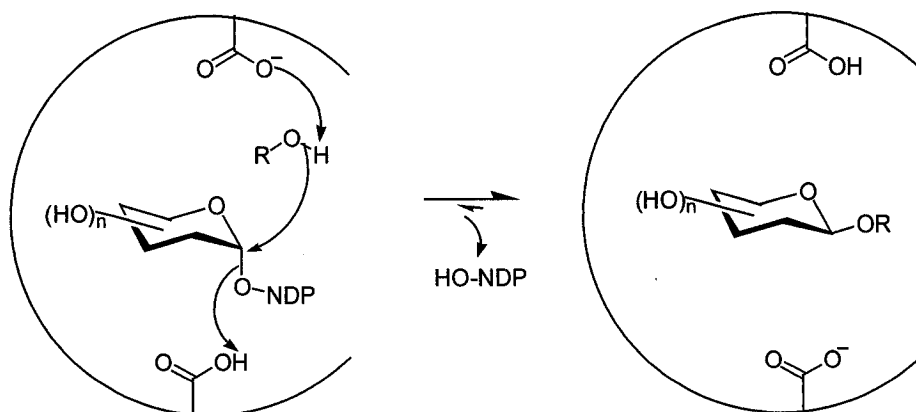


**Figure 18.** Representative mechanism of a GT-B inverting glycosyltransferase

In terms of substrate binding and product release, an ordered bi-bi mechanism has been proposed for both GT-A and GT-B inverting enzymes, although the order of binding and release is believed to be different for these two superfamilies.<sup>93</sup> With respect to GT-A enzymes, it has been proposed by Wong and coworkers that, in the case of the inverting family 10 human  $\alpha$ -(1 $\rightarrow$ 3)-fucosyltransferase V enzyme, the sugar nucleotide binds first, followed by the carbohydrate acceptor, and the desired product, an

oligosaccharide, is subsequently released first, followed by the nucleoside diphosphate leaving group.<sup>109</sup> This ordered bi-bi mechanistic sequence has also been suggested for other GT-A glycosyltransferases.<sup>111</sup> In contrast, for GT-B enzymes, the need for the aglycon to bind first followed by the sugar nucleotide donor has been demonstrated by Salas and coworkers with OleD, an inverting family 1 macrolide glycosyltransferase, through kinetic studies.<sup>112</sup> After sugar transfer, the nucleoside diphosphate was released first, followed by the newly glycosylated product. A similar binding motif has been suggested by Garavito and coworkers for the GT-B inverting family 1 glycosyltransferase known as GtfB, which transfers D-glucose to the vancomycin aglycon.<sup>113</sup> Attempts to observe a binary complex composed of UDP- $\alpha$ -D-glucose and GtfB were unsuccessful. This observation led the authors to suggest an ordered binding mechanism for GtfB substrates in which prior binding of the vancomycin aglycon is required to induce a conformational change in the enzyme, resulting in the creation of a functional subsite for UDP- $\alpha$ -D-glucose binding, although no data supporting this hypothesis has been published to date.

#### **1.4.3.2. Retaining Glycosyltransferases**

Retaining glycosyltransferases are enzymes that catalyze glycosidic bond formation with net retention of stereochemical configuration at the anomeric carbon of the product, as compared to the donor substrate. The mechanism for this type of glycosyltransferase was initially postulated to be analogous to that of glycosidases, which involves a double displacement reaction.<sup>108</sup> In this proposed mechanism, an acidic amino acid residue facilitates the acid-catalyzed leaving group departure of the nucleoside



diphosphate, which occurs simultaneously with nucleophilic attack by a second carboxylate to form a glycosyl-enzyme intermediate. In the second step, the first acidic amino acid residue functions as a general base to activate the incoming nucleophilic acceptor, which hydrolyzes the glycosyl-enzyme intermediate to produce the final product.<sup>105,114</sup> An example of this proposed double displacement mechanism is shown in Figure 19.

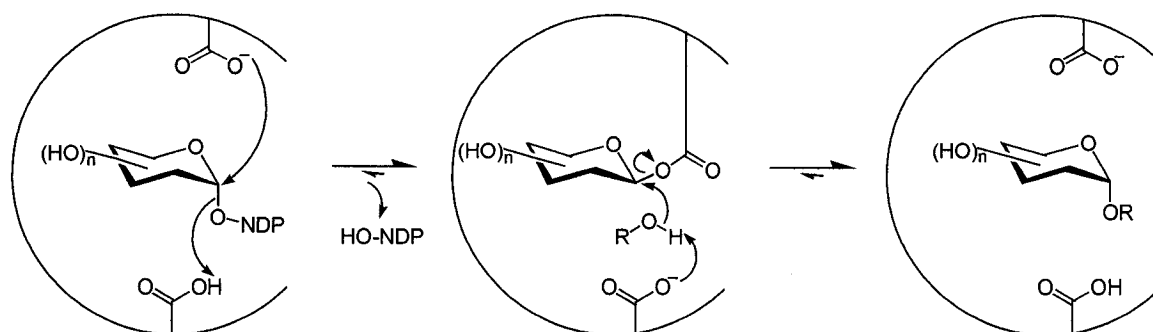


**Figure 19.** Proposed double displacement mechanism of a retaining glycosyltransferase

While it has been suggested that a divalent cation could play the role of Lewis acid and the nucleoside diphosphate leaving group could act as the catalytic base, the requirement for a catalytic nucleophile, properly positioned within the active site, still exists in the case of a double displacement retaining mechanism.<sup>108</sup> The first crystal structure of a retaining enzyme, a GT-A family 8  $\alpha$ -(1 $\rightarrow$ 4)-galactosyltransferase known as LgtC, was reported by Strynadka and coworkers in 2001.<sup>115</sup> The structure of this enzyme was solved in complex with  $Mn^{2+}$  and an unreactive sugar nucleotide, UDP- $\alpha$ -D-2FGal, in which the C-2 hydroxyl group of D-galactose was substituted by a fluorine atom. The inductive electron-withdrawing effect of the 2-deoxy-2-fluoro-substituent allowed this compound to act as an excellent enzyme inhibitor.<sup>115</sup> In addition, LgtC was also crystallized in complex with an acceptor analogue, 4'-deoxylactose, in which the

nucleophilic hydroxyl group at C-4' was replaced by a hydrogen atom. Interestingly, no  $\alpha$ -(1 $\rightarrow$ 4)-galactosyltransferase crystallographic evidence was found to support the presence of a catalytic nucleophile in the enzyme active site.<sup>115</sup>

In light of these results, Strynadka and coworkers proposed an alternative  $S_Ni$ -like retaining mechanism, which can also be described as a front-side  $S_N2$ -like reaction.<sup>115</sup> This mechanism involves a single transition state in which departure of the nucleoside diphosphate leaving group and incoming nucleophilic attack occur on the same face of the sugar. A representative example of the proposed  $S_Ni$ -like retaining mechanism is shown in Figure 20.

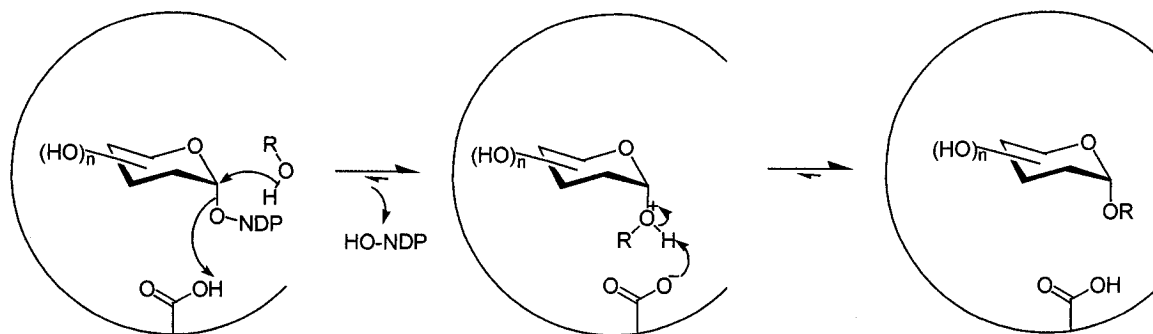


**Figure 20.** Proposed  $S_Ni$ -like mechanism of a retaining glycosyltransferase

Chemical precedence for this type of mechanism is derived from comprehensive conformational and kinetic studies conducted by Sinnott and Jencks on the solvolysis of D-glucose derivatives in various alcohols.<sup>116</sup> In addition, computational studies on LgtC recently confirmed that a one step  $S_Ni$ -like mechanism is energetically favourable.<sup>117</sup>  $S_Ni$ -like mechanisms have subsequently been proposed for several other retaining glycosyltransferases, including GT-B enzymes, based on a lack of defined catalytic nucleophile in their active sites.<sup>118,119,120</sup>

Also in 2001, a second crystal structure of a retaining  $\alpha$ -(1 $\rightarrow$ 3)-galactosyltransferase was reported by Gastinel and coworkers.<sup>121</sup> Interestingly, this enzyme belongs to the same family as LgtC and was crystallized in both the absence and presence of its UDP- $\alpha$ -D-galactose sugar nucleotide donor. In contrast to the  $S_Ni$ -like mechanism, Gastinel and coworkers proposed the formation of a glycosyl-enzyme intermediate based on crystallographic data, and suggested a double displacement mechanism for retaining glycosyltransferases. A specific glutamate residue, invariant in family 8 glycosyltransferases, was proposed as the catalytic nucleophile.<sup>121</sup> Moreover, it was suggested that another glutamate or aspartate residue might hydrolyze the glycosyl-enzyme intermediate in the second step of the double displacement mechanism, resulting in retention of anomeric stereochemistry.

In a more recent mechanistic twist, a catalytically relevant glycosyl-enzyme intermediate was observed with the Gln189Glu mutant of LgtC,<sup>122</sup> although the candidate catalytic nucleophile is quite far ( $\sim 9$  Å) from the anomeric reaction centre. Thus, a considerable conformational change would likely have to occur during catalysis for the candidate Asp190 residue to act as the catalytic nucleophile in a double displacement mechanism.<sup>108</sup>

The search for definitive evidence supporting the presence or lack thereof of a catalytic nucleophile in retaining glycosyltransferases continues. Only an increased number of crystal structures and/or a series of inspired mechanistic investigations will settle this debate. An improved understanding of glycosyltransferase catalysis will provide necessary insight for the rational design of effective inhibitors and the ability to evolve the substrate promiscuity of these ubiquitous biocatalysts.

#### **1.4.4. Substrate Promiscuity of Glycosyltransferases Involved in Natural Product Biosynthesis**

Glycosyltransferases involved in natural product biosynthesis are appealing enzymatic tools for drug discovery and development since they are responsible for decorating a structurally diverse array of aglycons with a large variety of biologically relevant sugar ligands. One perceived drawback of using enzymes in organic synthesis is that Nature has evolved enzymes to be substrate specific.<sup>123</sup> This has largely been proven false in the case of glycosyltransferases involved in secondary metabolite biosynthesis, as many examples now exist illustrating the tremendous substrate promiscuity of this class of biocatalyst with respect to both sugar nucleotide donor and acceptor substrates.<sup>79</sup>

The majority of substrate promiscuity studies have focused on GT-A enzymes, which are primarily responsible for oligosaccharide biosynthesis.<sup>87</sup> While GT-A enzymes are proving useful in preparing many biologically relevant oligosaccharides, the glycosylation of natural products is of particular interest in our laboratory, and thus this section will focus on glycosyltransferases involved in natural product biosynthesis. These enzymes are largely found in family 1 of the GT-B superfamily, which includes most prokaryotic enzymes responsible for glycosylating secondary metabolites as well as prokaryotic enzymes involved in primary metabolic pathways such as cell wall biosynthesis and various other insect and plant glycosyltransferases.<sup>87</sup>

Many wild-type GT-B glycosyltransferases involved in secondary metabolite biosynthesis have been shown to have surprisingly relaxed substrate specificities, although a few examples of less promiscuous enzymes have been reported.<sup>124,125</sup> This has allowed the efficient preparation of structurally diverse natural product libraries. Probably the best-characterized GT-B enzymes thus far are those involved in vancomycin

(3) biosynthesis as the crystal structures of both inverting family 1 glycosyltransferases have been solved.<sup>113,126</sup> In particular, GtfE, the vancomycin glycosyltransferase responsible for transferring D-glucose to the vancomycin aglycon, has demonstrated remarkable *in vitro* substrate promiscuity with respect to its sugar nucleotide donor as discussed in Section 1.3.3.<sup>80,81</sup>

In another example, Rohr and coworkers have demonstrated the *in vivo* sugar nucleotide promiscuity of ElmGT, a family 1 inverting glycosyltransferase responsible for the transfer of L-rhamnose to an intermediate in the elloramycin A biosynthetic pathway named 8-demethyltetracenomycin C (**27**), resulting in the formation of L-rhamnosyltetracenomycin C (**28**) (Figure 21).<sup>127</sup> Interestingly, ElmGT was able to accept a diverse array of both L- and D-configured dideoxysugars such as L-digitoxose, L-olivose, and D-olivose, and even D-glucose, a non-deoxygenated sugar in a <sup>4</sup>C<sub>1</sub> chair conformation, producing derivatives **29-32**, respectively. Surprisingly, ElmGT also demonstrated its ability to transfer a disaccharide consisting of two D-olivose units to **27**, producing derivative **33**.

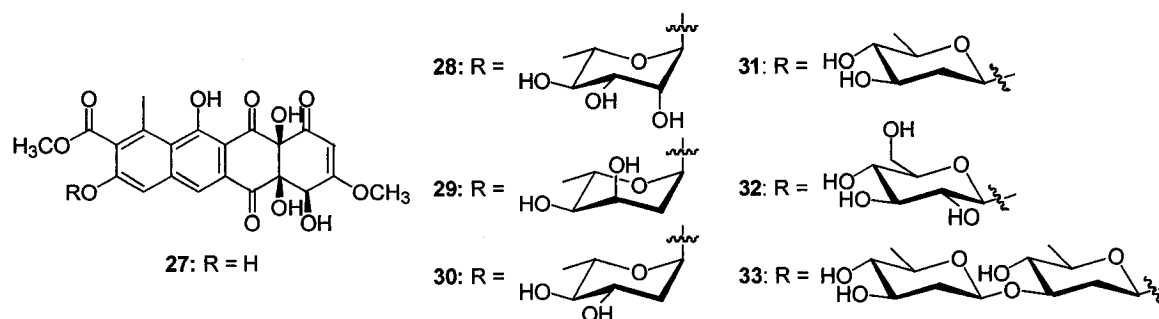


**Figure 21.** Structures of 8-demethyltetracenomycin C (**27**), L-rhamnosyltetracenomycin C (**28**), and glycosylated derivatives **29-33**

In addition to demonstrating sugar nucleotide promiscuity, GT-B glycosyltransferases are often promiscuous with respect to acceptor substrates. One *in*

*vitro* study illustrating this type of promiscuity was that of Walsh and coworkers in 2003 with NovM, a family 1 inverting glycosyltransferase responsible for attaching L-noviose (**34**), a 5,5-dimethylhexose, to novobiocic acid, an intermediate in the biosynthetic pathway of the aminocoumarin antibiotic novobiocin, forming desmethyldescarbamoyl novobiocin (**35**) (Figure 22).<sup>128</sup> Interestingly, NovM demonstrated relaxed specificity with a series of structurally variant coumarin aglycons as well as several simple phenols (**36-40**), providing impetus to further study the promiscuity of NovM with a variety of planar scaffolds.

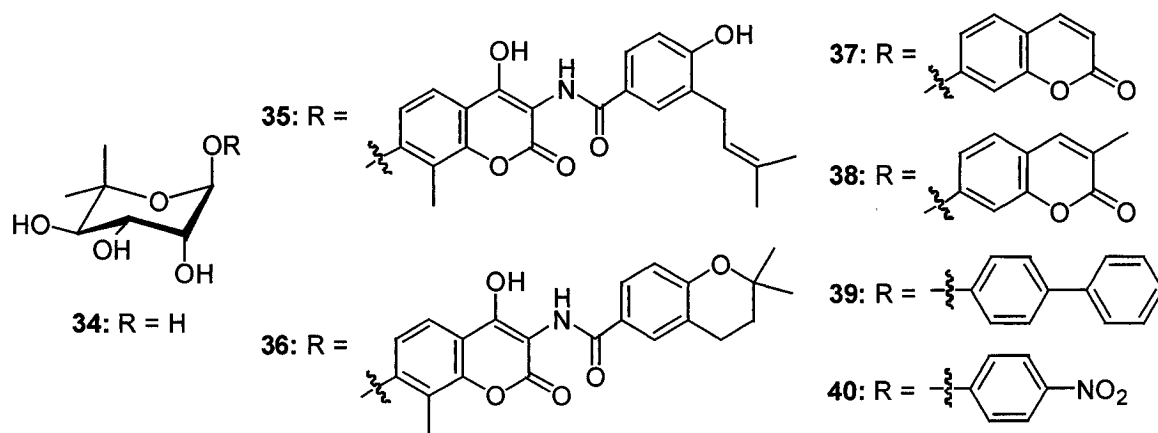


**Figure 22.** Structures of α-L-noviose (**34**), desmethyldescarbamoyl novobiocin (**35**) and derivatives **36-40**

A second GT-B glycosyltransferase displaying significant aglycon promiscuity is VinC, a polyketide-derived family 1 inverting enzyme responsible for the transfer of D-vicenisamine (**41**) to the vicenistatin aglycon in the last step of vicenistatin (**42**) biosynthesis (Figure 23).<sup>129</sup> Through *in vitro* studies, this glycosyltransferase proved useful in generating a structurally diverse library of vicenistatin derivatives with a variety of hydrophobic aglycon scaffolds (**43-45**). Of particular interest was the successful use of computational modelling studies to predict VinC promiscuity with a high degree of accuracy.<sup>129</sup>

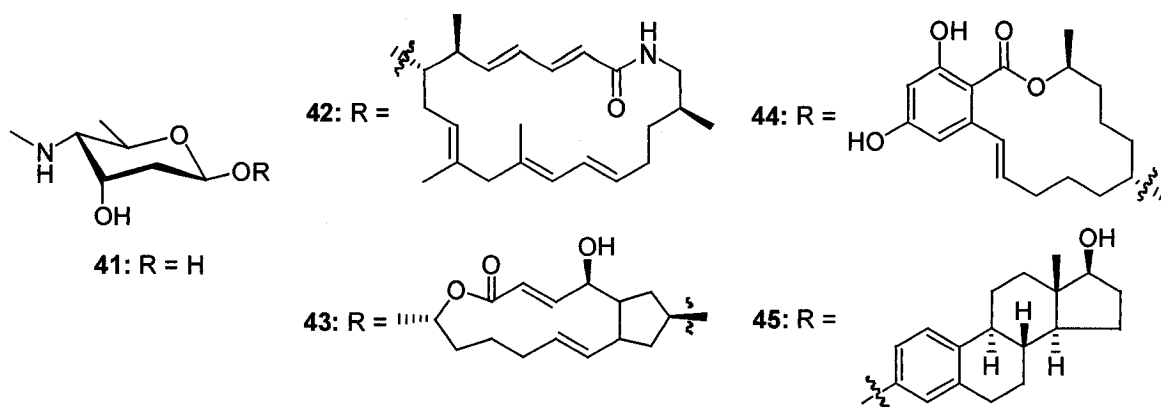


**Figure 23.** Structures of  $\beta$ -D-vicenisamine (41), vicenistatin (42), and representative derivatives 43-45

As evidenced by the aforementioned examples, GT-B enzymes are effective tools for preparing novel natural products for biological testing. The recent increase in glycosyltransferase crystal structures has resulted in a renewed interest in enzyme engineering and computational modelling studies.<sup>130</sup> In addition, the first high-throughput screening methodology has recently been developed using the GT-A family 42 sialyltransferase CstII for the directed evolution of glycosyltransferases.<sup>131</sup> Efforts to engineer and evolve GT-B glycosyltransferases are currently underway in numerous laboratories and this field will likely experience tremendous growth in the near future.

#### 1.4.5. JadS Glycosyltransferase

The putative JadS glycosyltransferase is believed to be responsible for the transfer of L-digitoxose from dTDP- $\beta$ -L-digitoxose (46) to the jadomycin B aglycon (7), resulting in the formation of the angucycline antibiotic jadomycin B (8) and the release of deoxythymidine diphosphate (dTDP) (47) (Figure 24).<sup>132</sup>

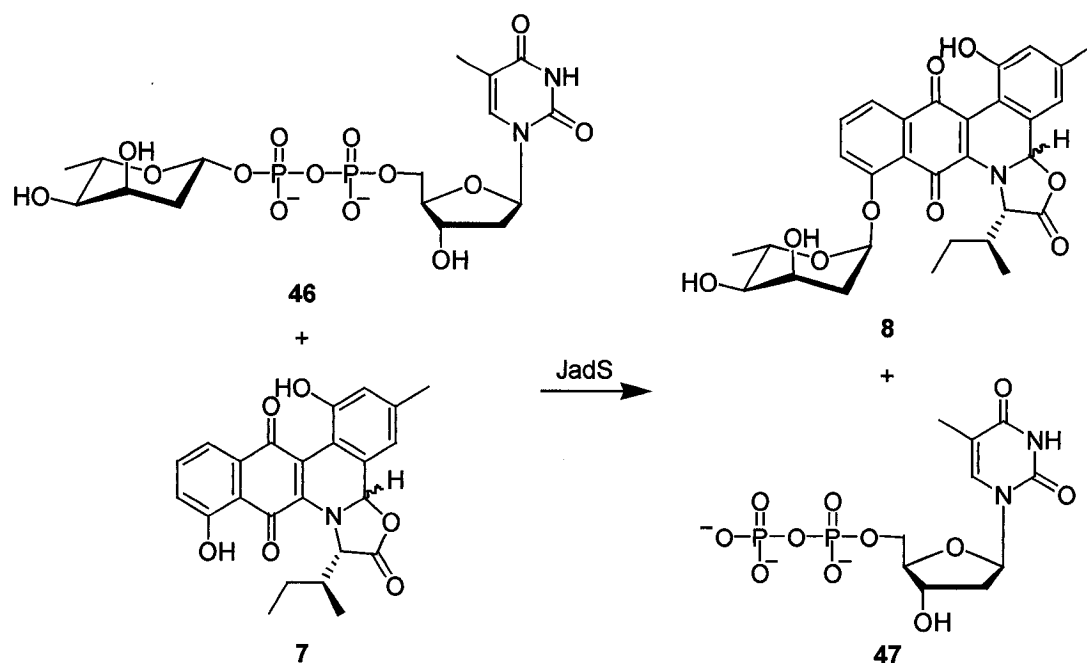


**Figure 24.** One of the last steps in the biosynthesis of jadomycin B (8)

The genes encoding the biosynthesis and subsequent transfer of L-digitoxose to the jadomycin B aglycon were identified in 2002 by Vining and coworkers.<sup>132</sup> Through gene disruption experiments and sequence comparisons with other dideoxysugar biosynthetic gene assemblies, genes *jadXOPQSTUV* were identified as being responsible for L-digitoxose biosynthesis and attachment.

The deduced amino acid sequence of the *jadS* gene displays significant sequence homology with other GT-B glycosyltransferases.<sup>132</sup> The closest sequence resemblance (44% identical amino acids) is to ElmGT, a family 1 inverting glycosyltransferase from *Streptomyces olivaceus* used in the biosynthesis of the antitumour agent elloramycin. The *jadS* gene sequence also resembles those of other GT-B glycosyltransferases from *Streptomyces* species used in the biosynthesis of secondary metabolites such as nogalamycin, landomycin, urdamycin, and daunorubicin (35-42% identical amino acids).



Based on resemblance to the aforementioned enzymes, JadS has tentatively been classified as a GT-B family 1 inverting glycosyltransferase. Both N-terminal and C-terminal His<sub>6</sub>-tagged constructs of JadS have recently been cloned, expressed, and purified using affinity chromatography in the Jakeman laboratory.<sup>133</sup>

## **1.5. Preparation of Sugar Nucleotides**

In order to explore the use of GT-B glycosyltransferases to prepare novel glycosylated natural products for potential therapeutic use, access to sugar nucleotides is required. A major limitation to probing the substrate promiscuity and potential application of these biocatalysts to the drug discovery and development process has been poor access to these enzyme substrates. Classical methods used to prepare sugar nucleotides make use of chemical synthesis, although enzymatic methods for the preparation of these substrates have recently been emerging. Both chemical and enzymatic approaches to synthesizing sugar nucleotides will be discussed in Sections 1.5.1 and 1.5.2, respectively.

### **1.5.1. Chemical Synthesis**

Although the enzymatic synthesis of sugar nucleotides is an emerging trend, chemical synthesis remains a robust and versatile method to prepare these enzyme substrates. There are two principal disconnection strategies used in the chemical synthesis of sugar nucleotides (Figure 25). The first method involves the coupling of a sugar-1-phosphate with an activated nucleoside 5'-monophosphate ester.<sup>134</sup> Although some sugar-1-phosphates are commercially available, others must be prepared via

multistep chemical syntheses and the nucleoside 5'-monophosphate ester is frequently activated as a morpholidate (**48**)<sup>135,136</sup> or an imidazolide (**49**)<sup>137,138</sup> (Figure 25). Although the addition of tetrazole as a catalyst has been shown to improve reaction times,<sup>139</sup> these coupling reactions often take several days and frequently result in only low to moderate yields.<sup>140,141</sup>

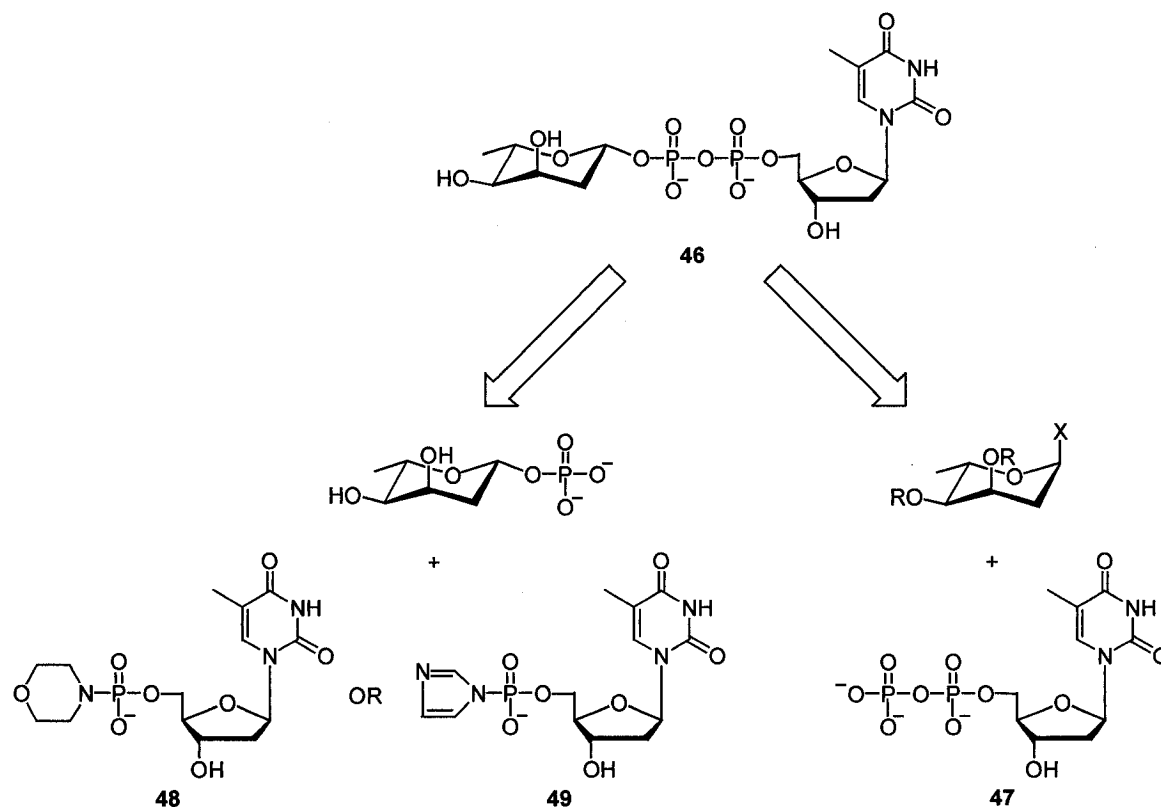


**Figure 25.** Two strategies for preparing sugar nucleotides using dTDP-β-L-digitoxose (**46**) as an example

In attempts to improve the synthesis of sugar nucleotides, the direct coupling of various glycosyl donors with nucleoside 5'-diphosphates has also been explored (Figure 25). Examples of glycosyl donors used in this approach include benzylated glycosyl bromides,<sup>142</sup> trimethylsilylated glycosyl iodides,<sup>143</sup> 2-(1,2-*trans*-glycopyranosyloxy)-3-methoxypyridines (MOP glycosides),<sup>144</sup> and triethylsilylated and benzylated epoxides.<sup>145,146</sup> These methodologies have generally resulted in similarly moderate yields

in the key coupling step, but eliminate the need for sugar-1-phosphates, using instead more easily accessible glycosyl donors. The major drawback of direct coupling approaches is the general lack of stereoselectivity obtained in the coupling of glycosyl donors with nucleoside 5'-diphosphates. In the majority of cases  $\alpha:\beta$  selectivity is approximately 1:1 and, even in cases where couplings are more selective, it is difficult to predict which diastereomer will predominate. It has been suggested that  $\alpha:\beta$  diastereomeric mixtures of sugar nucleotides are not problematic since glycosyltransferases are believed to select for the required diastereomer and not be significantly inhibited by sugar nucleotides of opposite anomeric configuration.<sup>142,143</sup> This being said, stereoselectivity is clearly advantageous in improving the yields of desired sugar nucleotide diastereomers, and facilitates kinetic studies without any possibility of interference from unwanted diastereomers.

### 1.5.2. Enzymatic Synthesis

Nature's answer to the question of sugar nucleotide synthesis involves sugar nucleotidyltransferase enzymes, also known as sugar pyrophosphorylases. These enzymes catalyze reactions in which a nucleophilic sugar-1-phosphate attacks the  $\alpha$ -phosphorus atom of a nucleoside 5'-triphosphate, resulting in the formation of a sugar nucleoside diphosphate and the release of pyrophosphate.

With respect to nucleotidyltransferase catalysis, two mechanistic hypotheses have been proposed based on kinetic data. The first proposed catalytic mechanism involves a ping-pong bi-bi mechanism where one substrate binds and one product is released prior to the binding of the second substrate and release of the second product.<sup>147</sup>

This mechanism requires the availability of a nucleophilic amino acid residue appropriately positioned in the active site to facilitate the formation of an enzyme-substrate covalent intermediate. The second proposed catalytic mechanism involves an ordered bi-bi mechanism in which both substrates must bind in a specific order and, after catalysis occurs, products are released in a defined sequence. Evidence supporting this alternative mechanism was reported in initial nucleotidyltransferase studies several decades ago.<sup>148,149,150</sup> Further kinetic studies on numerous nucleotidyltransferases in addition to crystal structure analysis has now established that most of these enzymes function via the second proposed ordered bi-bi catalytic mechanism.<sup>151,152,153</sup> Catalysis via this mechanism is analogous to an  $S_N2$ -type reaction since nucleophilic attack on one face of the  $\alpha$ -phosphorus atom occurs simultaneously with cleavage of the phosphodiester bond on the opposite face (Figure 26).<sup>152,153</sup>

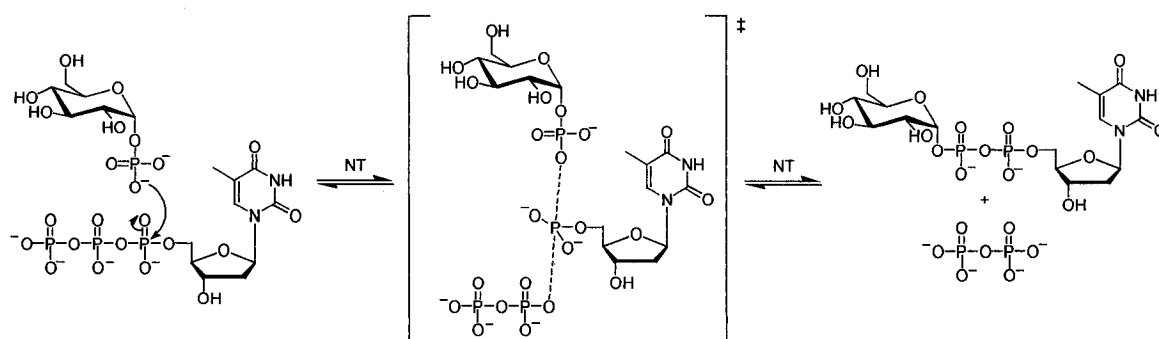


**Figure 26.** Representative mechanism of nucleotidyltransferase catalysis

With respect to the order of substrate binding and product release, in general, the nucleoside 5'-triphosphate first binds to the active site followed by binding of the sugar-1-phosphate, creating a ternary transition state. After catalysis occurs, the transition state collapses with the departure of pyrophosphate and the subsequent release of the desired sugar nucleoside diphosphate product.<sup>151,153</sup>

Interestingly, the analysis of nucleotidylyltransferase folds from solved crystal structures has revealed similarities to GT-A and GT-B glycosyltransferase folds.<sup>93,154</sup> Although no formal classification system analogous to glycosidases and glycosyltransferases currently exists for nucleotidylyltransferases, these ubiquitous enzymes have been discovered in eukaryotes, prokaryotes, and, most recently, archaea.<sup>151</sup>

Nucleotidylyltransferases are increasingly being used as an attractive alternative to chemical synthesis to prepare sugar nucleotides for glycorandomization and glycobiology studies. In order for these enzymes to be useful in generating libraries of sugar nucleotides, they must be substrate flexible, especially with respect to sugar-1-phosphates. Although some minor sugar-1-phosphate changes have been shown to negatively impact product yields,<sup>155</sup> nucleotidylyltransferases have, in general, demonstrated significant substrate promiscuity.<sup>151,156,157,158</sup> More detailed substrate promiscuity comparisons will be made in Section 2.4.1.

Several recent advances in this field have made the study and use of nucleotidylyltransferases more efficient. In order to produce structurally diverse libraries of sugar nucleotides using this enzymatic strategy, access to a wide variety of sugar-1-phosphates is required. As previously discussed, although some sugar-1-phosphates are commercially available, other sugar-1-phosphates, particularly deoxysugar-1-phosphates important for glycorandomization studies, are traditionally obtained via multistep chemical synthesis. The recent development of a substrate flexible sugar kinase via structure-based engineering has facilitated more efficient *in vitro* glycorandomization studies.<sup>159</sup> Site-directed mutagenesis has also been successfully applied to

nucleotidyltransferases, further expanding the sugar-1-phosphate promiscuity of these enzymes.<sup>160</sup> Finally, the recent development of an ESI-MS-based nucleotidyltransferase assay enables the expeditious determination of kinetic parameters and inhibition constants, enabling the efficient characterization of these biocatalysts with both natural and analogue substrates.<sup>161</sup> The development of additional techniques to aid in the efficient preparation of sugar nucleotides will continue to advance the study of glycosyltransferases, shedding more light on Nature's method of glycosylation.

## 1.6. Project Objectives

In order to first confirm the *in vitro* enzymatic activity of JadS and develop suitable assay conditions for unnatural substrates, catalysis with natural enzyme substrates, the jadomycin B aglycon (7) and dTDP- $\beta$ -L-digitoxose (46), is required. Furthermore, to study the substrate promiscuity of the JadS glycosyltransferase, and thus its potential for use in diversifying the carbohydrate functionalities attached to the jadomycin family of antibiotics, access to a library of structurally diverse analogue sugar nucleotides is also necessary. The following project objectives aimed to accomplish these goals:

- (1) Chemically synthesize the natural 2,6-dideoxysugar nucleotide substrate of JadS, dTDP- $\beta$ -L-digitoxose (46).
- (2) Explore various synthetic strategies to chemically prepare analogue sugar nucleotides from commercially available and synthetically prepared monosaccharides (51-56, Figure 27).
- (3) Investigate the efficiency of different sugar nucleotide purification strategies.

- (4) Evaluate the feasibility of enzymatically preparing analogue sugar nucleotides via probing the substrate promiscuity of several sugar nucleotidyltransferases.
- (5) Demonstrate JadS glycosyltransferase catalysis using dTDP- $\beta$ -L-digitoxose (**46**) and probe the substrate promiscuity of this enzyme using analogue sugar nucleotides.

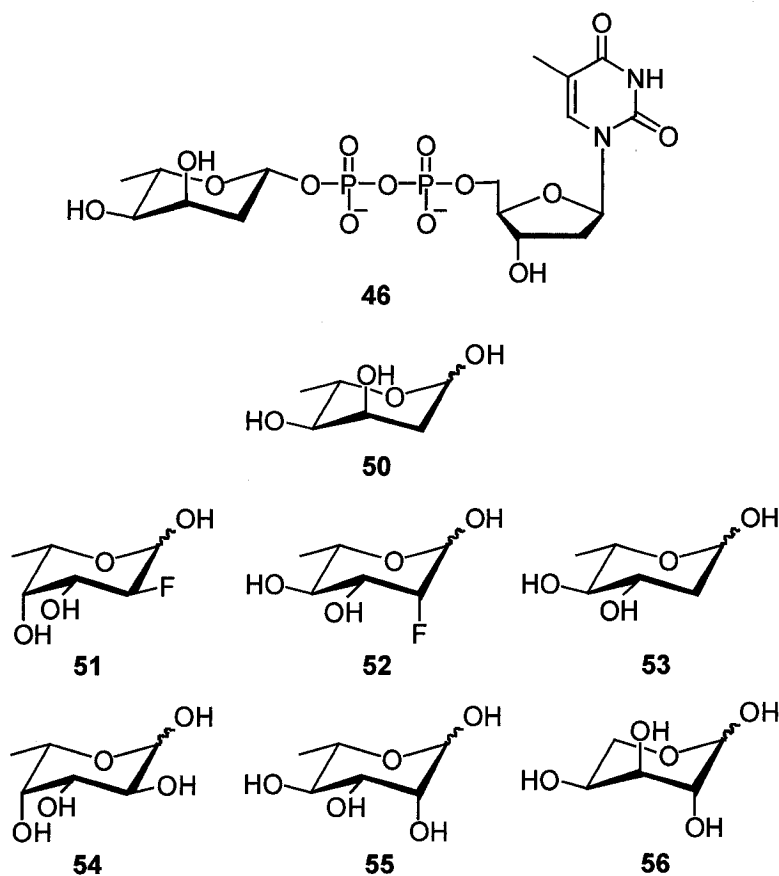


**Figure 27.** Structures of dTDP- $\beta$ -L-digitoxose (**46**), L-digitoxose (**50**) and proposed monosaccharide analogues **51-56**

## Chapter 2. Results and Discussion

---

### 2.1. Synthesis of L-Digitoxose

The 2,6-dideoxysugar L-digitoxose (**50**) is a component of numerous natural products of bacterial origin including both polyketide-derived antitumour antibiotics<sup>162,163</sup> and antifungal antibiotics<sup>164</sup> in addition to jadomycin B (**8**). Interestingly, D-digitoxose (**57**) (Figure 28) is a well-known constituent of cardiac<sup>165</sup> and plant<sup>166,167</sup> steroidal glycosides.

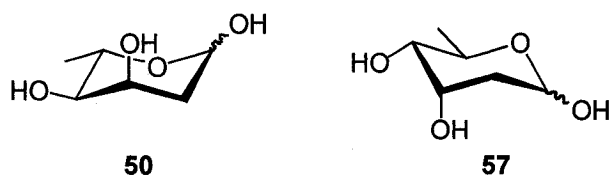


**Figure 28.** Structures of L-digitoxose (**50**) and D-digitoxose (**57**) enantiomers

As a result of their medicinal importance, there is significant interest in developing novel synthetic routes for the efficient preparation of deoxysugars, particularly 2,6-, 3,6-, and 4,6-dideoxyhexoses.<sup>168</sup> With respect to L-digitoxose (**50**), a number of syntheses based on significantly different strategies have been described.<sup>169,170,171,172,173,174</sup> A few of these routes rely on chiral synthon starting materials and numerous stereoselective reactions.<sup>169,170,171</sup> The disadvantage of this approach is that these strategies typically involve numerous diastereomeric separations and usually result in low overall yields.<sup>170,171</sup> Nevertheless, synthetic routes involving non-carbohydrate precursors can prove useful in facilitating the preparation of libraries of structurally related monosaccharides.<sup>169</sup> Other syntheses of L-digitoxose (**50**) originate from carbohydrate precursors, but typically also involve a large number of steps and



overall low yields.<sup>172,173</sup> To facilitate the project objective of preparing 2-deoxy-2-fluoro- and 2,6-dideoxysugar analogues of L-digitoxose (**50**), a synthetic strategy originating from a carbohydrate precursor was determined to be the best option. Of the synthetic routes previously described, the methodology of Brimacombe and coworkers was chosen due to its reasonable number of synthetic steps (six), its commercially available monosaccharide origin, (L-rhamnose (**55**)), and the opportunity to prepare several interesting analogues from synthetic intermediates.<sup>174</sup> A variation of this methodology was investigated and is described in Section 2.1.1.

#### 2.1.1. Method A

The key step in the synthetic strategy of Brimacombe and coworkers for preparing L-digitoxose (**50**) involves the reaction of methyl 2,3-*O*-benzylidene-4-*O*-(2-methoxyethoxymethyl)- $\alpha$ -L-rhamnopyranoside (**58**) or methyl 2,3-*O*-benzylidene-4-*O*-(2-methoxymethyl)- $\alpha$ -L-rhamnopyranoside (**59**) with *n*-butyllithium (*n*-BuLi) at -30 °C or below in THF (Figure 29).<sup>174</sup> This elimination reaction, first described by Klemer and Rodemeyer in 1974,<sup>175</sup> successfully produced desired 2-deoxy-3-ketosugars **60** and **61** in 41% and 38% yield, respectively, after careful silica gel chromatography in the hands of Brimacombe and coworkers.<sup>174</sup> In addition to these protected  $\alpha$ -L-rhamnopyranosides, methyl 2,3-*O*-benzylidene-4-*O*-methyl- $\alpha$ -L-rhamnopyranoside (**62**) was also previously used by Clode and coworkers to produce 2-deoxy-3-ketosugar **63** in 40% yield upon reaction with *n*-butyllithium at -30 °C or below in THF.<sup>176</sup> Interestingly, similarly protected 4-OH (**64**) and 4-*O*-benzyl (**65**) derivatives produced only complex mixtures of products under the aforementioned reaction conditions (Figure 29).<sup>176</sup>

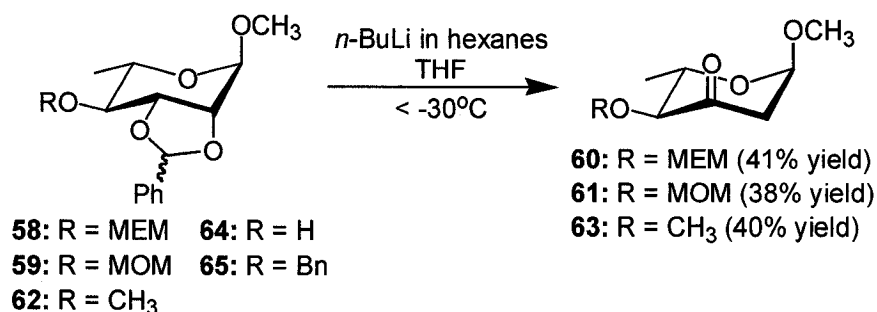


**Figure 29.** Klemm-Rodemeyer elimination reaction results reported by Brimacombe<sup>174</sup> and Clode<sup>176</sup>

In light of these results, fully protected  $\alpha$ -L-rhamnopyranosides **58**, **59**, and **62** were prepared to establish the efficacy of the Klemm-Rodemeyer elimination reaction in synthesizing 2-deoxy-3-ketosugars **60**, **61**, and **63**, respectively (Figure 30).

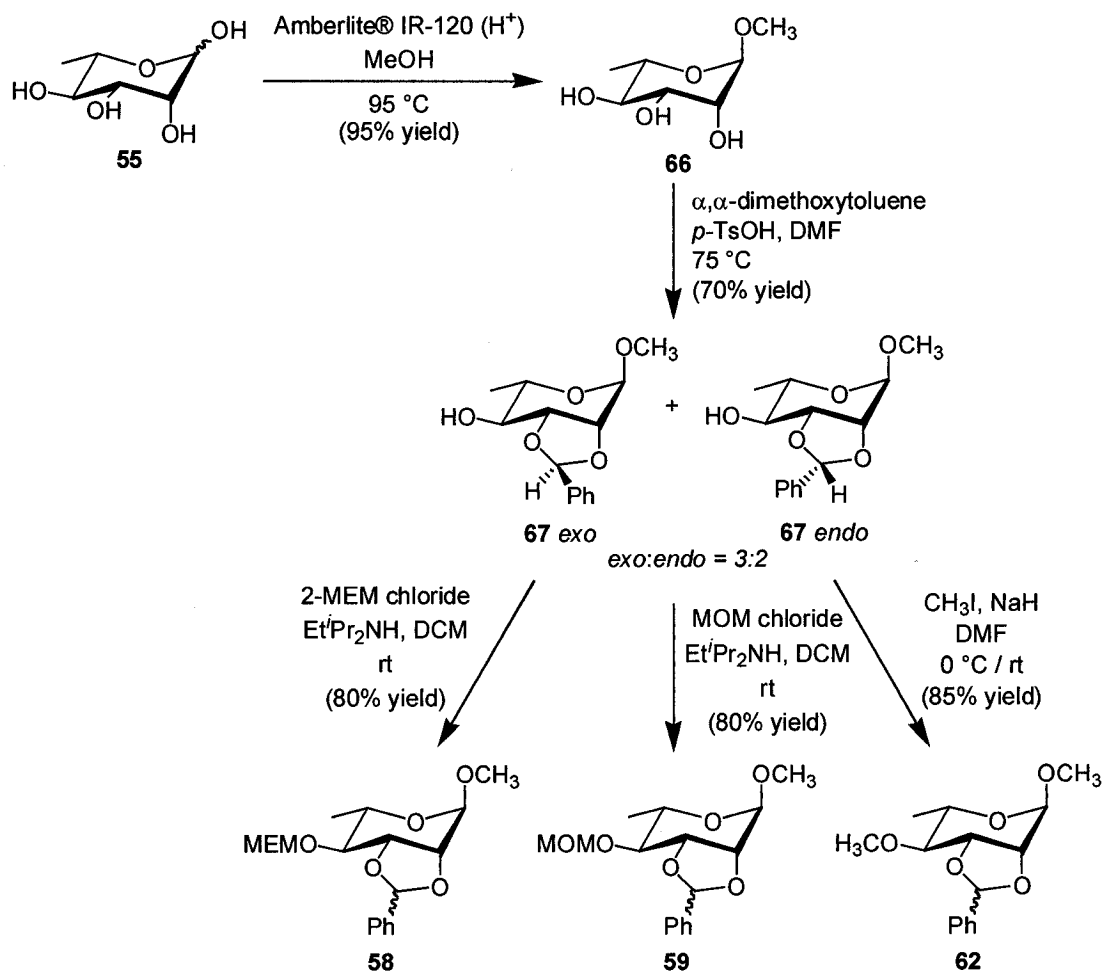


**Figure 30.** Klemm-Rodemeyer elimination reaction protecting group strategies

The first reaction in this protecting group sequence, common to all three protected  $\alpha$ -L-rhamnopyranoside derivatives, was a classical Fischer glycosidation (or glycosylation). L-Rhamnose (**55**) was easily converted to methyl glycoside **66** using Amberlite® IR-120 ( $H^+$ ) ion exchange resin in refluxing methanol,<sup>176</sup> affording methyl  $\alpha$ -L-rhamnopyranoside (**66**) in 95% yield as a crude yellow syrup that resisted crystallization and was not further purified. Secondly, *cis* hydroxyl groups at C-2 and C-3 of **66** were protected with a benzylidene acetal using  $\alpha,\alpha$ -dimethoxytoluene and *p*-toluenesulfonic acid in DMF.<sup>176</sup> Using this procedure, also common in the preparation of **58**, **59**, and **62**, methyl 2,3-*O*-benzylidene- $\alpha$ -L-rhamnopyranoside (**67**) was prepared in 70% yield as a diastereomeric colourless syrup after silica gel chromatography (3:2 *exo:endo*). In the last step of the synthesis of fully protected  $\alpha$ -L-rhamnopyranosides **58**, **59**, and **62**, the remaining free hydroxyl group at C-4 was protected with three different ether functionalities. Reaction of **67** with 2-methoxyethoxymethyl (MEM) chloride and ethyldiisopropylamine in DCM<sup>174</sup> produced **58** in 80% yield as a white solid after silica gel chromatography while reaction of **67** with methoxymethyl (MOM) chloride and ethyldiisopropylamine in DCM<sup>174</sup> produced **59**, similarly in 80% yield as a colourless syrup after silica gel chromatography. Finally, reaction of **67** with methyl iodide and sodium hydride in DMF<sup>177</sup> easily afforded **62** in 85% yield as a colourless syrup.

Suitably protected  $\alpha$ -L-rhamnopyranosides **58**, **59**, and **62** were subsequently used as starting materials in Klemm-Rodemeyer-type elimination reactions in attempts to improve the yields of desired 2-deoxy-3-ketosugars **60**, **61**, and **63**.

From a mechanistic standpoint, the Klemm-Rodemeyer elimination reaction is based on the preferential abstraction of the quasi-axial hydrogen atom attached to C-3 of

the carbohydrate ring, which is also part of the 1,3-dioxolane ring (Figure 31).<sup>178</sup> This abstraction results in the elimination of the benzylidene acetal as benzaldehyde and the concomitant formation of a 2-deoxy-3-ketosugar.

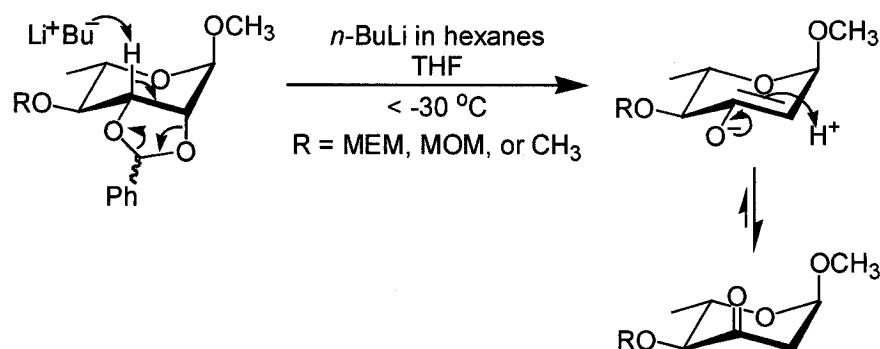


**Figure 31.** Mechanism of the Klemm-Rodemeyer elimination reaction

Klemm and Rodemeyer first observed this reaction using 2,3:4,6-di-*O*-benzylidene- $\alpha$ -D-mannopyranoside (**68**) and 2 equiv of *n*-butyllithium in THF at  $-30\text{ }^\circ\text{C}$ .<sup>175</sup> Under these conditions, the regiospecific synthesis of 2-deoxy-3-ketosugar **69** was observed with only a trace of 2,3-unsaturated byproduct **70** (Figure 32). This elimination reaction was subsequently used on a large scale (20 g) to synthesize the bioactive 2,6-dideoxysugar L-daunosamine<sup>179</sup> and related sugars<sup>180</sup> in high yield, although attempts by Horton and Weckerle to repeat the original result of Klemm and Rodemeyer resulted in complex mixtures of products, illustrating difficulties with the reproducibility of this reaction.<sup>178</sup>

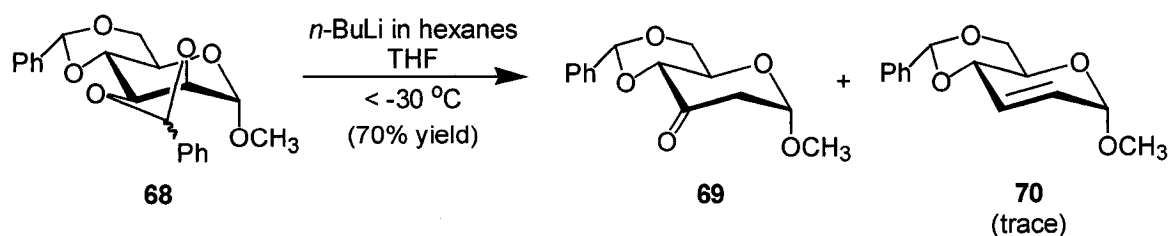


**Figure 32.** Synthesis of methyl 4,6-*O*-benzylidene- $\alpha$ -D-erythro-hexopyranosid-3-ulose (**69**) by Klemm and Rodemeyer<sup>175</sup>

Although Klemer and Rodemeyer were able to obtain only a trace of 2,3-unsaturated product **70**, it is important to note that three distinct possibilities exist for proton abstraction, resulting in different elimination products (Figure 33). Abstraction of a proton from C-2 of the 1,3-dioxolane ring results in the preparation of an alkene and the loss of a benzoate anion. Alternatively, abstraction of a proton from C-4 of the 1,3-dioxolane ring results in the production of an enolate, which subsequently tautomerizes to a C-4 ketone, and the release of benzaldehyde. Similarly, abstraction of a proton from C-5 of the 1,3-dioxolane ring results in the production of an enolate, which is converted to a C-5 ketone upon tautomerization, and the release of benzaldehyde. Horton and Weckerle have published an interesting summary of Klemer-Rodemeyer reactions with differing regiochemical outcomes for a variety of protected monosaccharides.<sup>178</sup> Their studies suggest that the regiochemical outcome of Klemer-Rodemeyer elimination reactions is often difficult to predict, especially in cases involving carbohydrates with conformationally flexible or distorted chair conformations.

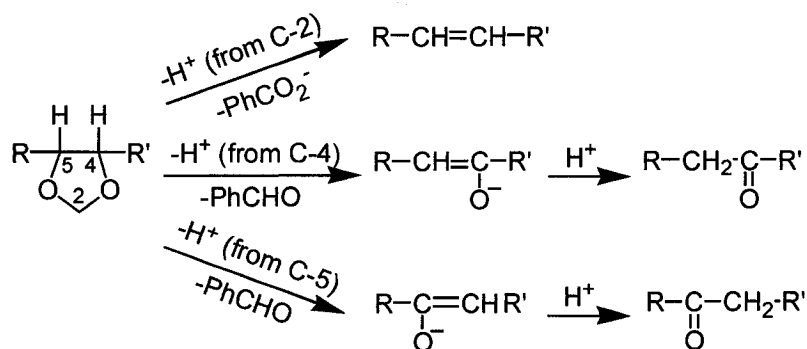


**Figure 33.** Possible Klemer-Rodemeyer reaction proton abstractions and corresponding products<sup>178</sup>

It is interesting to note that chemical precedence exists for selective base-induced elimination reactions involving 1,3-dioxolane rings in other types of organic molecules.<sup>181,182,183</sup> One of the first examples of this type of chemistry was reported in

1964 by Ramaswami and coworkers who discovered that 2-phenyl-1,3-dioxolane (**71**) rapidly evolved a gas on treatment with phenyllithium in ether at room temperature, which was shown to be ethylene (**72**) by mass spectrometry (Figure 34).<sup>184</sup>

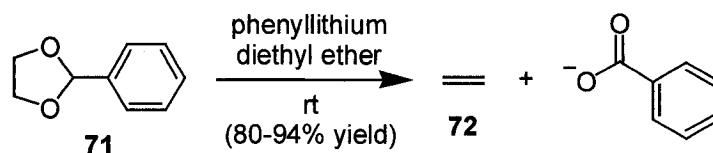


**Figure 34.** Base-induced elimination of ethylene (**72**) from 2-phenyl-1,3-dioxolane (**71**)<sup>184</sup>

Initial Klemmer-Rodemeyer-type experiments were conducted using 4-*O*-MEM-protected derivative **58**, which was previously reported to give a 41% yield of 2-deoxy-3-ketosugar **60** using 6 equiv of *n*-butyllithium in THF while keeping the internal reaction temperature below -30 °C for 1 h.<sup>174</sup> In my experience the highest isolated yield of 2-deoxy-3-ketosugar **60** achieved, using **58** as a starting material and similar reaction conditions as above, was 22% (Table 1, entry 1). The use of 4-*O*-MOM-protected derivative **59** to produce 2-deoxy-3-ketosugar **61** resulted in similarly low yields (16% at best) (Table 1, entry 2) and proved even more difficult to purify.

**Table 1.** Selected results from varying conditions of Klemmer-Rodemeyer elimination reaction with **58**, **59**, and **62**

entry	4- <i>O</i> -R group (compound)	base	equiv of base	temperature (°C)	time (h)	2-deoxy-3-ketosugar isolated yield (%)
1	MEM ( <b>58</b> )	<i>n</i> -BuLi	6	-40 to -30	1	22
2	MOM ( <b>59</b> )	<i>n</i> -BuLi	6	-40 to -30	1	16
3	CH <sub>3</sub> ( <b>62</b> )	<i>n</i> -BuLi	6	-40 to -30	1	19
4	CH <sub>3</sub> ( <b>62</b> )	<i>n</i> -BuLi	3	-40 to -30	3	23
5	CH <sub>3</sub> ( <b>62</b> )	<i>n</i> -BuLi	3	-75 to -65	20	5
6	CH <sub>3</sub> ( <b>62</b> )	<i>n</i> -BuLi	6	-75 to -65	20	no desired product
7	CH <sub>3</sub> ( <b>62</b> )	<i>n</i> -BuLi	3	-10 to 0	1	no desired product

Attention was subsequently turned to methyl 2,3-*O*-benzylidene-4-*O*-methyl- $\alpha$ -L-rhamnopyranoside (**62**) as a starting material for this reaction, which had previously been reported to afford 2-deoxy-3-ketosugar **63** in 40% yield by Clode and coworkers.<sup>176</sup> It was hoped that minimizing the size of the protecting group at C-4 of the carbohydrate ring would facilitate the desired abstraction of the C-3 proton. This theory was partially based on Morin's observation that the size of the C-4 protecting group of benzylidene acetal-protected methyl  $\alpha$ -L-rhamnopyranosides has a significant influence on the regiochemical outcome of the Klemm-Rodemeyer elimination reaction.<sup>185</sup> Specifically, Morin showed that when the C-4 hydroxyl group was protected with a bulky *tert*-butyldimethylsilyl (TBDMS) group as in  $\alpha$ -L-rhamnopyranoside **73**, the quasi-equatorial proton attached to C-2 is preferentially abstracted, affording exclusively 3-deoxy-2-ketosugar **74** (Figure 35).

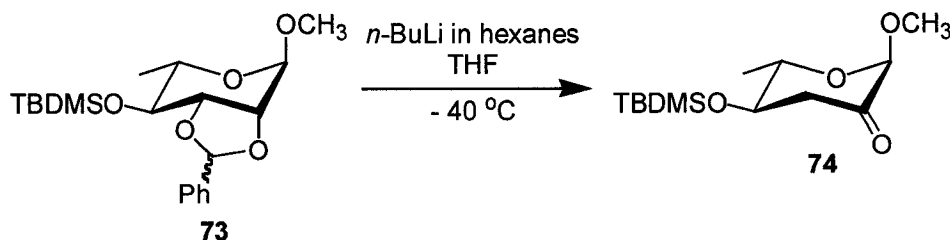


**Figure 35.** Regioselectivity of the Klemm-Rodemeyer reaction with 4-*O*-TBDMS-protected  $\alpha$ -L-rhamnopyranoside **73** as demonstrated by Morin<sup>185</sup>

On reaction of 4-*O*-methyl-protected derivative **62** with 6 equiv of *n*-butyllithium in THF, keeping the internal reaction temperature below -30 °C, the best isolated yield of 2-deoxy-3-ketosugar **63** obtained was 23% after silica gel chromatography (Table 1, entry 3). Many attempts were made to improve the yield of the Klemm-Rodemeyer reaction with **62** by varying the internal temperature of the reaction mixture, reaction

time, and the number of equiv of *n*-butyllithium (frequently titrated with 2,5-dimethoxybenzyl alcohol as an indicator<sup>186</sup>), with no success (Table 1, entries 4-7).

These disappointingly low yields prompted a careful analysis of the <sup>1</sup>H NMR spectra of the crude reaction mixtures. Surprisingly, this analysis revealed that only one diastereomer had primarily reacted after reaction times of 1-3 h under various reaction conditions, which was longer than the 30 min reaction time reported by Weckerle<sup>176</sup> with 4-*O*-methyl-protected derivative **62** as well as the 1 h reaction time reported by Brimacombe with 4-*O*-MEM- (**58**) and 4-*O*-MOM-protected (**59**) derivatives.<sup>174</sup> Through 1D nuclear Overhauser effect (NOE) NMR experiments, it was determined that the *exo* diastereomer reacted significantly faster than the *endo* diastereomer in the case of methyl 2,3-*O*-benzylidene-4-*O*-methyl- $\alpha$ -L-rhamnopyranoside (**62**) (Figure 36).

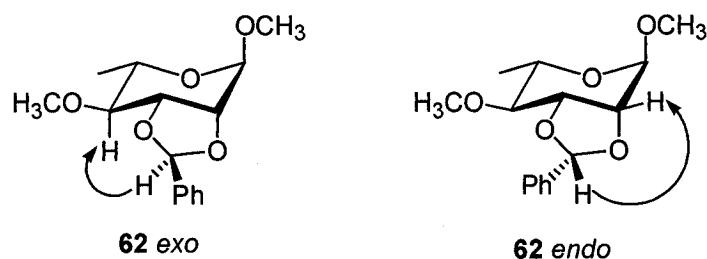


**Figure 36.** *Exo* and *endo* diastereomers of methyl 2,3-*O*-benzylidene-4-*O*-methyl- $\alpha$ -L-rhamnopyranoside (**62**) (arrows indicate strong 1D NOE interactions)

Of particular interest with respect to these observations are the conformational studies of Nánasi and coworkers on methyl 2,3-*O*-benzylidene- $\alpha$ -L-rhamnopyranoside (**67**) as well as 4-*O*-acetyl and 4-*O*-benzyl derivatives.<sup>187</sup> Their NMR spectroscopy-based investigations revealed that significant conformational differences exist in both the pyranoside and 1,3-dioxolane rings of *exo* and *endo* diastereomers of benzylidene acetal-protected  $\alpha$ -L-rhamnopyranosides. With respect to pyranoside rings, <sup>3</sup>*J*<sub>H-2,H-3</sub> values were consistently larger for *endo* diastereomers than for *exo* diastereomers, suggesting that the



corresponding dihedral angles are smaller in the case of *endo* diastereomers. Moreover, the coupling constant between the acetal carbon atom and quasi-axial proton H-3, which is also dependent on dihedral angle,<sup>188</sup> was consistently larger in *exo* diastereomers than in *endo* diastereomers of these  $\alpha$ -L-rhamnopyranosides. This indicates that the C-O-C-H dihedral angle between the acetal carbon atom and H-3 must be greater in the *exo* diastereomers as compared to the *endo* diastereomers. Together these conformational observations provide some insight into the differential reactivity of *exo* and *endo* diastereomers of  $\alpha$ -L-rhamnopyranosides **58**, **59**, and **62**.

In addition to establishing the lower reactivity of *endo* diastereomers, careful analysis of both <sup>1</sup>H NMR spectra of crude reaction mixtures and chromatographically separated products also allowed the identification of several Klemmer-Rodemeyer elimination reaction byproducts (Figure 37). The first byproduct, 3-deoxy-2-ketosugar **75** was observed in only trace quantities in the <sup>1</sup>H NMR spectra of several crude reaction mixtures and is attributed to proton abstraction from C-4 of the 1,3-dioxolane ring (C-2 of the monosaccharide ring) as previously shown in Figure 33. Secondly, a more significant quantity of alkene **76** was frequently identified and chromatographically isolated from crude reaction mixtures. Byproduct **76** is attributed to abstraction of the benzylic proton, H-2 in the 1,3-dioxolane ring, as previously shown in Figure 33. In addition to these two expected byproducts, a third compound (**77**), also observed in significant quantity, was chromatographically separated and characterized from several crude reaction mixtures. Byproduct **77** appears to result from two additional reactions of *n*-butyllithium with desired 2-deoxy-3-ketosugars **60**, **61**, and **63**. One reaction presumably involves the S<sub>N</sub>2 attack of *n*-butyllithium at the anomeric centre, displacing

the methoxy substituent, while the second reaction presumably involves the abstraction of H-4, resulting in ring opening and the formation of an enone. Copies of  $^1\text{H}$ ,  $^{13}\text{C}\{^1\text{H}\}$ , COSY, and  $^{13}\text{C}$ - $^1\text{H}$  HSQC NMR spectra of **77** are available in Appendix 1. A molecular formula of  $\text{C}_{11}\text{H}_{20}\text{O}_3$  for byproduct **77** was confirmed via high-resolution mass spectrometry, which is consistent with the proposed structure in Figure 37.

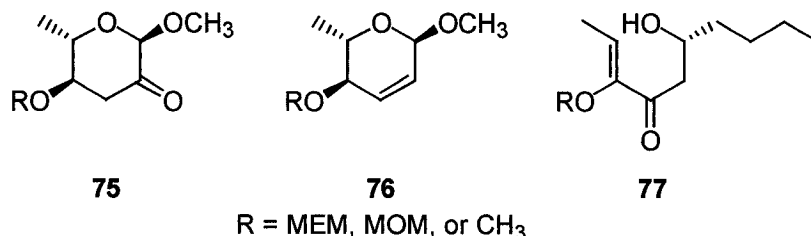


**Figure 37.** Several identified Klemer-Rodemeyer elimination reaction byproducts

In an attempt to address the diastereoselectivity issues associated with  $\alpha$ -L-rhamnopyranosides **58**, **59**, and **62**, an isopropylidene acetal was installed to protect the C-2 and C-3 hydroxyls of methyl  $\alpha$ -L-rhamnopyranoside (**66**) in lieu of the benzylidene acetal. Although largely unprecedented in a Klemer-Rodemeyer reaction, an isopropylidene acetal-protected  $\alpha$ -L-rhamnopyranoside was desirable for two reasons: (i) C-2 of the 1,3-dioxolane ring would no longer be chiral, eliminating diastereoselectivity issues; and, (ii) there would be no proton attached to C-2 of the 1,3-dioxolane ring, eliminating the possibility of an elimination product resulting from the previous abstraction of the benzylic proton. To facilitate this proposed Klemer-Rodemeyer reaction, methyl 2,3-*O*-isopropylidene- $\alpha$ -L-rhamnopyranoside (**78**) was prepared from methyl glycoside **66** using 2,2-dimethoxypropane as a solvent and *p*-toluenesulfonic acid as a catalyst, as previously described by Lipták and coworkers (Figure 38).<sup>189</sup> Following an extraction, isopropylidene-protected  $\alpha$ -L-rhamnopyranoside **78** was obtained as a colourless syrup in 92% yield and did not require further

purification. To fully protect **78**, a methyl ether was installed at the remaining C-4 hydroxyl group using methyl iodide and sodium hydride in DMF (Figure 38).<sup>177</sup> 4-*O*-Methyl-protected derivative **79** was subsequently obtained as a colourless syrup in 66% yield after silica gel chromatography.

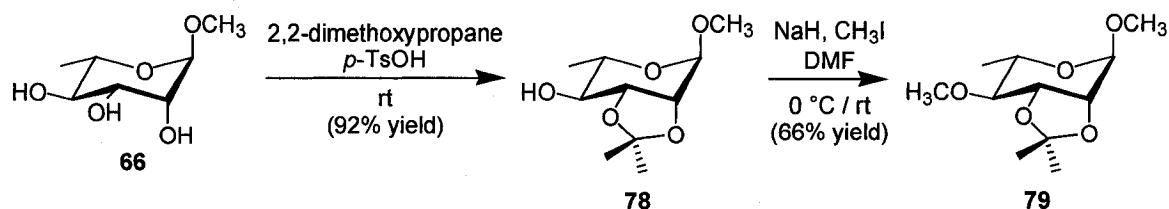


**Figure 38.** Synthesis of methyl 2,3-*O*-isopropylidene-4-*O*-methyl- $\alpha$ -L-rhamnopyranoside (**79**) from methyl  $\alpha$ -L-rhamnopyranoside (**66**)

The Klemm-Rodemeyer elimination reaction was first attempted with **79** in THF at -50 to -40 °C using 5 equiv of *n*-butyllithium, but after 2 h a significant quantity of starting material remained, and no desired product (**63**) was produced by analysis of the <sup>1</sup>H NMR spectrum of the crude reaction mixture (Figure 39). Warmer reaction temperatures (-10 to 0 °C) and lower equiv of *n*-butyllithium (2.5) facilitated the reaction of **79**, but only complex mixtures of products were obtained and none of the desired 2-deoxy-3-ketosugar (**63**) was observed in the <sup>1</sup>H NMR spectra of crude reaction mixtures.

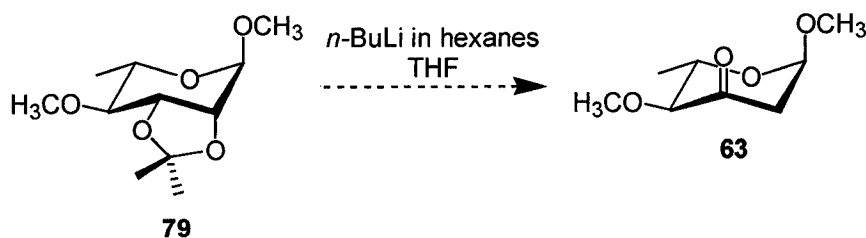


**Figure 39.** Proposed synthesis of methyl 2,6-dideoxy-4-*O*-methyl- $\alpha$ -L-erythro-hexopyranosid-3-ulose (**63**) from methyl 2,3-*O*-isopropylidene-4-*O*-methyl- $\alpha$ -L-rhamnopyranoside (**79**)

Interestingly, the conformation of methyl 4-*O*-acetyl-2,3-*O*-isopropylidene- $\alpha$ -L-rhamnopyranoside has also been studied by Nánasi and coworkers using NMR spectroscopy.<sup>187</sup> In terms of the pyranose ring, the conformation of this  $\alpha$ -L-rhamnopyranoside was found to be similar to the *exo* diastereomers of benzylidene acetal-protected  $\alpha$ -L-rhamnopyranosides, however; with respect to the 1,3-dioxolane ring, this compound possessed a conformation similar to the *endo* diastereomers of benzylidene acetal-protected  $\alpha$ -L-rhamnopyranosides. These conformational studies may provide some insight into the failure of the Klemmer-Rodemeyer reaction with methyl 2,3-*O*-isopropylidene-4-*O*-methyl- $\alpha$ -L-rhamnopyranoside (**79**).

The lack of success obtained using isopropylidene acetal-protected derivative **79**, as well as the nucleophilic role of *n*-butyllithium in byproduct formation, inspired an examination of one of the last Klemmer-Rodemeyer elimination reaction variables: the identity of the base. Although the majority of Klemmer-Rodemeyer reactions published to date report the use of *n*-butyllithium as a base,<sup>174,175,176,178,179,185</sup> a procedure has been described using *sec*-butyllithium (*s*-BuLi) as a base.<sup>190</sup> In this particular Klemmer-Rodemeyer elimination reaction, a tetrahydropyran-2-yl (THP) group was used to protect the C-4 hydroxyl of **67** and the transformation of  $\alpha$ -L-rhamnopyranoside **80** to 2-deoxy-3-ketosugar **81** was accomplished using 2 equiv of *sec*-butyllithium at -30 °C in THF, resulting in a yield of 40% after silica gel chromatography (Figure 40).<sup>190</sup>

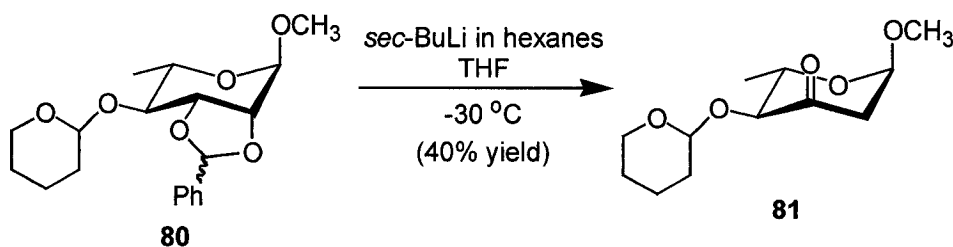


**Figure 40.** Synthesis of methyl 2,6-dideoxy-4-*O*-(tetrahydropyran-2-yl)- $\alpha$ -L-erythro-hexopyranosid-3-ulose (**81**) from methyl 2,3-*O*-benzylidene-4-*O*-(tetrahydropyran-2-yl)- $\alpha$ -L-rhamnopyranoside (**80**) by Klemer and Balkau<sup>190</sup>

The use of a THP group to protect the free hydroxyl group at C-4 was not pursued because this transformation introduces an additional chiral centre, further complicating the reaction as evidenced by the NOE studies on the differential reactivity of *exo* and *endo* diastereomers of **62**. In lieu of **80**, 4-*O*-methyl-protected (**62**) and 4-*O*-MEM-protected (**58**)  $\alpha$ -L-rhamnopyranosides were used in Klemer-Rodemeyer reactions with various bases (Table 2). Reaction of methyl 2,3-*O*-benzylidene-4-*O*-methyl- $\alpha$ -L-rhamnopyranoside (**62**) with lithium diisopropylamide (LDA) remained sluggish at successively higher temperatures, producing only a 6% yield of desired 2-deoxy-3-ketosugar **63** after 4 h at -30 to 0 °C with 2 equiv of base (Table 2, entries 1-2). Longer reaction times using **62** and LDA resulted in degradation, as no desired product was isolated after 23 h at -40 to 20 °C with 4 equivalents of base (Table 2, entry 3). Unfortunately, *tert*-butyllithium (*t*-BuLi) produced similar results, providing only a 5% yield of **63** after 3 h at -50 to -25 °C with 2 equiv of base (Table 2, entry 4). Interestingly, the use of *sec*-butyllithium as an alternative base provided an essential mixture of strong basicity and steric hindrance limiting byproducts resulting from participation of the base. Specifically, reaction of 4-*O*-MEM-protected  $\alpha$ -L-rhamnopyranoside **58** with 3 equiv of *s*-butyllithium at -50 to -35 °C for 4 h resulted in a dramatically improved 71% yield of 2-deoxy-3-ketosugar **60** after purification (Table 2,

entry 5), providing a pleasing conclusion to the Klemer-Rodemeyer elimination reaction study.

**Table 2.** Selected Klemer-Rodemeyer elimination reaction results with different bases

entry	4- <i>O</i> -R group (compound)	base	equiv of base	temperature (°C)	time (h)	2-deoxy-3-ketosugar isolated yield (%)
1	CH <sub>3</sub> ( <b>62</b> )	LDA	2	-50 to -25	3	4
2	CH <sub>3</sub> ( <b>62</b> )	LDA	2	-30 to 0	4	6
3	CH <sub>3</sub> ( <b>62</b> )	LDA	4	-40 to 20	23	no desired product
4	CH <sub>3</sub> ( <b>62</b> )	<i>t</i> -BuLi	2	-50 to -25	3	5
5	MEM ( <b>58</b> )	<i>s</i> -BuLi	3	-50 to -35	4	71

The fifth step in this synthetic route to L-digitoxose (**50**) involved a sodium borohydride reduction of 2-deoxy-3-ketosugar **60** to produce methyl 2,6-dideoxy-4-*O*-(2-methoxyethoxymethyl)- $\alpha$ -L-*ribo*-hexopyranoside (**82**) (Figure 41). This reaction proceeded stereoselectively, as reported by Brimacombe and coworkers,<sup>174</sup> resulting in a C3-OH axial:equatorial ratio of 10:1 and an 80% yield of **82** after silica gel chromatography. This high level of stereoselectivity presumably results from sodium borohydride attack via an equatorial trajectory, avoiding an energetically unfavourable 1,3-diaxial interaction with the axial methoxy group located at the anomeric centre.<sup>191,192</sup>

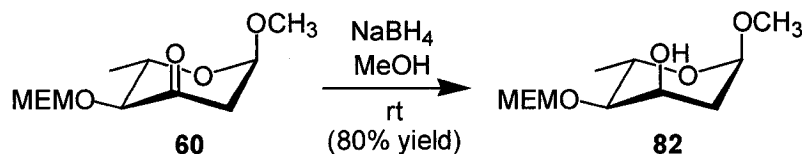


**Figure 41.** Sodium borohydride reduction of methyl 2,6-dideoxy-4-*O*-(2-methoxyethoxymethyl)- $\alpha$ -L-*erythro*-hexopyranosid-3-ulose (**60**) to methyl 2,6-dideoxy-4-*O*-(2-methoxyethoxymethyl)- $\alpha$ -L-*ribo*-hexopyranoside (**82**)

To facilitate the coupling of L-digitoxose (**50**) with a phosphate or nucleoside 5'-diphosphate, it was necessary to first deprotect at minimum the 4-*O*-MEM ether protecting group since MEM ethers are usually cleaved under acidic conditions and

2,6-dideoxysugar nucleotides are very acid labile. Brimacombe and coworkers previously reported the successful deprotection of **82** using 29% aqueous acetic acid, which was heated under gentle reflux for 2 h (Figure 42).<sup>174</sup> After silica gel chromatography, Brimacombe and coworkers obtained a syrup that crystallized over time, after which recrystallization from acetone afforded pure L-digitoxose in 70% yield as evidenced by melting point and elemental analysis.

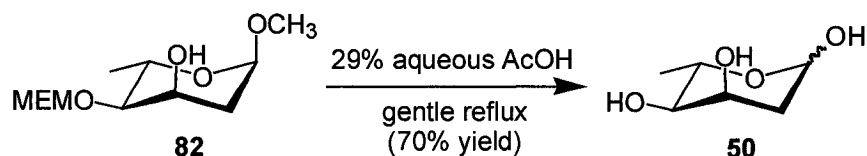


**Figure 42.** Method used by Brimacombe to deprotect methyl 2,6-dideoxy-4-*O*-(2-methoxyethoxymethyl)- $\alpha$ -L-ribo-hexopyranoside (**82**), affording L-digitoxose (**50**)<sup>174</sup>

Unfortunately, the deprotection of **82** proved more difficult than expected. After 2 h in refluxing 29% aqueous acetic acid, TLC analysis of the reaction mixture revealed the complete consumption of protected  $\alpha$ -L-rhamnopyranoside **82** and the formation of what appeared to be one new compound by TLC. Following concentration of the reaction mixture, analysis of the  $^1\text{H}$  NMR spectrum of the resulting yellow syrup revealed the presence of MEM protecting groups. This  $^1\text{H}$  NMR analysis was complicated by the possibility of five L-digitoxose (**50**) isomers upon deprotection:  $\alpha$  and  $\beta$  diastereomers of L-digitoxopyranose,  $\alpha$  and  $\beta$  diastereomers of L-digitoxofuranose, and the open chain *aldehyde* form of **50** (Figure 43). Interestingly, an equilibrated mixture of D-digitoxose in dimethylsulfoxide- $\text{d}_6$  has been quantitatively analyzed by NMR, revealing the following composition:  $\alpha$ -pyranose (11.2%),  $\beta$ -pyranose (67.3%),  $\alpha$ -furanose (8.4%),  $\beta$ -furanose (13.0), *aldehyde* form (0.1%).<sup>193</sup>

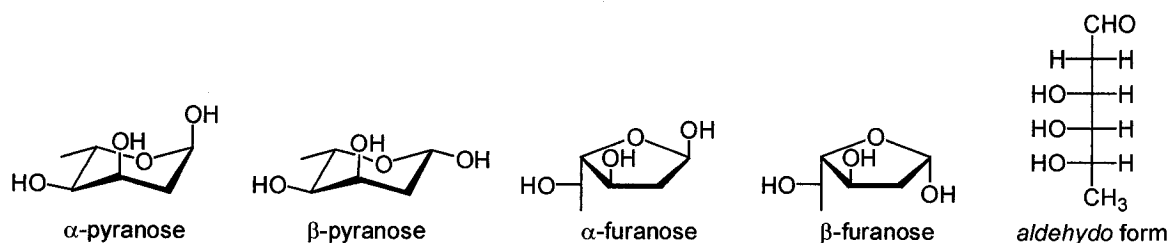


**Figure 43.** Five isomeric possibilities for L-digitoxose (**50**) after deprotection

Chromatography of the crude reaction mixture on silica gel using the same solvent conditions reported by Brimacombe and coworkers (9:1 EtOAc:MeOH)<sup>174</sup> did not assist in the purification of the desired product (**50**) as the <sup>1</sup>H NMR spectra obtained before and after silica gel chromatography were identical. The colourless syrup obtained via chromatography did not crystallize over time and several attempts to crystallize this syrup from acetone were unsuccessful. The identity of this syrup as 4-*O*-MEM- $\alpha/\beta$ -L-digitoxose was confirmed via ESI-MS (LRMS (ESI<sup>+</sup>) for C<sub>10</sub>H<sub>20</sub>O<sub>6</sub> (236.1 amu) = *m/z* 259.1 [M+Na]<sup>+</sup>). Higher concentrations of aqueous acetic acid and longer reaction times resulted in the complete degradation of this 2,6-dideoxysugar derivative.

In response to these results, efforts were re-directed toward designing and executing a more efficient, novel synthetic route to access elusive 2,6-dideoxysugar **50**, or a protected derivative thereof, which could be used directly in the coupling of **50** with a phosphate or nucleoside 5'-diphosphate.

### 2.1.2. Method B

With the previous success of the stereoselective sodium borohydride reduction in mind, a new synthetic plan was devised to access L-digitoxose (**50**) including the preparation of a 2-deoxy-3-ketosugar via a different means. This new strategy also originated from L-rhamnose (**55**) and involved the use of a glycal, a class of



monosaccharides that have long served as versatile intermediates in carbohydrate synthesis (Figure 44).

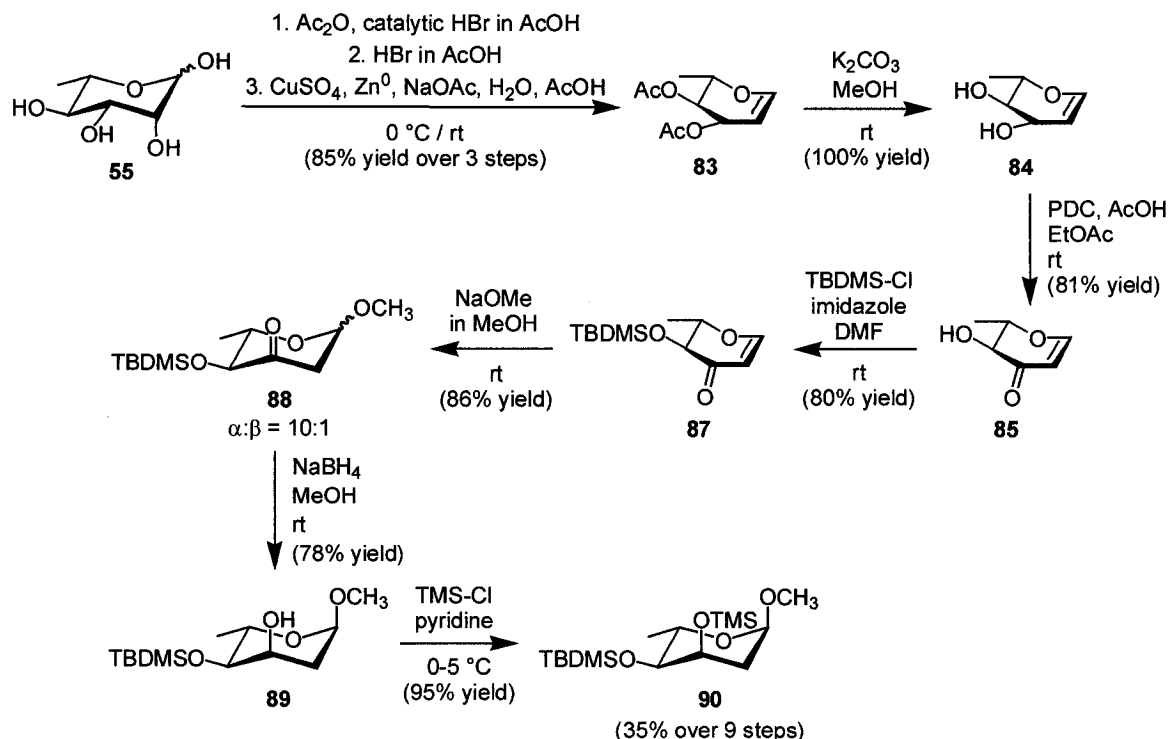


**Figure 44.** Novel synthesis of protected L-digitoxose derivative **90** via Method B

The first step in this synthetic route involved the preparation of 3,4-di-O-acetyl-L-rhamnal (**83**), a glycal, from L-rhamnose (**55**) using a one pot, three step modified procedure originally developed by Koreeda and coworkers.<sup>194</sup> This protocol first makes use of acetic anhydride and a catalytic amount of hydrogen bromide in acetic acid to fully acetylate L-rhamnose (**55**). After 30 min, all L-rhamnose (**55**) had dissolved and TLC analysis revealed that the acetylation reaction was complete. Additional hydrogen bromide in acetic acid was then added to facilitate the formation of an *in situ* glycosyl bromide. Although Koreeda and coworkers reported stirring this second step of the reaction protocol overnight, the bromination was found to be complete after only 1.5 h, allowing the completion of all three steps in the one pot procedure to be accomplished in

only one day. Following the formation of the desired acetylated L-rhamnosyl bromide, the reaction mixture was poured into a stirred suspension of copper sulfate, zinc, and sodium acetate in 33% aqueous acetic acid. This last step, a reductive elimination, was complete after vigorous stirring for 1.5 h in an ice-water bath. The desired product, 3,4-di-O-acetyl-L-rhamnal (**83**), was isolated in 85% yield over 3 steps in one day after a simple purification using a silica gel plug in a scintillated funnel.

3,4-Di-O-acetyl-L-rhamnal (**83**) was subsequently deacetylated using potassium carbonate in methanol as previously described by van Heerden and coworkers.<sup>195</sup> Although the original procedure involved the use of 0.008 equiv of potassium carbonate and a reaction time of 24 h at rt, by increasing the equiv of potassium carbonate 5 fold to 0.04, the reaction time was decreased to only 3 h at rt. In terms of work-up and purification, the reaction mixture was simply filtered through a short silica gel plug in a scintillated funnel and concentrated under reduced pressure to afford crystalline L-rhamnal (**84**) in essentially quantitative yield.

Regioselective oxidation of L-rhamnal (**84**) with pyridinium dichromate and acetic acid in EtOAc provided exclusively 1,5-anhydro-2,6-dideoxy-L-*erythro*-hex-1-en-3-ulose (**85**) following a modified procedure previously described by Czernecki and coworkers.<sup>196</sup> Although Czernecki and coworkers precipitated the resulting Cr(III) species using toluene, this procedure proved tedious and largely ineffective in our laboratory. Alternatively, the reaction mixture was passed successively through two short silica plugs which effectively bound the green Cr(III) species, facilitating an efficient purification of enulose **85**. Concentration of the filtrate under reduced pressure afforded white crystals of **85** in 81% yield.

In attempts to streamline the proposed synthetic method, the effect of sodium borohydride reduction on enulose **85** was investigated (Figure 45).

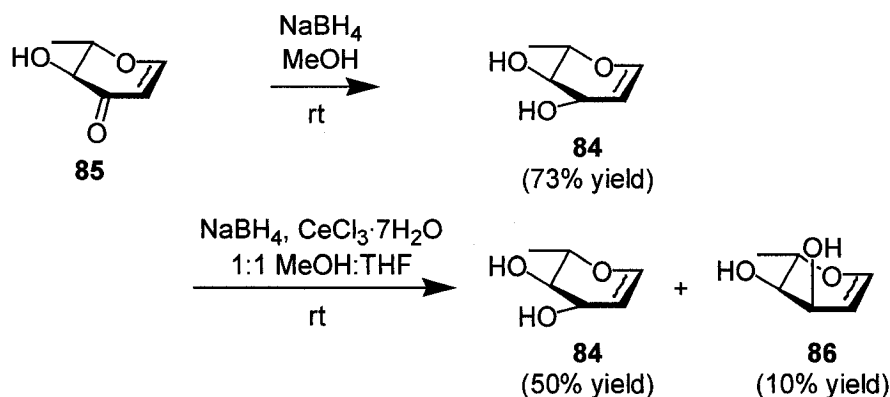


**Figure 45.** Reduction of 1,5-anhydro-2,6-dideoxy-L-erythro-hex-1-en-3-ulose (**85**) under various reduction conditions

Using conditions previously described for the preparation of **82** from 2-deoxy-3-ketosugar **60**,<sup>174</sup> reduction with sodium borohydride provided an inefficient route back to L-rhamninal (**84**). Interestingly, Luche reduction conditions,<sup>197</sup> which include a lanthanide salt such as  $\text{CeCl}_3 \cdot 7\text{H}_2\text{O}$  in addition to sodium borohydride, sometimes result in stereoselectivities opposite to reductions involving sodium borohydride alone.<sup>198</sup> The high regio- and stereoselectivity associated with Luche-type reductions was first noted by Danishefsky in 1983<sup>199</sup> and is postulated to result from the coordination of  $\text{CeCl}_3$ , a Lewis acid, with the carbonyl group, essentially blocking one face of the molecule.<sup>200</sup> In the case of enulose **85**, Luche-type reduction did result in a difference in stereoselectivity, but the 5:1 ratio of L-rhamninal (**84**):L-digitoxal (**86**) was very unfavourable (Figure 45).

To facilitate the efficient reduction of the 3-keto- functionality of enulose **85** to the corresponding axial hydroxyl group, access to a 2-deoxy-3-ketosugar analogous to those described in Method A (**60**, **61**, and **63**) was required. This transformation was accomplished in two easy steps by first protecting the remaining free hydroxyl group of

enulose **85** with a *tert*-butyldimethylsilyl (TBDMS) group using TBDMS chloride in DMF with imidazole serving as a catalyst as originally described by Corey and Venkateswarlu.<sup>201</sup> Following extraction and concentration under reduced pressure, TBDMS-protected enulose **87** was isolated in 80% yield and required no further purification. A TBDMS protecting group was chosen to protect enulose **85** because of its well-documented, non-acidic ease of removal using tetra-*n*-butylammonium fluoride (Bu<sub>4</sub>NF), also first described by Corey,<sup>201,202</sup> as well as its stability to reaction conditions in forthcoming synthetic steps.

To prepare 2,6-dideoxysugar **88** from TBDMS-protected enulose **87**, an efficient procedure involving sodium methoxide in methanol previously described by Köpper and Thiem was employed.<sup>192</sup> After dissolving **87** in 0.01 M sodium methoxide in methanol and stirring for only 1 h at rt, the reaction was deemed complete by TLC. After neutralization of the reaction mixture using Amberlite® IR-120 (H<sup>+</sup>) ion exchange resin (free acid form), filtration, and concentration under reduced pressure, methyl 2,6-dideoxy-4-*O*-(*tert*-butyldimethylsilyl)- $\alpha/\beta$ -L-*erythro*-hexopyranosid-3-ulose (**88**) was obtained as a pale yellow syrup in 86% yield as a 10:1  $\alpha:\beta$  mixture of diastereomers. Crude product **88** was used directly in the next synthetic step without any further purification.

Reduction of **88** with sodium borohydride provided easy access to an axially configured hydroxyl group at C-3 at this stage of the synthetic strategy. Using the same conditions previously described by Brimacombe for the sodium borohydride reduction of 4-*O*-MEM-protected 2-deoxy-3-ketosugar **60**,<sup>174</sup> 4-*O*-TBDMS-protected diastereomeric mixture **88** was efficiently reduced, resulting in a crude C3-OH  $\alpha:\beta$  ratio of 10:1.

Following silica gel chromatography, methyl 4-*O*-(*tert*-butyldimethylsilyl)-2,6-dideoxy- $\alpha$ -L-*ribo*-hexopyranoside (**89**) was isolated as a colourless syrup in 78% yield.

Lastly, the remaining C-3 free hydroxyl group was protected with a trimethylsilyl (TMS) group using TMS chloride and pyridine in a procedure analogous to one described by Hindsgaul for the TMS protection of various monosaccharides.<sup>143</sup> This reaction was complete by TLC after 1 h at 0-5 °C and fully protected L-digitoxose derivative **90** was isolated as a colourless syrup in 95% yield following extraction with H<sub>2</sub>O and concentration under reduced pressure. The 3-*O*-TMS functionality was chosen as a protecting group at this stage of the synthetic route because it could be easily removed using the same conditions as the 4-*O*-TBDMS group with Bu<sub>4</sub>NF after **90** was coupled with a nucleoside 5'-diphosphate. This work will be described in Section 2.3.1.

In summary, this novel synthetic route provides efficient access to protected L-digitoxose derivative **90** in 35% overall yield over nine steps. The benefits of this route over others previously described include the ease and speed of synthetic steps (7 of 9 steps completed in 3 h or less) as well as the lack of formal chromatography required (3 of 9 products purified using a short silica gel plug in a scintillated funnel, only 1 of 9 products purified using traditional silica gel chromatography). Also of notable interest is the high degree of regio- and stereoselectivity achieved in the oxidation of L-rhamnal (**84**) to enulose **85**, the Michael-type addition of sodium methoxide to 4-*O*-TBDMS-protected enulose **87**, and the sodium borohydride reduction of 2-deoxy-3-ketosugar **88**.

## 2.2. Monosaccharide Analogues Prepared from a Synthetic Intermediate

Several monosaccharide analogues were also prepared from 3,4-di-*O*-acetyl-L-rhamnal (**83**), an intermediate in the Method B synthesis of protected L-digitoxose derivative **90**. These analogues include two fluorinated 6-deoxysugar derivatives as well as one 2,6-dideoxysugar derivative (**94**, **95**, and **101**).

### 2.2.1. Fluorinated 6-Deoxysugar Analogues

Organically bound fluorine-containing compounds are very rare in nature and have been identified only in a small number of plants and microorganisms.<sup>203</sup> With respect to carbohydrates in particular, the first fluorine-containing sugar derivative, the 4'-fluoro-5'-*O*-sulfamoyladenoside nucleocidin (**91**), was isolated from an Indian soil sample containing *Streptomyces calvus* in 1957,<sup>204</sup> although it was not until 1969 that the correct fluorine-containing structure was elucidated (Figure 46).<sup>205</sup> More recently, the first fluorinase enzyme, a key component in the biosynthetic pathway of the ubiquitous toxin fluoroacetate, was discovered by O'Hagan and coworkers.<sup>206</sup>

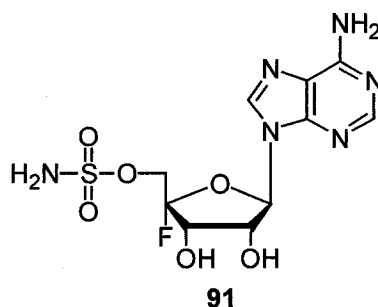


**Figure 46.** Structure of nucleocidin (**91**)

Despite the small number of isolated natural products containing fluorine in an organically bound state, there is significant interest in preparing fluorinated analogues of natural products since fluorine has demonstrated the ability to modify the chemical

properties, biological activity, and selectivity of certain pharmaceutically relevant compounds.<sup>58,203,207,208</sup> For example, fluorine atoms and fluoroalkyl groups are capable of increasing the lipophilicity of a molecule, which is important in drug pharmacokinetics such as absorption, distribution, metabolism, and excretion.<sup>203</sup> In addition, the electron-withdrawing ability of fluorine atoms increases the acidity of neighboring functional groups such as carboxylic acids or alcohols, and fluorine atoms can also act as hydrogen bond acceptors.

Of particular interest to carbohydrate chemists are fluorinated monosaccharides, specifically 2-deoxy-2-fluorosugars, which are increasingly being used as carbohydrate-active enzyme mechanistic probes and inhibitors.<sup>207</sup> Pioneering work by Withers established the significant utility 2-deoxy-2-fluorosugars, appropriately activated at the anomeric centre with a good leaving group, as retaining glycosidase mechanistic probes by demonstrating their ability to specifically label the catalytic nucleophile essential for a double displacement reaction mechanism.<sup>209,210,211</sup> More recently, 2-deoxy-2-fluorosugars have demonstrated their utility as glycosyltransferase inhibitors, allowing some insight into mechanistic details.<sup>212</sup> Considering the integral role of glycosylation in many biological processes, selective inhibition of certain mammalian glycosyltransferases may also serve as a medicinal tool in the treatment of cancer, tissue inflammation, and xenotransplant rejection.<sup>207</sup>

To facilitate the preparation of several 2-deoxy-2-fluorosugar analogues, the utility of Selectfluor®, an efficient electrophilic fluorinating agent, was explored (Figure 47). This reagent was developed in the early 1990s by Banks and coworkers<sup>213</sup> and quickly gained acceptance as a safe, easy to handle, non-toxic alternative<sup>207</sup> to more

traditional electrophilic fluorinating agents such as fluoroxytrifluoromethane ( $\text{CF}_3\text{OF}$ ),<sup>214</sup> perchloryl fluoride ( $\text{FClO}_3$ ),<sup>215,216</sup> and xenon difluoride ( $\text{XeF}_2$ ).<sup>217</sup>

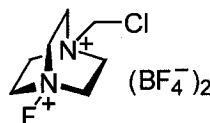


**Figure 47.** Structure of Selectfluor® (1-chloromethyl-4-fluoro-1,4-diazoniabicyclo[2.2.2]octane bis(tetrafluoroborate))

Selectfluor® was first employed with glycals by Wong and coworkers in 1997, who demonstrated that this reaction proceeds regiospecifically to produce only 2-deoxy-2-fluorosugars with concomitant introduction of a nucleophile at the anomeric centre.<sup>218</sup> Given this result, the reaction of Selectfluor® with 3,4-di-*O*-acetyl-L-rhamnal (**83**), an intermediate in the Method B synthesis of L-digitoxose derivative **90**, was investigated (Figure 48). On reaction of **83** with 2 equiv of Selectfluor® in 1:1 DMF:H<sub>2</sub>O, a mixture of four diastereomers (**92-93**) was obtained. This crude mixture of compounds was immediately acetylated using acetic anhydride and pyridine to afford fully acetylated fluorinated derivatives **94-95**. Careful chromatography allowed the separation of derivatives with a C-2 axial fluoro- substituent (**94**) from derivatives with a C-2 equatorial fluoro- substituent (**95**) in a **94:95** ratio of 3:2 as white crystalline solids in 60% overall yield over 2 steps.



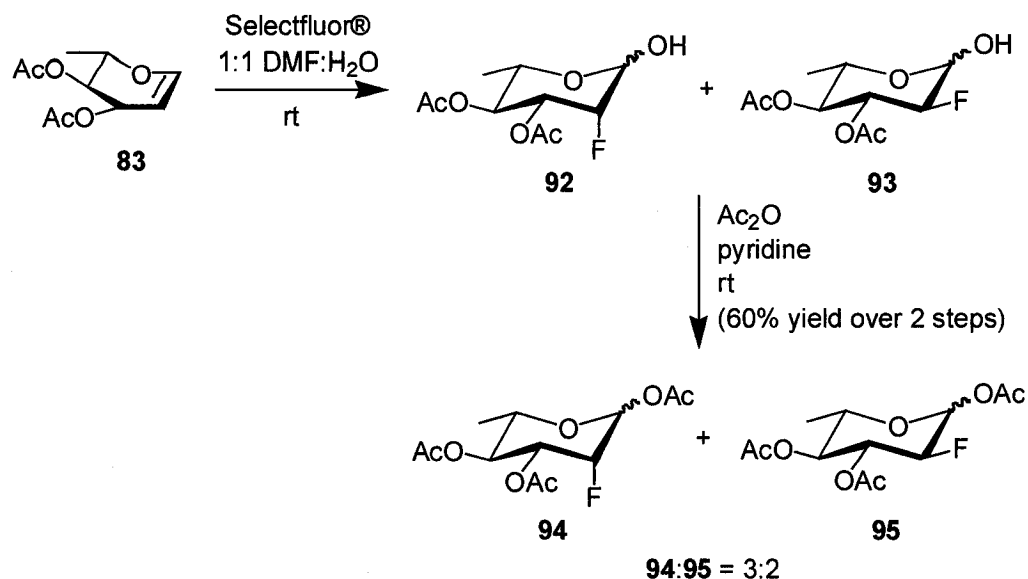


**Figure 48.** Synthesis of 1,3,4-tri-*O*-acetyl-2-deoxy-2-fluoro- $\alpha/\beta$ -L-rhamnopyranose (**94**) and 1,3,4-tri-*O*-acetyl-2,6-dideoxy-2-fluoro- $\alpha/\beta$ -L-glucopyranose (**95**) from 3,4-di-*O*-acetyl-L-rhamnal (**83**) using Selectfluor®

This result represented a significant improvement in yield and regioselectivity over a previous attempt to prepare 2-deoxy-2-fluorosugar derivatives of L-rhamnose (**55**) from acetylated glycal **83** with CF<sub>3</sub>OF.<sup>219</sup> Using this reagent, Butchard and Kent obtained a mixture of four products including 2-deoxy-2-fluoro-trifluoromethyl glycosides and as well as several 1,2-dideoxy-1,2-difluorosugar derivatives (**96-99**) (Figure 49). After multiple silica gel columns and serendipitous selective crystallizations, an overall isolated yield of 76% was obtained in an approximate **96:97:98:99** ratio of 3:2:1:1.

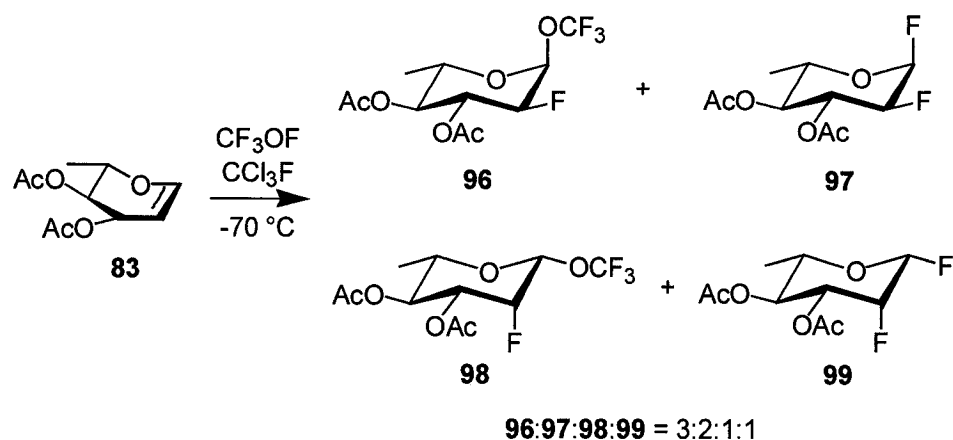


**Figure 49.** Reaction of 3,4-di-*O*-acetyl-L-rhamnal (**83**) with CF<sub>3</sub>OF by Butchard and Kent, producing **96-99**<sup>219</sup>

### 2.2.2. 2,6-Dideoxysugar Analogue

In addition to 2-deoxy-2-fluorosugar analogues **94** and **95**, it was recognized that 3,4-di-*O*-acetyl-L-rhamnal (**83**) could also be efficiently used to provide access to a 2,6-dideoxysugar analogue of L-digitoxose (**50**) named L-olivose (**100**) (Figure 50). These two 2,6-dideoxysugars are C-3 epimers and thus the preparation of L-olivose (**102**) was of particular interest for probing the promiscuity of the JadS glycosyltransferase exclusively at C-3 after conversion of **100** to a sugar nucleotide.

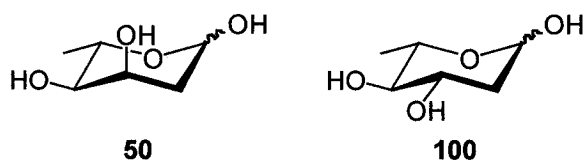


**Figure 50.** Structures of L-digitoxose (**50**) and L-olivose (**100**)

A recently reported methodology used to prepare 2-deoxy- and 2,6-dideoxysugars from glycals is that of Lam and Gervay-Hague, which involves a simple one-pot procedure using hydrogen bromide in acetic acid, glacial acetic acid, and acetic anhydride

in DCM.<sup>220</sup> This synthetic approach was successfully used to prepare 1,3,4-tri-*O*-acetyl- $\alpha/\beta$ -L-olivopyranose (**101**) in 68% yield after silica gel chromatography (Figure 51).



**Figure 51.** Synthesis of 1,3,4-tri-*O*-acetyl- $\alpha/\beta$ -L-olivopyranose (**101**) from 3,4-di-*O*-acetyl-L-rhamnal (**83**)

## 2.3. Chemical Synthesis of Sugar Nucleotides

The chemical synthesis and purification of sugar nucleotides represents a significant challenge for synthetic organic chemists. While traditional indirect coupling procedures require access to appropriate sugar-1-phosphates<sup>134</sup> and often necessitate long reaction times of several days,<sup>140,141</sup> more recently developed direct coupling methods frequently suffer from poor stereoselectivity,<sup>142,143,146</sup> and both approaches typically result in only low to moderate yields (Section 1.5.1).<sup>140,141,142,143,146</sup> Moreover, sugar nucleotides are water-soluble and pH sensitive, necessitating careful handling and complicating purification protocols. A variety of strategies used to chemically synthesize both a 2,6-dideoxysugar nucleotide (Section 2.3.1) and analogue sugar nucleotides (Sections 2.3.2 and 2.3.3) will be described.

### 2.3.1. Preparation of a 2,6-Dideoxysugar Nucleotide

As discussed in Section 1, 2,6-dideoxysugars are important structural components of a wide variety of natural products. Unfortunately, a significant limitation of investigations into the substrate promiscuity of Leloir-type glycosyltransferases is poor

access to 2,6-dideoxysugar nucleotide substrates.<sup>87</sup> The chemical synthesis of these elusive compounds is plagued by several factors. First and foremost, the absence of an electron-withdrawing substituent at C-2 results in a much more labile glycosidic bond, which is prone to hydrolysis or anomerization.<sup>221</sup> Moreover, the lack of stereodirecting substituent at both C-2 and C-6 presents a considerable challenge for dictating anomeric stereoselectivity.<sup>64</sup> Since the JadS glycosyltransferase catalyzes  $\alpha$ -glycoside biosynthesis and has putatively been identified by sequence homology with related enzymes to function via an inverting mechanism,<sup>132</sup> access to  $\beta$ -linked sugar nucleotides is desired. This requirement adds yet another layer of difficulty to synthetic approaches aimed at accessing 2-deoxyglycosides since the  $\beta$  anomers of these compounds are thermodynamically unfavorable due to the anomeric effect.<sup>221</sup>

To facilitate the preparation of sugar nucleotides from protected L-digitoxose derivative **90**, two retrosynthetic strategies were considered as discussed in Section 1.5.1 (Figure 25). As previously described, the classical approach to sugar nucleotide synthesis involves the initial synthesis of a sugar-1-phosphate, which is subsequently coupled with an activated nucleoside 5'-monophosphate ester.<sup>134</sup> In addition to common limitations of this approach such as long reaction times and low overall yields, 2-deoxysugar-1-phosphates have generally been reported to be very difficult to prepare and isolate due to their instability,<sup>222</sup> although one study demonstrating the stereoselective generation of several 2,6-dideoxysugar-1-phosphates has recently been reported.<sup>223</sup> The second synthetic strategy used to prepare sugar nucleotides involves the direct coupling of electrophilic glycosyl donors with nucleoside 5'-diphosphates. Two direct coupling approaches involving a 2,6-dideoxyglycosyl iodide<sup>224</sup> derived from an anomeric

trimethylsilyl group and a 2,6-dideoxyglycosyl chloride<sup>223</sup> derived from an anomeric hydroxyl group have been reported. The benefit of this type of approach is that only one challenging coupling reaction and purification protocol has to be explored in lieu of the two couplings and purifications required in the preparation and coupling of a 2,6-dideoxysugar-1-phosphate. Thus, initial efforts were directed toward this second synthetic approach of which the first step was to establish suitable conditions for the preparation of an electrophilic 2,6-dideoxyglycosyl halide from previously prepared methyl 4-*O*-(*tert*-butyldimethylsilyl)-2,6-dideoxy-3-*O*-(trimethylsilyl)- $\alpha$ -L-ribo-hexopyranoside (**90**).

A synthetic strategy facilitating the direct conversion of protected methyl glycoside **90** to a glycosyl halide was desired (Figure 52), as this route would circumvent the need to first hydrolyze the anomeric methoxy group. This type of deprotection is usually accomplished under acidic conditions,<sup>174</sup> which prompted efforts to avoid this step due to the difficulties encountered in this type of transformation in Section 2.1.1. In addition, TMS and TBDMS protecting groups are largely unstable to acid<sup>225</sup> and it was desired that these protecting groups remain intact until after coupling **90** with a nucleoside 5'-diphosphate. Lastly, by avoiding deprotection of the anomeric centre, the risk of mutarotation, which could give rise to undesirable furanose ring forms, is reduced.

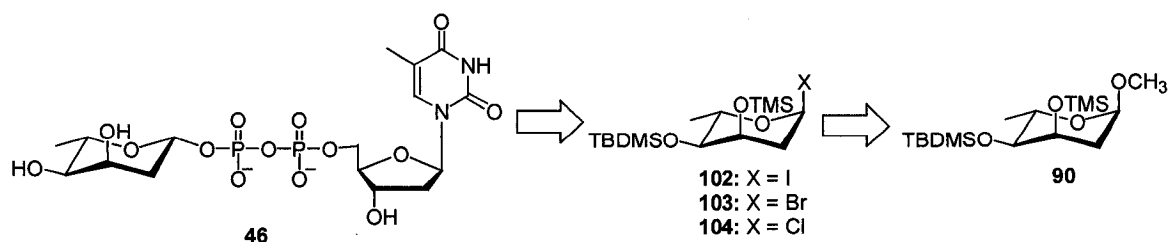


**Figure 52.** Proposed retrosynthetic strategy to access dTDP- $\beta$ -L-digitoxose from protected L-digitoxose derivative **90**

An analysis of synthetic options available to efficiently accomplish the direct conversion of methyl 2,6-dideoxyglycoside **90** to a glycosyl halide (**102**, **103**, or **104**) provided several possibilities. With respect to glycosyl iodides, Thiem and Meyer have reported the preparation of 2,3,4,6-tetra-*O*-acetyl- $\alpha$ -D-galactopyranosyl iodide (**105**) from methyl 2,3,4,6-tetra-*O*-acetyl- $\alpha$ -D-galactopyranoside (**106**) using 4 equiv of trimethylsilyl iodide (TMS-I) in toluene for 2 h at 80 °C, after which time **105** was isolated in 65% yield (Figure 53).<sup>226</sup> In the same publication, Thiem and Meyer also described the preparation of several 2-deoxyglycosyl iodides using 1.2 equiv of TMS-I in toluene for 15 min at rt, after which time a quantitative yield was obtained,<sup>226</sup> although the majority of these procedures involved anomeric acetates, which are more commonly used than methyl glycosides in this type of transformation.<sup>220</sup>

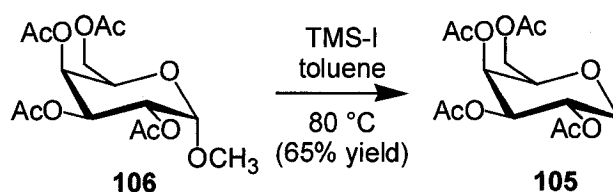


**Figure 53.** Synthesis of 2,3,4,6-tetra-*O*-acetyl- $\alpha$ -D-galactopyranosyl iodide (**105**) from methyl glycoside **106** by Thiem and Meyer<sup>226</sup>

In a similar reaction, Uchiyama and Hindsgaul have reported the *in situ* formation of 2-deoxyglycosyl iodide **107** from a trimethylsilyl-protected anomeric ether (**108**) using 1 molar equivalent of TMS-I in DCM at -78 °C for 30 min (Figure 54).<sup>143</sup> After this transformation was complete, newly formed iodide **107** was reacted directly with UDP for 4 h at an unspecified temperature, affording UDP-2-deoxy- $\alpha$ -D-galactose (**109**) in 40% yield ( $\alpha$ : $\beta$  = 3:1) following chromatography.

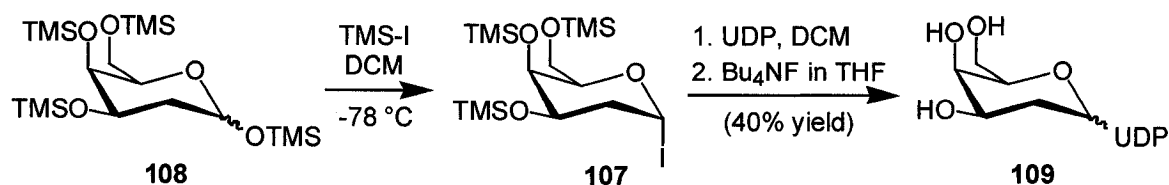


**Figure 54.** Synthesis of UDP-2-deoxy-α-D-galactose (**109**) via 2-deoxyglycosyl iodide **107** by Uchiyama and Hindsgaul<sup>143</sup>

Given these results, several attempts were made to prepare L-digitoxosyl iodide **102** from methyl 2,6-dideoxyglycoside **90**. Initial efforts focused on using 1 molar equivalent of TMS-I with **90** in DCM at a reaction temperatures of -78 °C, 0 °C, and rt. Reaction monitoring by TLC revealed the formation of a new compound of similar retention factor ( $R_f$ ) to starting material **90** in reactions conducted at 0 °C and rt, while no reaction was observed at -78 °C after several hours. Analysis of <sup>1</sup>H NMR spectra of crude reaction mixtures revealed that the new compound formed at 0 °C and rt was the β diastereomer of α-configured methyl 2,6-dideoxyglycoside **90**, illustrating that some anomerization was taking place. No signals corresponding to a possible 2,6-dideoxyglycosyl iodide were observed in the <sup>1</sup>H NMR spectra. Reactions involving increased equiv of TMS-I produced similar results and no 2,6-dideoxyglycosyl iodide was ever observed by TLC or <sup>1</sup>H NMR. Despite these results, it was reasoned that 2,6-dideoxyglycosyl iodide **102** may have been forming *in situ*, but was too unstable to observe by TLC or <sup>1</sup>H NMR. Thus, several reactions were attempted involving the direct addition of UDP to reaction mixtures after stirring **90** with 1 molar equivalent of TMS-I in DCM for 15 min or 1 h at -78 or 0 °C in an effort to demonstrate the formation of an *in situ* glycosyl iodide via formation of a 2,6-dideoxysugar nucleotide product. These efforts unfortunately failed, as no 2,6-dideoxysugar nucleotide product formation was detected by <sup>1</sup>H or <sup>31</sup>P{<sup>1</sup>H} NMR spectroscopy.

At this point, efforts were re-directed toward the synthesis of more stable 2,6-dideoxyglycosyl chlorides and bromides. Of the aforementioned glycosyl halides, glycosyl chlorides are the most stable electrophiles, so initial efforts were aimed at surveying methods available for the direct conversion of methyl 2,6-dideoxyglycoside **90** to 2,6-dideoxyglycosyl chloride **104**. No literature precedent was discovered for this type of transformation with a 2-deoxy- or 2,6-dideoxysugar, although it should be acknowledged that reactions of this type involving anomeric hydroxyl groups and oxalyl chloride have previously been described.<sup>223</sup> Although fairly unpopular, several methods facilitating the direct conversion of a methyl glycoside to a glycosyl chloride have been reported for non-deoxygenated carbohydrates<sup>227,228,229</sup> as well as a 3,6-dideoxysugar.<sup>230</sup> Chlorinating conditions used in these procedures include dichloromethyl methyl ether and a Lewis acid such as  $\text{BF}_3 \cdot \text{Et}_2\text{O}$  or  $\text{ZnCl}_2$ ,<sup>227</sup> boron trichloride and 2,6-*di*-*tert*butyl-4-methylpyridine,<sup>228</sup> acyl chloride and  $\text{ZnCl}_2$ ,<sup>229</sup> as well as hydrogen chloride and TMS chloride.<sup>230</sup> Given the inherent instability of 2,6-dideoxysugars as well as the TMS and TBDMS acid-sensitive protecting groups of **90**, none of these protocols seemed suitable for the preparation of **104** from methyl 2,6-dideoxyglycoside **90**.

Attention was subsequently turned to methods that could be used to directly prepare 2,6-dideoxyglycosyl bromide **103** from methyl 2,6-dideoxyglycoside **90**. The vast majority of publications describing this transformation involve trimethylsilyl bromide (TMS-Br). This versatile reagent has been quite extensively used to generate glycosyl bromides from 2-deoxysugar anomeric acetates,<sup>226</sup> 2,6-dideoxysugar anomeric hydroxyls,<sup>223,231</sup> non-deoxygenated methyl glycosides<sup>232</sup> and methyl 3,4,6-trideoxyglycosides<sup>233</sup> as well as from numerous methyl 2,6-dideoxyglycosides.<sup>234,235,236</sup>



All three procedures reporting the conversion of methyl 2,6-dideoxyglycosides to 2,6-dideoxyglycosyl bromides involved the use of approximately 2 equiv of TMS-Br and anhydrous benzene as a solvent at rt, while reaction times varied from 8-24 h.<sup>234,235,236</sup> Interestingly, some variation was observed with respect to ratios of products obtained using the aforementioned reaction conditions. For example, after stirring for 18 h, Monneret and coworkers discovered that  $\beta$ -configured methyl 2,6-dideoxyglycoside **110** had been transformed into both desired 2,6-dideoxyglycosyl bromide **111**, as well as  $\alpha$ -configured methyl 2,6-dideoxyglycoside **112**, while a small amount of unreacted starting material also remained (Figure 55).<sup>234</sup> The ratio of these products was not disclosed and this crude mixture was immediately used in the next synthetic step, which involved the formation of a disaccharide.

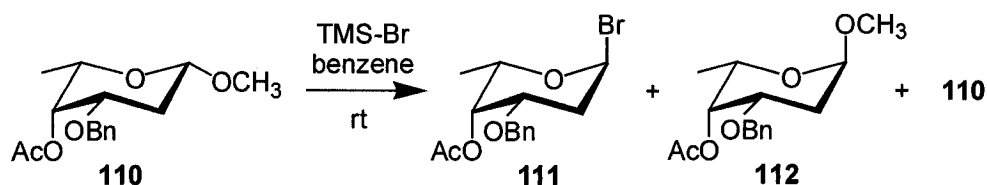


**Figure 55.** Synthesis of 2,6-dideoxyglycosyl bromide **111** from  $\beta$ -configured methyl 2,6-dideoxyglycoside **110** by Monneret and coworkers<sup>234</sup>

Using similar reaction conditions, Thiem and Meyer reported the conversion of two methyl 2,6-dideoxyglycosides (**113-114**) to their corresponding 2,6-dideoxyglycosyl bromides (**115-116**), after 8 h at rt with 2 equiv of TMS-Br in quantitative yield (Figure 56).<sup>236</sup>

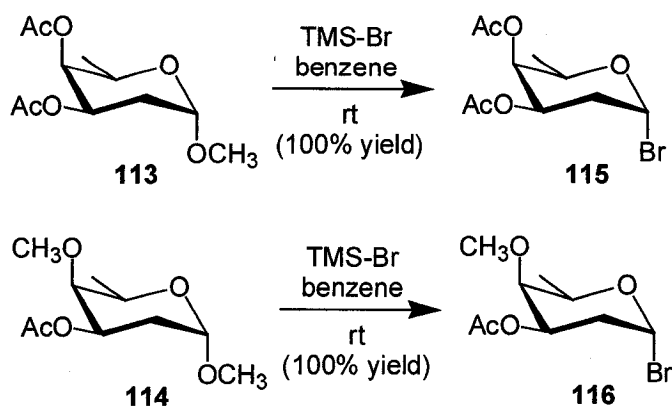


**Figure 56.** Synthesis of 2,6-dideoxyglycosyl bromides **115** and **116** from methyl 2,6-dideoxyglycosides **113** and **114**, respectively, by Thiem and Meyer<sup>236</sup>

Thus, methyl 2,6-dideoxyglycoside **90** was initially reacted with 2 equiv of TMS-Br in both toluene and DCM for 8 h at rt (Figure 57). Analysis of <sup>1</sup>H NMR spectra of crude reaction mixtures after careful concentration under reduced pressure revealed 2,6-dideoxyglycosyl bromide **103** as the major product along with β-configured methyl 2,6-dideoxyglycoside **117** as a minor product in both cases although the proportion of byproduct **117** was higher when toluene was used as a solvent by <sup>1</sup>H NMR integration. Additional experiments with DCM as a solvent revealed reaction with **90** was complete using just 1 equiv of TMS-Br after only 1 h (Figure 58). Using only 1 equiv of TMS-Br for this shorter reaction time period also resulted in the suppression of byproducts, as exclusively 2,6-dideoxyglycosyl bromide **103** was prepared by <sup>1</sup>H NMR (δ 6.46 (br d,  $J_{1,2a} = 4.0$  Hz, 1 H, H-1)) under these conditions. Interestingly, longer reaction times (15 h) with **90** and 1 equiv of TMS-Br resulted in complete conversion to β-configured methyl 2,6-dideoxyglycoside **117** by <sup>1</sup>H NMR.

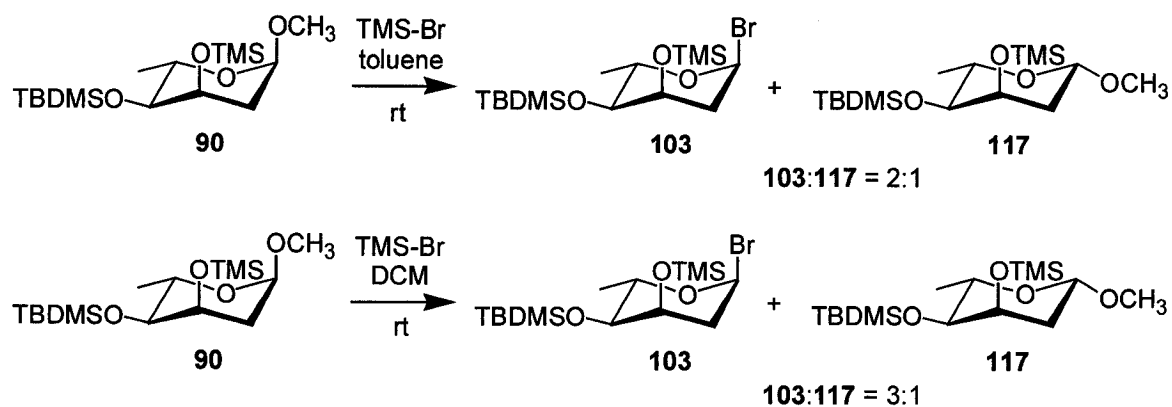


**Figure 57.** Synthesis of 2,6-dideoxyglycosyl bromide **103** from methyl 2,6-dideoxyglycoside **90** using 2 equiv of TMS-Br in toluene and DCM

Following careful concentration under reduced pressure, 2,6-dideoxyglycosyl bromide **103** was added directly to a second flask containing UDP ( $\text{Bu}_4\text{N}^+$  salt titrated to pH 6 as previously described by Ernst and Klaffke<sup>145,146</sup>), triethylamine, and 3 Å molecular sieves in DCM (Figure 58). After stirring this coupling reaction for 2 h at rt, all 2,6-dideoxyglycosyl bromide **103** had reacted or was degraded upon TLC and no further reaction progress was evident by HPLC.

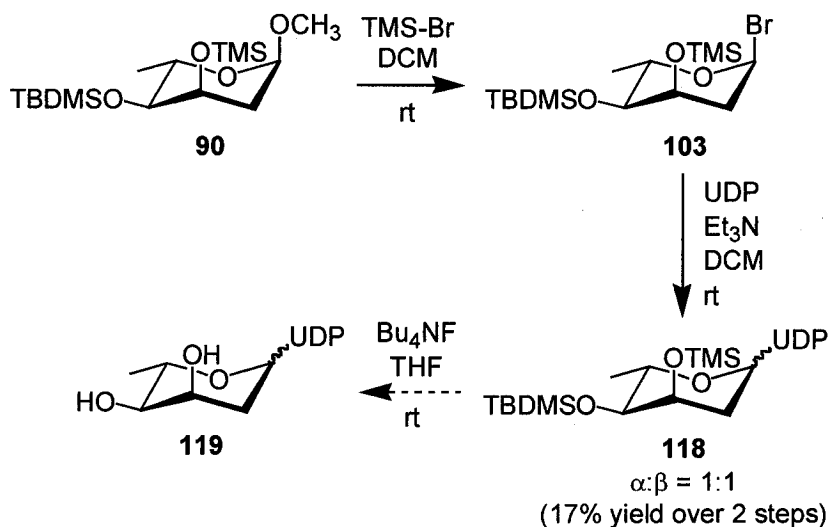


**Figure 58.** Synthesis of UDP- $\alpha/\beta$ -L-digitoxose (**119**) via 2,6-dideoxyglycosyl bromide **103**, produced using 1 equiv of TMS-Br from methyl 2,6-dideoxyglycoside **90**

After filtration of molecular sieves and concentration under reduced pressure, the reaction mixture was re-dissolved in H<sub>2</sub>O and immediately adjusted to pH 8 using triethylamine as silyl-protected 2,6-dideoxysugar nucleotide **118** readily decomposed at pH values below 8. Alkaline phosphatase was subsequently added to degrade unreacted UDP to uridine and inorganic phosphate, which greatly facilitated the purification process. 2,6-Dideoxysugar nucleotide **118** was efficiently purified using C18 reversed-phase chromatography with H<sub>2</sub>O and MeOH (both containing 0.1% NH<sub>4</sub>HCO<sub>3</sub> as previously described by Kahne and coworkers<sup>223</sup>), which afforded **118** in 17% yield over 2 steps by UV spectroscopy. Of particular note was the instability of protected 2,6-dideoxysugar nucleotide **118** to C18 reversed-phase ion-pair chromatography conditions involving the use of aqueous tributylammonium acetate (pH 4)<sup>237</sup> (Section 2.3.2.2) and aqueous tributylammonium bicarbonate buffers (pH 6) (Section 2.3.3.3).

Following the successful purification of silyl-protected UDP- $\alpha/\beta$ -L-digitoxose derivative **118**, the compound was carefully concentrated under reduced pressure, re-dissolved in THF, and Bu<sub>4</sub>NF (1.5 equiv per silyl protecting group) was added to facilitate the removal of silyl protecting groups. After 30 min at rt, HPLC analysis revealed the complete consumption of **118** ( $t_R$  = 9.23 min) and the formation of two new peaks: one major ( $t_R$  = 5.88 min) and one minor ( $t_R$  = 5.70 min). Following cation exchange (Dowex® ion exchange resin, Na<sup>+</sup> form), the deprotection reaction products were analyzed via <sup>1</sup>H and <sup>31</sup>P{<sup>1</sup>H} NMR, which revealed that presence of both UDP and UDP- $\alpha/\beta$ -L-digitoxose (**119**) in an unfavourable 4:1 ratio. This analysis was confirmed via LC-MS as molecular ions of both UDP and **119** were detected.

Tetra-*n*-butylammonium fluoride in THF has previously been used to successfully remove both trimethylsilyl<sup>143</sup> and triethylsilyl<sup>145</sup> protecting groups from sugar nucleotides, although deprotection of this type has not been reported with a 2,6-dideoxysugar nucleotide. Future deprotection efforts will focus on using Bu<sub>4</sub>NF in THF at 0 °C or lower as reported by Kirschning and coworkers for the TBDMS deprotection of a 2,6-dideoxyglycoside.<sup>62</sup>

The aforementioned synthetic scheme and purification protocol was developed using UDP in lieu of dTDP because of the significantly higher cost of the latter nucleoside 5'-diphosphate (dTDP: 50 mg = \$274.00 CAD as opposed to UDP: 1 g = \$270.00 CAD from Sigma-Aldrich).<sup>e</sup> Once suitable deprotection conditions are established, the aforementioned synthetic route will be used to prepare dTDP- $\alpha/\beta$ -L-digitoxose (**46**).

### 2.3.2. Preparation of Analogue Sugar Nucleotides via an Indirect Coupling Methodology

To facilitate the synthesis of analogue sugar nucleotides from commercially available monosaccharides L-fucose (**54**), L-rhamnose (**55**), and L-arabinose (**56**), several traditional indirect coupling strategies employing nucleoside 5'-monophosphates activated using morpholidates<sup>135,136,139</sup> and imidazolides<sup>137,138</sup> were considered in addition to more recent approaches involving *N*-methylimidazolides<sup>238</sup> and *N*-methylpyrrolidines.<sup>239</sup> Of the available options, a synthetic strategy involving nucleoside 5'-monophosphate activation via *N*-methylimidazole was chosen due of the speed and simplicity of this approach.<sup>238</sup> This nucleoside 5'-monophosphate activation

---

<sup>e</sup> Sigma-Aldrich Canada, [http://www.sigmaaldrich.com/Area\\_of\\_Interest/The\\_Americas/Canada.html](http://www.sigmaaldrich.com/Area_of_Interest/The_Americas/Canada.html) (Accessed: 22/02/07).

method was first reported by Bogachev in 1996 for use in preparing nucleoside 5'-triphosphates<sup>240</sup> and has subsequently been used in the Jakeman laboratory to synthesize nucleoside 5'-triphosphate analogues.<sup>237</sup> In 2001, Marlow and Kiessling extended this nucleoside 5'-monophosphate activation method for use in the synthesis of sugar nucleotides, reporting the preparation of UDP- $\alpha$ -D-galactofuranose (**120**) via coupling of UMP-*N*-methylimidazolid (**121**) with  $\alpha$ -D-galactofuranose-1-phosphate (**122**) (Figure 59).<sup>238</sup> After 2 h at rt, the reaction was deemed complete and an 83% conversion to product was observed by  $^{31}\text{P}\{^1\text{H}\}$  NMR. Following purification by preparative-scale ion exchange HPLC, UDP- $\alpha$ -D-galactofuranose (**120**) was obtained in 35% yield as determined by UV spectroscopy.<sup>238</sup>

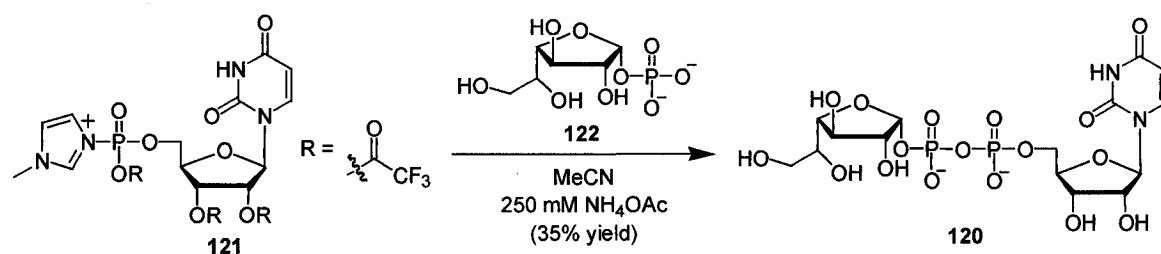


**Figure 59.** Synthesis of UDP- $\alpha$ -D-galactofuranose (**120**) via coupling of UMP-*N*-methylimidazolid (**121**) with  $\alpha$ -D-galactofuranose-1-phosphate (**122**) by Marlow and Kiessling<sup>238</sup>

In order to investigate the use of this synthetic strategy to prepare analogue sugar nucleotides, access to sugar-1-phosphates derived from L-fucose (**54**), L-rhamnose (**55**), and L-arabinose (**56**) was first required. The synthesis of these precursors is described below in Section 2.3.2.1.

### 2.3.2.1. Synthesis of Sugar-1-Phosphates

Many indirect coupling strategies employed to prepare sugar nucleotides involve the use of  $\alpha$ -D-sugar-1-phosphates, several of which are commercially available. Other more exotic  $\alpha$ -D-sugar-1-phosphates are often easily accessed via numerous synthetic approaches as the  $\alpha$  anomers of these phosphorylated sugars are thermodynamically favoured due to the anomeric effect.<sup>155,222,241,242</sup> Although  $\alpha$ -D-sugar nucleotides are useful in the study of many glycosyltransferases involved in the biosynthesis of oligosaccharides and glycoconjugates, most natural product glycosyltransferases require  $\beta$ -L-sugar nucleotide substrates to form  $\alpha$ -glycosides via an inverting mechanism (Section 1.4.3.1). Since the  $\beta$  anomers of sugar-1-phosphates are formed under kinetic control, and are susceptible to anomerization under acidic conditions, fewer synthetic routes have been developed to efficiently prepare this class of compounds.

While  $\beta$  anomers of sugar-1-phosphates are usually more difficult to access in high diastereomeric excess, some exceptions to this general rule exist, such as in the case of  $\beta$ -L-fucose-1-phosphate (**123**). Since the C-2 hydroxyl group of L-fucose (**54**) is equatorial in the  ${}^1C_4$  chair conformation, protection of C-2 with an acyl functionality facilitates neighbouring group participation, which promotes the formation of the desired  $\beta$  anomer (Figure 60).

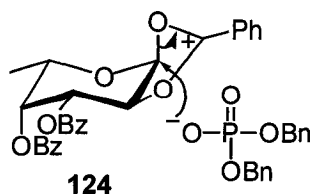


**Figure 60.** Influence of neighbouring group participation on the trajectory of dibenzyl phosphate attack in the case of 2,3,4-tri-*O*-benzoyl- $\alpha$ -L-fucopyranosyl bromide (**124**)

To prepare  $\beta$ -L-fucose-1-phosphate (**123**), a modified procedure based on a synthetic route reported by Wong and coworkers was employed (Figure 61).<sup>243</sup> The first step in this strategy involved the benzylation of L-fucose (**54**) using benzoyl chloride and pyridine, which easily afforded 1,2,3,4-tetra-*O*-benzoyl- $\alpha/\beta$ -L-fucopyranose (**125**) in 94% yield after 3 h at rt. Bromination of **125** with phosphorus tribromide and H<sub>2</sub>O in DCM as described by Liang and Grindley<sup>244</sup> was similarly facile, producing 2,3,4-tri-*O*-benzoyl- $\alpha$ -L-fucopyranosyl bromide (**124**) as a white crystalline solid in 96% yield after 4 h at rt. The key phosphorylation step involved the use of dibenzyl phosphate, silver triflate, and 2,4,6-collidine in DCM at -40 °C for 4 h, after which time the reaction mixture was allowed to slowly warm to rt overnight. <sup>1</sup>H and <sup>31</sup>P{<sup>1</sup>H} NMR analysis of the crude reaction mixture revealed that exclusively the  $\beta$  anomer of the desired phosphorylated product (**126**) had been produced with the only contaminants visible by NMR being 2,4,6-collidine and a small amount of hydrolyzed glycosyl bromide. To streamline the purification protocol, the crude reaction mixture was used directly in the next deprotection step where 2,4,6-collidine and the degraded glycosyl bromide were easily extracted into the organic layer after hydrogenolysis of the benzyl protecting groups. Following hydrogenolysis of **126** using 10% Pd/C in 1 M aqueous NaHCO<sub>3</sub> and MeOH, newly deprotected product 2,3,4-tri-*O*-acetyl- $\beta$ -L-fucose-1-phosphate (**127**) was deacetylated using 1 M aqueous NaOH over 3 h while gradually warming from 0 °C to rt. After neutralizing the pH of the reaction mixture with 1 M aqueous acetic acid, cation exchange, lyophilization, and trituration with ethanol to remove residual NH<sub>4</sub>OAc,  $\beta$ -L-fucose-1-phosphate (**123**) was obtained as a white solid in 39% yield over 3 steps.



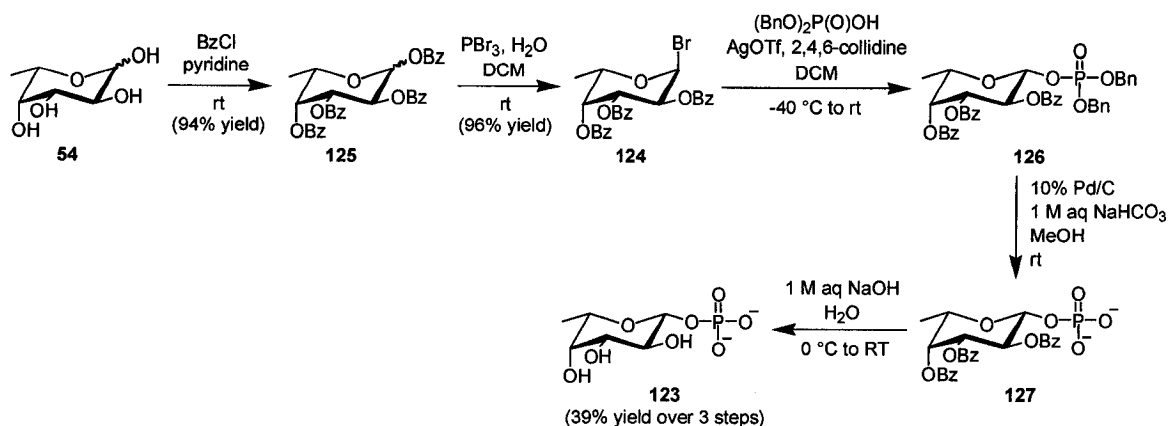


**Figure 61.** Synthesis of  $\beta$ -L-fucose-1-phosphate (**123**)

Several NMR experiments were used to confirm the anomeric stereochemistry of  $\beta$ -L-fucose-1-phosphate (**123**). In addition to the traditional  $^3J_{\text{H-1,H-2}}$  value extracted from the  $^1\text{H}$  NMR spectrum, which is quite definitive in itself for **123** with a value of 8.0 Hz, a coupled  $^{13}\text{C}$ - $^1\text{H}$  HSQC NMR experiment was employed to measure the value of  $^1J_{\text{C-1,H-1}}$ . The use of this coupling constant to determine anomeric stereochemistry was first reported by Bock and coworkers in the 1970s,<sup>245,246</sup> and is now extensively employed in the assignment of anomeric stereochemistry of disaccharide linkages.<sup>247</sup> Its use in the structural determination of other glycosides<sup>220</sup> as well as sugar nucleotides<sup>248</sup> has also been reported. Bock and coworkers demonstrated that the magnitude of  $^1J_{\text{C-1,H-1}}$  values could be reliably linked to the orientation of the C-1 substituent, providing convenient access to information regarding anomeric stereochemistry of hexopyranoses.<sup>245,246</sup> *O*-Linked glycosides with axially-oriented protons at C-1 typically have a  $^1J_{\text{C-1,H-1}}$  value of 158-162 Hz, while *O*-linked glycosides with equatorially-oriented protons at C-1 typically have a  $^1J_{\text{C-1,H-1}}$  value of 169-171 Hz.<sup>246</sup> Only glycosides with similar anomeric functionalities can be compared, as the electronegativity of the C-1 substituent affects  $^1J_{\text{C-1,H-1}}$  values, although a relative difference of *ca.* 10 Hz is often still observed between

$\alpha$  and  $\beta$  anomers.<sup>245</sup> Given these observations, commercially available  $\alpha$ -D-glucose-1-phosphate (**128**) and  $\alpha$ -D-mannose-1-phosphate (**129**) were first evaluated as standards and  $^1J_{C-1,H-1}$  values of 169 Hz and 170 Hz, respectively, were observed. These values correspond well with literature expectations due to their equatorially-oriented C-1 protons (Figure 62).<sup>245,246</sup>

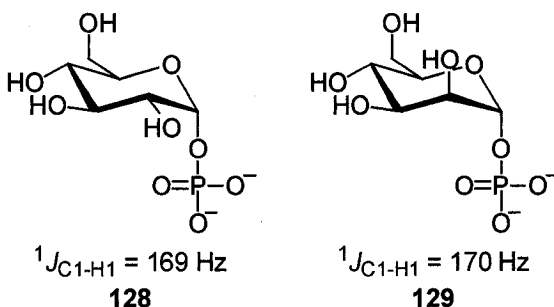


**Figure 62.** Structures and  $^1J_{C-1,H-1}$  values of  $\alpha$ -D-glucose-1-phosphate (**128**) and  $\alpha$ -D-mannose-1-phosphate (**129**)

On extension of this characterization approach to  $\beta$ -L-fucose-1-phosphate (**123**), a  $^1J_{C-1,H-1}$  value of 162 Hz was obtained, further supporting the formation of the desired  $\beta$  anomer (Figure 63). In addition, through space correlations observed using 1D NOE and 2D NOESY NMR experiments were consistent with all coupling constants, confirming the exclusive formation of  $\beta$ -L-fucose-1-phosphate (**123**).

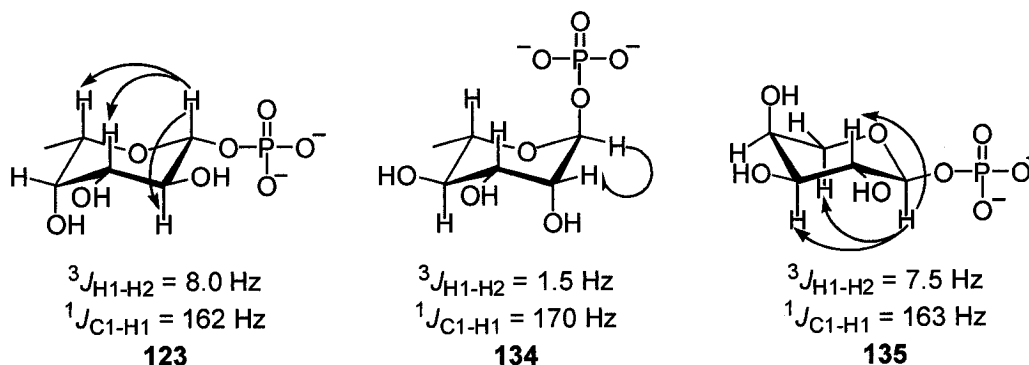


**Figure 63.** NMR characterization data supporting the preparation of  $\beta$ -L-fucose-1-phosphate (**123**),  $\alpha$ -L-rhamnose-1-phosphate (**134**), and  $\alpha$ -L-arabinose-1-phosphate (**135**) (arrows indicate strong 1D NOE interactions)

Efforts were also directed toward preparing  $\beta$ -L-rhamnose-1-phosphate due to the structural similarity of L-rhamnose (**55**) and L-digitoxose (**50**) (Figure 27) and the biological relevance of dTDP- $\beta$ -L-rhamnose, a sugar nucleotide involved in bacterial cell wall biosynthesis and thus an antibiotic target.<sup>153</sup> Of the small number of published procedures describing the preparation of  $\beta$ -L-rhamnose-1-phosphate,<sup>138,249,250,251</sup> that of Zhao and Thorson was most attractive due to its ease and stereoselectivity as well as its similarity to the synthetic strategy previously described for the preparation of  $\beta$ -L-fucose-1-phosphate (**123**) (Figure 64).<sup>138</sup> The first step in this synthesis involved the acetylation of L-rhamnose (**55**) using acetic anhydride and pyridine, which easily afforded acetylated derivative **130** in quantitative yield. Subsequent bromination of **130** with phosphorus tribromide and H<sub>2</sub>O in DCM<sup>244</sup> produced glycosyl bromide **131** in 89% yield. Phosphorylation of **131** with dibenzyl phosphate, silver triflate, and 2,4,6-collidine again produced exclusively one anomer as in the case of  $\beta$ -L-fucose-1-phosphate (**123**). This crude reaction mixture was carried directly through to deprotection steps as described above for **123** to enhance synthetic route efficiency, producing **134** in 43% over 3 steps.

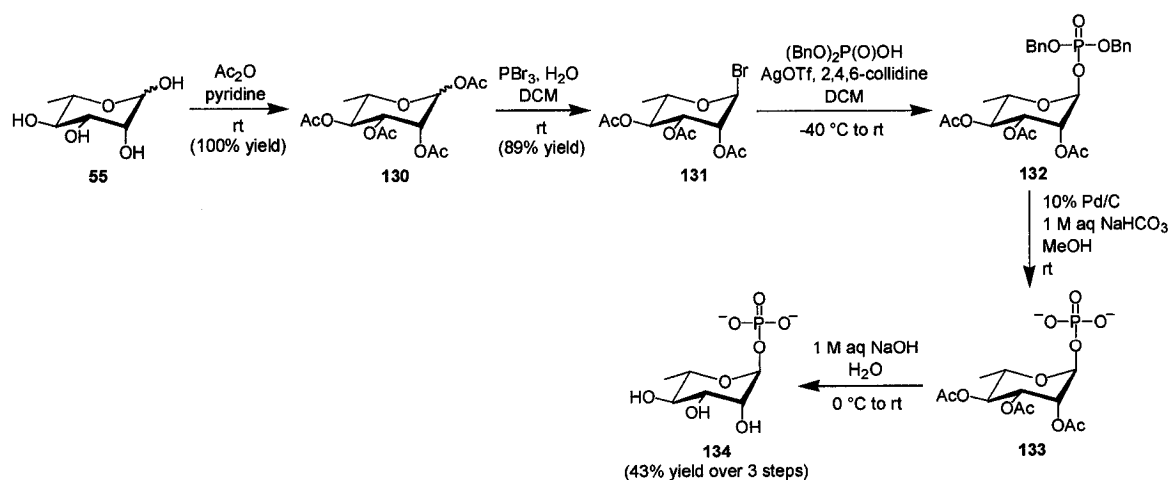


**Figure 64.** Synthesis of  $\alpha$ -L-rhamnose-1-phosphate (**134**)

It was anticipated that the single diastereomer prepared using this procedure would be  $\beta$ -L-rhamnose-1-phosphate as Zhao and Thorson reported a yield of 78% after chromatography in the initial phosphorylation step of the synthesis of this compound.<sup>138</sup> An analysis of  $^1\text{H}$ ,  $^{31}\text{P}\{^1\text{H}\}$ , and  $^{13}\text{C}\{^1\text{H}\}$  NMR data of **134** generally revealed good agreement with that of Zhao and Thorson.<sup>138</sup> Of particular interest with respect to anomeric stereochemistry were  $^3J_{\text{H1-H2}}$  values. In the case of **134**,  $^3J_{\text{H1-H2}}$  was equal to 1.5 Hz; however, no  $^3J_{\text{H1-H2}}$  value was reported by Zhao and Thorson,<sup>138</sup> possibly due to characterization of  $\beta$ -L-rhamnose-1-phosphate as a triethylammonium salt (1.6 equiv), which can result in decreased spectral resolution. The similarities between our characterization data for **134** with that of Zhao and Thorson initially supported the belief that  $\beta$ -L-rhamnose-1-phosphate had been prepared via kinetic control under the conditions described above. Nevertheless, measurement of the  $^1J_{\text{C1-H1}}$  value of **134** resulted in a coupling constant of 170 Hz, suggesting that an equatorially-oriented proton was present at C-1 and the opposite anomer,  $\alpha$ -L-rhamnose-1-phosphate (**134**), had actually been prepared using the aforementioned methodology (Figure 64). Further 1D NOE and 2D NOESY NMR experiments confirmed this hypothesis as irradiation of equatorially-oriented H-1 resulted in only one through space correlation to equatorially-oriented H-2 whereas, in the case of  $\beta$ -L-fucose-1-phosphate (**123**), strong correlations were observed from axially-oriented H-1 to both H-3 and H-5, also both in axial orientations (Figure 63). Interestingly, Prihar and Behrman reported the preparation of both  $\alpha$ -L-rhamnose-1-phosphate (**134**) and  $\beta$ -L-rhamnose-1-phosphate in 1973 using a methodology involving *o*-phenylene phosphorochloridate and 2,3,4-tri-*O*-acetyl- $\alpha/\beta$ -L-rhamnopyranose (**131**).<sup>251</sup> Moreover,  $^1\text{H}$  NMR analysis revealed the  $^3J_{\text{H1-H2}}$  value of  $\alpha$ -L-rhamnose-1-phosphate

(**134**) to be 1.5 Hz, while a value of 1.0 Hz was reported for  $\beta$ -L-rhamnose-1-phosphate, illustrating the similarity between the H1-C1-C2-H2 dihedral angles of  $\alpha$  and  $\beta$  anomers of this compound. Based on the effects of neighboring group participation, it would be anticipated that this coupling procedure would yield  $\alpha$ -L-rhamnose-1-phosphate (**134**).

Using a similar procedure to those described above,  $\alpha$ -L-arabinose-1-phosphate (**135**) was also prepared due to the structural similarities between L-digitoxose (**50**) and L-arabinose (**56**) (Figure 27). Also of particular interest was the structural similarity between L-arabinose (**56**) and 6-deoxy-L-altrose, the sugar component of the jadomycin B analogue ILEVS1080 (**25**) (Figure 15), as the only difference between these two monosaccharides is a C-5 methyl group, present in 6-deoxy-L-altrose, but absent in **56**. In a similar fashion to L-rhamnose (**55**), L-arabinose (**56**) was first acetylated using acetic anhydride and pyridine, generating acetylated derivative **136** in 99% yield (Figure 65). Subsequent bromination with phosphorus tribromide and H<sub>2</sub>O in DCM afforded acetylated glycosyl bromide **137** in 78% yield. Phosphorylation using dibenzyl phosphate, silver triflate, and 2,4,6-collidine in DCM at -40 °C to rt again proceeded stereoselectively, affording only one phosphorylated anomer (**138**) on analysis of the crude reaction mixture. As described above, this crude reaction mixture was directly subjected to hydrogenolysis to deprotect benzyl phosphate esters, producing acetylated sugar-1-phosphate derivative **139**, after which time a simple extraction was used to remove organic-soluble impurities. Following deacetylation using 1 M aqueous NaOH and cation exchange,  $\alpha$ -L-arabinose-1-phosphate (**135**) was obtained in 40% yield over 3 steps.

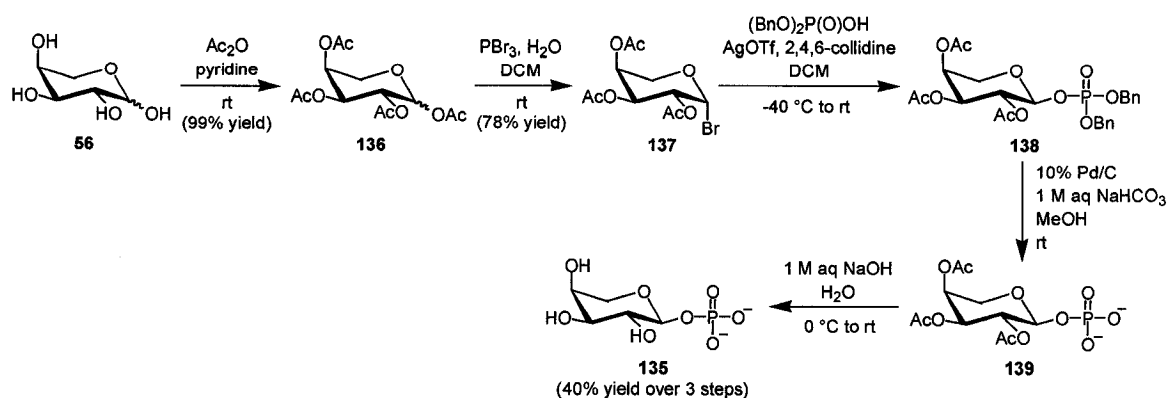


**Figure 65.** Synthesis of α-L-arabinose-1-phosphate (**135**)

On examination of the  $^1\text{H}$  NMR spectrum of **135**, a  $^3J_{\text{H1-H2}}$  value of 7.5 Hz was observed. This, along with other  $^1\text{H}$  NMR coupling constants, suggests that α-L-arabinose-1-phosphate (**135**) is predominantly in a  $^4\text{C}_1$  chair conformation. In this conformation, two of the three hydroxyl groups of **135** are equatorial whereas in the  $^1\text{C}_4$  chair conformation, only one of the three hydroxyl groups of **135** would be equatorial, making the  $^4\text{C}_1$  chair conformation energetically favourable. Although the anomeric effect would stabilize the opposite  $^1\text{C}_4$  chair conformation, a 1,3-diaxial interaction between C-1 and C-3 substituents significantly destabilizes this conformation, leading to the predominance of the  $^4\text{C}_1$  chair conformation. With respect to anomeric stereochemistry, a  $^1J_{\text{C1-H1}}$  value of 163 Hz was obtained for **135**, suggesting the formation of the α anomer, which is consistent with the observed  $^3J_{\text{H1-H2}}$  value of 7.5 Hz and the expected result based on neighbouring group participation (Figure 63). Furthermore, 1D NOE and 2D NOESY NMR experiments, with strong correlations to H-2, H-3, and H-5a on irradiation of H-1, lent additional support to the aforementioned conformational and stereochemical conclusions.

This synthetic approach to prepare sugar-1-phosphates has been extended to 2-deoxy-2-fluorosugars by Stephanie Lucas, a summer student in the Jakeman laboratory.

Phosphorylation of several fluorinated glycosyl bromides using the aforementioned methodology resulted in the stereoselective formation of 2-deoxy-2-fluoro- $\alpha$ -L-rhamnose-1-phosphate (**140**), 2,6-dideoxy-2-fluoro- $\beta$ -L-glucose-1-phosphate (**141**), and 2-deoxy-2-fluoro- $\beta$ -L-fucose-1-phosphate (**142**), all possessing 1,2-*trans* stereochemistry (Figure 66).<sup>252</sup>

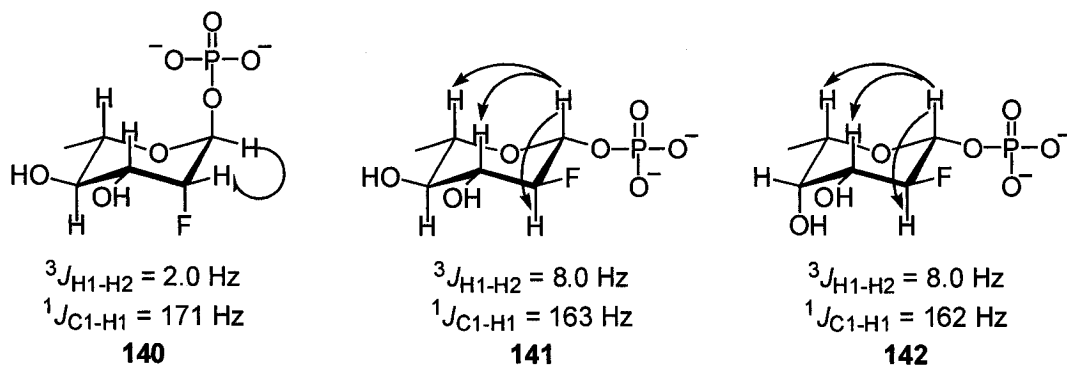


**Figure 66.** NMR characterization data supporting the preparation of 2-deoxy-2-fluoro- $\alpha$ -L-rhamnose-1-phosphate (**140**), 2,6-dideoxy-2-fluoro- $\beta$ -L-glucose-1-phosphate (**141**), and 2-deoxy-2-fluoro- $\beta$ -L-fucose-1-phosphate (**142**) (arrows indicate strong 1D NOE interactions)

Fluorinated sugar-1-phosphates **140**, **141**, and **142** will be tested for utility as nucleotidyltransferase inhibitors as well as glycosyltransferase inhibitors after conversion to sugar nucleotides via coupling with activated nucleoside 5'-monophosphates.

### 2.3.2.2. Coupling of Sugar-1-Phosphates with *N*-Methylimidazole Nucleoside 5'-Monophosphate Donors

The synthesis of sugar nucleotides via an indirect coupling approach requires the initial generation of an electrophilic nucleoside 5'-monophosphate, which is subsequently coupled with a sugar-1-phosphate. In this case, electrophilic NMP-*N*-methylimidazolides were generated from adenosine 5'-monophosphate (**143**) and uridine 5'-monophosphate

(144) via two rapid *in situ* steps as previously described by Marlow and Kiessling<sup>238</sup> as well as Mohamady and Jakeman<sup>237</sup> (Figure 67). The first step involved the trifluoroacetylation of nucleoside 5'-monophosphates using an excess of trifluoroacetic anhydride in the presence of triethylamine and dimethylaniline in MeCN, which was complete after 15 min at rt. Following the removal of volatile components under reduced pressure, the addition of *N*-methylimidazole facilitated the formation of NMP-*N*-methylimidazolides 145 and 121 in only an additional 15 min at rt. The successful generation of these activated species was confirmed by <sup>31</sup>P{<sup>1</sup>H} NMR as AMP- (145) and UMP-*N*-methylimidazolides (121) were detected as singlets with distinctive <sup>31</sup>P{<sup>1</sup>H} chemical shifts of -11.0 and -10.8 ppm, respectively.<sup>238</sup>

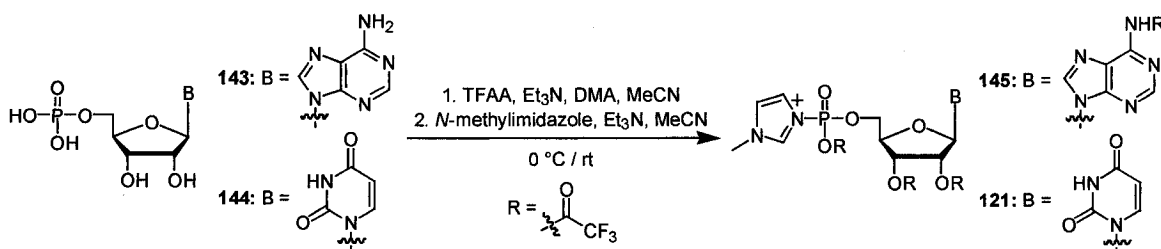


**Figure 67.** Preparation of AMP- (145) and UMP-*N*-methylimidazolides (121)

As nucleoside 5'-monophosphates are hygroscopic and contain equiv of H<sub>2</sub>O, previously published coupling procedures often necessitate the removal of this moisture before use of NMPs in coupling reactions via azeotroping with pyridine.<sup>253,139</sup> *N*-Methylimidazolide activation circumvents this requirement as H<sub>2</sub>O is conveniently removed via reaction with excess equivalents of trifluoroacetic anhydride. It was also determined that nucleoside 5'-monophosphate triethylammonium salts<sup>238</sup> are not required, as the reaction sequence worked well with commercially available nucleoside 5'-monophosphates in free acid form.<sup>237</sup>



With respect to organic bases, both *N,N*-dimethylaniline and triethylamine were employed in the initial acylation reaction as this mixture of bases was found to be optimal in the first study describing this activation method by Bogachev.<sup>240</sup> It was reasoned that *N,N*-dimethylaniline ( $pK_a = 4.8$ ), a weaker base than triethylamine ( $pK_a = 10.9$ ), is better suited for mild acylation; however, triethylamine was useful in preventing degradation of nucleosides which can result from the acidification of the reaction mixture after trifluoroacetic anhydride addition.<sup>240</sup> Higher sugar nucleotide yields were obtained using *N,N*-dimethylaniline in contrast to another report from our laboratory describing the synthesis of nucleoside 5'-triphosphate analogues in which this reagent was found to have no effect on product formation and was omitted.<sup>237</sup>

Following the *in situ* activation of nucleoside 5'-monophosphates **143** and **144**, NMP-*N*-methylimidazolides **145** and **121**, were independently coupled with 2 equiv of various sugar-1-phosphates (**128**, **135**, **123**, **134**) in MeCN (Figure 68). An excess of sugar-1-phosphate was used in an attempt to suppress side reactions as reported by Bogachev,<sup>240</sup> although unreacted sugar-1-phosphates were quantitatively recovered during the purification process and could be used again in future reactions after cation exchange. The coupling reactions, monitored by  $^{31}\text{P}\{^1\text{H}\}$  NMR, were deemed complete after 2 h at rt, after which time they were quenched with cold 250 mM aqueous  $\text{NH}_4\text{OAc}$  (pH 7) to facilitate product deacylation.<sup>238</sup> This 2 h reaction time is of notable significance when compared with reaction times of 1-3 days, which are frequently reported for synthetic routes involving morpholidate-activated nucleoside 5'-monophosphates.<sup>140,141,254</sup> Sugar nucleotide products were purified using automated C18 reversed-phase ion-pair chromatography.

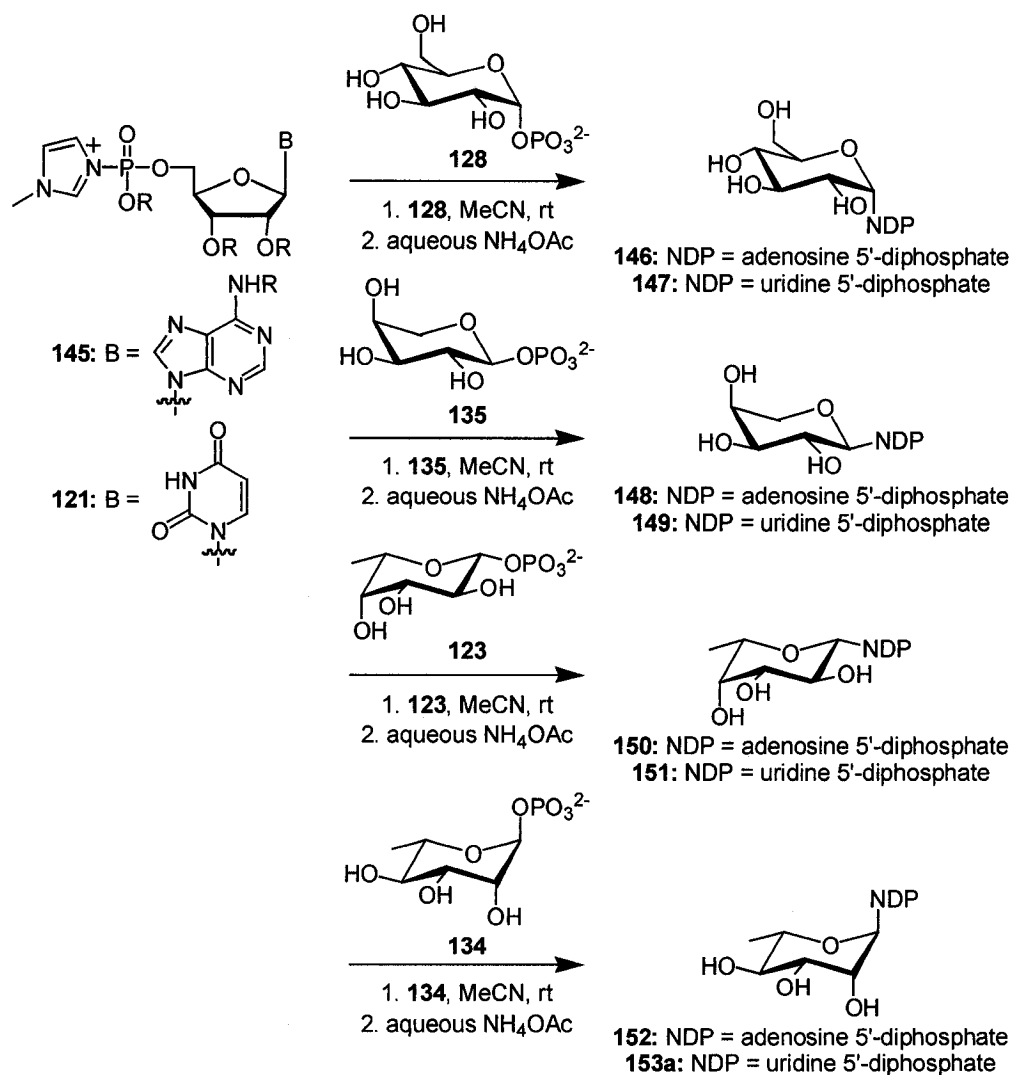


**Figure 68.** Reaction of sugar-1-phosphates with NMP-*N*-methylimidazolides to prepare sugar nucleotides **146-153a**

Commercially available α-D-glucose-1-phosphate (**128**) and AMP-*N*-methylimidazolide (**145**) were initially employed to test this synthetic procedure. Following coupling and purification, ADP-α-D-glucose (**146**) was isolated in 48% yield over 4 steps. This protocol was extended to UMP (**144**), a pyrimidine base-containing nucleotide, which resulted in the preparation of UDP-α-D-glucose (**147**) in 35% yield over 4 steps. On extension of this coupling procedure to synthetically prepared sugar-1-phosphates α-L-arabinose-1-phosphate (**135**), β-L-fucose-1-phosphate (**123**), and

$\alpha$ -L-rhamnose-1-phosphate (**134**), conversions to product of approximately 40-50% by  $^{31}\text{P}\{^1\text{H}\}$  NMR were obtained in all cases. Purification of this series of sugar nucleotides required the removal of dinucleoside diphosphates (NppNs), which were the main byproducts in all reactions, presumably resulting from the self-condensation of NMP-*N*-methylimidazolides. In the case of sugar nucleotides **146-149**, 10 mM aqueous tributylammonium acetate (pH 4) was used as an ion-pair reagent in C18 reversed-phase chromatography as previously described by Mohamady and Jakeman;<sup>237</sup> however, this purification methodology could not be easily extended to sugar nucleotides **150-153a**. The purification of these four  $\beta$ -L-fucose- and  $\alpha$ -L-rhamnose-containing sugar nucleotides (**150-153a**) was instead achieved by changing the ion-pair reagent to 10 mM aqueous tributylammonium bicarbonate, which enabled the separation of sugar nucleotides from NppNs. A summary of results obtained via this coupling procedure is shown in Table 3.

**Table 3.** Yields of sugar nucleotides prepared via coupling of sugar-1-phosphates with NMP-*N*-methylimidazolides

product	sugar-1-phosphate	NMP	reaction time (h)	yield by UV <sup>*,±</sup> (%)
<b>146</b>	$\alpha$ -D-glucose-1-phosphate	AMP	2	48
<b>147</b>	$\alpha$ -D-glucose-1-phosphate	UMP	2	35
<b>148</b>	$\alpha$ -L-arabinose-1-phosphate	AMP	2	35
<b>149</b>	$\alpha$ -L-arabinose-1-phosphate	UMP	2	32
<b>150</b>	$\beta$ -L-fucose-1-phosphate	AMP	2	28
<b>151</b>	$\beta$ -L-fucose-1-phosphate	UMP	2	26
<b>152</b>	$\alpha$ -L-rhamnose-1-phosphate	AMP	2	25
<b>153a</b>	$\alpha$ -L-rhamnose-1-phosphate	UMP	2	30

\* Yields are reported for purified products over 4 steps from NMPs.

± UV yields were determined at  $\lambda_{\text{max}}$  260 nm ( $\epsilon = 1.51 \times 10^4 \text{ M}^{-1}\text{cm}^{-1}$ ) for products containing adenosine and  $\lambda_{\text{max}}$  261 nm ( $\epsilon = 1.01 \times 10^4 \text{ M}^{-1}\text{cm}^{-1}$ ) for products containing uridine.

In summary, the coupling of nucleoside 5'-monophosphate-*N*-methylimidazolides with sugar-1-phosphates is a fast, reproducible method to prepare sugar nucleotides, although the purification of these compounds can prove tedious due to the formation of NppNs. The moderate yields obtained using this synthetic strategy are generally comparable to yields reported using the popular morpholidate method of nucleoside 5'-monophosphate activation,<sup>140,141,254</sup> although the increased electrophilicity NMP-*N*-methylimidazolides facilitates much shorter coupling times than previously reported methods.<sup>140,141,254</sup>

### **2.3.3. Preparation of Analogue Sugar Nucleotides via Direct Coupling Methodologies**

To circumvent the difficulties associated with indirect coupling methodologies such as the necessity to first prepare sugar-1-phosphates and sugar nucleotide purification from dinucleoside diphosphates, several direct coupling strategies were explored to synthesize sugar nucleotides. As discussed in Section 1.5.1, previous synthetic approaches of this type involved the coupling of nucleoside 5'-diphosphates with benzylated glycosyl bromides,<sup>142</sup> trimethylsilylated glycosyl iodides,<sup>143</sup> 2-(1,2-*trans*-glycopyranosyloxy)-3-methoxypyridines (MOP glycosides),<sup>144</sup> and triethylsilylated and benzylated epoxides.<sup>145,146</sup>

#### **2.3.3.1. Nucleoside 5'-Diphosphate-*N*-Methylimidazolidone Donors**

Initial direct coupling efforts focused on an extension of the nucleoside 5'-monophosphate-*N*-methylimidazolidone procedure. It was reasoned that this approach could be expanded to generate nucleoside 5'-diphosphate-*N*-methylimidazolidone donors,

which could subsequently be coupled with monosaccharides selectively deprotected at the anomeric centre with the assistance of a base.

To investigate this novel approach to the synthesis of sugar nucleotides, uridine 5'-diphosphate (**154**) was used as a model nucleoside 5'-diphosphate in attempts to generate a UDP-*N*-methylimidazolidone donor (Figure 69). Uridine 5'-diphosphate was first trifluoroacetylated and subsequently treated with *N*-methylimidazole in an attempt to prepare UDP-*N*-methylimidazolidone as described for the generation of NMP-*N*-methylimidazolidones in Section 2.3.1.2. Unfortunately,  $^{31}\text{P}\{^1\text{H}\}$  and  $^{31}\text{P}$ - $^1\text{H}$  HSQC NMR analysis of products generated via this reaction sequence revealed the presence of two singlets corresponding to UMP-*N*-methylimidazolidone (**121**) and inorganic phosphate (**155**). These products presumably result from nucleophilic attack of *N*-methylimidazole at the  $\alpha$  phosphorus instead of the desired  $\beta$  phosphorus atom, resulting in displacement of the entire  $\beta$  phosphate group in lieu of a single trifluoroacetyl functionality. Based on these results, this approach was not further pursued.

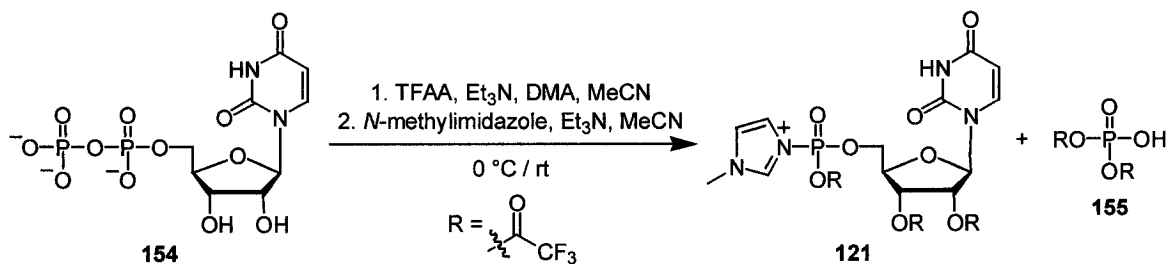


**Figure 69.** Reaction attempt to generate a UDP-*N*-methylimidazolidone electrophile for coupling with a selectively deprotected monosaccharide

### 2.3.3.2. Glycosyl Iodide Donors

Of the direct coupling methods previously described,<sup>142,143,144,145,146</sup> that of Uchiyama and Hindsgaul involving the coupling of trimethylsilylated glycosyl iodides

with nucleoside 5'-diphosphates<sup>143</sup> was most attractive due to the directness of this route and the ease of *in situ* protecting group removal with tetra-*n*-butylammonium fluoride. Specifically, Uchiyama and Hindsgaul demonstrated the rapid conversion of L-arabinose, D-galactose, and several deoxysugars from the D-galactose series, to uridine diphosphosugars via the *in situ* formation of trimethylsilyl-protected glycosyl iodides, followed by coupling with UDP, and deprotection using Bu<sub>4</sub>NF.<sup>143</sup> Moderate yields of 30 to 49% were obtained over 3 steps after purification via treatment with alkaline phosphatase followed by ion exchange chromatography.<sup>143</sup> Of particular interest were the  $\alpha$ : $\beta$  stereoselectivities obtained in the key coupling step with UDP using this series of monosaccharide donors. According to Uchiyama and Hindsgaul,  $\alpha$ : $\beta$  ratios of 1:1 were frequently observed, although several exceptions were noted in the case of deoxysugars where  $\alpha$ : $\beta$  ratios of 3:1 and 1:3 were reported for UDP-2-deoxy- $\alpha$ -D-galactose and UDP-4-deoxy- $\alpha$ -D-galactose, respectively.<sup>143</sup>

L-Rhamnose (**55**) was chosen as a model monosaccharide along with UDP to investigate this approach due to difficulties associated with preparing  $\beta$ -L-rhamnose-1-phosphate for reaction with NMP-*N*-methylimidazolides (Section 2.3.1.1). Initial protection of L-rhamnose (**55**) using trimethylsilyl chloride and pyridine proceeded smoothly, affording trimethylsilyl-protected derivative **156** in quantitative yield (Figure 70). Reaction of **156** with 1 molar equivalent of trimethylsilyl iodide in DCM resulted in essentially quantitative conversion to glycosyl iodide **157** by <sup>1</sup>H NMR ( $\delta$  6.69 (br s, 1 H, H-1)) after only 1 h at rt, which was used directly in the subsequent UDP coupling step to prepare UDP- $\alpha$ / $\beta$ -L-rhamnose (**153b**) after *in situ* deprotection with Bu<sub>4</sub>NF.

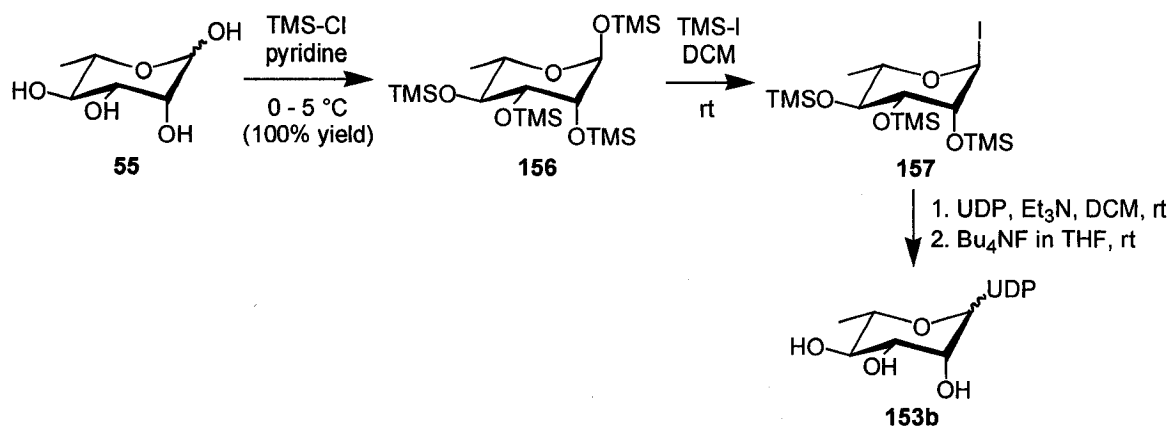


**Figure 70.** Synthesis of UDP- $\alpha/\beta$ -L-rhamnose (**153b**) via coupling of 2,3,4-tri-*O*-trimethylsilyl- $\alpha$ -L-rhamnopyranosyl iodide (**157**) with UDP

Several variables were investigated to improve the yield of the coupling reaction between 2,3,4-tri-*O*-trimethylsilyl- $\alpha$ -L-rhamnopyranosyl iodide (**157**) and UDP as evidenced by percentage conversions to product via integration of  $^{31}\text{P}\{^1\text{H}\}$  NMR spectra (Table 4). The addition of 3 Å molecular sieves improved the conversion to product from 17% to 29%, indicating that these drying agents were useful in removing H<sub>2</sub>O associated with hygroscopic nucleoside 5'-diphosphates, thus limiting degradation of glycosyl iodide **157**. Furthermore, the addition of 1 molar equivalent of triethylamine in conjunction with 3 Å molecular sieves also improved the conversion to product from 29% to 49%. As discussed in the synthesis of UDP- $\alpha/\beta$ -L-digitoxose (**119**) (Section 2.3.1), UDP was titrated to pH 6 with tetrabutylammonium hydroxide prior to the coupling reaction as reported to be optimal by Ernst and Klaffke.<sup>145,146</sup> Nonetheless, it was reasoned that the addition of a non-protonated tertiary amine base could potentially enhance glycosyl iodide (**157**) and sugar nucleotide product (**153b**) stability, since these compounds are acid-sensitive, without interfering with the nucleophilicity of UDP. Although 1 molar equivalent of triethylamine appeared to enhance conversions to product, an additional equivalent of triethylamine was of no further benefit.

**Table 4.** Effect of variables on the percentage conversion of UDP to UDP- $\alpha/\beta$ -L-rhamnose (**153b**) on coupling with 2,3,4-tri-*O*-trimethylsilyl- $\alpha$ -L-rhamnopyranosyl iodide (**157**)

variable	conversion to product by $^{31}\text{P}\{^1\text{H}\}$ NMR (%)
no molecular sieves	17
molecular sieves	29
molecular sieves + 1 equiv $\text{Et}_3\text{N}$	49
molecular sieves + 2 equiv $\text{Et}_3\text{N}$	44

After establishing improved coupling reaction conditions as described above, other variables such as solvent and reaction temperature were explored to investigate the effects of these variables on the  $\alpha:\beta$  stereoselectivity of UDP- $\alpha/\beta$ -L-rhamnose (**153b**) (Table 5). Interestingly, no difference was observed between the use of MeCN and DCM as solvents at rt with respect to stereoselectivity, both affording  $\alpha:\beta$  ratios of 2:1. In addition, decreasing the reaction temperature to  $-40\text{ }^\circ\text{C}$  in an attempt to increase the proportion of the kinetically favoured  $\beta$  anomer resulted in no difference with respect to the  $\alpha:\beta$  ratio of UDP- $\alpha/\beta$ -L-rhamnose (**153b**), again affording 2:1  $\alpha:\beta$  stereoselectivity. As evidenced in Table 5, conversions to **153b** from UDP ranged from 24% to 32% by  $^{31}\text{P}\{^1\text{H}\}$  NMR under the reaction conditions described above. Purification of UDP- $\alpha/\beta$ -L-rhamnose (**153b**) was attempted via automated ion exchange chromatography using aqueous  $\text{NH}_4\text{OAc}$  buffer as an eluent. Unfortunately, lyophilization of potential sugar nucleotide products resulted in their complete decomposition. This can possibly be attributed to the high ionic strength of lyophilized aqueous solutions as similar problems have previously been reported with other sugar nucleotides.<sup>258</sup>



**Table 5.** Effect of variables on the  $\alpha$ : $\beta$  ratio of UDP- $\alpha$ / $\beta$ -L-rhamnose (**153b**) when prepared via coupling of 2,3,4-tri-*O*-trimethylsilyl- $\alpha$ -L-rhamnopyranosyl iodide (**157**) with UDP

solvent	temperature (°C)	reaction time (h)	conversion to <b>153b</b> by $^{31}\text{P}\{^1\text{H}\}$ NMR (%) <sup>*</sup>	$\alpha$ : $\beta$ ratio
DCM	rt	2	32	2:1
MeCN	rt	2	27	2:1
DCM	-40	2	24	2:1

<sup>\*</sup>Conversions are reported for crude products over 2 steps (coupling and deprotection).

Although it was pleasing that UDP- $\beta$ -L-rhamnose was prepared, albeit as the minor component in a mixture of diastereomers (**153b**), it was reasoned that improved  $\beta$  selectivity could possibly be obtained using a less reactive electrophile such as a glycosyl bromide.

### 2.3.3.3. Glycosyl Bromide Donors

As it was originally believed that reaction of acetylated L-rhamnosyl bromide (**131**) with dibenzyl phosphate, silver triflate, and 2,4,6-collidine in DCM produced  $\beta$ -L-rhamnose-1-phosphate (Section 2.3.1.1), the reaction of glycosyl bromide **131** with UDP was also explored in an attempt to enhance the proportion of the desired  $\beta$  anomer in the preparation of UDP- $\alpha$ / $\beta$ -L-rhamnose (**153b**). Initial coupling reactions involving acetylated L-rhamnosyl bromide (**131**) and UDP in DCM were very sluggish at rt, as determined by TLC and HPLC (Figure 71). After 72 h at rt, all glycosyl bromide (**131**) had reacted or degraded by TLC and no additional reaction progress was observed by HPLC. Following treatment with alkaline phosphatase to degrade unreacted UDP, which simplified the purification process, acetyl protecting groups were removed using 2:2:1

MeOH:H<sub>2</sub>O:Et<sub>3</sub>N.<sup>223</sup> Purification via C18 reversed-phase ion-pair chromatography using 10 mM aqueous tributylammonium acetate buffer (pH 4) and MeOH afforded a single sugar nucleotide anomer (**153a**) in 11% yield (Table 6).

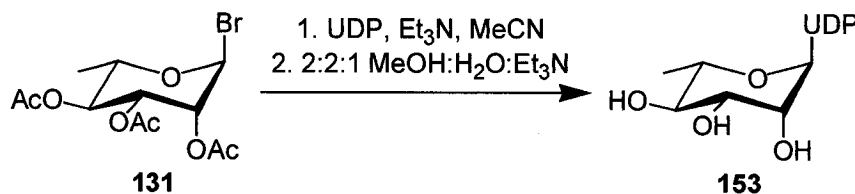


**Figure 71.** Stereoselective synthesis of UDP- $\alpha$ -L-rhamnose (**153a**) via coupling of 2,3,4-tri-*O*-acetyl- $\alpha$ -L-rhamnopyranosyl bromide (**131**) with UDP

To increase the rate of the reaction and improve the yield, the coupling of acetylated L-rhamnosyl bromide (**131**) and UDP was repeated using MeCN as a solvent at 80 °C. After 0.5 h, all glycosyl bromide (**131**) had reacted or degraded as indicated by TLC, and <sup>31</sup>P{<sup>1</sup>H} and <sup>31</sup>P-<sup>1</sup>H HSQC NMR analysis revealed the presence of a sugar nucleotide product (**153a**) (~ 50% conversion to product). Following deprotection and purification as described above, a yield of 43% was obtained (Table 6). It should be noted that additional equivalents of glycosyl bromide resulted in significantly lower conversions to product of approximately 25% and consequently lower yields, largely due to an increased number of monophosphate byproducts visible as singlets in <sup>31</sup>P{<sup>1</sup>H} NMR spectra.

**Table 6.** Effect of variables on the yield of UDP- $\alpha$ -L-rhamnose (**153a**) when prepared via direct coupling of 2,3,4-tri-*O*-acetyl- $\alpha$ -L-rhamnopyranosyl bromide (**131**) and UDP

solvent	temperature (°C)	reaction time (h)	equiv of bromide	yield of <b>153a</b> by UV <sup>*,±</sup> (%)	$\alpha$ : $\beta$ ratio
DCM	rt	72	1	11	1:0
MeCN	80	0.5	1	43	1:0
MeCN	80	0.5	2	23	1:0

<sup>\*</sup>Yields are reported for purified products over 2 steps (coupling and deprotection).

<sup>±</sup> UV yields were determined at  $\lambda_{\text{max}}$  261 nm ( $\epsilon = 1.01 \times 10^4 \text{ M}^{-1}\text{cm}^{-1}$ ).

The single sugar nucleotide anomer isolated using this coupling procedure was originally believed to be UDP- $\beta$ -L-rhamnose since a  $^3J_{H-1,H-2}$  value of 1.5 Hz was observed for sugar nucleotide **153a**, which was in agreement with the  $^3J_{H-1,H-2}$  value obtained from the sugar-1-phosphate product (**134**) prepared via coupling of acetylated L-rhamnosyl bromide (**131**) and dibenzyl phosphate (Section 2.3.1.1). However, on examination of a coupled HSQC NMR experiment, a  $^1J_{C-1,H-1}$  value 170 Hz was observed for **153a**, supporting the formation of an  $\alpha$  anomer, especially as a  $^1J_{C-1,H-1}$  value of 161 Hz has previously been reported for dTDP- $\beta$ -L-rhamnose.<sup>248</sup> In addition, only one strong through space correlation was observed between H-1 and H-2 via 1D NOE NMR experiments on **153a** in contrast to  $\beta$ -L-fucose-1-phosphate where additional strong correlations to H-3 and H-5 were observed on irradiation of H-1 (Figure 72).

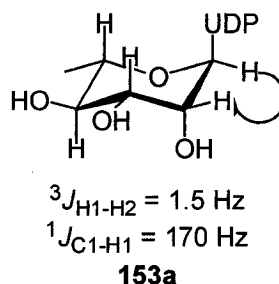


**Figure 72.** NMR characterization data supporting the preparation of UDP- $\alpha$ -L-rhamnose (**153a**) via direct coupling of 2,3,4-tri-*O*-acetyl- $\alpha$ -L-rhamnopyranosyl bromide (**131**) with UDP (arrow indicates a strong 1D NOE interaction)

This result can be explained via neighbouring group participation since glycosyl bromide **131** was protected with acyl groups. In the case of acetylated L-rhamnosyl bromide **131**, attack from the bottom face of the monosaccharide, which would provide access to UDP- $\beta$ -L-rhamnose, is blocked by the 1,3-dioxolane ring formed via neighbouring group participation (Figure 73). In contrast, the top face of the acetylated monosaccharide is open to nucleophilic attack by UDP, resulting in the exclusive

preparation of UDP- $\alpha$ -L-rhamnose (**153a**). This analysis inspired a hypothesis that this approach could be extended to prepare diastereomerically pure sugar nucleotides of desired anomeric configuration via direct coupling of nucleoside 5'-diphosphates with acylated glycosyl bromides derived from D-mannose (**158**) and L-fucose (**54**) (Figure 73). In the case of D-mannose (**158**), the 1,3-dioxolane ring produced via neighbouring group participation protects the top face of the monosaccharide from attack, promoting nucleoside 5'-diphosphate nucleophilic attack exclusively from the bottom face, resulting in the preparation of the desired  $\alpha$  anomer. The equatorial hydroxyl group at C-2 also results in the protection of the top face of L-fucose (**54**), but encourages the preparation of the desired  $\beta$  anomer due to a  ${}^1C_4$  chair conformation.

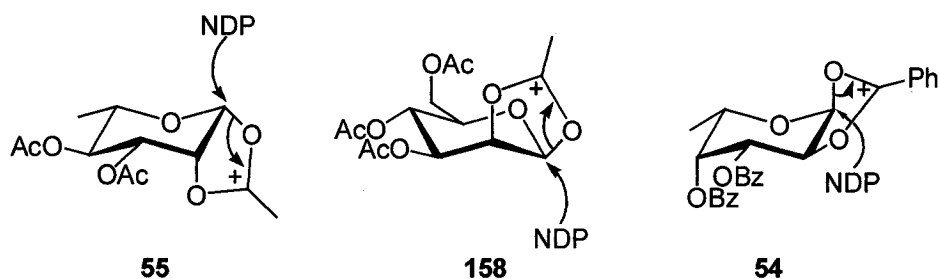


**Figure 73.** Influence of neighbouring group participation on the trajectory of NDP attack for acylated glycosyl bromides derived from L-rhamnose (**55**), D-mannose (**158**), and L-fucose (**54**)

GDP- $\alpha$ -D-mannose (**159**) and GDP- $\beta$ -L-fucose (**160**) are two of seven principal sugar nucleotides utilized by Leloir glycosyltransferases in mammalian systems.<sup>255</sup> Significant interest therefore exists to develop efficient synthetic routes to these sugar nucleotides for use as substrates for glycosyltransferases, which are increasingly being used to prepare complex oligosaccharides and glycoconjugates for biological study.<sup>130,256</sup> The majority of chemical syntheses described thus far to access **159** and **160** involve the initial preparation of sugar-1-phosphates, which were subsequently coupled with

activated nucleoside 5'-diphosphates.<sup>243,257,258,259</sup> One exception, however, is a direct coupling methodology reported by Arlt and Hindsgaul in 1995 that involved the synthesis of GDP- $\beta$ -L-fucose (**160**) via coupling of a benzylated glycosyl bromide, clearly not amenable to neighbouring group participation, with GDP in DCM at rt.<sup>142</sup> Using this strategy, three sugar nucleotides were synthesized in yields ranging from 10-30% from reducing sugars D-galactose, L-arabinose, and L-fucose (**54**) with  $\alpha:\beta$  stereoselectivities ranging from 1:1 to 3:1.<sup>142</sup>

To ascertain the feasibility of a new direct coupling approach using acylated glycosyl bromides and nucleoside 5'-diphosphates, acetylated D-mannosyl bromide (**161**) was first prepared in excellent yield via acetylation of D-mannose (**158**) using acetic anhydride and pyridine followed by reaction of acetylated derivative **162** with phosphorus tribromide and H<sub>2</sub>O in DCM (Figure 77).<sup>244</sup> Acetylated D-mannosyl bromide (**161**) was coupled with UDP (previously titrated to pH 6 with Bu<sub>4</sub>NOH and lyophilized<sup>145,146</sup>) at 80 °C in MeCN as previously described for UDP- $\alpha$ -L-rhamnose (**153a**). After 0.5 h, all the glycosyl bromide had been consumed or degraded as indicated by TLC and a sugar nucleotide product (**163**) was visible by <sup>31</sup>P{<sup>1</sup>H} NMR. This coupling reaction was repeated using acetylated D-mannosyl bromide (**161**) and GDP to extend the utility of this procedure for use with a nucleoside 5'-diphosphate containing a biologically relevant purine base (Figure 74). Using the aforementioned reaction conditions, the coupling reaction was again complete after 0.5 h, producing sugar nucleotide **159**.

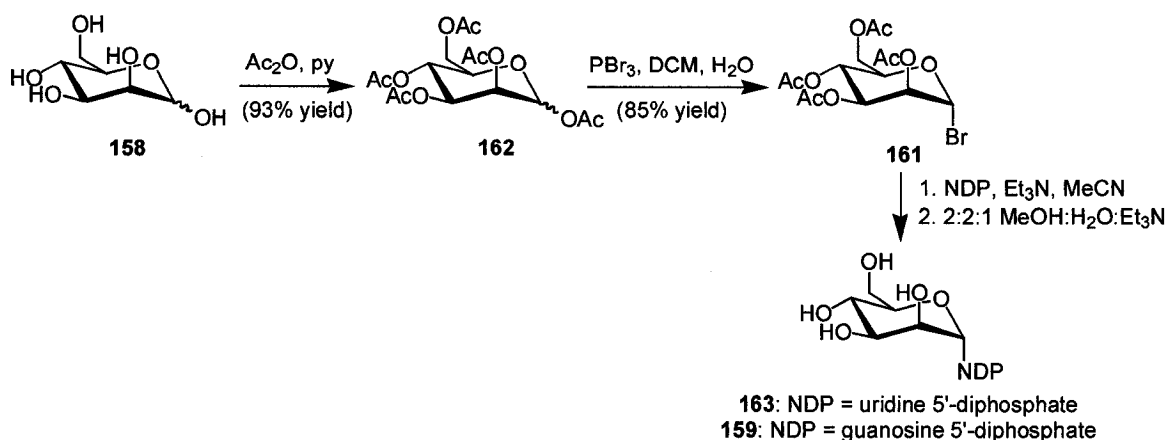


**Figure 74.** Stereoselective synthesis of UDP- $\alpha$ -D-mannose (**163**) and GDP- $\alpha$ -D-mannose (**159**) via direct displacement of acetylated D-mannosyl bromide (**161**) with NDPs

Sugar nucleotides **159** and **163** were subsequently treated with alkaline phosphatase to degrade unreacted nucleoside 5'-diphosphates, deacetylated using 2:2:1 MeOH:H<sub>2</sub>O:Et<sub>3</sub>N,<sup>223</sup> and purified using C18 reversed-phase ion-pair chromatography. In lieu of 10 mM aqueous tributylammonium acetate (pH 4), a new aqueous buffer, 10 mM aqueous tributylammonium bicarbonate (pH 6), was prepared by bubbling CO<sub>2</sub> gas (obtained via the sublimation of dry ice) through an aqueous solution containing 10 mM tributylamine. There were two main advantages to this new aqueous ion-pair buffer. First, the pH of the buffer was 6, so there was far less chance of acid-sensitive sugar nucleotides degrading on the column and there is no need to neutralize column fractions prior to concentration under reduced pressure. Second, in the case of tributylammonium bicarbonate buffer, the anionic counterion is volatile, simplifying the purification protocol since sugar nucleotides can be directly applied to cation exchange resin to easily generate desired salt forms without any interference from carbonic acid. In contrast, in the case of tributylammonium acetate buffer, ammonium salts of sugar nucleotides were generated to facilitate the formation of NH<sub>4</sub>OAc. Although NH<sub>4</sub>OAc is known to sublime upon lyophilization, samples must often be freeze-dried several times to

completely remove this salt depending on the concentration of  $\text{NH}_4\text{OAc}$  in the sample. To help facilitate the complete removal of  $\text{NH}_4\text{OAc}$ , samples were triturated several times with ethanol following lyophilization, which eventually facilitated the removal of this salt, although omission of this step was obviously desirable. After purification of sugar nucleotides **159** and **163** via C18 reversed-phase ion-pair chromatography using 10 mM aqueous tributylammonium bicarbonate buffer and MeOH followed by cation exchange, **159** and **163** were obtained as white solids following lyophilization. Sugar nucleotide yields, determined by both UV spectroscopy and mass, ranged from 29–38% for UDP- $\alpha$ -D-mannose (**163**) and GDP- $\alpha$ -D-mannose (**159**).

Structural characterization of purified sugar nucleotides **163** and **159** supported the exclusive preparation of UDP- $\alpha$ -D-mannose (**163**) and GDP- $\alpha$ -D-mannose (**159**), as predicted by neighboring group participation (Table 7). As with L-rhamnose (**55**),<sup>250</sup> both  $\alpha$  and  $\beta$  anomers of glycosides derived from D-mannose (**158**) have similarly small  $^3J_{\text{H-1,H-2}}$  values differing by approximately 1 Hz and  $^3J_{\text{H-1,H-2}}$  values were not actually observed in the case of sugar nucleotides **163** and **159** due to the linewidths of the  $^1\text{H}$  NMR spectra. To unambiguously determine the anomeric configuration of D-manno-linked sugar nucleotides,  $^1J_{\text{C-1,H-1}}$  values were determined. These values, 170 Hz for UDP- $\alpha$ -D-mannose (**163**) and 173 Hz for GDP- $\alpha$ -D-mannose (**159**), along with an anomeric H-1" chemical shift of 5.49 ppm for both of these sugar nucleotides, fully supported the assignment of **163** and **159** as  $\alpha$  anomers (Table 7).<sup>245,246</sup>

**Table 7.** Characterization of D-manno- and L-fuco-linked sugar nucleotides

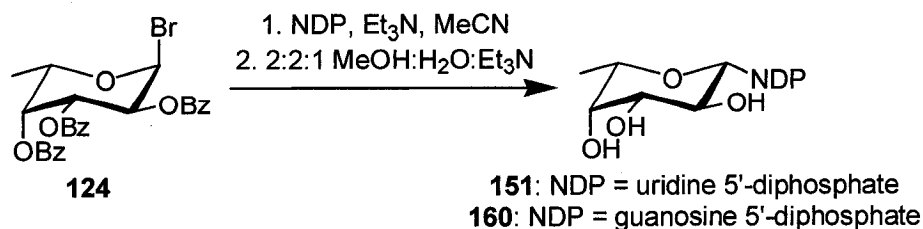
product	sugar	NDP	yield by UV <sup>*,‡</sup> (%)	yield by mass <sup>*</sup> (%)	$\delta$ H-1'' (ppm)	$^3J_{H-1'',H-2''}$ (Hz)	$^1J_{C-1'',H-1''}$ (Hz)
<b>163</b>	D-mannose	UDP	29	33	5.49	n/o <sup>§</sup>	170
<b>159</b>	D-mannose	GDP	35	38	5.49	n/o <sup>§</sup>	173
<b>151</b>	L-fucose	UDP	26	31	4.84	8.0	163
<b>160</b>	L-fucose	GDP	31	35	4.90	8.0	160

<sup>\*</sup> Yields are reported for purified products over 2 steps (coupling and deprotection).

<sup>‡</sup> UV yields were determined at  $\lambda_{\max}$  261 nm ( $\epsilon = 1.01 \times 10^4 \text{ M}^{-1}\text{cm}^{-1}$ ) for products containing uridine and  $\lambda_{\max}$  253 nm ( $\epsilon = 1.37 \times 10^4 \text{ M}^{-1}\text{cm}^{-1}$ ) for products containing guanosine.

<sup>§</sup> n/o = not observed (br d,  $^3J_{H-1'',P} = 8.0 \text{ Hz}$ ).

This methodology and purification strategy was extended to L-fucose (**54**), which was predicted to produce  $\beta$  anomers of sugar nucleotides via coupling of acylated glycosyl bromides with nucleoside 5'-diphosphates based on neighbouring group participation (Figure 73). To test the generality of this approach with different acyl groups, benzoylated L-fucosyl bromide (**124**) was first prepared from **54** in excellent yield as described in Section 2.3.1.1. Upon coupling glycosyl bromide **124** independently with both UDP and GDP at 80 °C for 0.5 h, only one sugar nucleotide anomer was obtained in both cases (Figure 75). Following purification via the protocol described above for **163** and **159**, UDP- $\beta$ -L-fucose (**151**) and GDP- $\beta$ -L-fucose (**160**) were obtained as white solids in yields ranging from 26–35% as determined by both UV spectroscopy and mass (Table 7).

**Figure 75.** Stereoselective synthesis of UDP- $\beta$ -L-fucose (**151**) and GDP- $\beta$ -L-fucose (**160**) via direct displacement of benzoylated L-fucosyl bromide (**124**) with NDPs



With respect to NMR characterization,  $^3J_{H-1'',H-2''}$  values of 8.0 Hz, obtained for both UDP- $\beta$ -L-fucose (**151**) and GDP- $\beta$ -L-fucose (**160**), were very diagnostic in assigning  $\beta$  anomeric configurations to **151** and **160** (Table 7). For consistency, and to further support the claim of  $\beta$  diastereomer formation,  $^1J_{C-1'',H-1''}$  values were also determined for **151** and **160**. These values, 163 Hz for UDP- $\beta$ -L-fucose (**151**) and 160 Hz for GDP- $\beta$ -L-fucose (**160**), were entirely consistent with literature expectations for  $\alpha$ - and  $\beta$ -linked *O*-glycosides.<sup>245,246</sup>

In summary, this novel methodology,<sup>260</sup> employing the well-known concept of neighbouring group participation, represents a simple, efficient procedure for preparing diastereomerically pure  $\alpha$ -D-manno- and  $\beta$ -L-fuco-linked sugar nucleoside diphosphates from reducing sugars in only four synthetic steps. This approach could theoretically be extended to prepare various  $\alpha$ -D-manno- and  $\beta$ -L-fuco-linked sugar nucleotide derivatives synthetically modified at any position except C-2 for use as glycosyltransferase probes. Similarly, this procedure may also be amenable for use in the synthesis of sugar nucleotide derivatives modified at the nucleobase.<sup>261</sup>

## 2.4. Enzymatic Synthesis of Sugar Nucleotides

As described in Section 1.5.2, the *in vitro* preparation of sugar nucleotides, through the use of sugar nucleotidyltransferases, is quickly emerging as an attractive alternative to chemical synthesis.<sup>73,151,155,156,157,158,160</sup> These enzymatic strategies offer several advantages over chemical synthesis including mild, aqueous reaction conditions and high yields as well as a lack of stereochemistry to be concerned with as these biocatalysts couple two phosphates. In addition, several nucleotidyltransferases have

recently been shown to be promiscuous with respect to their sugar-1-phosphate and/or nucleoside 5'-triphosphate substrates,<sup>151,155,156,158</sup> invoking interest in studying the substrate promiscuity of additional wild-type and engineered enzymes. To this end, the scope and limitations of the enzymatic preparation of sugar nucleotides using three nucleotidyltransferases and a variety of sugar-1-phosphates and nucleoside 5'-triphosphates will be described in Section 2.4.1.

#### **2.4.1. Substrate Promiscuity of Three Nucleotidyltransferases**

Three bacterial nucleotidyltransferases were used to investigate the enzyme-catalyzed preparation of sugar nucleotides: Cps2L (*Streptococcus pneumoniae* R6), RmlA (*Streptococcus mutans* UA159), and RmlA3 (*Aneurinibacillus thermoaerophilus* DSM 10155). All of these enzymes are  $\alpha$ -D-glucose-1-phosphate thymidyltransferases involved in primary metabolic processes, and as such catalyze the preparation of dTDP- $\alpha$ -D-glucose from  $\alpha$ -D-glucose-1-phosphate and deoxythymidine 5'-triphosphate (dTTP) in the presence of a divalent metal cation (Figure 76). Cps2L and RmlA thymidyltransferases were cloned, expressed, and purified in the Jakeman laboratory by Prof. Roy Mosher and Sheryl Knowles, whereas the pRmlA3 plasmid was kindly provided by Prof. Joseph Lam (Department of Molecular and Cellular Biology, University of Guelph).

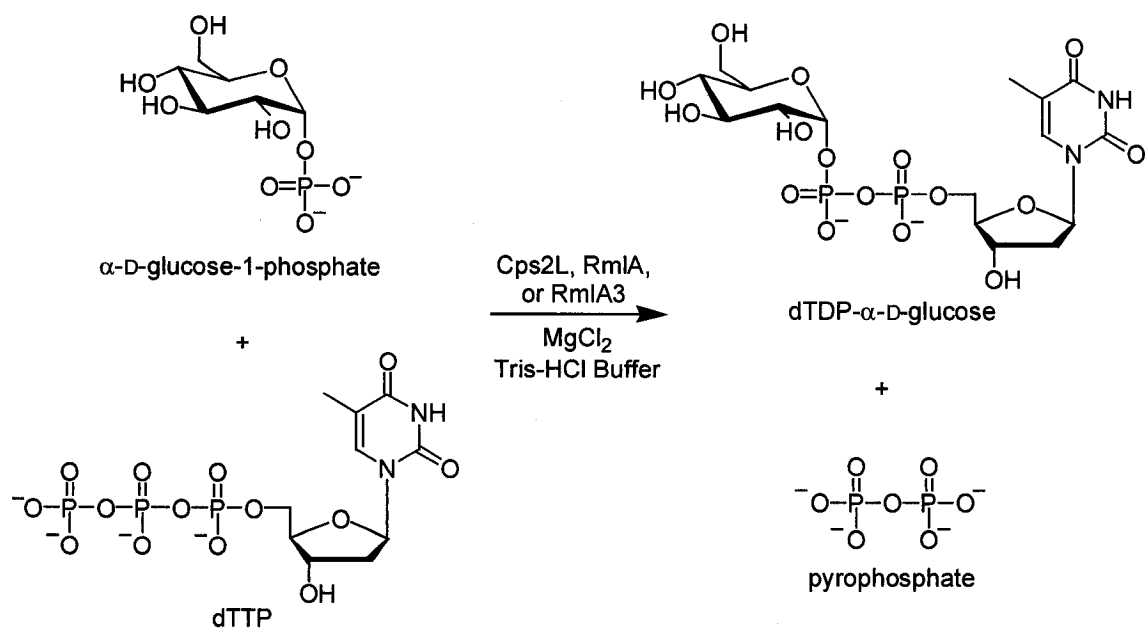


**Figure 76.** Reaction catalyzed by Cps2L, RmlA, and RmlA3  $\alpha\text{-D-glucose-1-phosphate}$  thymidyltransferases

The five commercially available  $\alpha\text{-D-sugar-1-phosphates}$  selected for this study were  $\alpha\text{-D-glucose-1-phosphate}$  ( $\alpha\text{-D-Glc-1-P}$ ),  $\alpha\text{-D-glucosamine-1-phosphate}$  ( $\alpha\text{-D-GlcNH}_2\text{-1-P}$ ),  $N\text{-acetyl-}\alpha\text{-D-glucosamine-1-phosphate}$  ( $\alpha\text{-D-GlcNAc-1-P}$ ),  $\alpha\text{-D-galactose-1-phosphate}$  ( $\alpha\text{-D-Gal-1-P}$ ), and  $\alpha\text{-D-mannose-1-phosphate}$  ( $\alpha\text{-D-Man-1-P}$ ) (Figure 77). In addition, three L-sugar-1-phosphates, prepared via chemical synthesis as described in Section 2.3.1.1,  $\beta\text{-L-fucose-1-phosphate}$  ( $\beta\text{-L-Fuc-1-P}$ ),  $\alpha\text{-L-rhamnose-1-phosphate}$  ( $\alpha\text{-L-Rha-1-P}$ ), and  $\alpha\text{-L-arabinose-1-phosphate}$  ( $\alpha\text{-L-Ara-1-P}$ ), were also included as potential substrates in this investigation (Figure 77).

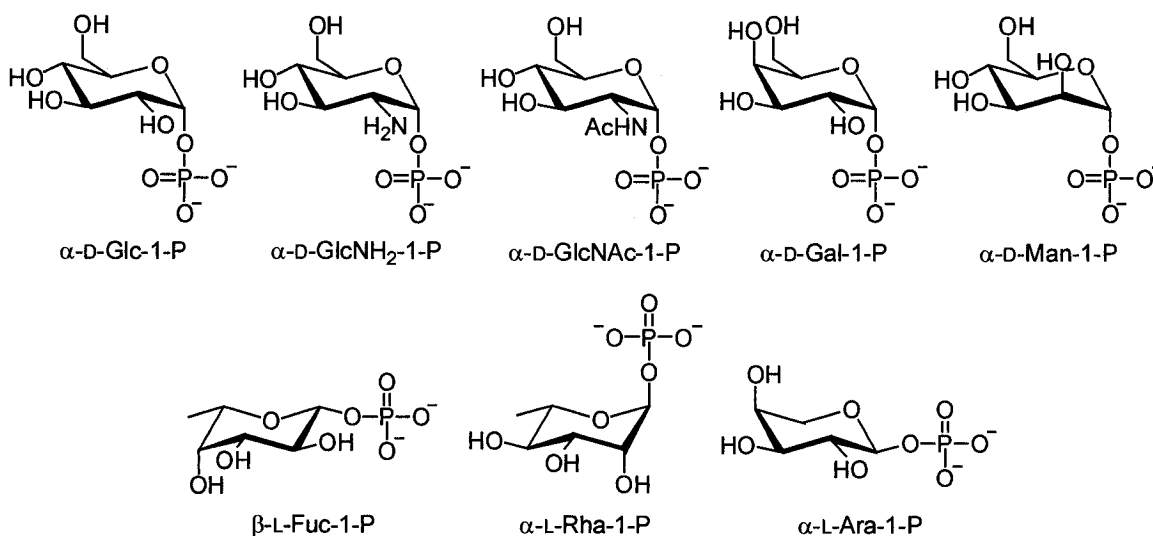


**Figure 77.** Structures of sugar-1-phosphates used in thymidyltransferase substrate promiscuity studies

The five  $\alpha$ -D-sugar-1-phosphates in Figure 77, divergent in structure from  $\alpha$ -D-Glc-1-P, were selected to probe the substrate promiscuity of the three thymidyltransferases toward changes in configuration at the C-2 and C-4 stereocentres of the various monosaccharides. Synthetic access to L-sugar-1-phosphates also provided an opportunity to study substrates of alternative anomeric configuration ( $\alpha$ -L-Ara-1-P) and different conformation ( $\alpha$ -L-Rha-1-P,  $\beta$ -L-Fuc-1-P). Of particular interest was the study of  $\beta$ -L-Fuc-1-P, as  $\beta$ -L-sugar nucleotides in the  ${}^1C_4$  chair conformation are substrates for many family 1 (GT-B) glycosyltransferases involved in the biosynthesis of natural products.<sup>34,35,36,168</sup>

With respect to nucleoside 5'-triphosphate (NTP) substrates, five commercially available NTPs, adenosine 5'-triphosphate (ATP), cytidine 5'-triphosphate (CTP), guanosine 5'-triphosphate (GTP), deoxythymidine 5'-triphosphate (dTTP), and uridine 5'-triphosphate (UTP), were tested independently with all sugar-1-phosphates described above (Figure 78).

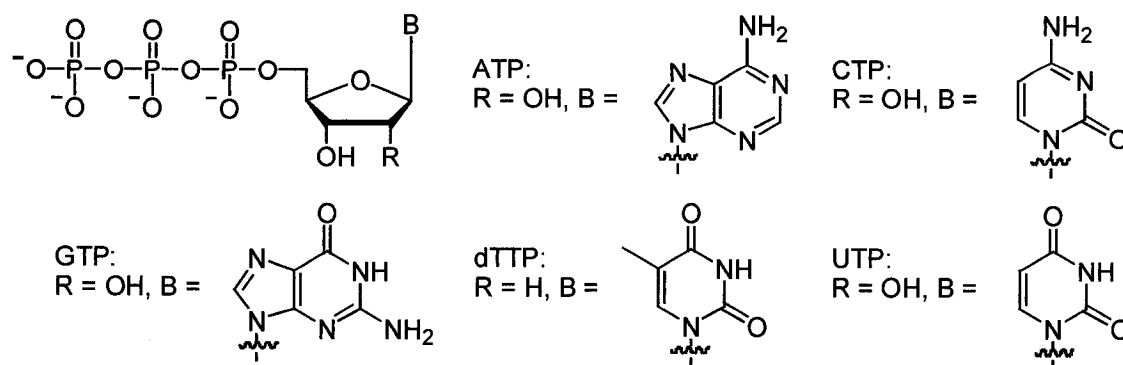


**Figure 78.** Structures of NTPs used in thymidyltransferase substrate promiscuity studies

To assess the potential synthetic utility of Cps2L, RmlA, and RmlA3 thymidyltransferases, enzymatic reactions were conducted using millimolar substrate concentrations similar to those previously described<sup>155,157,158</sup> in the presence of inorganic pyrophosphatase,<sup>151,157,158</sup> which served to degrade pyrophosphate, a potential inhibitor<sup>151</sup> produced as a reaction byproduct, to inorganic phosphate. Aliquots of each enzymatic reaction were quenched with methanol after incubation at 37 °C and centrifuged to precipitate proteins prior to HPLC and ESI-MS/MS analysis. In the absence of thymidyltransferase, NTP, sugar-1-phosphate, or  $\text{MgCl}_2$ , no product formation was observed.

A summary of the substrate promiscuity of Cps2L, RmlA, and RmlA3 thymidyltransferases, determined after 30 min, is presented in white in Figure 79. The incubation of  $\alpha$ -D-Glc-1-P with both dTTP and UTP consistently produced very high levels of conversion to product (87–100%) with all three enzymes, indicating that UTP was readily accepted as an alternative NTP with  $\alpha$ -D-Glc-1-P. Similarly, incubation of all three thymidyltransferases with  $\alpha$ -D-GlcNH<sub>2</sub>-1-P and both dTTP and UTP, independently, also produced high levels of conversion (77–96%) after 30 min at 37 °C.

When the reaction of other  $\alpha$ -D-sugar-1-phosphates with dTTP was explored, it was found that  $\alpha$ -D-GlcNAc-1-P,  $\alpha$ -D-Gal-1-P, and  $\alpha$ -D-Man-1-P were also accepted by all three enzymes at reasonable conversions after 30 min (greater than 50% in all but one case), demonstrating that changes in configuration at C-2 and C-4, and even substitution of an acetyl group at C-2, were tolerated by Cps2L, RmlA, and RmlA3. Interestingly, when both alternative  $\alpha$ -D-sugar-1-phosphates and alternative NTPs were incubated with these three enzymes, conversions after 30 min decreased significantly in all cases except with  $\alpha$ -D-GlcNH<sub>2</sub>-1-P and UTP, illustrating that these enzymes readily tolerate only one change in either sugar-1-phosphate or NTP.

Of particular significance was the acceptance of the chemically synthesized  $\beta$ -L-Fuc-1-P substrate by all three nucleotidyltransferases after 30 min at 37 °C, albeit at conversions ranging from 3 –10%. Not surprisingly,  $\alpha$ -L-Rha-1-P and  $\alpha$ -L-Ara-1-P were not accepted by any enzyme with any NTP, demonstrating the stringent anomeric stereospecificity of these thymidyltransferases.

The initial incubation of enzymatic reactions for 30 min at 37 °C provided an excellent survey of relative enzyme specificity. However, in order to more fully assess the synthetic potential of these biocatalysts, reactions resulting in conversions to product of less than 50% after 30 min were incubated for 24 h at 37 °C. A summary of these results, shown in black in Figure 79, illustrates that significant improvements in conversion were obtained in the majority of cases with all thymidyltransferases after incubation for 24 h at 37 °C. For example, all three enzymes were able to synthesize dTDP- $\beta$ -L-Fuc in greater than 70% conversion after 24 h as compared to conversions of only 3–10% after 30 min. Secondly, in the case of RmlA3, conversions of eight

substrates after 30 min ranged from 3–29%, whilst conversions after 24 h with the same group of substrates had increased to 90–99%.

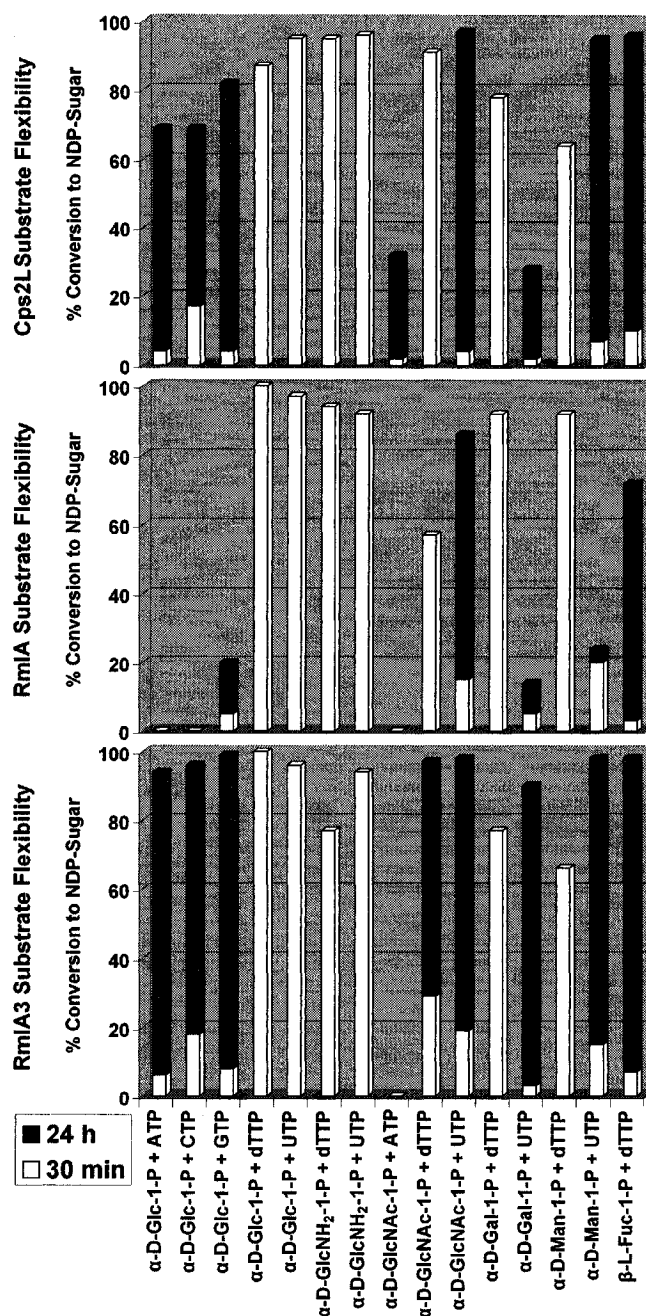


**Figure 79.** Substrate promiscuity of Cps2L, RmlA, and RmlA3 thymidyltransferases after 30 min and 24 h incubations at 37 °C

The improved conversions to product observed after 24 h incubations at 37 °C with all three thymidyltransferases suggests that Cps2L, RmlA, and RmlA3 are stable

over a significant portion of the 24 h time period. Of particular note is that RmlA3, a thermophilic enzyme, and Cps2L, a mesophilic enzyme, generally demonstrated comparable levels of activity over the 24 h time period at 37 °C. Conversion figures obtained after 24 h clearly indicate the potential synthetic utility of these three enzymes, particularly as neither substrate nor product inhibition was observed at millimolar concentrations. Also of significance is the ability of all three enzymes to prepare dTDP- $\beta$ -L-Fuc in high yield after incubation at 37 °C for 24 h. This is potentially surprising considering that dTDP- $\beta$ -L-Rha is a competitive inhibitor of *P. aeruginosa* RmlA with micromolar affinity,<sup>150,153</sup> and epimerization at C-2 and C-4 of the hexopyranose ring are the only stereochemical differences between these sugar nucleotide products. It is also significant to note that only minimal degradation (typically less than 5%) of NTPs and NDP-sugars to NMPs and NDPs was observed over the 24 h incubation period, illustrating the stability of substrates and products at 37 °C under the reported reaction conditions. While the substrate promiscuity of other thermophilic nucleotidyltransferases have been reported,<sup>151,262</sup> these results provide incentive to study the substrate promiscuity of a psychrophilic enzyme, which would potentially function at even lower temperatures than those reported herein and further minimize the degradation of substrates and products over a given time period.

In comparison with the substrate promiscuity of other characterized nucleotidyltransferases,<sup>151,155,158,262,263</sup> Cps2L, RmlA, and RmlA3 rank very high in terms of the number of sugar-1-phosphates and NTPs they will accept, and the excellent conversions to product obtained demonstrate the potential of these enzymes to provide efficient access to a variety of sugar nucleotides. In particular, the  $\alpha$ -D-glucose-1-



phosphate thymidyltransferase E<sub>p</sub> (*Salmonella enterica* LT2)<sup>155,158</sup> has demonstrated a broad sugar-1-phosphate promiscuity, but produced significantly lower conversions with UTP than dTTP in several cases. Moreover, thermostable  $\alpha$ -D-glucose-1-phosphate uridylyltransferase UDPG-PPase (*Pyrococcus furiosus* DSM 3638)<sup>151</sup> also demonstrated broad sugar-1-phosphate promiscuity, but produced much lower conversions with dTTP than UTP in all but one case. In addition, UDPG-PPase would not accept ATP, a purine nucleotide, in contrast to Cps2L and RmlA3, which demonstrated catalysis with ATP and  $\alpha$ -D-Glc-1-P in excellent yield (69% and 94%, respectively) after 24 h at 37 °C. Interestingly, thermostable  $\alpha$ -D-glucose-1-phosphate thymidyltransferase ST0452 (*Sulfolobus tokadaii* strain 7),<sup>262</sup> has demonstrated stringent substrate specificity with respect to both sugar-1-phosphates and NTPs. Using ST0452, no catalysis was observed with  $\alpha$ -D-GlcNH<sub>2</sub>-1-P,  $\alpha$ -D-Gal-1-P, or  $\alpha$ -D-Man-1-P and any NTP and, in addition, ATP, CTP, or GTP nucleotides were not accepted with any sugar-1-phosphate. In another example, the  $\alpha$ -D-glucose-1-phosphate uridylyltransferase GalU (*Streptococcus pneumoniae*)<sup>263</sup> has also exhibited rather stringent substrate specificity with respect to NTPs as no catalysis was observed with either ATP or UTP with  $\alpha$ -D-Glc-1-P.

It is interesting to note that, in general, nucleotidyltransferases involved in secondary metabolism have been reported to be more substrate stringent than the primary metabolic enzymes described above.<sup>264,265</sup> In the case of SgcA1, an  $\alpha$ -D-glucose-1-phosphate thymidyltransferase from the gene cluster of the enediyne antibiotic C-1027,<sup>265</sup> it was found that, out of six sugar-1-phosphates tested, only  $\alpha$ -D-Glc-1-P was accepted. In addition, of five potential NTP substrates, only dTTP and UTP (only 6% conversion) were accepted by SgcA1, demonstrating the stringent specificity of this

enzyme.<sup>265</sup> Similarly, the stringent substrate specificity of the aminoglycoside antibiotic  $\alpha$ -D-glucosamine-1-phosphate thymidyltransferase BtrD<sup>264</sup> has also been disclosed as only two  $\alpha$ -D-sugar-1-phosphates of six substrates tested were reportedly accepted by the enzyme. In addition, BtrD was found to be incapable of accepting ATP, CTP, or GTP nucleotides with any sugar-1-phosphate.<sup>264</sup> Interestingly, Spencer and coworkers have very recently reported this initial characterization of BtrD to be incorrect and instead suggest that BtrD actually functions as a deacetylase.<sup>266</sup>

In summary, Cps2L, RmlA, and RmlA3, three primary metabolic thymidyltransferases, have clearly exhibited their ability to use both dTTP and UTP nucleotides along with six sugar-1-phosphates to efficiently prepare dTDP- and UDP-sugars. In addition, Cps2L and RmlA3 have demonstrated their utility in the preparation of ADP-, CDP-, and GDP-sugars with conversions to product ranging from 69–99%, illustrating the potential synthetic utility of these nucleotidyltransferases over others involved in primary and secondary metabolic processes. This is also the first report<sup>267</sup> to demonstrate the ability of bacterial nucleotidyltransferases to prepare dTDP- $\beta$ -L-Fuc in high conversions ranging from 72–98% after incubation at 37 °C for 24 h. The lower temperature required for catalysis compared to the thermostable archaeal UDPG-PPase<sup>151</sup> may offer a significant advantage when utilizing less stable sugar-1-phosphates or NTPs. In conclusion, these three enzymes provide a convenient route to the efficient preparation of a library of fifteen sugar nucleotides with a variety of sugars and nucleotide bases. Kinetic studies on these thymidyltransferases will provide more insight into their substrate promiscuity.

## Chapter 3. Experimental

---

### 3.1. General Methods

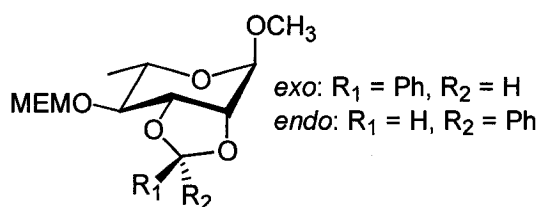
With the exclusion of certain solvents, chemicals were purchased commercially and used without further purification unless otherwise specified. Anhydrous DCM and THF were dried and purified via filtration through alumina using an Innovative Technology solvent purification system. All other solvents were reagent grade unless otherwise noted. Analytical thin-layer chromatography was performed on glass-backed TLC plates pre-coated with silica gel (SiliCycle™, 250  $\mu$ m) and compounds were detected by UV absorbance (254 nm) and/or by spraying with a KMnO<sub>4</sub> visualization solution (3 g KMnO<sub>4</sub>, 20 g K<sub>2</sub>CO<sub>3</sub>, 5 mL 5% w/v aqueous NaOH, 300 mL H<sub>2</sub>O). Analytical HPLC of sugar nucleotide reaction mixtures and purified products was performed using a Hewlett Packard Series 1050 instrument equipped with an Agilent Zorbax 5  $\mu$ m Rx-C18 column (150 cm x 4.6 mm). Compounds containing nucleoside base chromophores were monitored at an absorbance of 254 nm over a linear gradient from 90:10 A:B to 40:60 A:B over 8.0 min followed by a plateau at 40:60 A:B from 8.0 to 10.0 min at 1.0 mL/min where A was an aqueous buffer containing 12 mM Bu<sub>4</sub>NBr, 10 mM KH<sub>2</sub>PO<sub>4</sub>, and 5% v/v HPLC grade MeCN (pH 4) and B was HPLC-grade MeCN (hereafter denoted as Method A). Automated normal-phase silica gel and C18 reversed-phase chromatography was performed on a Biotage SP1™ flash chromatography system. Normal-phase silica gel benchtop chromatography was performed using SiliCycle™ 230-400 mesh ultra pure silica. Hydrogenolysis was performed using a Parr Model 3911 pressure reaction apparatus. UV-Visible spectroscopy was conducted using a Molecular

Devices SpectraMax Plus<sup>384</sup> spectrometer. Melting points were measured in open capillary tubes using a Gallenkamp melting point apparatus and are reported uncorrected. Nuclear magnetic resonance experiments were conducted using either a Bruker/Tecmag AC-250 spectrometer or a Bruker AVANCE 500 MHz spectrometer. 1D NOE and 2D NOESY NMR experiments were performed with mixing times of 750 ms and 500 ms, respectively. Chemical shifts are reported in parts per million (ppm) relative to a tetramethylsilane internal standard at 0.00 ppm for samples in CDCl<sub>3</sub>, while spectra recorded in D<sub>2</sub>O were referenced to the solvent peak at 4.79 ppm. <sup>31</sup>P{<sup>1</sup>H} spectra were referenced relative to an external 85% aqueous H<sub>3</sub>PO<sub>4</sub> standard at 0.00 ppm, while <sup>19</sup>F{<sup>1</sup>H} spectra were referenced relative to an external 0.5% v/v CF<sub>3</sub>C<sub>6</sub>H<sub>5</sub> standard in CDCl<sub>3</sub> at -63.72 ppm. All <sup>1</sup>H and <sup>13</sup>C{<sup>1</sup>H} NMR assignments were confirmed using COSY, HSQC, and/or HMBC 2D NMR experiments. High-resolution electron ionization (EI) mass spectrometry measurements were obtained using a DuPont CEC 21-110B double-focusing magnetic sector instrument with an ionization voltage of 70 V. Both low- and high-resolution electrospray ionization (ESI) mass spectrometry measurements on chemically synthesized compounds were obtained using a ThermoFinnigan LCQ duo ion trap instrument operating in flow-injection mode with a flow rate of 25 μL/min and a spray voltage of -4 kV. Low-resolution ESI mass spectrometry measurements on enzymatically synthesized compounds were obtained using an Applied Biosystems hybrid triple quadrupole linear ion trap (2000 Q TRAP®) instrument and a spray voltage of -4 kV. During sample analysis, the solvent (7:3 MeCN:H<sub>2</sub>O containing 2 mM NH<sub>4</sub>OAc) was constantly infused into the ion source at 10 μL/min using a built-in syringe pump. After collection of an enhanced mass spectrum,

enzymatically prepared sugar nucleotide product ions were fragmented via an enhanced product ion scan using a collision energy of -60 V. Tandem LC-MS analysis was performed using an Agilent 1100 Series LC system coupled to an Applied Biosystems hybrid triple quadrupole linear ion trap (4000 Q TRAP®) instrument as previously described.<sup>268</sup>

### 3.2. Synthesis and Characterization of Compounds

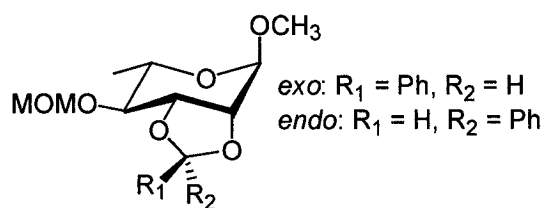
#### Methyl 2,3-*O*-benzylidene-4-*O*-(2-methoxyethoxymethyl)- $\alpha$ -L-rhamnopyranoside (**58**)



This compound was prepared by an adaptation of a procedure described by Brimacombe and coworkers.<sup>174</sup> A diastereomeric mixture of methyl 2,3-*O*-benzylidene- $\alpha$ -L-rhamnopyranoside acetals (**67**) (0.73 g, 2.7 mmol) was dissolved in DCM (6 mL) in a round-bottomed flask. Following the dropwise addition of ethyldiisopropylamine (1.1 mL, 6.3 mmol) and 2-methoxyethoxymethyl chloride (0.70 mL, 6.1 mmol), the reaction mixture was stirred at rt for 48 h, after which time TLC analysis (35:65 EtOAc:hexanes,  $R_f$  product **58** = 0.67) revealed that all starting material had been consumed. After concentration under reduced pressure, the resulting crude orange syrup was re-dissolved in DCM (25 mL) and washed with 1 M aqueous HCl (25 mL) and H<sub>2</sub>O (25 mL). After drying over Na<sub>2</sub>SO<sub>4</sub>, the organic layer was concentrated under reduced pressure and purified via benchtop silica gel chromatography (isocratic 17:83 EtOAc:hexanes), affording 4-*O*-MEM-protected derivative **58** as a white solid (0.78 g, 2.2 mmol, 80%

yield).  $^1\text{H}$  NMR (250 MHz,  $\text{CDCl}_3$ ):  $\delta$  *exo* diastereomer: 7.59-7.32 (m, 5 H, Ph), 6.15 (s, 1 H, PhCH), 5.06 (br s, 1 H, H-1), 4.82 (d,  $J_{\text{H,H}} = 6.7$  Hz, 2 H,  $\text{OCH}_2\text{O}$ ), 4.47 (dd,  $J_{2,3} = 5.5$  Hz,  $J_{3,4} = 7.2$  Hz, 1 H, H-3), 4.10 (br d, 1 H, H-2), 3.86-3.41 (m, 6 H, H-4, H-5,  $\text{OCH}_2\text{CH}_2\text{O}$ ), 3.38 (s, 3 H,  $\text{OCH}_3$ ), 3.37 (s, 3 H,  $\text{OCH}_3$ ), 1.36 (d,  $J_{5,6} = 6.1$  Hz, 3 H, H<sub>3</sub>-6); *endo* diastereomer: 7.59-7.32 (m, 5 H, Ph), 5.88 (s, 1 H, PhCH), 5.09 (br s, 1 H, H-1), 4.79 (d,  $J_{\text{H,H}} = 6.7$  Hz, 2 H,  $\text{OCH}_2\text{O}$ ), 4.30 (dd,  $J_{2,3} = 6.4$  Hz,  $J_{3,4} = 6.6$  Hz, 1 H, H-3), 4.19 (br d, 1 H, H-2), 3.86-3.41 (m, 6 H, H-4, H-5,  $\text{OCH}_2\text{CH}_2\text{O}$ ), 3.39 (s, 3 H,  $\text{OCH}_3$ ), 3.32 (s, 3 H,  $\text{OCH}_3$ ), 1.31 (d,  $J_{5,6} = 6.4$  Hz, 3 H, H<sub>3</sub>-6). The reported PhCH  $^1\text{H}$  NMR data is consistent with that of Brimacombe and coworkers.<sup>174</sup>

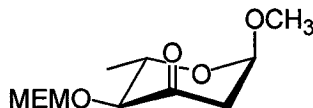
**Methyl 2,3-*O*-benzylidene-4-*O*-(methoxymethyl)- $\alpha$ -L-rhamnopyranoside (**59**)**



This compound was prepared by an adaptation of a procedure described by Brimacombe and coworkers.<sup>174</sup> A diastereomeric mixture of methyl 2,3-*O*-benzylidene- $\alpha$ -L-rhamnopyranoside acetals (**67**) (1.91 g, 7.20 mmol) was dissolved in DCM (15 mL) in a round-bottomed flask. Following the dropwise addition of ethyldiisopropylamine (2.1 mL, 12 mmol) and methoxymethyl chloride (1.3 mL, 17 mmol), the reaction mixture was stirred at rt for 48 h, after which time TLC analysis (35:65 EtOAc:hexanes,  $R_f$  product **59** = 0.71) revealed that all starting material had been consumed. After concentration under reduced pressure, the resulting crude yellow syrup was dissolved in DCM (50 mL) and washed with 1 M aqueous HCl (50 mL) and  $\text{H}_2\text{O}$  (50 mL). After

drying over Na<sub>2</sub>SO<sub>4</sub>, the organic layer was concentrated under reduced pressure and purified via silica gel chromatography (isocratic 12:88 EtOAc:hexanes), affording 4-*O*-MOM-protected derivative **59** as a colourless syrup (1.79 g, 5.77 mmol, 80% yield). <sup>1</sup>H NMR (250 MHz, CDCl<sub>3</sub>): δ *exo diastereomer*: 7.59-7.31 (m, 5 H, Ph), 6.15 (s, 1 H, PhCH), 4.92 (br d, 1 H, H-1), 4.71 (d, *J*<sub>H,H</sub> = 6.4 Hz, 2 H, OCH<sub>2</sub>O), 4.49 (dd, *J*<sub>2,3</sub> = 5.5 Hz, *J*<sub>3,4</sub> = 7.0 Hz, 1 H, H-3), 4.10 (br d, 1 H, H-2), 3.80-3.45 (m, 2 H, H-4, H-5), 3.40 (s, 3 H, OCH<sub>3</sub>), 3.38 (s, 3 H, OCH<sub>3</sub>), 1.37 (d, *J*<sub>5,6</sub> = 6.1 Hz, 3 H, H<sub>3</sub>-6); *endo diastereomer*: 7.59-7.31 (m, 5 H, Ph), 5.90 (s, 1 H, PhCH), 4.98 (br d, 1 H, H-1), 4.67 (d, *J*<sub>H,H</sub> = 6.4 Hz, 2 H, OCH<sub>2</sub>O), 4.32 (dd, *J*<sub>2,3</sub> = 6.4 Hz, *J*<sub>3,4</sub> = 6.6 Hz, 1 H, H-3), 4.19 (br d, 1 H, H-2), 3.80-3.45 (m, 2 H, H-4, H-5), 3.44 (s, 3 H, OCH<sub>3</sub>), 3.37 (s, 3 H, OCH<sub>3</sub>), 1.31 (d, *J*<sub>5,6</sub> = 6.1 Hz, 3 H, H<sub>3</sub>-6). The reported PhCH <sup>1</sup>H NMR data is consistent with that of Brimacombe and coworkers.<sup>174</sup>

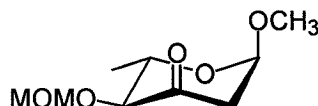
**Methyl 2,6-dideoxy-4-*O*-(2-methoxyethoxymethyl)-α-*L*-erythro-hexopyranosid-3-ulose (60)**



This compound was prepared by an adaptation of a procedure described by Brimacombe and coworkers.<sup>174</sup> A diastereomeric mixture of methyl 2,3-*O*-benzylidene-4-*O*-(2-methoxyethoxymethyl)-α-*L*-rhamnopyranoside acetals (**58**) (382 mg, 1.08 mmol) was dissolved in anhydrous THF (12 mL) in a two-necked round-bottomed flask fitted with a thermometer under a nitrogen atmosphere. After cooling this solution to -50 °C, *sec*-butyllithium in cyclohexane (1.0 M, 3.3 mL, 3.2 mmol) was added dropwise while keeping the internal temperature of the reaction mixture below -40 °C. After maintaining a temperature at or below -35 °C for 4 h, TLC analysis (35:65 EtOAc:hexanes, *R<sub>f</sub>* product

**60** = 0.21) revealed that all starting material had been consumed and the reaction mixture was allowed to warm up to -10 °C. The reaction mixture was poured into an ice-water mixture containing 10% w/v aqueous NH<sub>4</sub>Cl (20 mL) and extracted with DCM (2 x 20 mL). The combined organic extracts were washed with H<sub>2</sub>O (40 mL), dried over Na<sub>2</sub>SO<sub>4</sub>, and concentrated under reduced pressure. The resulting crude yellow syrup was purified via benchtop silica gel chromatography (isocratic 35:65 EtOAc:hexanes), which afforded 2-deoxy-3-ketosugar **60** as pale yellow crystals (190. mg, 0.767 mmol, 71% yield). <sup>1</sup>H NMR (250 MHz, CDCl<sub>3</sub>): δ 5.04 (dd, *J*<sub>1,2ax</sub> = 4.2 Hz, *J*<sub>1,2eq</sub> = 1.1 Hz, 1 H, H-1), 4.91 (d, *J*<sub>H,H</sub> = 7.0 Hz, 1 H, OCH<sub>2</sub>O), 4.86 (d, 1 H, OCH<sub>2</sub>O), 4.02-3.52 (m, 6 H, H-4, H-5, OCH<sub>2</sub>CH<sub>2</sub>O), 3.39 (s, 3 H, OCH<sub>3</sub>), 3.34 (s, 3 H, OCH<sub>3</sub>), 2.75 (dd, *J*<sub>2ax,2eq</sub> = 13.9 Hz, 1 H, H-2ax), 2.58 (dd, 1 H, H-2eq), 1.42 (d, *J*<sub>5,6</sub> = 5.8 Hz, 3 H, H<sub>3</sub>-6). The reported <sup>1</sup>H NMR data is consistent with that of Brimacombe and coworkers.<sup>174</sup>

**Methyl 2,6-dideoxy-4-*O*-(methoxymethyl)-α-*L*-erythro-hexopyranosid-3-ulose (61)**

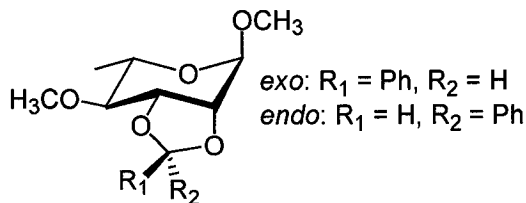


This compound was prepared by an adaptation of a procedure described by Brimacombe and coworkers.<sup>174</sup> A diastereomeric mixture of methyl 2,3-*O*-benzylidene-4-*O*-(methoxymethyl)-α-*L*-rhamnopyranoside acetals (**59**) (559 mg, 2.10 mmol) was dissolved in anhydrous THF (18 mL) in a two-necked round-bottomed flask fitted with a thermometer under a nitrogen atmosphere. After cooling this mixture to -50 °C, *n*-butyllithium in hexanes (1.8 M, 6.9 mL, 12 mmol) was added dropwise while keeping the internal temperature of the reaction mixture below -40 °C. After maintaining a temperature at or below -30 °C for 1 h, TLC analysis (35:65 EtOAc:hexanes, *R<sub>f</sub>* product



**61** = 0.45) revealed that all starting material had been consumed and the reaction mixture was allowed to warm up to -10 °C. The reaction mixture was poured into an ice-water mixture containing 10% w/v aqueous NH<sub>4</sub>Cl (30 mL) and extracted with DCM (2 x 30 mL). The combined organic extracts were washed with H<sub>2</sub>O (30 mL), dried over Na<sub>2</sub>SO<sub>4</sub>, and concentrated under reduced pressure. The resulting crude yellow syrup was purified via benchtop silica gel chromatography (isocratic 22:78 EtOAc:hexanes), which afforded 2-deoxy-3-ketosugar **61** as a colourless solid (69 mg, 0.34 mmol, 16% yield). <sup>1</sup>H NMR (250 MHz, CDCl<sub>3</sub>): δ 5.04 (dd,  $J_{1,2ax} = 4.6$  Hz,  $J_{1,2eq} = 1.2$  Hz, 1 H, H-1), 4.83 (d,  $J_{H,H} = 7.0$  Hz, 1 H, OCH<sub>2</sub>O), 4.69 (d, 1 H, OCH<sub>2</sub>O), 4.10-3.86 (m, 2 H, H-4, H-5), 3.44 (s, 3 H, OCH<sub>3</sub>), 3.37 (s, 3 H, OCH<sub>3</sub>), 2.77 (dd,  $J_{2ax,2eq} = 14.0$  Hz, 1 H, H-2ax), 2.59 (dd, 1 H, H-2eq), 1.44 (d,  $J_{5,6} = 5.8$  Hz, 3 H, H<sub>3</sub>-6). The reported <sup>1</sup>H NMR data is consistent with that of Brimacombe and coworkers.<sup>174</sup>

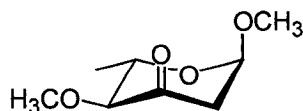
#### Methyl 2,3-*O*-benzylidene-4-*O*-methyl- $\alpha$ -L-rhamnopyranoside (**62**)



This compound was prepared via an adaptation of a methylation procedure described by Brimacombe.<sup>177</sup> A diastereomeric mixture of methyl 2,3-*O*-benzylidene- $\alpha$ -L-rhamnopyranoside acetals (**67**) (0.81 g, 3.2 mmol) was dissolved in DMF (15 mL) in a round-bottomed flask and cooled to 0 °C in an ice-water bath containing NaCl. Sodium hydride (0.61 g, 25 mmol) was added in small portions and the reaction mixture was stirred for 1 h at 0 °C. Methyl iodide (2.8 mL, 45 mmol) was subsequently added

dropwise and the reaction mixture was stirred at rt for 2.5 h, after which time TLC analysis (35:65 EtOAc:hexanes,  $R_f$  product **62** = 0.73) revealed that all starting material had been consumed. Anhydrous MeOH (10 mL) was added to decompose excess reagents and the reaction mixture was stirred for an additional 0.5 h at rt. Following concentration under reduced pressure, EtOAc (50 mL) and H<sub>2</sub>O (50 mL) were added to dissolve the oily residue and the resulting aqueous and organic layers were separated. The organic layer was washed with H<sub>2</sub>O (3 x 40 mL), dried over Na<sub>2</sub>SO<sub>4</sub>, and concentrated under reduced pressure to afford **62** as a pale yellow syrup (0.73 g, 2.7 mmol, 85% yield). <sup>1</sup>H NMR (500 MHz, CDCl<sub>3</sub>):  $\delta$  *exo* diastereomer: 7.55-7.33 (m, 5 H, Ph), 6.16 (s, 1 H, PhCH), 4.90 (br s, 1 H, H-1), 4.47 (dd,  $J_{2,3}$  = 5.5 Hz,  $J_{3,4}$  = 7.2 Hz, 1 H, H-3), 4.09 (br d, 1 H, H-2), 3.69-3.61 (m, 1 H, H-5), 3.60 (s, 3 H, OCH<sub>3</sub>), 3.36 (s, 3 H, OCH<sub>3</sub>), 3.11 (dd,  $J_{4,5}$  = 9.3 Hz, 1 H, H-4), 1.35 (d,  $J_{5,6}$  = 6.0 Hz, 3 H, H<sub>3</sub>-6); *endo* diastereomer: 7.55-7.33 (m, 5 H, Ph), 5.89 (s, 1 H, PhCH), 4.98 (br s, 1 H, H-1), 4.27 (dd,  $J_{2,3}$  = 6.3 Hz,  $J_{3,4}$  = 6.9 Hz, 1 H, H-3), 4.19 (br d, 1 H, H-2), 3.69-3.61 (m, 1 H, H-5), 3.48 (s, 3 H, OCH<sub>3</sub>), 3.38 (s, 3 H, OCH<sub>3</sub>), 3.01 (dd,  $J_{4,5}$  = 9.4 Hz, 1 H, H-4), 1.28 (d,  $J_{5,6}$  = 6.0 Hz, 3 H, H<sub>3</sub>-6). The reported <sup>1</sup>H NMR data is consistent with that of Clode and coworkers.<sup>176</sup>

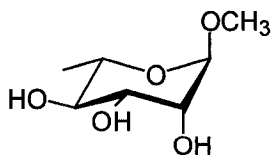
#### Methyl 2,6-dideoxy-4-*O*-methyl- $\alpha$ -L-erythro-hexopyranosid-3-ulose (**63**)



This compound was prepared by an adaptation of a procedure described by Brimacombe and coworkers.<sup>174</sup> A diastereomeric mixture of methyl 2,3-*O*-benzylidene-4-*O*-methyl- $\alpha$ -L-rhamnopyranoside acetals (**62**) (373 mg, 1.40 mmol) was dissolved in

anhydrous THF (11 mL) in a two-necked round-bottomed flask fitted with a thermometer under a nitrogen atmosphere. After cooling this solution to -50 °C, *n*-butyllithium in hexanes (1.5 M, 2.9 mL, 4.2 mmol) was added dropwise while keeping the internal temperature of the reaction mixture below -40 °C. After maintaining a temperature at or below -30 °C for 3 h, TLC analysis (10:90 EtOAc:hexanes,  $R_f$  product **63** = 0.17) revealed that all starting material had been consumed and the reaction mixture was allowed to warm up to -10 °C. The reaction mixture was poured into an ice-water mixture containing 10% w/v aqueous NH<sub>4</sub>Cl (20 mL) and extracted with DCM (2 x 20 mL). The combined organic extracts were washed with H<sub>2</sub>O (20 mL), dried over Na<sub>2</sub>SO<sub>4</sub>, and concentrated under reduced pressure. The resulting yellow syrup was purified via benchtop silica gel chromatography (isocratic 10:90 EtOAc:hexanes), which afforded 2-deoxy-3-ketosugar **63** as a colourless solid (56 mg, 0.32 mmol, 23% yield). <sup>1</sup>H NMR (500 MHz, CDCl<sub>3</sub>): δ 5.03 (dd,  $J_{1,2ax}$  = 4.0 Hz,  $J_{1,2eq}$  = 1.4 Hz, 1 H, H-1), 3.92 (m, 1 H, H-5), 3.53 (s, 3 H, OCH<sub>3</sub>), 3.42 (d,  $J_{4,5}$  = 9.6 Hz, 1 H, H-4), 3.33 (s, 3 H, OCH<sub>3</sub>), 2.75 (dd,  $J_{2ax,2eq}$  = 14.0 Hz, 1 H, H-2ax), 2.58 (dd, 1 H, H-2eq), 1.40 (d,  $J_{5,6}$  = 6.1 Hz, 3 H, H<sub>3</sub>-6). The reported <sup>1</sup>H NMR data is consistent with that of Clode and coworkers.<sup>176</sup>

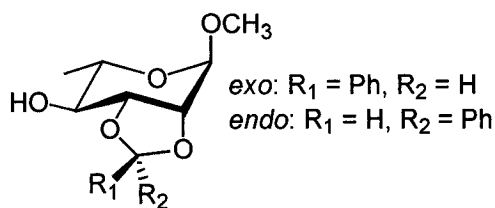
#### Methyl α-L-rhamnopyranoside (**66**)



This compound was prepared by an adaptation of a procedure described by Clode and coworkers.<sup>176</sup> L-Rhamnose monohydrate (30.0 g, 183 mmol), anhydrous MeOH (500 mL), Amberlite® IR-120 (H<sup>+</sup>) resin (30 g dry mass, washed with 1 M aqueous HCl and

MeOH prior to the reaction, free acid form), and 3 Å molecular sieves (20 g) were combined in a round-bottomed flask and heated to 95 °C under a nitrogen atmosphere. After 24 h, no starting material remained by TLC (6:3:1 DCM:EtOAc:EtOH,  $R_f$  product **66** = 0.40). Following filtration and concentration under reduced pressure, methyl glycoside **66** was isolated as a yellow syrup that resisted crystallization attempts (30.8 g, 173 mmol, 95% yield).  $^1\text{H}$  NMR (500 MHz,  $\text{D}_2\text{O}$ ):  $\delta$  4.72 (d,  $J_{1,2}$  = 2.0 Hz, 1 H, H-1), 3.96 (dd,  $J_{2,3}$  = 3.5 Hz, 1 H, H-2), 3.74 (dd,  $J_{3,4}$  = 10.0 Hz, 1 H, H-3), 3.70 (dq,  $J_{4,5}$  = 9.5 Hz,  $J_{5,6}$  = 6.0 Hz, 1 H, H-5), 3.46 (dd, 1 H, H-4), 3.43 (s, 3 H,  $\text{OCH}_3$ ), 1.33 (d, 3 H,  $\text{H}_3\text{-6}$ ).

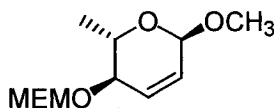
#### Methyl 2,3-*O*-benzylidene- $\alpha$ -L-rhamnopyranoside (**67**)



This compound was prepared by an adaptation of a procedure described by Clode and coworkers.<sup>176</sup> Methyl- $\alpha$ -L-rhamnopyranoside (**66**) (5.20 g, 29.2 mmol) and *p*-toluenesulfonic acid monohydrate (0.019 g, 0.010 mmol) were dissolved in DMF (31 mL) in a round-bottomed flask.  $\alpha,\alpha$ -Dimethoxytoluene (5.2 mL, 35 mmol) was added dropwise to this solution and the round-bottomed flask was fitted with an air condensor, which was attached to a water aspirator through a drying tube containing Drierite®. The reaction mixture was heated to 75 °C and stirred for 24 h, after which time TLC analysis revealed that no starting material remained (35:65 EtOAc:hexanes,  $R_f$  product **67** = 0.57). The reaction mixture was poured into an ice-saturated aqueous  $\text{NaHCO}_3$  solution (50 mL) and extracted with DCM (75 mL). The organic layer was washed with  $\text{H}_2\text{O}$  (75 mL),

dried over Na<sub>2</sub>SO<sub>4</sub>, and concentrated to afford a crude colourless liquid. The components of this liquid were separated via benchtop silica gel chromatography (isocratic 25:75 EtOAc:hexanes), which resulted in the recovery of excess  $\alpha,\alpha$ -dimethoxytoluene in addition to the desired diastereomeric products (**67**, 3:2 *exo:endo*), isolated as a colourless syrup (5.46 g, 20.4 mmol, 70% yield). <sup>1</sup>H NMR (250 MHz, CDCl<sub>3</sub>):  $\delta$  *exo diastereomer*: 7.55-7.30 (m, 5 H, Ph), 6.14 (s, 1 H, PhCH), 4.89 (br s, 1 H, H-1), 4.42-3.44 (m, 4 H, H-2, H-3, H-4, H-5), 3.38 (s, 3 H, OCH<sub>3</sub>), 2.58 (d,  $J_{4,OH}$  = 4.3 Hz, 1 H, OH), 1.36 (d,  $J_{5,6}$  = 6.1 Hz, 3 H, H<sub>3</sub>-6); *endo diastereomer*: 7.55-7.30 (m, 5 H, Ph), 5.90 (s, 1 H, PhCH), 4.91 (br s, 1 H, H-1), 4.42-3.44 (m, 4 H, H-2, H-3, H-4, H-5), 3.41 (s, 3 H, OCH<sub>3</sub>), 2.64 (d,  $J_{4,OH}$  = 4.9 Hz, 1 H, OH), 1.30 (d,  $J_{5,6}$  = 6.4 Hz, 3 H, H<sub>3</sub>-6). The reported <sup>1</sup>H NMR data is consistent with that of Clode and coworkers.<sup>176</sup>

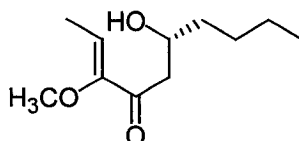
**Methyl 2,3,6-trideoxy-4-*O*-(2-methoxyethoxymethyl)- $\alpha$ -L-erythro-hex-2-enopyranoside (**76**)**



This compound was isolated as a byproduct from several Klemer-Rodemeyer reactions in which a diastereomeric mixture of methyl 2,3-*O*-benzylidene-4-*O*-(2-methoxyethoxymethyl)- $\alpha$ -L-rhamnopyranoside (**58**) was used as a starting material to prepare methyl 2,6-dideoxy-4-*O*-(2-methoxyethoxymethyl)- $\alpha$ -L-erythro-hexopyranosid-3-ulose (**60**) via reaction with *n*-butyllithium. Similar byproducts were also observed in the crude <sup>1</sup>H NMR spectra of analogous reactions aimed at preparing 4-*O*-MOM-protected (**61**) and 4-*O*-methyl-protected (**63**) 2-deoxy-3-ketosugars. <sup>1</sup>H NMR (500 MHz, CDCl<sub>3</sub>):  $\delta$  6.03 (br d,  $J_{4,5}$  = 10.0 Hz, 1 H, H-4), 5.74 (ddd,  $J_{3,5}$  = 0.5 Hz,  $J_{5,6}$  = 2.5 Hz, 1 H, H-5), 4.86 (d,  $J_{H,H}$  = 7.0 Hz, 1 H, OCH<sub>2</sub>O), 4.81 (m, 1 H, H-6), 4.77 (d, 1 H,

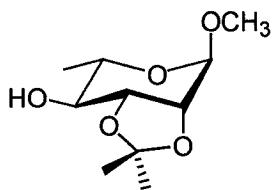
OCH<sub>2</sub>O), 3.88-3.54 (m, 6 H, H-2, H-3, OCH<sub>2</sub>CH<sub>2</sub>O), 3.42 (s, 3 H, OCH<sub>3</sub>), 3.39 (s, 3 H, OCH<sub>3</sub>), 1.30 (d,  $J_{2,CH3} = 5.5$  Hz, 3 H, CHCH<sub>3</sub>); <sup>13</sup>C{<sup>1</sup>H} NMR (126 MHz, CDCl<sub>3</sub>): δ 131.7 (C-4), 126.6 (C-5), 95.5 (C-6), 95.1 (OCH<sub>2</sub>O), 75.5, 71.8, 67.3, 66.0 (C-2, C-3, OCH<sub>2</sub>CH<sub>2</sub>O), 59.2 (OCH<sub>3</sub>), 55.7 (OCH<sub>3</sub>), 18.3 (CHCH<sub>3</sub>).

**(6R)-6-Hydroxy-3-methoxy-dec-2-en-4-one (77)**



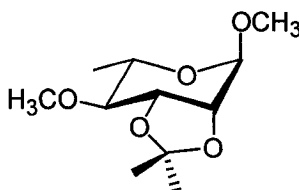
This compound was isolated as a byproduct from several Klemm-Rodemeyer reactions in which a diastereomeric mixture of methyl 2,3-*O*-benzylidene-4-*O*-methyl- $\alpha$ -L-rhamnopyranoside acetals (**62**) was used as a starting material to prepare methyl 2,6-dideoxy-4-*O*-methyl- $\alpha$ -L-*erythro*-hexopyranosid-3-ulose (**63**) via reaction with *n*-butyllithium. Similar byproducts were also observed in the crude <sup>1</sup>H NMR spectra of analogous reactions aimed at preparing 4-*O*-MEM- (**60**) and 4-*O*-MOM-protected (**61**) 2-deoxy-3-ketosugars. NMR spectra of this compound can be found in Appendix 1. <sup>1</sup>H NMR (500 MHz, CDCl<sub>3</sub>): δ 6.29 (q,  $J_{1,2} = 7.0$  Hz, 1 H, H-2), 4.07 (m, 1 H, H-6), 3.66 (s, 3 H, OCH<sub>3</sub>), 3.09 (br s, 1 H, OH), 2.80 (dd,  $J_{5a,6} = 2.5$  Hz,  $J_{5a,5b} = 17.5$  Hz, 1 H, H-5a), 2.66 (dd,  $J_{5b,6} = 9.0$  Hz, 1 H, H-5b), 1.84 (d, 3 H, H<sub>3</sub>-1), 1.57-1.22 (m, 6 H, CH<sub>2</sub>CH<sub>2</sub>CH<sub>2</sub>), 0.91 (t,  $J_{H,H} = 5.0$  Hz, 3 H, CH<sub>2</sub>CH<sub>3</sub>); <sup>13</sup>C{<sup>1</sup>H} NMR (126 MHz, CDCl<sub>3</sub>): δ 198.5 (C=O), 154.9 (C-3), 124.8 (C-2), 67.9 (C-6), 60.0 (OCH<sub>3</sub>), 44.4 (C-5), 36.3 (CH<sub>2</sub>), 27.7 (CH<sub>2</sub>), 22.6 (CH<sub>2</sub>), 14.0 (CH<sub>2</sub>CH<sub>3</sub>), 11.4 (C-1); calcd 200.1412 amu for C<sub>11</sub>H<sub>20</sub>O<sub>3</sub>, HRMS (EI<sup>+</sup>) found 200.1408 +/-0.0008 amu.

### Methyl 2,3-*O*-isopropylidene- $\alpha$ -L-rhamnopyranoside (**78**)



This compound was prepared by an adaptation of a procedure described by Brimacombe and coworkers.<sup>189</sup> Methyl- $\alpha$ -L-rhamnopyranoside (**66**) (6.39 g, 35.9 mmol) was dissolved in 2,2-dimethoxypropane (22 mL, 180 mmol) in a round-bottomed flask. *p*-Toluenesulfonic acid monohydrate (0.12 g, 0.63 mmol) was added and the resulting reaction mixture was stirred for 30 min at rt, after which time TLC analysis (6:3:1 DCM:EtOAc:EtOH,  $R_f$  product **78** = 0.43) revealed the complete consumption of starting material. The reaction mixture was diluted with DCM (60 mL) and the organic layer was washed with 5% w/v aqueous NaHCO<sub>3</sub> (30 mL) and H<sub>2</sub>O (3 x 30 mL). The organic layer was dried over Na<sub>2</sub>SO<sub>4</sub> and concentrated under reduced pressure to afford **78** as a pale yellow syrup (7.20 g, 33.0 mmol, 92% yield). <sup>1</sup>H NMR (500 MHz, CDCl<sub>3</sub>):  $\delta$  4.86 (br s, 1 H, H-1), 4.14-4.00 (m, 2 H, H-2, H-3), 3.58 (m, 1 H, H-5), 3.36 (s, 3 H, OCH<sub>3</sub>), 3.31 (m, 1 H, H-4), 1.51 (s, 3 H, C(CH<sub>3</sub>)<sub>2</sub>), 1.34 (s, 3 H, C(CH<sub>3</sub>)<sub>2</sub>), 1.28 (d,  $J_{5,6}$  = 6.6 Hz, 3 H, H<sub>3</sub>-6).

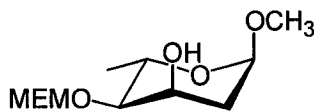
**Methyl 2,3-*O*-isopropylidene-4-*O*-methyl- $\alpha$ -L-rhamnopyranoside (79)**



This compound was prepared via an adaptation of a methylation procedure described by Brimacombe.<sup>177</sup> Methyl 2,3-*O*-isopropylidene- $\alpha$ -L-rhamnopyranoside (**78**) (2.75 g, 12.6 mmol) was dissolved in DMF (150 mL) in a round-bottomed flask and cooled to 0 °C in an ice-water bath containing NaCl. Sodium hydride (2.40 g, 100. mmol) was added in small portions and the reaction mixture was stirred for 1 h at 0 °C. Methyl iodide (11 mL, 180 mmol) was subsequently added dropwise and the resulting reaction mixture was stirred for 1 h at rt, after which time TLC analysis (35:65 EtOAc:hexanes,  $R_f$  product **79** = 0.78) revealed that all starting material had been consumed. Anhydrous MeOH (46 mL) was added to decompose excess reagents and the reaction mixture was stirred for 0.5 h at rt. Following concentration under reduced pressure, EtOAc (160 mL) and H<sub>2</sub>O (160 mL) were added to dissolve the oily residue and the resulting aqueous and organic layers separated. The organic layer was washed with H<sub>2</sub>O (3 x 130 mL), dried over Na<sub>2</sub>SO<sub>4</sub>, and concentrated under reduced pressure to afford a crude pale yellow syrup. This crude product was purified via benchtop silica gel chromatography (isocratic 10:90 EtOAc:hexanes), resulting in the isolation of methylated derivative **79** as a colorless syrup (1.93 g, 8.32 mmol, 66% yield). <sup>1</sup>H NMR (500 MHz, CDCl<sub>3</sub>):  $\delta$  4.83 (br s, 1 H, H-1), 4.14-4.08 (m, 2 H, H-2, H-3), 3.57 (m, 1 H, H-5), 3.53 (s, 3 H, OCH<sub>3</sub>), 3.36 (s, 3 H, OCH<sub>3</sub>), 2.96 (dd,  $J_{3,4}$  = 9.6 Hz,  $J_{4,5}$  = 6.3 Hz, 1 H, H-4), 1.54 (s, 3 H, C(CH<sub>3</sub>)<sub>2</sub>), 1.35 (s, 3 H, C(CH<sub>3</sub>)<sub>2</sub>), 1.28 (d,  $J_{5,6}$  = 6.3 Hz, 3 H, H<sub>3</sub>-6).

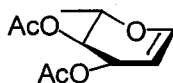


**Methyl 2,6-dideoxy-4-*O*-(2-methoxyethoxymethyl)- $\alpha$ -L-ribo-hexopyranoside (**82**)**



This compound was prepared by an adaptation of a procedure described by Brimacombe and coworkers.<sup>174</sup> Methyl 2,6-dideoxy-4-*O*-(2-methoxyethoxymethyl)- $\alpha$ -L-*erythro*-hexopyranosid-3-ulose (**60**) (560. mg, 2.26 mmol) was dissolved in HPLC-grade MeOH (25 mL) in a round-bottomed flask and NaBH<sub>4</sub> (810. mg, 21.4 mmol) was added in small portions. The reaction mixture was stirred at rt for 1 h, after which time TLC analysis (75:25 EtOAc:hexanes, *R<sub>f</sub>* product **82** = 0.22) revealed that all starting material had been consumed. The reaction mixture was concentrated under reduced pressure and re-dissolved in DCM (30 mL), which was subsequently washed with H<sub>2</sub>O (10 mL). After drying over Na<sub>2</sub>SO<sub>4</sub> and concentration under reduced pressure, a crude yellow syrup was obtained, which was purified via benchtop silica gel chromatography (isocratic 75:25 EtOAc:hexanes) to afford 2,6-dideoxysugar **82** as a pale yellow syrup (453 mg, 1.81 mmol, 80% yield). <sup>1</sup>H NMR (500 MHz, CDCl<sub>3</sub>):  $\delta$  4.90 (d, *J*<sub>H,H</sub> = 7.5 Hz, 1 H, OCH<sub>2</sub>O), 4.78 (d, 1 H, OCH<sub>2</sub>O), 4.74 (br d, *J*<sub>1,2ax</sub> = 4.0 Hz, 1 H, H-1), 4.15 (m, 1 H, H-3), 4.02 (dq, *J*<sub>4,5</sub> = 9.5 Hz, *J*<sub>5,6</sub> = 6.5 Hz, 1 H, H-5), 3.86-3.55 (m, 4 H, OCH<sub>2</sub>CH<sub>2</sub>O), 3.40 (s, 3 H, OCH<sub>3</sub>), 3.38 (s, 3 H, OCH<sub>3</sub>), 3.28 (dd, *J*<sub>3,4</sub> = 3.0 Hz, 1 H, H-4), 2.13 (ddd, *J*<sub>1,2eq</sub> = 1.0 Hz, *J*<sub>2ax,2eq</sub> = 15.0 Hz, *J*<sub>2eq,3</sub> = 3.5 Hz, 1 H, H-2eq), 1.89 (dt, *J*<sub>2ax,3</sub> = 3.5 Hz, 1 H, H-2ax), 1.42 (d, 3 H, H<sub>3</sub>-6). The reported <sup>1</sup>H NMR data is consistent with that of Brimacombe and coworkers.<sup>174</sup>

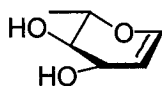
### 3,4-Di-*O*-acetyl-L-rhamnal (**83**)



This compound was prepared by an adaptation of a procedure described by Koreeda and coworkers.<sup>194</sup> L-Rhamnose monohydrate (5.00 g, 27.4 mmol) was added to a round-bottomed flask, which was subsequently cooled to 0-5 °C in an ice-water bath. Acetic anhydride (16.0 mL, 145 mmol) was added and the round-bottomed flask was fitted with a septum. A small amount of 33% HBr in acetic acid (250  $\mu$ L, 1.4 mmol) was added through the septum, the ice-water bath was removed, and the reaction mixture was stirred for 1 h at rt, after which time all solid had dissolved and TLC analysis (35:65 EtOAc:hexanes,  $R_f$  acetylated product = 0.35) revealed the complete consumption of starting material. Additional 33% HBr in acetic acid (26.0 mL, 144 mmol) was added and the resulting reaction mixture was stirred for 1.5 h, after which time TLC analysis (35:65 EtOAc:hexanes,  $R_f$  brominated product = 0.48) revealed that the bromination reaction was complete. Anhydrous NaOAc (12.5 g, 152 mmol) was subsequently added to neutralize excess HBr in acetic acid and the reaction mixture was poured into a suspension of CuSO<sub>4</sub>·5H<sub>2</sub>O (1.25 g, 5.01 mmol), Zn<sup>0</sup> dust (50.0 g, 765 mmol), and NaOAc·3H<sub>2</sub>O (62.5 g, 459 mmol) in a solution of H<sub>2</sub>O (50 mL) and acetic acid (25 mL). The resulting reaction mixture was cooled to 0-5 °C in an ice-water bath and stirred vigorously for 1.5 h, after which time the reaction was deemed complete by TLC (25:75 EtOAc:hexanes,  $R_f$  product **83** = 0.60). The reaction mixture was filtered through a short plug of Celite® and the solid was washed successively with EtOAc (500 mL) and H<sub>2</sub>O

(500 mL).<sup>f</sup> After partitioning organic and aqueous layers of the filtrate, the organic layer was washed with H<sub>2</sub>O (500 mL), saturated aqueous NaHCO<sub>3</sub> (500 mL), and saturated aqueous NaCl (250 mL). Following drying over Na<sub>2</sub>SO<sub>4</sub> and concentration under reduced pressure, a crude yellow syrup was obtained. Purification via a short silica gel plug in a scintillated funnel (isocratic 10:90 EtOAc:hexanes) afforded **83** as a colorless syrup (4.99 g, 23.3 mmol, 85% yield). <sup>1</sup>H NMR (500 MHz, CDCl<sub>3</sub>): δ 6.43 (dd, *J*<sub>1,2</sub> = 6.3 Hz, *J*<sub>1,3</sub> = 1.3 Hz, 1 H, H-1), 5.34 (ddd, *J*<sub>2,3</sub> = 3.0 Hz, *J*<sub>3,4</sub> = 6.0 Hz, 1 H, H-3), 5.03 (dd, *J*<sub>4,5</sub> = 8.3 Hz, 1 H, H-4), 4.78 (dd, 1 H, H-2), 4.11 (dq, *J*<sub>5,6</sub> = 6.5 Hz, 1 H, H-5), 2.09 (s, 3 H, C(O)CH<sub>3</sub>), 2.04 (s, 3 H, C(O)CH<sub>3</sub>), 1.31 (d, 3 H, H<sub>3</sub>-6); <sup>13</sup>C{<sup>1</sup>H} NMR (125 MHz, CDCl<sub>3</sub>): δ 170.6 (CH<sub>3</sub>CO<sub>2</sub>), 169.9 (CH<sub>3</sub>CO<sub>2</sub>), 146.0 (C-1), 98.8 (C-2), 72.5 (C-5), 71.8 (C-4), 68.3 (C-3), 21.0 (CH<sub>3</sub>CO<sub>2</sub>), 20.9 (CH<sub>3</sub>CO<sub>2</sub>), 16.5 (C-6). The reported <sup>1</sup>H and <sup>13</sup>C{<sup>1</sup>H} NMR data is consistent with that of van Heerden and coworkers.<sup>195</sup>

#### L-Rhamnal (**84**)

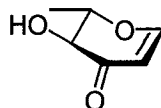


This compound was prepared by an adaptation of a procedure described by van Heerden and coworkers.<sup>195</sup> 3,4-Di-*O*-acetyl-L-rhamnal (**83**) (2.84 g, 13.3 mmol) was dissolved in HPLC-grade MeOH (15 mL) in a round-bottomed flask. Potassium carbonate (72 mg, 0.52 mmol) was added and the resulting reaction mixture was stirred vigorously for 3 h at rt, after which time TLC analysis (100% EtOAc, *R<sub>f</sub>* product **84** = 0.36) confirmed that the reaction was complete. The reaction mixture was filtered

<sup>f</sup> The solid collected during the Celite® filtration should be washed with H<sub>2</sub>O immediately after washing with EtOAc while the solid still contains some organic solvent. Dried solids containing zinc with trace organic solvents can readily combust.

through a short silica gel plug in a scintillated funnel, which was washed with HPLC-grade MeOH (25 mL). Concentration of the filtrate under reduced pressure afforded white crystals of **84** (1.73 g, 13.3 mmol, 100% yield).  $^1\text{H}$  NMR (500 MHz,  $\text{CDCl}_3$ ):  $\delta$  6.31 (dd,  $J_{1,2} = 6.0$  Hz,  $J_{1,3} = 1.5$  Hz, 1 H, H-1), 4.69 (dd,  $J_{2,3} = 2.0$  Hz, 1 H, H-2), 4.21 (ddd,  $J_{3,4} = 7.5$  Hz, 1 H, H-3), 3.84 (dq,  $J_{4,5} = 10.0$  Hz,  $J_{5,6} = 6.0$  Hz, 1 H, H-5), 3.40 (dd, 1 H, H-4), 1.38 (d, 3 H,  $\text{H}_3$ -6);  $^{13}\text{C}\{^1\text{H}\}$  NMR (125 MHz,  $\text{CDCl}_3$ ):  $\delta$  144.8 (C-1), 102.7 (C-2), 75.2 (C-4), 74.5 (C-5), 70.2 (C-3), 17.1 (C-6); mp 73-74 °C (lit.<sup>196</sup> mp 72-73 °C).

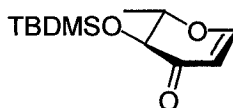
#### 1,5-Anhydro-2,6-dideoxy-L-erythro-hex-1-en-3-ulose (**85**)



This compound was prepared by an adaptation of a procedure described by Czernecki and coworkers.<sup>196</sup> L-Rhamnal (**84**) (2.74 g, 21.1 mmol) was dissolved in HPLC-grade EtOAc (260 mL) in a round-bottomed flask. Glacial acetic acid (2.6 mL, 45.5 mmol) was added dropwise followed by 3 Å molecular sieves (*ca.* 30) and the resulting solution was stirred for 15 min at rt. Pyridinium dichromate (4.54 g, 12.1 mmol) was subsequently added and the reaction mixture was stirred for 17 h at rt, after which time the reaction was deemed complete by TLC (100% EtOAc,  $R_f$  product **85** = 0.77). The reaction mixture was filtered through two short silica gel plugs in scintillated funnels, washing with HPLC- grade EtOAc, to remove the Cr(III) species. After the second filtration, white crystals of enulose **85** were obtained (2.19 g, 17.1 mmol, 81% yield) following concentration of the filtrate under reduced pressure.  $^1\text{H}$  NMR (500 MHz,  $\text{CDCl}_3$ ):  $\delta$  7.39 (d,  $J_{1,2} = 5.8$  Hz, 1 H, H-1), 5.46 (d, 1 H, H-2), 4.20 (dq,  $J_{4,5} = 13.0$

Hz,  $J_{5,6} = 6.0$  Hz, 1 H, H-5), 3.98 (d, 1 H, H-4), 1.58 (d, 3 H, H<sub>3</sub>-6);  $^{13}\text{C}\{^1\text{H}\}$  NMR (125 MHz,  $\text{CDCl}_3$ ):  $\delta$  194.2 (C=O), 164.7 (C-1), 103.5 (C-2), 80.0 (C-5), 72.8 (C-4), 18.0 (C-6); mp 87-88 °C (lit. mp<sup>196</sup> 92-93 °C, lit. mp<sup>269</sup> 86 °C). The reported  $^1\text{H}$  NMR data is consistent with that of Paulsen and Bünsch.<sup>269</sup>

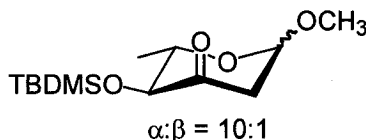
**1,5-Anhydro-4-*O*-(*tert*-butyldimethylsilyl)-2,6-dideoxy-L-*erythro*-hex-1-en-3-ulose (87)**



This compound was prepared via an adaptation of a *tert*-butyldimethylsilyl derivatization procedure described by Corey and Venkateswarlu.<sup>201</sup> 1,5-Anhydro-2,6-dideoxy-L-*erythro*-hex-1-en-3-ulose (**85**) (1.54 g, 12.0 mmol) was dissolved in anhydrous DMF (15 mL) in a round-bottomed flask under a nitrogen atmosphere. Imidazole (2.05 g, 30.1 mmol) and *tert*-butyldimethylsilyl chloride (2.17 g, 14.4 mmol) were added and the reaction mixture was stirred for 19 h at rt, after which time TLC analysis (10:90 EtOAc:hexanes,  $R_f$  product **87** = 0.38) revealed the complete consumption of starting material. The reaction mixture was diluted with EtOAc (50 mL) and extracted with  $\text{H}_2\text{O}$  (3 x 50 mL). After drying over  $\text{Na}_2\text{SO}_4$  and concentration under reduced pressure, TBDMS-protected derivative **87** was obtained as a colorless syrup (2.33 g, 9.61 mmol, 80% yield).  $^1\text{H}$  NMR (500 MHz,  $\text{CDCl}_3$ ):  $\delta$  7.29 (d,  $J_{1,2} = 6.0$  Hz, 1 H, H-1), 5.35 (d, 1 H, H-2), 4.32 (dq,  $J_{4,5} = 11.5$  Hz,  $J_{5,6} = 6.0$  Hz, 1 H, H-5), 4.02 (d, 1 H, H-4), 1.52 (d, 3 H, H<sub>3</sub>-6), 0.95 (s, 9 H,  $\text{C}(\text{CH}_3)_3$ ), 0.24 (s, 3 H,  $\text{Si}(\text{CH}_3)_2$ ), 0.12 (s, 3 H,  $\text{Si}(\text{CH}_3)_2$ );  $^{13}\text{C}\{^1\text{H}\}$  NMR (125 MHz,  $\text{CDCl}_3$ ):  $\delta$  193.7 (C=O), 162.3 (C-1), 105.0

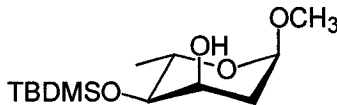
(C-2), 80.2 (C-5), 75.3 (C-4), 26.0 (C(CH<sub>3</sub>)<sub>3</sub>), 25.83 (C(CH<sub>3</sub>)<sub>3</sub>), 25.80 (C(CH<sub>3</sub>)<sub>3</sub>), 18.7 (C(CH<sub>3</sub>)<sub>3</sub>), 18.2 (C-6), -3.9 (Si(CH<sub>3</sub>)<sub>2</sub>), -5.4 (Si(CH<sub>3</sub>)<sub>2</sub>).

**Methyl 4-*O*-(*tert*-butyldimethylsilyl)-2,6-dideoxy- $\alpha/\beta$ -L-*erythro*-hexopyranosid-3-ulose (88)**



This compound was prepared via an adaptation of a 1,4-addition procedure described by Köpper and Thiem.<sup>192</sup> 1,5-Anhydro-4-*O*-(*tert*-butyldimethylsilyl)-2,6-dideoxy-L-*erythro*-hex-1-en-3-ulose (**87**) (85 mg, 0.35 mmol) was dissolved in 0.01 M NaOMe in MeOH (7.1 mL) and the resulting reaction mixture was stirred for 1 h at rt, after which time TLC analysis (10:90 EtOAc:hexanes, *R<sub>f</sub>* diastereomeric product **88** = 0.35 and 0.27) revealed the complete consumption of starting material. The reaction mixture was neutralized to pH 7 using Amberlite® IR-120 (H<sup>+</sup>) ion exchange resin (free acid form), filtered, and concentrated under reduced pressure to afford **88** as a pale yellow syrup in an  $\alpha:\beta$  ratio of 10:1 (81 mg, 0.30 mmol, 86% yield). <sup>1</sup>H NMR (500 MHz, CDCl<sub>3</sub>):  $\delta$   $\alpha$  diastereomer: 5.06 (br d, *J*<sub>1,2ax</sub> = 4.5 Hz, 1 H, H-1), 3.96 (dq, *J*<sub>4,5</sub> = 9.5 Hz, *J*<sub>5,6</sub> = 6.5 Hz, 1 H, H-5), 3.88 (d, 1 H, H-4), 3.36 (s, 3 H, OCH<sub>3</sub>), 2.75 (dd, *J*<sub>2ax,2eq</sub> = 14.0 Hz, 1 H, H-2ax), 2.61 (br d, 1 H, H-2eq), 1.44 (d, 3 H, H<sub>3</sub>-6), 0.95 (s, 9 H, C(CH<sub>3</sub>)<sub>3</sub>), 0.20 (s, 3 H, Si(CH<sub>3</sub>)<sub>2</sub>), 0.06 (s, 3 H, Si(CH<sub>3</sub>)<sub>2</sub>);  $\beta$  diastereomer: 4.59 (dd, *J*<sub>1,2a</sub> = 9.5 Hz, *J*<sub>1,2e</sub> = 2.5 Hz, 1 H, H-1); <sup>13</sup>C{<sup>1</sup>H} NMR (125 MHz, CDCl<sub>3</sub>):  $\delta$   $\alpha$  diastereomer: 203.4 (C=O), 99.6 (C-1), 80.5 (C-4), 70.7 (C-5), 54.8 (OCH<sub>3</sub>), 46.5 (C-2), 25.94 (C(CH<sub>3</sub>)<sub>3</sub>), 25.93 (C(CH<sub>3</sub>)<sub>3</sub>), 25.91 (C(CH<sub>3</sub>)<sub>3</sub>), 19.2 (C-6), 18.7 (C(CH<sub>3</sub>)<sub>3</sub>), -4.1 (Si(CH<sub>3</sub>)<sub>2</sub>), -5.4 (Si(CH<sub>3</sub>)<sub>2</sub>).

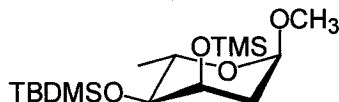
**Methyl 4-*O*-(*tert*-butyldimethylsilyl)-2,6-dideoxy- $\alpha$ -L-ribo-hexopyranoside (**89**)**



This compound was prepared by an adaptation of a reduction procedure described by Brimacombe and coworkers.<sup>174</sup> Methyl 4-*O*-(*tert*-butyldimethylsilyl)-2,6-dideoxy- $\alpha/\beta$ -L-*erythro*-hexopyranosid-3-ulose (**88**) (1.78 g, 6.49 mmol) was dissolved in HPLC-grade MeOH (72 mL) in a round-bottomed flask. Sodium borohydride (2.33 g, 61.7 mmol) was subsequently added in small portions and the reaction mixture was stirred for 1 h at rt, after which time TLC analysis (10:90 EtOAc:hexanes,  $R_f$  product **89** = 0.16) revealed the reaction was complete. The reaction mixture was concentrated under reduced pressure, re-dissolved in DCM (50 mL), and washed with H<sub>2</sub>O (25 mL). The organic layer was dried over MgSO<sub>4</sub> and concentrated under reduced pressure to yield crude **89** as a pale yellow syrup. Purification via automated silica gel chromatography using a Biotage 40M (40 mm x 15 cm) column (solvent system = 5:95 A:B (10 CV), linear gradient to 10:90 A:B (5 CV), 10:90 A:B (2 CV) where A = EtOAc and B = hexanes; flow-rate = 40 mL/min), afforded diastereomerically pure **89** as a colorless syrup (1.40 g, 5.06 mmol, 78% yield). <sup>1</sup>H NMR (500 MHz, CDCl<sub>3</sub>):  $\delta$  4.70 (br d,  $J_{1,2ax}$  = 4.0 Hz, 1 H, H-1), 3.96 (dq,  $J_{4,5}$  = 9.5 Hz,  $J_{5,6}$  = 6.0 Hz, 1 H, H-5), 3.91 (m, 1 H, H-3), 3.36 (s, 3 H, OCH<sub>3</sub>), 3.32 (dd,  $J_{3,4}$  = 3.0 Hz, 1 H, H-4), 3.05 (d,  $J_{3,OH}$  = 5.5 Hz, 1 H, OH), 2.14 (dd,  $J_{2ax,2eq}$  = 15.0 Hz,  $J_{2eq,3}$  = 3.0 Hz, 1 H, H-2eq), 1.88 (dt,  $J_{2ax,3}$  = 3.5 Hz, 1 H, H-2ax), 1.24 (d, 3 H, H<sub>3</sub>-6), 0.92 (s, 9 H, C(CH<sub>3</sub>)<sub>3</sub>), 0.11 (s, 3 H, Si(CH<sub>3</sub>)<sub>2</sub>), 0.10 (s, 3 H, Si(CH<sub>3</sub>)<sub>2</sub>); <sup>13</sup>C{<sup>1</sup>H} NMR (125 MHz, CDCl<sub>3</sub>):  $\delta$  98.2 (C-1), 74.8 (C-4), 67.8 (C-3), 63.2

(C-5), 55.3 (OCH<sub>3</sub>), 35.4 (C-2), 25.94 (C(CH<sub>3</sub>)<sub>3</sub>), 25.93 (C(CH<sub>3</sub>)<sub>3</sub>), 25.92 (C(CH<sub>3</sub>)<sub>3</sub>), 18.3 (C-6), 18.2 (C(CH<sub>3</sub>)<sub>3</sub>), -4.1 (Si(CH<sub>3</sub>)<sub>2</sub>), -4.5 (Si(CH<sub>3</sub>)<sub>2</sub>).

**Methyl 4-*O*-(*tert*-butyldimethylsilyl)-2,6-dideoxy-3-*O*-(trimethylsilyl)- $\alpha$ -L-ribo-hexopyranoside (**90**)**

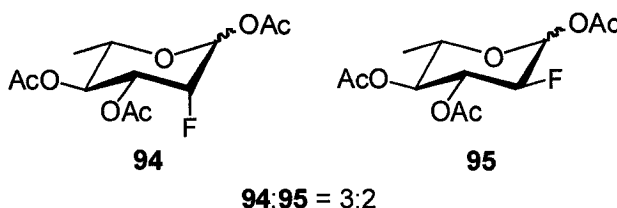


This compound was prepared by an adaptation of a trimethylsilyl derivatization procedure described by Uchiyama and Hindsgaul.<sup>143</sup> Methyl 4-*O*-(*tert*-butyldimethylsilyl)-2,6-dideoxy- $\alpha$ -L-ribo-hexopyranoside (**89**) (460 mg, 1.66 mmol) was dissolved in anhydrous pyridine (8 mL) in a round-bottomed flask under a nitrogen atmosphere and cooled to 0-5 °C in an ice-water bath. Trimethylsilyl chloride (320  $\mu$ L, 2.49 mmol) was added dropwise and the reaction mixture was stirred for 1 h at 0-5 °C, after which time TLC analysis (10:90 EtOAc:hexanes,  $R_f$  product **90** = 0.50) revealed the reaction was complete. The reaction mixture was diluted with hexanes (50 mL) and washed with H<sub>2</sub>O (5 x 20 mL). The organic layer was dried over Na<sub>2</sub>SO<sub>4</sub> and concentrated under reduced pressure to afford **90** as a colorless syrup (549 mg, 1.57 mmol, 95% yield), which required no further purification. <sup>1</sup>H NMR (500 MHz, CDCl<sub>3</sub>):  $\delta$  4.62 (dd,  $J_{1,2ax}$  = 4.0 Hz,  $J_{1,2eq}$  = 3.5 Hz, 1 H, H-1), 4.08 (dq,  $J_{4,5}$  = 10.0 Hz,  $J_{5,6}$  = 6.5 Hz, 1 H, H-5), 3.94 (m, 1 H, H-3), 3.32 (dd,  $J_{3,4}$  = 3.0 Hz, 1 H, H-4), 3.31 (s, 3 H, OCH<sub>3</sub>), 1.97 (ddd,  $J_{2ax,2eq}$  = 14.0 Hz,  $J_{2eq,3}$  = 5.0 Hz, 1 H, H-2eq), 1.78 (dt,  $J_{2ax,3}$  = 4.0 Hz, 1 H, H-2ax), 1.19 (d, 3 H, H<sub>3</sub>-6), 0.90 (s, 9 H, C(CH<sub>3</sub>)<sub>3</sub>), 0.12 (s, 9 H, Si(CH<sub>3</sub>)<sub>3</sub>), 0.07 (s, 3 H, Si(CH<sub>3</sub>)<sub>2</sub>), 0.06 (s, 3 H, Si(CH<sub>3</sub>)<sub>2</sub>); <sup>13</sup>C{<sup>1</sup>H} NMR (125 MHz, CDCl<sub>3</sub>):  $\delta$  97.9 (C-1), 74.9 (C-4), 68.1 (C-3), 65.9 (C-5), 55.1 (OCH<sub>3</sub>), 36.5 (C-2), 26.08 (C(CH<sub>3</sub>)<sub>3</sub>), 26.07



(C(CH<sub>3</sub>)<sub>3</sub>), 26.06 (C(CH<sub>3</sub>)<sub>3</sub>), 18.33 (C(CH<sub>3</sub>)<sub>3</sub>), 18.31 (C(CH<sub>3</sub>)<sub>3</sub>), 18.27 (C-6), 0.66 (Si(CH<sub>3</sub>)<sub>3</sub>), 0.65 (Si(CH<sub>3</sub>)<sub>3</sub>), 0.64 (Si(CH<sub>3</sub>)<sub>3</sub>), -3.8 (Si(CH<sub>3</sub>)<sub>2</sub>), -4.6 (Si(CH<sub>3</sub>)<sub>2</sub>); calcd 348.2152 amu for C<sub>16</sub>H<sub>36</sub>O<sub>4</sub>Si<sub>2</sub>, HRMS (EI<sup>+</sup>) found 348.2151 +/-0.0008 amu.

**1,3,4-Tri-*O*-acetyl-2-deoxy-2-fluoro- $\alpha/\beta$ -L-rhamnopyranose (**94**) and 1,3,4-Tri-*O*-acetyl-2,6-dideoxy-2-fluoro- $\alpha/\beta$ -L-glucopyranose (**95**)**



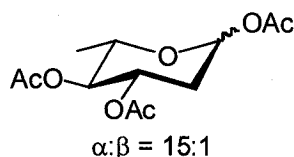
These compounds were prepared by an adaptation of a fluorination procedure described by Stick and Watts.<sup>114</sup> 3,4-Di-*O*-acetyl-L-rhamnol (**83**) (3.26 g, 15.2 mmol) was dissolved in a mixture of 1:1 H<sub>2</sub>O:DMF (190 mL) in a round-bottomed flask. Selectfluor® (10.78 g, 30.44 mmol) was added and the resulting reaction mixture was stirred for 4 h at rt, after which time TLC analysis (25:75 EtOAc:hexanes, *R<sub>f</sub>* products **92** and **93** = 0.32, 0.26, 0.15) revealed the reaction was complete. The reaction mixture was concentrated under reduced pressure and partitioned between EtOAc (50 mL) and H<sub>2</sub>O (50 mL). After drying the organic layer over MgSO<sub>4</sub> and concentration under reduced pressure, a crude yellow syrup was obtained (2.93 g), which was taken directly on to the next acetylation step. Acetic anhydride (2.2 mL, 23 mmol) and pyridine (1.9 mL, 23 mmol) were added to the mixture of crude fluorinated products (**92** and **93**) and the resulting reaction mixture was stirred for 3 h at rt, after which time TLC analysis (25:75 EtOAc:hexanes, *R<sub>f</sub>* product **94** = 0.33, *R<sub>f</sub>* product **95** = 0.38) revealed the reaction was complete. The reaction mixture was diluted with cold H<sub>2</sub>O (50 mL) and extracted with DCM (2 x 50 mL). The organic layer was washed with 1 M aqueous HCl (3 x 50 mL),

H<sub>2</sub>O (50 mL), saturated aqueous NaHCO<sub>3</sub> (2 x 50 mL), and again with H<sub>2</sub>O (50 mL). The organic layer was dried over MgSO<sub>4</sub> and concentrated under reduced pressure, generating a crude yellow syrup. Purification via automated silica gel chromatography using a Biotage 40M (40 mm x 15 cm) column (solvent system = 10:90 A:B (15 CV), linear gradient to 15:85 A:B (3 CV), 15:85 A:B (10 CV) where A = EtOAc and B = hexanes; flow-rate = 40 mL/min) afforded 1,3,4-tri-*O*-acetyl-2-deoxy-2-fluoro- $\alpha/\beta$ -L-rhamnopyranose (**94**) and 1,3,4-tri-*O*-acetyl-2,6-dideoxy-2-fluoro- $\alpha/\beta$ -L-glucopyranose (**95**) as white crystalline solids in a 3:2 ratio (2.66 g, 9.10 mmol, 60% yield over 2 steps).

<sup>1</sup>H NMR (500 MHz, CDCl<sub>3</sub>):  $\delta$  **94** ( $\alpha:\beta$  = 15:1)  *$\alpha$  diastereomer*: 6.21 (dd,  $J_{1,F}$  = 6.5 Hz,  $J_{1,2}$  = 2.0 Hz, 1 H, H-1), 5.23 (ddd,  $J_{2,3}$  = 2.5 Hz,  $J_{3,F}$  = 28.0 Hz,  $J_{3,4}$  = 10.0 Hz, 1 H, H-3); 5.16 (dd,  $J_{4,5}$  = 9.5 Hz, 1 H, H-4), 4.74 (ddd,  $J_{2,F}$  = 49.0 Hz, 1 H, H-2), 3.95 (dq,  $J_{5,6}$  = 6.5 Hz, 1 H, H-5), 2.16 (s, 3 H, C(O)CH<sub>3</sub>), 2.11 (s, 3 H, C(O)CH<sub>3</sub>), 2.07 (s, 3 H, C(O)CH<sub>3</sub>), 1.24 (d, 3 H, H<sub>3</sub>-6); **95** ( $\alpha:\beta$  = 3:2)  *$\alpha$  diastereomer*: 6.35 (br d,  $J_{1,2}$  = 4.0 Hz, 1 H, H-1), 5.51 (ddd,  $J_{2,3}$  = 9.5 Hz,  $J_{3,F}$  = 12.0 Hz,  $J_{3,4}$  = 9.5 Hz, 1 H, H-3); 4.80 (dd,  $J_{4,5}$  = 9.5 Hz, 1 H, H-4), 4.62 (ddd,  $J_{2,F}$  = 53.0 Hz, 1 H, H-2), 3.98 (dq,  $J_{5,6}$  = 6.0 Hz, 1 H, H-5), 2.19 (s, 3 H, C(O)CH<sub>3</sub>), 2.08 (s, 3 H, C(O)CH<sub>3</sub>), 2.06 (s, 3 H, C(O)CH<sub>3</sub>), 1.19 (d, 3 H, H<sub>3</sub>-6);  *$\beta$  diastereomer*: 5.76 (dd,  $J_{1,F}$  = 3.0 Hz,  $J_{1,2}$  = 8.0 Hz, 1 H, H-1); 5.33 (ddd,  $J_{2,3}$  = 9.0 Hz,  $J_{3,F}$  = 14.5 Hz,  $J_{3,4}$  = 9.5 Hz, 1 H, H-3); 4.79 (dd,  $J_{4,5}$  = 9.5 Hz, 1 H, H-4), 4.42 (ddd,  $J_{2,F}$  = 51.0 Hz, 1 H, H-2), 3.73 (dq,  $J_{5,6}$  = 6.0 Hz, 1 H, H-5), 2.17 (s, 3 H, C(O)CH<sub>3</sub>), 2.09 (s, 3 H, C(O)CH<sub>3</sub>), 2.05 (s, 3 H, C(O)CH<sub>3</sub>), 1.23 (d, 3 H, H<sub>3</sub>-6); <sup>19</sup>F{<sup>1</sup>H} NMR (235 MHz, CDCl<sub>3</sub>):  $\delta$  **94** ( $\alpha:\beta$  = 3:2)  *$\alpha$  diastereomer*: 103.2 (s, F-2);  *$\beta$  diastereomer*: 104.4 (s, F-2); **95** ( $\alpha:\beta$  = 15:1)  *$\alpha$  diastereomer*: 101.5 (s, F-2);  *$\beta$  diastereomer*: 102.3 (s, F-2); **94**: mp

130-132 °C (lit.<sup>219</sup> mp 136 °C); **95**: mp 125-127 °C (lit.<sup>219</sup> 126 °C). The reported <sup>1</sup>H NMR data is consistent with selected data described by Butchard and Kent.<sup>219</sup>

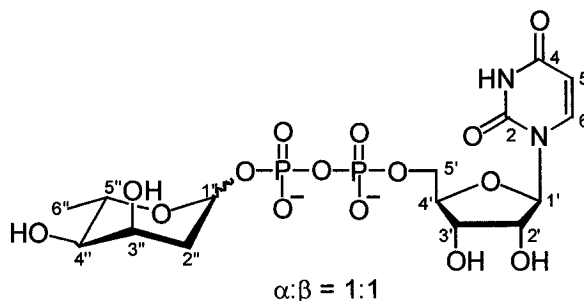
**1,3,4-Tri-*O*-acetyl- $\alpha/\beta$ -L-olivopyranose (**101**)**



This compound was prepared by an adaptation of a procedure described by Lam and Gervay-Hague.<sup>220</sup> Di-*O*-acetyl-L-rhamnal (**83**) (500. mg, 2.33 mmol) was dissolved in anhydrous DCM (3 mL) in a round-bottomed flask under a nitrogen atmosphere. Glacial acetic acid (1.5 mL, 26 mmol) and acetic anhydride (3.0 mL, 14 mmol) were added and the resulting solution was cooled to 0-5 °C in an ice-water bath for 15 min. 33% Hydrogen bromide in acetic acid (93  $\mu$ L) was added and the reaction mixture was stirred for 21 h at rt, after which time TLC analysis (35:65 EtOAc:hexanes,  $R_f$  product **101** = 0.42) revealed the reaction was complete. Anhydrous NaOAc (400 mg) was added to neutralize the reaction mixture, which was stirred at rt for an additional 30 min. The resulting heterogeneous mixture was diluted with DCM (25 mL) and filtered through a short plug of Celite® in a scintillated funnel, which was washed with additional DCM (25 mL). Following concentration under reduced pressure, the crude product was purified via automated silica gel chromatography using a Biotage 25M (25 mm x 15 cm) column (solvent system = 10:90 A:B (5 CV), linear gradient to 25:75 A:B (5 CV), 25:75 A:B (9 CV) where A = EtOAc and B = hexanes; flow-rate = 25 mL/min), affording pure **101** as a colorless syrup in an  $\alpha:\beta$  ratio of 15:1 (435 mg, 1.59 mmol, 68% yield). <sup>1</sup>H NMR (500 MHz, CDCl<sub>3</sub>):  $\delta$   $\alpha$  diastereomer: 6.19 (br d,  $J_{1,2ax} = 4.0$  Hz, 1 H, H-1), 5.27

(ddd,  $J_{2ax,3} = 9.5$  Hz,  $J_{2eq,3} = 5.5$  Hz,  $J_{3,4} = 9.5$  Hz, 1 H, H-3), 4.80 (dd,  $J_{4,5} = 10.0$  Hz, 1 H, H-4), 3.95 (dq,  $J_{5,6} = 6.5$  Hz, 1 H, H-5), 2.26 (ddd,  $J_{1,2eq} = 1.5$  Hz,  $J_{2ax,2eq} = 13.5$  Hz, 1 H, H-2eq), 2.12 (s, 3 H, C(O)CH<sub>3</sub>), 2.07 (s, 3 H, C(O)CH<sub>3</sub>), 2.03 (s, 3 H, C(O)CH<sub>3</sub>), 1.92 (ddd, 1 H, H-2ax), 1.19 (d, 3 H, H<sub>3</sub>-6);  $\beta$  diastereomer: 5.77 (dd,  $J_{1,2ax} = 10.0$  Hz,  $J_{1,2eq} = 2.0$  Hz, 1 H, H-1);  $^{13}\text{C}\{^1\text{H}\}$  NMR (125 MHz, CDCl<sub>3</sub>):  $\delta$   $\alpha$  diastereomer: 170.2 (C(O)CH<sub>3</sub>), 169.9 (C(O)CH<sub>3</sub>), 169.1 (C(O)CH<sub>3</sub>), 90.8 (C-1), 74.1 (C-4), 68.4 (C-3), 68.2 (C-5), 34.1 (C-2), 21.0 (C(O)CH<sub>3</sub>), 20.9 (C(O)CH<sub>3</sub>), 20.7 (C(O)CH<sub>3</sub>), 17.6 (C-6). The reported  $^1\text{H}$  and  $^{13}\text{C}\{^1\text{H}\}$  NMR data is consistent with that of Bols and coworkers.<sup>270</sup>

#### UDP- $\alpha/\beta$ -L-digitoxose (119)



Methyl 4-*O*-(*tert*-butyldimethylsilyl)-2,6-dideoxy-3-*O*-(trimethylsilyl)- $\alpha$ -L-ribo-hexopyranoside (**90**) (53 mg, 0.15 mmol) was dissolved in anhydrous DCM (750  $\mu\text{L}$ ) in a round-bottomed flask under a nitrogen atmosphere. Trimethylsilyl bromide (20  $\mu\text{L}$ , 0.15 mmol) was added and the reaction mixture was stirred for 1 h at rt, after which time TLC (10:90 EtOAc:hexanes,  $R_f$  2,6-dideoxyglycosyl bromide **103** = 0.65)<sup>g</sup> revealed the complete consumption of **90**. One third of the reaction mixture was removed via syringe, carefully concentrated under reduced pressure, and re-dissolved in CDCl<sub>3</sub>.  $^1\text{H}$  NMR

<sup>g</sup> 2,6-Dideoxyglycosyl bromide **103** degrades on silica gel and two other compounds, presumably resulting from this degradation process, were also visible on the TLC plate (10:90 EtOAc:hexanes,  $R_f$  = 0.45 and 0.16).

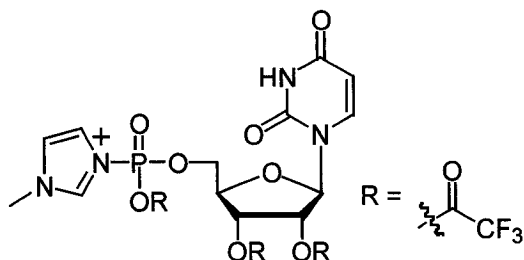
analysis of the crude reaction mixture supported the presence of 2-deoxyglycosyl bromide **103** ( $\delta$  6.46 (br d,  $J_{1,2a} = 4.0$  Hz, 1 H, H-1)), which appeared to be formed in near quantitative yield. In a second round-bottomed flask, uridine 5'-diphosphate (tetrabutylammonium salt (2.3 equiv by  $^1\text{H}$  NMR), 96 mg, 0.10 mmol) was dissolved in dry DCM (2.0 mL) under a nitrogen atmosphere. Anhydrous triethylamine (14  $\mu\text{L}$ , 0.10 mmol) and 3 Å molecular sieves (*ca.* 10) were added and the resulting solution was stirred for 15 min at rt. The remaining two thirds of the first reaction mixture containing 2,6-dideoxyglycosyl bromide **103** was subsequently transferred via cannula to the second round-bottomed flask containing UDP. The resulting reaction mixture was stirred for 2 h at rt, after which time TLC (10:90 EtOAc:hexanes) revealed that all 2,6-dideoxyglycosyl bromide (**103**) has been consumed or degraded and HPLC analysis of the reaction mixture (Method A) revealed the presence of a new peak at 9.23 min. The reaction mixture was filtered through a scintillated funnel to remove molecular sieves and carefully concentrated without heating under reduced pressure. The resulting crude yellow syrup was re-dissolved in  $\text{H}_2\text{O}$  (3 mL) and the pH of this aqueous solution was immediately adjusted to 8 using triethylamine. Alkaline phosphatase (50 EU<sup>h</sup>) was added to facilitate the degradation of unreacted UDP to uridine and inorganic phosphate to simplify the purification protocol. This enzymatic reaction mixture was stirred for 4 h at rt, after which time the degradation of UDP was complete by HPLC. The reaction mixture was purified via automated C18 reversed-phase chromatography using a Biotage 12M (12 mm x 15 cm) column (solvent system = 100:0 A:B (10 CV) followed by a linear gradient to 0:100 A:B (30 CV) where A = 0.1% w/v aqueous  $\text{NH}_4\text{CO}_3$  and B = 0.1% w/v

---

<sup>h</sup> 1 EU = the amount of enzyme needed to catalyze the transformation of 1  $\mu\text{mol}$  of substrate per min

$\text{NH}_4\text{CO}_3$  in HPLC-grade MeOH; A and B chilled in a 4 °C fridge prior to use; flow-rate = 10 mL/min; UV detection at 254 nm). Concentration of appropriate fractions under reduced pressure afforded silyl-protected 2,6-dideoxysugar nucleotide **118** ( $^{31}\text{P}\{^1\text{H}\}$  NMR (202 MHz,  $\text{D}_2\text{O}$ , pH 6):  $\delta$  -11.6 (2 d, attached to D-ribose), -14.0 (2 d, attached to L-digitoxose)) in 17% yield over 2 steps by UV spectroscopy ( $\lambda_{\text{max}}$  261 nm,  $\epsilon = 1.01 \times 10^4 \text{ M}^{-1}\text{cm}^{-1}$ ). Protected 2,6-dideoxysugar nucleotide derivative **118** was subsequently dissolved in anhydrous THF (2.0 mL) in a round-bottomed flask under a nitrogen atmosphere. Tetra-*n*-butylammonium fluoride (1.0 M solution in THF, 50.  $\mu\text{L}$ , 0.050 mmol) was added and the reaction mixture was stirred for 0.5 h at rt, after which time HPLC analysis (Method A) revealed the complete disappearance of **118** and the formation of a major new peak at 5.88 min and a minor new peak at 5.70 min. The reaction mixture was concentrated under reduced pressure, re-dissolved in  $\text{H}_2\text{O}$  (5 mL), and extracted with HPLC-grade DCM (5 mL). The aqueous layer was subsequently applied to a column filled with Dowex® 50W-X8 cation exchange resin ( $\text{Na}^+$  form, 100-200 mesh). Following elution with  $\text{H}_2\text{O}$ , appropriate fractions were pooled and concentrated under reduced pressure. Unfortunately, the retention time of the major peak was found to correspond to UDP, while the minor peak corresponded to UDP- $\alpha/\beta$ -L-digitoxose (**119**, disodium salt) by  $^1\text{H}$  NMR (**119**:UDP = 1:4), demonstrating the instability of protected 2,6-dideoxysugar nucleotide **118** toward tetra-*n*-butylammonium fluoride at rt. This analysis was confirmed via LC-MS. LRMS (ESI $^-$ ) for  $\text{C}_9\text{H}_{14}\text{N}_2\text{O}_{12}\text{P}_2$  (UDP free acid, 404.0 amu) =  $m/z$  403.0 [ $\text{M}-\text{H}$ ] $^-$ , LRMS (ESI $^-$ ) for  $\text{C}_{15}\text{H}_{24}\text{N}_2\text{O}_{15}\text{P}_2$  (UDP- $\alpha/\beta$ -L-digitoxose (**119**) free acid, 534.1 amu) =  $m/z$  533.2 [ $\text{M}-\text{H}$ ] $^-$ .

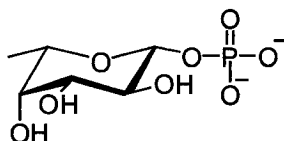
### UMP-*N*-methylimidazolid (121)



This compound was prepared by an adaptation of a procedure described by Marlow and Kiessling.<sup>238</sup> Uridine 5'-monophosphate (free acid, 32 mg, 0.10 mmol) was suspended in anhydrous MeCN (300  $\mu\text{L}$ ) in a round-bottomed flask under a nitrogen atmosphere. Anhydrous triethylamine (140.  $\mu\text{L}$ , 1.01 mmol) and anhydrous dimethylaniline (50.  $\mu\text{L}$ , 0.40 mmol) were added and the resulting mixture was cooled to 0-5  $^{\circ}\text{C}$  with stirring. Trifluoroacetic anhydride (140  $\mu\text{L}$ , 0.99 mmol) and anhydrous MeCN (100  $\mu\text{L}$ ) were combined in a second round-bottomed flask under a nitrogen atmosphere, similarly cooled to 0-5  $^{\circ}\text{C}$  in an ice-water bath, and subsequently added to the first heterogeneous mixture via cannula. The ice-water bath was removed and the reaction mixture was stirred for 15 min at rt, after which time all UMP appeared to dissolve and excess trifluoroacetic anhydride and trifluoroacetic acid were carefully removed via concentration of the reaction mixture under reduced pressure. The resulting pale yellow syrup was re-dissolved in anhydrous MeCN (100  $\mu\text{L}$ ) under a nitrogen atmosphere and cooled to 0-5  $^{\circ}\text{C}$  in an ice-water bath. In a third round-bottomed flask, *N*-methylimidazole (24  $\mu\text{L}$ , 0.30 mmol) and triethylamine (70  $\mu\text{L}$ , 0.51 mmol) were dissolved in anhydrous MeCN (100  $\mu\text{L}$ ) under a nitrogen atmosphere and cooled to 0-5  $^{\circ}\text{C}$  in an ice-water bath. The contents of this third flask were then added via cannula to the newly trifluoroacetylated UMP solution and the resulting reaction mixture was

stirred under a nitrogen atmosphere at 0-5 °C in an ice-water bath for 15 min to generate the desired UMP-*N*-methylimidazolidone donor (**121**), which was bright yellow in colour. The essentially quantitative formation of this species was confirmed by  $^{31}\text{P}\{^1\text{H}\}$  NMR as the UMP-*N*-methylimidazolidone donor (**121**) appeared as a singlet with a distinctive -10.8 ppm chemical shift, which was consistent with NMR data reported by Mohamady and Jakeman<sup>237</sup> as well as Marlow and Kiessling.<sup>238</sup> This electrophile was used directly in coupling reactions with various sugar-1-phosphates as described in the preparation of **147**, **149**, **151**, and **153a**.

#### **β-L-Fucose-1-phosphate (123)**



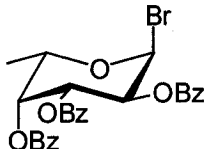
This compound was prepared by an adaptation of a phosphorylation procedure described by Zhao and Thorson.<sup>138</sup> A mixture of dibenzyl phosphate (1.58 g, 5.68 mmol), silver triflate (1.33 g, 5.16 mmol), and 2,4,6-collidine (890 μL, 6.71 mmol) was dissolved in anhydrous DCM (6.0 mL) in a round-bottomed flask. This solution was stirred under a nitrogen atmosphere in the absence of light for 1 h. 2,3,4-Tri-*O*-benzoyl-α-L-fucopyranosyl bromide (**124**) (1.82 g, 5.16 mmol) was dissolved in anhydrous DCM (5.0 mL) in a second round-bottomed flask under a nitrogen atmosphere and both flasks were cooled to -40°C in a dry ice-acetone bath. The contents of the second round-bottomed flask were then added dropwise via cannula to the first flask and the resulting reaction mixture was stirred for 4 h at -40°C under a nitrogen atmosphere in the absence of light. After 4 h, no more dry ice was added and the reaction mixture was allowed to



slowly warm to rt while stirring overnight. After 12 h at rt, TLC analysis (35:65 EtOAc:hexanes,  $R_f$  dibenzylphosphorylated product **126** = 0.22) revealed that the reaction was complete. The reaction mixture was diluted with DCM (20 mL) and the organic layer was washed with H<sub>2</sub>O (20 mL), saturated aqueous K<sub>2</sub>CO<sub>3</sub> (2 x 20 mL), and again H<sub>2</sub>O (2 x 20 mL). The organic layer was dried over Na<sub>2</sub>SO<sub>4</sub> and concentrated under reduced pressure. It was found that exclusively one diastereomer of dibenzylphosphorylated product **126** had been produced and the only byproducts visible in the <sup>1</sup>H NMR spectrum of the crude product were 2,4,6-collidine and a small amount of hydrolyzed glycosyl bromide. To streamline the purification procedure, the crude dibenzylphosphorylated product was used directly in the next deprotection step where 2,4,6-collidine and the small amount of hydrolyzed glycosyl bromide were easily extracted into the organic layer after hydrogenolysis of the benzyl groups protecting the phosphate. In preparation for hydrogenolysis, 10% Pd/C (500 mg) and 1 M aqueous NaHCO<sub>3</sub> (8.4 mL) were first added to the hydrogenolysis jar. The crude protected sugar-1-phosphate was subsequently dissolved in MeOH (20 mL), added to the jar, and subjected to hydrogenolysis under a 50 psi hydrogen atmosphere for 1 h, after which time no starting material was visible by TLC. The reaction mixture was filtered through a short plug of Celite® in a scintillated funnel (rinsing with MeOH) to remove the Pd/C catalyst. The filtrate was concentrated under reduced pressure and partitioned between DCM (25 mL) and H<sub>2</sub>O (25 mL). To remove the acetyl groups protecting the monosaccharide, the aqueous layer was diluted with H<sub>2</sub>O (total volume = 15 mL) and cooled to 0-5°C in an ice-water bath. 1 M Aqueous NaOH (12 mL) was added dropwise and the reaction mixture was allowed to warm slowly to rt over 3 h. The pH was then

carefully adjusted to 7.0-7.5 with cold 1 M aqueous acetic acid and the reaction mixture was concentrated to ~ 5 mL in volume and applied to an Amberlite® IR-120 (H<sup>+</sup>) cation exchange column (free acid form). The sugar-1-phosphate was eluted with H<sub>2</sub>O and fractions containing the desired product were pooled. The pH of these fractions was immediately adjusted to 7.0-7.5 with 1 M aqueous NH<sub>4</sub>OH and the sugar-1-phosphate was concentrated under reduced pressure and lyophilized. Trituration with ethanol followed by vortexing and centrifugation at 4 °C facilitated the successful removal of remaining NH<sub>4</sub>OAc. After concentration under reduced pressure, the sugar-1-phosphate was re-dissolved in H<sub>2</sub>O (~ 2 mL) and lyophilized a second time, affording β-L-fucose-1-phosphate (**123**, diammonium salt) as a white solid (559 mg, 2.01 mmol, 39% yield over 3 steps). <sup>1</sup>H NMR (500 MHz, D<sub>2</sub>O, pH 6): δ 4.86 (dd, *J*<sub>1,P</sub> = 7.5 Hz, *J*<sub>1,2</sub> = 8.0 Hz, 1 H, H-1), 3.84 (br q, *J*<sub>5,6</sub> = 6.5 Hz, 1 H, H-5), 3.76 (br d, *J*<sub>3,4</sub> = 3.5 Hz, 1 H, H-4), 3.71 (dd, *J*<sub>2,3</sub> = 10.0 Hz, 1 H, H-3), 3.55 (dd, 1 H, H-2), 1.28 (d, 3 H, H<sub>3</sub>-6); <sup>13</sup>C{<sup>1</sup>H} NMR (126 MHz, D<sub>2</sub>O, pH 6): δ 97.6 (C-1), 72.8 (C-3), 71.8 (C-2), 71.3 (C-4), 71.2 (C-5), 15.5 (C-6); Coupled <sup>13</sup>C-<sup>1</sup>H HSQC: <sup>1</sup>*J*<sub>C-1,H-1</sub> = 162 Hz; <sup>31</sup>P{<sup>1</sup>H} NMR (202 MHz, D<sub>2</sub>O, pH 6): δ 1.37 (s); LRMS (ESI) for C<sub>6</sub>H<sub>13</sub>O<sub>8</sub>P (free acid, 244.1 amu) = *m/z* 243.1 [M-H]<sup>-</sup>. The reported <sup>1</sup>H and <sup>13</sup>C{<sup>1</sup>H} NMR data is consistent with that of Hindsgaul and coworkers<sup>258</sup> as well as Barker and coworkers.<sup>259</sup>

### 2,3,4-Tri-*O*-benzoyl- $\alpha$ -L-fucopyranosyl bromide (**124**)

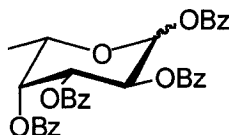


This compound was prepared by an adaptation of a bromination procedure described by Liang and Grindley.<sup>244</sup> 1,2,3,4-Tetra-*O*-benzoyl- $\alpha/\beta$ -L-fucopyranose (**125**) (1.04 g, 1.79 mmol) was dissolved in DCM (6 mL) in a round-bottomed flask that was stoppered with a septum and cooled to 0-5 °C in an ice-water bath. Phosphorus tribromide (285  $\mu$ L, 3.02 mmol) and H<sub>2</sub>O (190  $\mu$ L, 10.5 mmol) were added dropwise to this solution. After 10 min, the reaction mixture was warmed to rt and stirred for 2 h, after which time the reaction was deemed complete by TLC (35:65 EtOAc:hexanes, *R<sub>f</sub>* product **124** = 0.78).<sup>i</sup> The reaction mixture was diluted with DCM (25 mL) and washed with H<sub>2</sub>O (2 x 40 mL), saturated aqueous NaHCO<sub>3</sub> (40 mL), and saturated aqueous NaCl (2 x 40 mL). The organic layer was dried over Na<sub>2</sub>SO<sub>4</sub> and concentrated to afford a pale orange syrup (928 mg, 1.72 mmol, 96% yield). <sup>1</sup>H NMR (500 MHz, CDCl<sub>3</sub>):  $\delta$  8.13-7.24 (m, 15 H, Ph), 6.94 (d, *J*<sub>1,2</sub> = 4.0 Hz, 1 H, H-1), 6.01 (dd, *J*<sub>2,3</sub> = 10.5 Hz, *J*<sub>3,4</sub> = 3.5 Hz, 1 H, H-3), 5.84 (dd, *J*<sub>4,5</sub> = 1.0 Hz, 1 H, H-4), 5.61 (dd, 1 H, H-2), 4.69 (br q, *J*<sub>5,6</sub> = 6.5 Hz, 1 H, H-5), 1.36 (d, 3 H, H<sub>3</sub>-6); <sup>13</sup>C{<sup>1</sup>H} NMR (125 MHz, CDCl<sub>3</sub>):  $\delta$  165.8 (C=O), 165.7 (C=O), 165.5 (C=O), 133.7 (Ph), 133.6 (Ph), 133.3 (Ph), 130.2 (Ph), 130.0 (Ph), 129.9 (Ph), 129.7 (Ph), 129.1 (Ph), 129.0 (Ph), 128.7 (Ph), 128.6 (Ph), 128.3 (Ph), 89.4 (C-1),

<sup>i</sup> Glycosyl bromide **124** degrades on silica gel TLC plates, presumably to the corresponding hemiacetals, which had an *R<sub>f</sub>* of 0.41 in 35:65 EtOAc:hexanes.

70.9 (C-4), 70.5 (C-5), 69.3 (C-3), 68.7 (C-2), 15.8 (C-6).<sup>j</sup> The reported  $^1\text{H}$  and  $^{13}\text{C}\{^1\text{H}\}$  NMR data is consistent with that of Wong and coworkers.<sup>243</sup>

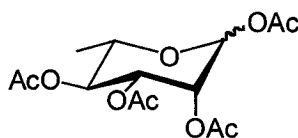
### 1,2,3,4-Tetra-*O*-benzoyl- $\alpha/\beta$ -L-fucopyranose (**125**)



This compound was prepared by an adaptation of a benzylation procedure described by Wong and coworkers.<sup>243</sup> L-Fucose (2.00 g, 12.2 mmol) and pyridine (40 mL) were combined in a round-bottomed flask and the resulting mixture was cooled to 0–5 °C in an ice-water bath. Benzoyl chloride (7.20 mL, 62.1 mmol) was added dropwise and the ice-water bath was removed. The reaction mixture was stirred for 3 h at rt, after which time the reaction was deemed complete by TLC (35:65 EtOAc:hexanes,  $R_f$  product **125** = 0.64). The reaction mixture was poured into an ice-water mixture (100 mL) and extracted with EtOAc (2 x 100 mL). The combined organic extracts were washed with cold 1 M aqueous HCl (3 x 200 mL), H<sub>2</sub>O (200 mL), saturated aqueous NaHCO<sub>3</sub> (200 mL), and saturated aqueous NaCl (200 mL). The organic layer was dried over Na<sub>2</sub>SO<sub>4</sub> and concentrated to afford a light brown solid in an  $\alpha$ : $\beta$  ratio of 15:1 (6.68 g, 11.5 mmol, 94% yield).  $^1\text{H}$  NMR (500 MHz, CDCl<sub>3</sub>):  $\delta$   $\alpha$  diastereomer: 8.17–7.23 (m, 20 H, Ph), 6.87 (d,  $J_{1,2}$  = 3.5 Hz, 1 H, H-1), 6.08 (dd,  $J_{2,3}$  = 10.5 Hz,  $J_{3,4}$  = 3.3 Hz, 1 H, H-3), 5.99 (dd, 1 H, H-2), 5.90 (dd,  $J_{4,5}$  = 1.0 Hz, 1 H, H-4), 4.64 (br q,  $J_{5,6}$  = 6.5 Hz, 1 H, H-5), 1.32 (d, 3 H, H<sub>3</sub>-6).

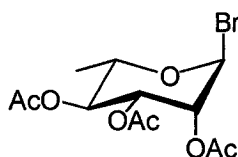
<sup>j</sup> Not all phenyl  $^{13}\text{C}\{^1\text{H}\}$  resonances were observed, presumably due to spectral overlap in the 133.7 – 128.3 ppm region.

### 1,2,3,4-Tetra-*O*-acetyl- $\alpha/\beta$ -L-rhamnopyranose (**130**)



L-Rhamnose monohydrate (5.00 g, 27.4 mmol) and pyridine (18 mL) were combined in a round-bottomed flask. Acetic anhydride (21 mL, 220 mmol) was added and the reaction mixture was stirred for 1 h at rt, after which time the reaction was deemed complete by TLC (50:50 EtOAc:hexanes,  $R_f$  product **130** = 0.60). The reaction mixture was diluted with an ice-water solution (50 mL) and extracted with DCM (3 x 50 mL). The combined organic extracts were washed with 1 M aqueous HCl (3 x 50 mL), H<sub>2</sub>O (2 x 50 mL), saturated aqueous NaHCO<sub>3</sub> (50 mL), and again H<sub>2</sub>O (50 mL). After drying over Na<sub>2</sub>SO<sub>4</sub> and concentration under reduced pressure, acetylated product **130** was obtained as a pale yellow syrup in an  $\alpha$ : $\beta$  ratio of 3:1 (9.11 g, 27.4 mmol, 100% yield). <sup>1</sup>H NMR (500 MHz, CDCl<sub>3</sub>):  $\delta$   $\alpha$  *diastereomer*: 6.02 (d,  $J_{1,2}$  = 2.0 Hz, 1 H, H-1), 5.31 (dd,  $J_{2,3}$  = 3.5 Hz,  $J_{3,4}$  = 10.5 Hz, 1 H, H-3), 5.25 (dd, 1 H, H-2), 5.12 (dd,  $J_{4,5}$  = 10.0 Hz, 1 H, H-4), 3.94 (dq,  $J_{5,6}$  = 6.5 Hz, 1 H, H-5), 2.17 (s, 3 H, C(O)CH<sub>3</sub>), 2.16 (s, 3 H, C(O)CH<sub>3</sub>), 2.07 (s, 3 H, C(O)CH<sub>3</sub>), 2.01 (s, 3 H, C(O)CH<sub>3</sub>), 1.23 (d, 3 H, H<sub>3</sub>-6);  $\beta$  *diastereomer*: 5.84 (d,  $J_{1,2}$  = 1.5 Hz, 1 H, H-1), 5.48 (dd,  $J_{2,3}$  = 3.0 Hz, 1 H, H-2), 5.08 (m, 2 H, H-3, H-4), 3.67 (dq,  $J_{5,6}$  = 6.0 Hz, 1 H, H-5), 2.21 (s, 3 H, C(O)CH<sub>3</sub>), 2.10 (s, 3 H, C(O)CH<sub>3</sub>), 2.06 (s, 3 H, C(O)CH<sub>3</sub>), 2.00 (s, 3 H, C(O)CH<sub>3</sub>), 1.29 (d, 3 H, H<sub>3</sub>-6).

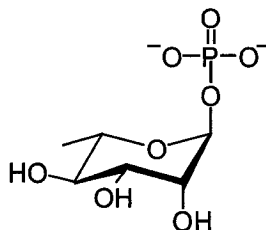
### 2,3,4-Tri-*O*-acetyl- $\alpha$ -L-rhamnopyranosyl bromide (**131**)



Following the procedure used for the preparation of glycosyl bromide **124**, 1,2,3,4-tetra-*O*-acetyl- $\alpha/\beta$ -L-rhamnopyranose (**130**) (3.11 g, 9.36 mmol) was reacted with phosphorus tribromide (1.50 mL, 15.9 mmol) and H<sub>2</sub>O (1.01 mL, 56.2 mmol) in DCM (30 mL). The aforementioned protocol afforded 2,3,4-tri-*O*-acetyl- $\alpha$ -L-rhamnopyranosyl bromide (**131**) (35:65 EtOAc:hexanes,  $R_f$  = 0.72)<sup>k</sup> as an orange syrup (2.95 g, 8.35 mmol, 89% yield). <sup>1</sup>H NMR (500 MHz, CDCl<sub>3</sub>):  $\delta$  6.27 (br s, 1 H, H-1), 5.67 (dd,  $J_{2,3}$  = 3.5 Hz,  $J_{3,4}$  = 10.0 Hz, 1 H, H-3), 5.45 (dd,  $J_{1,2}$  = 1.5 Hz, 1 H, H-2), 5.16 (dd,  $J_{4,5}$  = 10.0 Hz, 1 H, H-4), 4.11 (dq,  $J_{5,6}$  = 6.0 Hz, 1 H, H-5), 2.18 (s, 3 H, C(O)CH<sub>3</sub>), 2.08 (s, 3 H, C(O)CH<sub>3</sub>), 2.01 (s, 3 H, C(O)CH<sub>3</sub>), 1.29 (d, 3 H, H<sub>3</sub>-6); <sup>13</sup>C{<sup>1</sup>H} NMR (125 MHz, CDCl<sub>3</sub>):  $\delta$  169.9 (C(O)CH<sub>3</sub>), 169.8 (C(O)CH<sub>3</sub>), 169.6 (C(O)CH<sub>3</sub>), 83.7 (C-1), 72.5 (C-2), 71.1 (C-5), 70.3 (C-4), 67.9 (C-3), 20.8 (C(O)CH<sub>3</sub>), 20.7 (C(O)CH<sub>3</sub>), 20.6 (C(O)CH<sub>3</sub>), 17.0 (C-6). The reported <sup>1</sup>H and <sup>13</sup>C{<sup>1</sup>H} NMR data is consistent with that of Thorson and coworkers.<sup>271</sup>

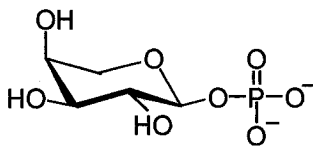
<sup>k</sup> Glycosyl bromide **131** degrades on silica gel TLC plates, presumably to the corresponding hemiacetals, which had an  $R_f$  of 0.24 in 35:65 EtOAc:hexanes.

### $\alpha$ -L-Rhamnose-1-phosphate (**134**)



Following the procedure used for the preparation of  $\beta$ -L-fucose-1-phosphate (**123**), 2,3,4-tri-*O*-acetyl- $\alpha$ -L-rhamnopyranosyl bromide (**131**) (2.56 g, 7.25 mmol) was reacted with dibenzyl phosphate (2.22 g, 7.98 mmol), silver triflate (1.86 g, 7.25 mmol), and 2,4,6-collidine (1.25 mL, 9.43 mmol) in anhydrous DCM. Hydrogenolysis was performed on the crude dibenzylphosphorylated product (**132**) (35:65 EtOAc:hexanes,  $R_f$  = 0.27), as previously described using 10% Pd/C (700 mg) and 1 M aqueous  $\text{NaHCO}_3$  (11.8 mL) in MeOH (30 mL). Deacetylation was accomplished by diluting **133** with  $\text{H}_2\text{O}$  (total volume = 20 mL) and adding 1 M aqueous NaOH (17 mL). After purification, cation exchange, and lyophilization as described for **123**,  $\alpha$ -L-rhamnose-1-phosphate (**134**, diammonium salt) was obtained as a white solid (868 mg, 3.12 mmol, 43% yield over 3 steps).  $^1\text{H}$  NMR (500 MHz,  $\text{D}_2\text{O}$ , pH 6):  $\delta$  5.31 (dd,  $J_{1,\text{P}}$  = 8.0 Hz,  $J_{1,2}$  = 1.5 Hz, 1 H, H-1), 4.00 (dd,  $J_{2,3}$  = 3.5 Hz, 1 H, H-2), 3.93 (m, 2 H, H-3, H-5), 3.44 (dd,  $J_{3,4}$  = 10.0 Hz,  $J_{4,5}$  = 10.0 Hz, 1 H, H-4), 1.30 (d,  $J_{5,6}$  = 6.5 Hz, 3 H, H<sub>3</sub>-6);  $^{13}\text{C}\{^1\text{H}\}$  NMR (126 MHz,  $\text{D}_2\text{O}$ , pH 6):  $\delta$  95.1 (C-1), 72.3 (C-4), 70.9 (C-2), 69.7 (C-3), 68.8 (C-5), 16.8 (C-6); Coupled  $^{13}\text{C}$ - $^1\text{H}$  HSQC:  $^1J_{\text{C-1,H-1}}$  = 170 Hz;  $^{31}\text{P}\{^1\text{H}\}$  NMR (202 MHz,  $\text{D}_2\text{O}$ , pH 6):  $\delta$  1.34 (s); LRMS (ESI) for  $\text{C}_6\text{H}_{13}\text{O}_8\text{P}$  (free acid, 244.1 amu) =  $m/z$  243.0  $[\text{M-H}]^-$ . The reported  $^1\text{H}$  and  $^{13}\text{C}\{^1\text{H}\}$  NMR data is consistent with that of Zhao and Thorson, which was reported referring to the  $\beta$  diastereomer.<sup>138</sup>

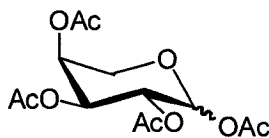
### $\alpha$ -L-Arabinose-1-phosphate (**135**)



Following the procedure used for the preparation of  $\beta$ -L-fucose-1-phosphate (**123**), 2,3,4-tri-*O*-acetyl- $\beta$ -L-arabinopyranosyl bromide (**137**) (1.75 g, 5.16 mmol) was reacted with dibenzyl phosphate (1.58 g, 5.68 mmol), silver triflate (1.33 g, 5.16 mmol), and 2,4,6-collidine (890.  $\mu$ L, 6.71 mmol) in anhydrous DCM. Hydrogenolysis was performed on the crude dibenzylphosphorylated product (**138**) (35:65 EtOAc:hexanes,  $R_f$  = 0.31), as previously described using 10% Pd/C (500 mg) and 1 M aqueous  $\text{NaHCO}_3$  (8.4 mL) in MeOH (20 mL). Deacetylation was accomplished by diluting **139** with  $\text{H}_2\text{O}$  (total volume = 15 mL) and adding 1 M aqueous NaOH (12 mL). After purification, cation exchange, and lyophilization as described for **123**,  $\alpha$ -L-arabinose-1-phosphate (**135**, diammonium salt) was obtained as a white solid (544 mg, 2.06 mmol, 40% yield over 3 steps).  $^1\text{H}$  NMR (500 MHz,  $\text{D}_2\text{O}$ , pH 6):  $\delta$  4.82 (dd,  $J_{1,\text{P}}$  = 8.0 Hz,  $J_{1,2}$  = 7.5 Hz, 1 H, H-1), 3.96 (m, 1 H, H-4), 3.95 (m, 1 H, H-5a), 3.73 (dd,  $J_{2,3}$  = 9.5 Hz,  $J_{3,4}$  = 3.0 Hz, 1 H, H-3), 3.70 (br d,  $J_{5\text{a},5\text{b}}$  = 12.0 Hz, 1 H, H-5b), 3.61 (dd, 1 H, H-2);  $^{13}\text{C}\{^1\text{H}\}$  NMR (126 MHz,  $\text{D}_2\text{O}$ , pH 6):  $\delta$  97.8 (C-1), 72.2 (C-3), 71.9 (C-2), 68.1 (C-4), 66.1 (C-5); Coupled  $^{13}\text{C}$ - $^1\text{H}$  HSQC:  $^1J_{\text{C-1,H-1}}$  = 163 Hz;  $^{31}\text{P}\{^1\text{H}\}$  NMR (202 MHz,  $\text{D}_2\text{O}$ , pH 7):  $\delta$  2.45 (s). LRMS (ESI $^-$ ) for  $\text{C}_5\text{H}_{11}\text{O}_8\text{P}$  (free acid, 230.1 amu) =  $m/z$  229.0  $[\text{M-H}]^-$ .

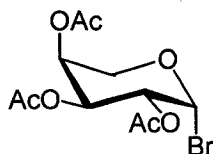


### 1,2,3,4-Tetra-*O*-acetyl- $\alpha/\beta$ -L-arabinopyranose (**136**)



Following the procedure used for the preparation of acetylated derivative **130**, L-arabinose (3.00 g, 20.0 mmol) was reacted with acetic anhydride (15.1 mL, 160. mmol) in pyridine (12.9 mL). The aforementioned protocol afforded 1,2,3,4-tetra-*O*-acetyl- $\alpha/\beta$ -L-arabinopyranose (**136**) (35:65 EtOAc:hexanes,  $R_f$  = 0.45) as a pale yellow syrup in an  $\alpha$ : $\beta$  ratio of 2:3 (6.32 g, 19.9 mmol, 99% yield).  $^1\text{H}$  NMR (500 MHz,  $\text{CDCl}_3$ ):  $\delta$   $\alpha$  *diastereomer*: 5.67 (d,  $J_{1,2}$  = 7.0 Hz, 1 H, H-1), 5.30 (m, 1 H, H-2), 5.31 (m, 1 H, H-4), 5.12 (dd,  $J_{2,3}$  = 9.5 Hz,  $J_{3,4}$  = 3.5 Hz, 1 H, H-3), 3.95 (m, 2 H, H<sub>2</sub>-5), 2.14 (s, 3 H, C(O)CH<sub>3</sub>), 2.13 (s, 3 H, C(O)CH<sub>3</sub>), 2.07 (s, 3 H, C(O)CH<sub>3</sub>), 2.05 (s, 3 H, C(O)CH<sub>3</sub>);  $\beta$  *diastereomer*: 6.35 (d,  $J_{1,2}$  = 3.0 Hz, 1 H, H-1), 5.34 (m, 1 H, H-2), 4.39 (m, 1 H, H-4), 4.24 (m, 1 H, H-3), 3.95 (m, 2 H, H<sub>2</sub>-5), 2.16 (s, 3 H, C(O)CH<sub>3</sub>), 2.15 (s, 3 H, C(O)CH<sub>3</sub>), 2.12 (s, 3 H, C(O)CH<sub>3</sub>), 2.03 (s, 3 H, C(O)CH<sub>3</sub>).

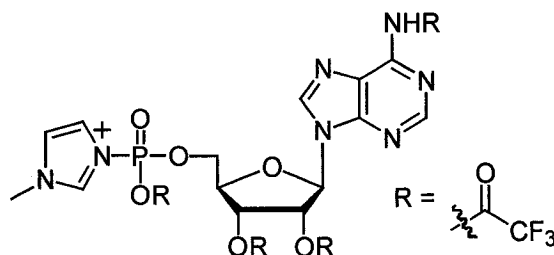
### 2,3,4-Tri-*O*-acetyl- $\beta$ -L-arabinopyranosyl bromide (**137**)



Following the procedure used for the preparation of glycosyl bromide **124**, 1,2,3,4-tetra-*O*-acetyl- $\alpha/\beta$ -L-arabinopyranose (**136**) (2.50 g, 7.86 mmol) was reacted with phosphorus tribromide (1.20 mL, 12.7 mmol) and H<sub>2</sub>O (850  $\mu\text{L}$ , 47.2 mmol) in DCM (25 mL). The aforementioned protocol afforded 2,3,4-tri-*O*-acetyl- $\beta$ -L-arabinopyranosyl

bromide (**137**) (35:65 EtOAc:hexanes,  $R_f = 0.73$ )<sup>1</sup> as a white solid (2.09 g, 6.16 mmol, 78% yield). <sup>1</sup>H NMR (500 MHz, CDCl<sub>3</sub>): δ 6.70 (d,  $J_{1,2} = 4.0$  Hz, 1 H, H-1), 5.41 (dd,  $J_{2,3} = 10.5$  Hz,  $J_{3,4} = 3.5$  Hz, 1 H, H-3), 5.40 (m, 1 H, H-4), 5.09 (dd, 1 H, H-2), 4.21 (br d,  $J_{5a,5b} = 13.5$  Hz, 1 H, H-5a), 3.94 (dd, 1 H, H-5b), 2.16 (s, 3 H, C(O)CH<sub>3</sub>), 2.12 (s, 3 H, C(O)CH<sub>3</sub>), 2.03 (s, 3 H, C(O)CH<sub>3</sub>); <sup>13</sup>C{<sup>1</sup>H} NMR (125 MHz, CDCl<sub>3</sub>): δ 170.1 (C(O)CH<sub>3</sub>), 170.0 (C(O)CH<sub>3</sub>), 169.8 (C(O)CH<sub>3</sub>), 89.7 (C-1), 68.0 (C-2), 67.9 (C-4), 67.6 (C-3), 64.7 (C-5), 20.8 (C(O)CH<sub>3</sub>), 20.7 (C(O)CH<sub>3</sub>), 20.6 (C(O)CH<sub>3</sub>).

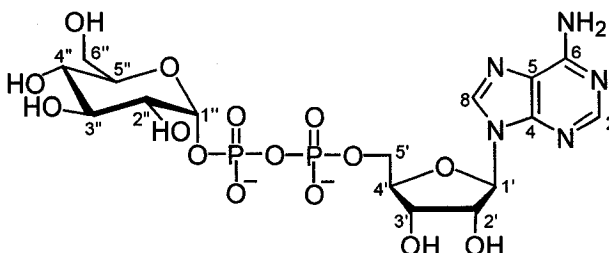
#### AMP-*N*-methylimidazolid (145)



Following the procedure used for the preparation of UMP-*N*-methylimidazolid (**121**), adenosine 5'-monophosphate (free acid, 35 mg, 0.10 mmol) was treated to the identical conditions as those described for **121** to prepare AMP-*N*-methylimidazolid (**145**). The essentially quantitative formation of this species was confirmed by <sup>31</sup>P{<sup>1</sup>H} NMR as the AMP-*N*-methylimidazolid donor (**145**) appeared as a singlet with a distinctive -11.0 ppm chemical shift, which was consistent with NMR data reported by Mohamady and Jakeman.<sup>237</sup> This electrophile was used directly in coupling reactions with various sugar-1-phosphates as described in the preparation of **146**, **148**, **150**, and **152**.

<sup>1</sup> Glycosyl bromide **137** degrades on silica gel TLC plates, presumably to the corresponding hemiacetals, which had an  $R_f$  of 0.17 in 35:65 EtOAc:hexanes.

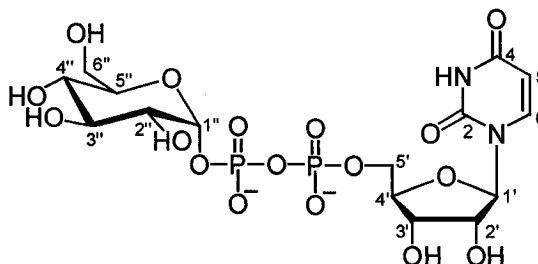
### ADP- $\alpha$ -D-glucose (146)



This compound was prepared by an adaptation of a procedure described by Marlow and Kiessling.<sup>238</sup>  $\alpha$ -D-Glucose-1-phosphate (tributylammonium salt (1.45 equiv), 106 mg, 0.200 mmol) was dissolved in anhydrous MeCN (1.0 mL) in a round-bottomed flask under a nitrogen atmosphere. 3 Å Molecular sieves were added and the resulting mixture was stirred for 15 min at rt. A solution of AMP-*N*-methylimidazolid (145) (~ 0.10 mmol) in anhydrous MeCN (~ 200  $\mu$ L) was subsequently added via cannula from a second round-bottomed flask under a nitrogen atmosphere. Reaction progress was monitored by  $^{31}\text{P}\{^1\text{H}\}$  NMR via taking small aliquots of the reaction mixture (~ 50  $\mu$ L) and diluting with anhydrous MeCN (~ 500  $\mu$ L). After 2 h, all AMP-*N*-methylimidazolid (145) had been consumed or degraded and the reaction mixture was quenched with 250 mM aqueous  $\text{NH}_4\text{OAc}$  (3 mL). The resulting aqueous solution was extracted with HPLC-grade DCM (3 mL) to remove organic-soluble reaction components. The product-containing aqueous layer was purified via automated C18 reversed-phase ion-pair chromatography using a Biotage 25M (25 mm x 15 cm) column (solvent system = 100:0 A:B (2 CV), linear gradient to 70:30 A:B (5 CV), 70:30 A:B (5 CV), linear gradient to 50:50 A:B (5 CV), 50:50 A:B (8 CV) where A = an aqueous solution containing 10 mM tributylamine and 30 mM glacial acetic acid and B = HPLC-grade MeOH; flow-rate = 25 mL/min; UV detection at 254 nm). Fractions containing the

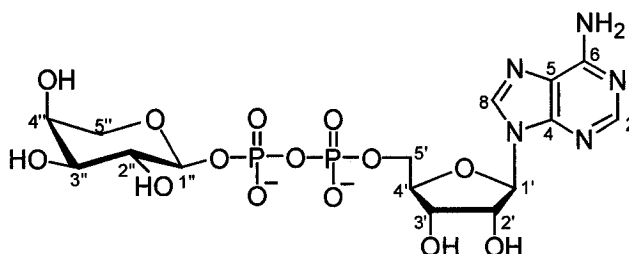
desired sugar nucleotide product were adjusted to pH 7 using a 1 M aqueous  $\text{NH}_4\text{OH}$  solution and concentrated under reduced pressure to a volume of  $\sim 5$  mL. The sugar nucleotide product was then passed through an Amberlite® IR-120 ( $\text{H}^+$ ) cation exchange column (free acid form) and acidic fractions were immediately neutralized to pH 7 using a dilute aqueous  $\text{NH}_4\text{OH}$  solution. Following concentration under reduced pressure, the sugar nucleotide was re-dissolved in  $\text{H}_2\text{O}$  ( $\sim 2$  mL) and lyophilized. Trituration with ethanol followed by vortexing and centrifugation at  $4^\circ\text{C}$  facilitated the successful removal of remaining  $\text{NH}_4\text{OAc}$ . After concentration under reduced pressure, the sugar nucleotide product was re-dissolved in  $\text{H}_2\text{O}$  ( $\sim 2$  mL) and lyophilized a second time to afford ADP- $\alpha$ -D-glucose (**146**, diammonium salt) as a white solid in 48% yield by UV spectroscopy ( $\lambda_{\text{max}}$  260 nm,  $\epsilon = 1.51 \times 10^4 \text{ M}^{-1}\text{cm}^{-1}$ ).  $^1\text{H}$  NMR (500 MHz,  $\text{D}_2\text{O}$ , pH 6):  $\delta$  8.54 (s, 1 H, H-8), 8.30 (s, 1 H, H-2), 6.18 (d,  $J_{1',2'} = 6.0$  Hz, 1 H, H-1'), 5.63 (dd,  $J_{1'',\text{P}} = 7.5$  Hz,  $J_{1'',2''} = 3.5$  Hz, 1 H, H-1''), 4.81 (dd,  $J_{2',3'} = 5.5$  Hz, 1 H, H-2'), 4.58 (dd,  $J_{3',4'} = 3.5$  Hz, 1 H, H-3'), 4.44 (m, 1 H, H-4'), 4.27 (m, 2 H, H-5a', H-5b'), 3.92 (ddd,  $J_{4'',5''} = 10.0$  Hz,  $J_{5'',6a''} = 2.0$  Hz,  $J_{5'',6b''} = 4.0$  Hz, 1 H, H-5''), 3.87 (dd,  $J_{6a'',6b''} = 12.5$  Hz, 1 H, H-6a''), 3.81 (dd,  $J_{2'',3''} = 10.0$  Hz,  $J_{3'',4''} = 9.5$  Hz, 1 H, H-3''), 3.77 (dd, 1 H, H-6b''), 3.55 (m, 1 H, H-2''), 3.47 (dd, 1 H, H-4'');  $^{13}\text{C}\{^1\text{H}\}$  NMR (126 MHz,  $\text{D}_2\text{O}$ , pH 6):  $\delta$  155.7 (C-6), 152.9 (C-2), 149.2 (C-4), 139.8 (C-8), 118.7 (C-5), 95.6 (C-1''), 86.9 (C-1'), 83.9 (C-4'), 74.3 (C-2'), 72.9 (C-5''), 72.8 (C-3''), 71.6 (C-2''), 70.4 (C-3'), 69.2 (C-4''), 65.3 (C-5'), 60.4 (C-6'');  $^{31}\text{P}\{^1\text{H}\}$  NMR (202 MHz,  $\text{D}_2\text{O}$ , pH 6):  $\delta$  -11.1 (d,  $J_{\text{P,P}} = 20.8$  Hz), -12.7 (d);  $t_{\text{R}}$  **146** = 5.58 min (Method A); LRMS (ESI $^-$ ) for  $\text{C}_{16}\text{H}_{25}\text{N}_5\text{O}_{15}\text{P}_2$  (free acid, 589.1 amu) =  $m/z$  588.0  $[\text{M-H}]^-$ . The reported  $^1\text{H}$  and  $^{13}\text{C}\{^1\text{H}\}$  NMR data is consistent with that of Lee and coworkers.<sup>156</sup>

### UDP- $\alpha$ -D-glucose (147)



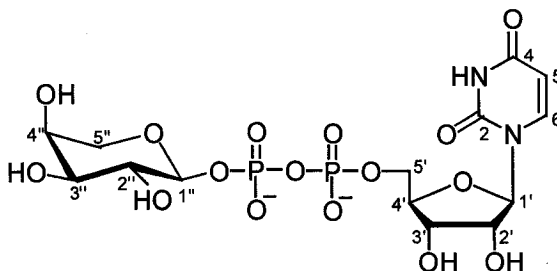
Following the procedure used for the preparation of ADP- $\alpha$ -D-glucose (**146**),  $\alpha$ -D-glucose-1-phosphate (tributylammonium salt (1.45 equiv), 106 mg, 0.200 mmol) was coupled with UMP-*N*-methylimidazolid (**121**) ( $\sim 0.10$  mmol) to prepare UDP- $\alpha$ -D-glucose (**147**). After purification as described for **146**, UDP- $\alpha$ -D-glucose (**147**, diammonium salt) was obtained as a white solid in 35% yield by UV spectroscopy ( $\lambda_{\text{max}}$  261 nm,  $\epsilon = 1.01 \times 10^4 \text{ M}^{-1}\text{cm}^{-1}$ ).  $^1\text{H}$  NMR (500 MHz,  $\text{D}_2\text{O}$ , pH 6):  $\delta$  7.91 (d,  $J_{5,6} = 8.5$  Hz, 1 H, H-6), 5.93 (m, 2 H, H-1', H-5), 5.55 (dd,  $J_{1',\text{P}} = 7.0$  Hz,  $J_{1'',2''} = 3.5$  Hz, 1 H, H-1''), 4.33 (dd, 2 H, H-2', H-3'), 4.24 (m, 1 H, H-4'), 4.18 (m, 2 H, H-5a', H-5b'), 3.85 (ddd,  $J_{4'',5''} = 9.5$  Hz,  $J_{5'',6a''} = 2.0$  Hz,  $J_{5'',6b''} = 4.5$  Hz, 1 H, H-5''), 3.81 (dd,  $J_{6a'',6b''} = 12.5$  Hz, 1 H, H-6a''), 3.73 (dd, 1 H,  $J_{2'',3''} = 9.5$  Hz,  $J_{3'',4''} = 9.5$  Hz, H-3''), 3.72 (dd, 1 H, H-6b''), 3.48 (m, 1 H, H-2''), 3.42 (dd, 1 H, H-4'');  $^{13}\text{C}\{^1\text{H}\}$  NMR (126 MHz,  $\text{D}_2\text{O}$ , pH 6):  $\delta$  166.3 (C-4), 151.9 (C-2), 141.7 (C-6), 102.7 (C-5), 95.6 (C-1''), 88.4 (C-1'), 83.3 (C-4'), 73.8 (C-2'), 72.9 (C-5'), 72.8 (C-3'), 71.6 (C-2''), 69.7 (C-3'), 69.2 (C-4''), 65.0 (C-5'), 60.4 (C-6'');  $^{31}\text{P}\{^1\text{H}\}$  NMR (202 MHz,  $\text{D}_2\text{O}$ , pH 6):  $\delta$  -11.1 (d,  $J_{\text{P,P}} = 20.8$  Hz), -12.8 (d);  $t_{\text{R}}$  **147** = 5.49 min (Method A); LRMS (ESI $^-$ ) for  $\text{C}_{15}\text{H}_{24}\text{N}_2\text{O}_{17}\text{P}_2$  (free acid, 566.1 amu) =  $m/z$  565.1  $[\text{M}-\text{H}]^-$ . The reported  $^1\text{H}$  and  $^{13}\text{C}\{^1\text{H}\}$  NMR data is consistent with that of Lee and coworkers.<sup>156</sup>

### ADP- $\alpha$ -L-arabinose (**148**)



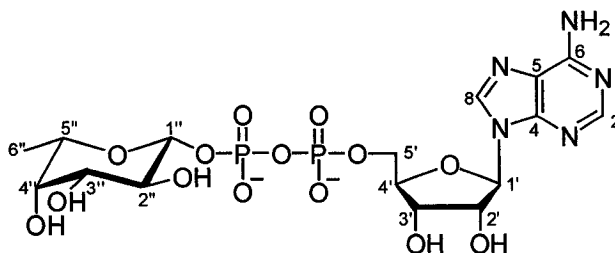
Following the procedure used for the preparation of ADP- $\alpha$ -D-glucose (**146**),  $\alpha$ -L-arabinose-1-phosphate (**135**) (tributylammonium salt (1.49 equiv), 102 mg, 0.200 mmol) was coupled with AMP-*N*-methylimidazolid (**145**) ( $\sim 0.10$  mmol) to prepare ADP- $\alpha$ -L-arabinose (**148**). After purification as described for **146**, ADP- $\alpha$ -L-arabinose (**148**, diammonium salt) was obtained as a white solid in 35% yield by UV spectroscopy ( $\lambda_{\text{max}}$  260 nm,  $\epsilon = 1.51 \times 10^4 \text{ M}^{-1}\text{cm}^{-1}$ ).  $^1\text{H}$  NMR (500 MHz,  $\text{D}_2\text{O}$ , pH 6):  $\delta$  8.46 (s, 1 H, H-8), 8.21 (s, 1 H, H-2), 6.10 (d,  $J_{1',2'} = 6.0$  Hz, 1 H, H-1'), 4.85 (dd,  $J_{1'',\text{P}} = 7.5$  Hz,  $J_{1'',2''} = 8.0$  Hz, 1 H, H-1''), 4.73 (dd,  $J_{2',3'} = 5.5$  Hz, 1 H, H-2'), 4.49 (dd,  $J_{3',4'} = 3.5$  Hz, 1 H, H-3'), 4.35 (m, 1 H, H-4'), 4.18 (m, 2 H, H-5a', H-5b'), 3.87 (m, 1 H, H-4''), 3.85 (dd,  $J_{4'',5a''} = 2.5$  Hz,  $J_{5a'',5b''} = 12.5$  Hz, 1 H, H-5a''), 3.63 (m, 2 H, H-3'', H-5b''), 3.60 (dd,  $J_{2'',3''} = 10.0$  Hz, 1 H, H-2'');  $^{13}\text{C}\{^1\text{H}\}$  NMR (126 MHz,  $\text{D}_2\text{O}$ , pH 6):  $\delta$  155.7 (C-6), 152.9 (C-2), 149.2 (C-4), 139.9 (C-8), 118.7 (C-5), 98.7 (C-1''), 86.9 (C-1'), 84.0 (C-4'), 74.3 (C-2'), 71.9 (C-2''), 71.2 (C-3''), 71.1 (C-3'), 68.0 (C-4''), 66.5 (C-5''), 65.3 (C-5');  $^{31}\text{P}\{^1\text{H}\}$  NMR (202 MHz,  $\text{D}_2\text{O}$ , pH 6):  $\delta$  -11.1 (d,  $J_{\text{P,P}} = 20.2$  Hz), -13.0 (d);  $t_{\text{R}}$  **148** = 5.34 min (Method A); LRMS (ESI $^-$ ) for  $\text{C}_{15}\text{H}_{23}\text{N}_5\text{O}_{14}\text{P}_2$  (free acid, 559.1 amu) =  $m/z$  558.1  $[\text{M}-\text{H}]^-$ .

### UDP- $\alpha$ -L-arabinose (**149**)



Following the procedure used for the preparation of ADP- $\alpha$ -D-glucose (**146**),  $\alpha$ -L-arabinose-1-phosphate (**135**) (tributylammonium salt (1.49 equiv), 102 mg, 0.200 mmol) was coupled with UMP-*N*-methylimidazolid (**121**) ( $\sim 0.10$  mmol) to prepare UDP- $\alpha$ -L-arabinose (**149**). After purification as described for **146**, UDP- $\alpha$ -L-arabinose (**149**, diammonium salt) was obtained as a white solid in 32% yield by UV spectroscopy ( $\lambda_{\text{max}}$  261 nm,  $\epsilon = 1.01 \times 10^4 \text{ M}^{-1}\text{cm}^{-1}$ ).  $^1\text{H}$  NMR (500 MHz,  $\text{D}_2\text{O}$ , pH 6):  $\delta$  7.91 (d,  $J_{5,6} = 8.5$  Hz, 1 H, H-6), 5.93 (m, 2 H, H-1', H-5), 4.85 (dd,  $J_{1'',\text{P}} = 7.5$  Hz,  $J_{1'',2''} = 8.0$  Hz, 1 H, H-1''), 4.34 (m, 2 H, H-2', H-3'), 4.24 (m, 1 H, H-4'), 4.17 (m, 2 H, H-5a', H-5b'), 3.90 (m, 1 H, H-4''), 3.88 (dd,  $J_{4'',5a''} = 2.5$  Hz,  $J_{5a'',5b''} = 12.5$  Hz, 1 H, H-5a''), 3.66 (m, 2 H, H-3'', H-5b''), 3.60 (dd,  $J_{2'',3''} = 9.5$  Hz, 1 H, H-2'');  $^{13}\text{C}\{^1\text{H}\}$  NMR (126 MHz,  $\text{D}_2\text{O}$ , pH 6):  $\delta$  166.4 (C-4), 152.0 (C-2), 141.7 (C-6), 102.8 (C-5), 98.7 (C-1''), 88.3 (C-1'), 83.4 (C-4'), 73.8 (C-2'), 71.9 (C-3''), 71.2 (C-2''), 69.8 (C-3'), 68.0 (C-4''), 66.5 (C-5''), 65.0 (C-5');  $^{31}\text{P}\{^1\text{H}\}$  NMR (202 MHz,  $\text{D}_2\text{O}$ , pH 6):  $\delta$  -11.2 (d,  $J_{\text{P,P}} = 20.2$  Hz), -13.0 (d);  $t_{\text{R}}$  **149** = 5.37 min (Method A); LRMS (ESI) for  $\text{C}_{14}\text{H}_{22}\text{N}_2\text{O}_{16}\text{P}_2$  (free acid, 536.1 amu) =  $m/z$  535.1  $[\text{M-H}]^-$ . The reported  $^1\text{H}$ ,  $^{13}\text{C}\{^1\text{H}\}$ , and  $^{31}\text{P}\{^1\text{H}\}$  NMR data is consistent with that of Ernst and Klaffke.<sup>145</sup>

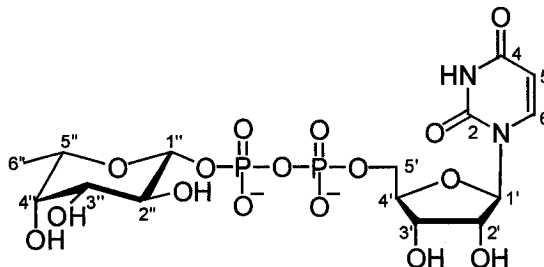
### ADP- $\beta$ -L-fucose (150)



Following the procedure used for the preparation of ADP- $\alpha$ -D-glucose (**146**),  $\beta$ -L-fucose-1-phosphate (**123**) (tributylammonium salt (1.53 equiv), 106 mg, 0.200 mmol) was coupled with AMP-*N*-methylimidazolid (**145**) ( $\sim 0.10$  mmol) to prepare ADP- $\beta$ -L-fucose (**150**). After purification as described for **146**, ADP- $\beta$ -L-fucose (**150**, diammonium salt) was obtained as a white solid in 28% yield by UV spectroscopy ( $\lambda_{\max}$  260 nm,  $\epsilon = 1.51 \times 10^4 \text{ M}^{-1}\text{cm}^{-1}$ ).  $^1\text{H}$  NMR (500 MHz,  $\text{D}_2\text{O}$ , pH 6):  $\delta$  8.55 (s, 1 H, H-8), 8.30 (s, 1 H, H-2), 6.18 (d,  $J_{1',2'} = 6.0$  Hz, 1 H, H-1'), 4.95 (dd,  $J_{1'',\text{P}} = 8.0$  Hz,  $J_{1'',2''} = 8.0$  Hz, 1 H, H-1''), 4.82 (dd,  $J_{2',3'} = 5.5$  Hz, 1 H, H-2'), 4.59 (dd,  $J_{3',4'} = 3.5$  Hz, 1 H, H-3'), 4.44 (m, 1 H, H-4'), 4.26 (m, 2 H, H-5a', H-5b'), 3.79 (br q,  $J_{5'',6''} = 6.5$  Hz, 1 H, H-5''), 3.74 (br d,  $J_{3'',4''} = 3.0$  Hz, 1 H, H-4''), 3.68 (dd,  $J_{2'',3''} = 10.0$  Hz, 1 H, H-3''), 3.59 (dd,  $J_{1'',2''} = 7.5$  Hz, 1 H, H-2''), 1.25 (d, 3 H, H<sub>3</sub>-6'');  $^{13}\text{C}\{^1\text{H}\}$  NMR (126 MHz,  $\text{D}_2\text{O}$ , pH 6):  $\delta$  155.7 (C-6), 153.0 (C-2), 149.3 (C-4), 139.9 (C-8), 118.7 (C-5), 98.4 (C-1''), 86.8 (C-1'), 84.0 (C-4'), 74.3 (C-2'), 72.5 (C-3''), 71.5 (C-5''), 71.2 (C-4''), 71.1 (C-2''), 70.5 (C-3'), 65.3 (C-5'), 15.4 (C-6'');  $^{31}\text{P}\{^1\text{H}\}$  NMR (202 MHz,  $\text{D}_2\text{O}$ , pH 6):  $\delta$  -11.1 (d,  $J_{\text{P,P}} = 20.8$  Hz), -12.9 (d);  $t_{\text{R}}$  **150** = 5.84 min (Method A); LRMS (ESI<sup>+</sup>) for  $\text{C}_{16}\text{H}_{25}\text{N}_5\text{O}_{14}\text{P}_2$  (free acid, 573.1 amu) =  $m/z$  572.1 [ $\text{M-H}$ ]<sup>-</sup>.

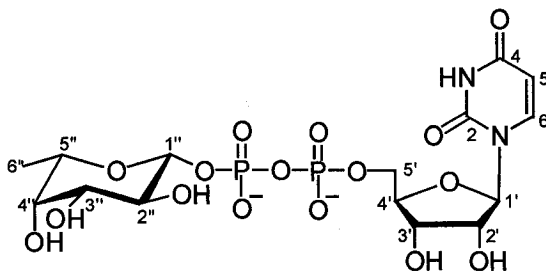


### UDP- $\beta$ -L-fucose (151) (Method 1)



Following the procedure used for the preparation of ADP- $\alpha$ -D-glucose (**146**),  $\beta$ -L-fucose-1-phosphate (**123**) (tributylammonium salt (1.53 equiv), 106 mg, 0.200 mmol) was coupled with UMP-*N*-methylimidazolid (**121**) ( $\sim 0.10$  mmol) to prepare UDP- $\beta$ -L-fucose (**151**). Following purification as described for **146**, UDP- $\beta$ -L-fucose (**151**, diammonium salt) was obtained as a white solid in 26% yield by UV spectroscopy ( $\lambda_{\text{max}}$  261 nm,  $\epsilon = 1.01 \times 10^4 \text{ M}^{-1}\text{cm}^{-1}$ ).  $^1\text{H}$  NMR (500 MHz,  $\text{D}_2\text{O}$ , pH 6):  $\delta$  7.84 (d,  $J_{5,6} = 8.0$  Hz, 1 H, H-6), 5.91 (d,  $J_{1',2'} = 4.5$  Hz, 1 H, H-1'), 5.88 (d, 1 H, H-5), 4.84 (dd,  $J_{1'',\text{P}} = 8.0$  Hz,  $J_{1'',2''} = 8.0$  Hz, 1 H, H-1''), 4.29 (m, 2 H, H-2', H-3'), 4.19 (m, 1 H, H-4'), 4.12 (m, 2 H, H-5a', H-5b'), 3.73 (br q,  $J_{5'',6''} = 6.5$  Hz, 1 H, H-5''), 3.65 (br d,  $J_{3'',4''} = 3.5$  Hz, 1 H, H-4''), 3.59 (dd,  $J_{2'',3''} = 10.0$  Hz, 1 H, H-3''), 3.47 (dd,  $J_{1'',2''} = 8.0$  Hz, 1 H, H-2''), 1.17 (d, 3 H, H-3-6'');  $^{13}\text{C}\{^1\text{H}\}$  NMR (126 MHz,  $\text{D}_2\text{O}$ , pH 6):  $\delta$  167.4 (C-4), 152.8 (C-2), 141.5 (C-6), 102.8 (C-5), 98.5 (C-1''), 88.4 (C-1'), 83.3 (C-4'), 73.8 (C-2'), 72.5 (C-3''), 71.5 (C-5''), 71.2 (C-4''), 71.1 (C-2''), 69.8 (C-3'), 65.0 (C-5'), 15.5 (C-6'');  $^{31}\text{P}\{^1\text{H}\}$  NMR (202 MHz,  $\text{D}_2\text{O}$ , pH 6):  $\delta$  -11.2 (d,  $J_{\text{P,P}} = 20.2$  Hz), -12.9 (d);  $t_{\text{R}}$  **151** = 5.60 min (Method A); LRMS (ESI $^+$ ) for  $\text{C}_{15}\text{H}_{24}\text{N}_2\text{O}_{16}\text{P}_2$  (free acid, 550.1 amu) =  $m/z$  549.1  $[\text{M-H}]^-$ . The reported  $^1\text{H}$  and  $^{13}\text{C}\{^1\text{H}\}$  NMR data is consistent with that of Augé and coworkers.<sup>272</sup>

## UDP- $\beta$ -L-fucose (151) (Method 2)



Uridine 5'-diphosphate (tetrabutylammonium salt (2.3 equiv by  $^1\text{H}$  NMR), 96 mg, 0.10 mmol) was dissolved in anhydrous MeCN (3.0 mL) in a round-bottomed flask fitted with a condensor under a nitrogen atmosphere. Anhydrous triethylamine (14  $\mu\text{L}$ , 0.10 mmol) and 3 Å molecular sieves (*ca.* 10) were added and the resulting solution was stirred at rt for 15 min. In a second round-bottomed flask, 2,3,4-tri-*O*-benzoyl- $\alpha$ -L-fucopyranosyl bromide (**124**) (56 mg, 0.10 mmol) was dissolved in anhydrous MeCN (2.0 mL) under a nitrogen atmosphere and transferred via cannula to the first flask containing UDP. The reaction mixture was heated at 80 °C for 30 min, after which time all glycosyl bromide had been consumed or degraded as indicated by TLC. Following filtration of molecular sieves and concentration under reduced pressure, the crude reaction mixture was re-dissolved in  $\text{H}_2\text{O}$  (3 mL) and the pH of this aqueous solution was immediately adjusted to 8 using triethylamine. Alkaline phosphatase (50 EU) was added to degrade residual UDP to uridine and inorganic phosphate, simplifying the purification protocol. The enzymatic reaction was stirred at rt for 16 h, after which time the degradation process was deemed complete by HPLC (Method A,  $t_{\text{R}}$  UDP = 5.88 min,  $t_{\text{R}}$  uridine = 1.50 min). The reaction mixture was subsequently concentrated under reduced pressure and re-dissolved in 2:2:1 MeOH: $\text{H}_2\text{O}$ :Et $_3\text{N}$  (3.0 mL) to remove acyl protecting groups. The resulting solution was stirred at rt for 24 h, after which time the

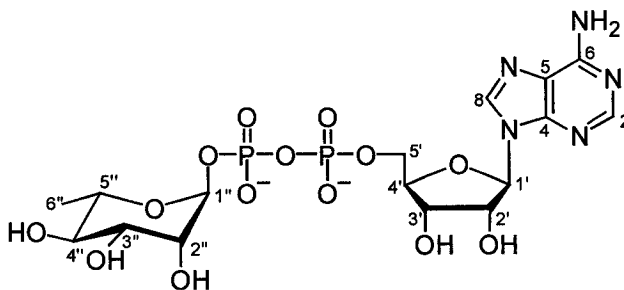
reaction mixture was concentrated under reduced pressure and re-dissolved in 10 mM aqueous tributylammonium bicarbonate buffer (~ 2 mL) in preparation for purification via C18 reversed-phase ion-pair chromatography. The 10 mM aqueous tributylammonium bicarbonate buffer was prepared by adding tributylamine (10 mmol/L) to H<sub>2</sub>O and bubbling CO<sub>2</sub> (obtained from the sublimation of dry ice) through the solution, which was cooled in an ice bath, until all tributylamine appeared to dissolve (~ 3 h). The resulting aqueous buffer was chilled in a 4 °C fridge if not used directly following its preparation. Automated C18 reversed-phase ion-pair chromatography was performed using a Biotage 25M (25 mm x 15 cm) C18 reversed-phase column (solvent system = 100:0 A:B (2 CV) followed by a linear gradient to 60:40 A:B (15 CV) and a plateau at 60:40 A:B (2 CV) where A = 10 mM aqueous tributylammonium bicarbonate buffer (pH 6) and B = HPLC-grade MeOH; flow rate of 25 mL/min; UV detection at 254 nm). Fractions containing the desired sugar nucleotide were combined and concentrated under reduced pressure to ~ 5 mL in volume. This solution was applied to a column filled with Dowex® 50W-X8 cation exchange resin (Na<sup>+</sup> form, 100-200 mesh) and the sugar nucleotide product was eluted with H<sub>2</sub>O. Fractions containing the desired product were concentrated under reduced pressure and lyophilized to afford UDP-β-L-fucose (**151**, disodium salt) as a white solid. NMR Analysis of **151** revealed a small quantity of an *n*-propyl-containing counterion (not connected to the sugar nucleotide by COSY NMR analysis). It was postulated that this impurity was present in the tributylamine.<sup>m</sup> To obtain a final product in one salt form for accurate yield analysis by mass, the sugar nucleotide was re-dissolved in a 0.1% w/v aqueous NH<sub>4</sub>HCO<sub>3</sub> solution and purified using

---

<sup>m</sup> This chemical was subsequently purchased in higher purity, which circumvented this difficulty.

a Biotage 12M (12 mm x 15 cm) C18 reversed-phase column (solvent system = 100:0 A:B (4 CV) followed by a linear gradient to 0:100 A:B (3 CV) and a plateau at 0:100 A:B (4 CV) where A = 0.1% w/v aqueous  $\text{NH}_4\text{HCO}_3$  and B = 0.1% w/v  $\text{NH}_4\text{HCO}_3$  in HPLC-grade MeOH; flow rate of 10 mL/min; UV detection at 254 nm). After concentration under reduced pressure, the sugar nucleotide was re-dissolved in  $\text{H}_2\text{O}$  (~ 2 mL) and lyophilized a second time to afford UDP- $\beta$ -L-fucose (**151**), free from *n*-propyl-containing organic impurities (18 mg, 0.031 mmol, 31% yield by mass, 26% yield by UV spectroscopy at  $\lambda_{\text{max}}$  261 nm,  $\epsilon = 1.01 \times 10^4 \text{ M}^{-1}\text{cm}^{-1}$  over 2 steps). Coupled  $^{13}\text{C}$ - $^1\text{H}$  HSQC:  $^1J_{\text{C-1"},\text{H-1}"}$  = 163 Hz. Other characterization data obtained for UDP- $\beta$ -L-fucose (**151**) prepared via Method 2 was identical to that of **151** prepared via Method 1, which was consistent with  $^1\text{H}$  and  $^{13}\text{C}\{^1\text{H}\}$  NMR data reported by Augé and coworkers.<sup>272</sup>

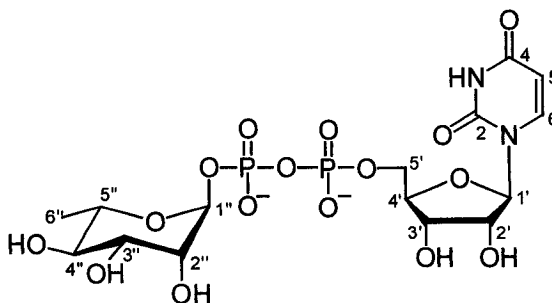
#### ADP- $\alpha$ -L-rhamnose (**152**)



Following the procedure used for the preparation of ADP- $\alpha$ -D-glucose (**146**),  $\alpha$ -L-rhamnose-1-phosphate (**134**) (tributylammonium salt (1.48 equiv), 104 mg, 0.200 mmol) was coupled with AMP-*N*-methylimidazolide (**145**) (~ 0.10 mmol) to prepare ADP- $\alpha$ -L-rhamnose (**152**). Following purification as described for **146**, ADP- $\alpha$ -L-rhamnose (**152**, diammonium salt) was obtained as a white solid in 25% yield by UV spectroscopy ( $\lambda_{\text{max}}$  260 nm,  $\epsilon = 1.51 \times 10^4 \text{ M}^{-1}\text{cm}^{-1}$ ).  $^1\text{H}$  NMR (500 MHz,  $\text{D}_2\text{O}$ , pH 6):  $\delta$

8.55 (s, 1 H, H-8), 8.29 (s, 1 H, H-2), 6.15 (d,  $J_{1',2'} = 6.0$  Hz, 1 H, H-1'), 5.43 (dd,  $J_{1'',P} = 7.5$  Hz,  $J_{1'',2''} = 1.5$  Hz, 1 H, H-1''), 4.77 (dd,  $J_{2',3'} = 4.5$  Hz, 1 H, H-2'), 4.53 (dd,  $J_{3',4'} = 4.0$  Hz, 1 H, H-3'), 4.40 (m, 1 H, H-4'), 4.22 (m, 2 H, H-5a', H-5b'), 4.03 (m, 1 H, H-2''), 3.90 (dq,  $J_{4'',5''} = 10.0$  Hz,  $J_{5'',6''} = 6.5$  Hz, 1 H, H-5''), 3.87 (dd,  $J_{2'',3''} = 3.5$  Hz,  $J_{3'',4''} = 9.5$  Hz, 1 H, H-3''), 3.41 (dd, 1 H, H-4''), 1.24 (d, 3 H, H<sub>3-6''</sub>);  $^{13}\text{C}\{^1\text{H}\}$  NMR (126 MHz, D<sub>2</sub>O, pH 6):  $\delta$  155.0 (C-6), 154.3 (C-2), 150.9 (C-4), 140.9 (C-8), 118.8 (C-5), 96.4 (C-1''), 87.1 (C-1'), 84.1 (C-4'), 74.4 (C-2'), 72.1 (C-4''), 70.5 (C-3'), 70.4 (C-2''), 69.7 (C-5''), 69.6 (C-3''), 65.2 (C-5'), 16.8 (C-6'');  $^{31}\text{P}\{^1\text{H}\}$  NMR (202 MHz, D<sub>2</sub>O, pH 6):  $\delta$  -11.4 (d,  $J_{P,P} = 20.2$  Hz), -13.8 (d);  $t_R$  **152** = 5.67 min (Method A); LRMS (ESI<sup>+</sup>) for C<sub>16</sub>H<sub>25</sub>N<sub>5</sub>O<sub>14</sub>P<sub>2</sub> (free acid, 573.1 amu) =  $m/z$  572.1 [M-H]<sup>+</sup>.

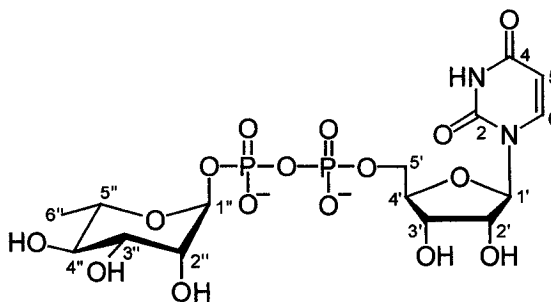
#### UDP- $\alpha$ -L-rhamnose (**153a**) (Method 1)



Following the procedure used for the preparation of ADP- $\alpha$ -D-glucose (**146**),  $\alpha$ -L-rhamnose-1-phosphate (**134**) (tributylammonium salt (1.48 equiv), 104 mg, 0.200 mmol) was coupled with UMP-*N*-methylimidazolidine (**121**) (~ 0.10 mmol) to prepare UDP- $\alpha$ -L-rhamnose (**153a**). After purification as described for **146**, UDP- $\alpha$ -L-rhamnose (**153a**, diammonium salt) was obtained as a white solid in 30% yield by UV spectroscopy ( $\lambda_{\text{max}}$  261 nm,  $\epsilon = 1.01 \times 10^4 \text{ M}^{-1}\text{cm}^{-1}$ ).  $^1\text{H}$  NMR (500 MHz, D<sub>2</sub>O, pH 6):  $\delta$  7.99 (d,  $J_{5,6} = 8.0$  Hz, 1 H, H-6), 6.02 (m, 2 H, H-1', H-5), 5.47 (dd,  $J_{1'',P} = 7.5$  Hz,  $J_{1'',2''} = 1.5$  Hz, 1 H,

H-1''), 4.41 (m, 2 H, H-2', H-3'), 4.33 (m, 1 H, H-4'), 4.25 (m, 2 H, H-5a', H-5b'), 4.08 (m, 1 H, H-2''), 3.95 (dq,  $J_{4'',5''} = 9.5$  Hz,  $J_{5'',6''} = 6.5$  Hz, 1 H, H-5''), 3.91 (dd,  $J_{2'',3''} = 3.5$  Hz,  $J_{3'',4''} = 10.0$  Hz, 1 H, H-3''), 3.48 (dd, 1 H, H-4''), 1.33 (d, 3 H, H<sub>3</sub>-6'');  $^{13}\text{C}\{^1\text{H}\}$  NMR (126 MHz, D<sub>2</sub>O, pH 6):  $\delta$  167.5 (C-4), 152.9 (C-2), 141.5 (C-6), 102.8 (C-5), 96.4 (C-1''), 88.4 (C-1'), 83.2 (C-4'), 73.8 (C-2'), 72.1 (C-4''), 70.5 (C-2''), 70.4 (C-3''), 69.7 (C-5''), 69.6 (C-3'), 65.0 (C-5'), 16.8 (C-6'');  $^{31}\text{P}\{^1\text{H}\}$  NMR (202 MHz, D<sub>2</sub>O, pH 6):  $\delta$  -11.5 (d,  $J_{\text{P,P}} = 20.4$  Hz), -13.9 (d);  $t_{\text{R}}$  **153a** = 5.58 min (Method A); LRMS (ESI<sup>+</sup>) for C<sub>15</sub>H<sub>24</sub>N<sub>2</sub>O<sub>16</sub>P<sub>2</sub> (free acid, 550.1 amu) =  $m/z$  549.1 [M-H]<sup>+</sup>. The reported  $^1\text{H}$  NMR data is consistent with selected data reported by Barber and Behrman.<sup>250</sup>

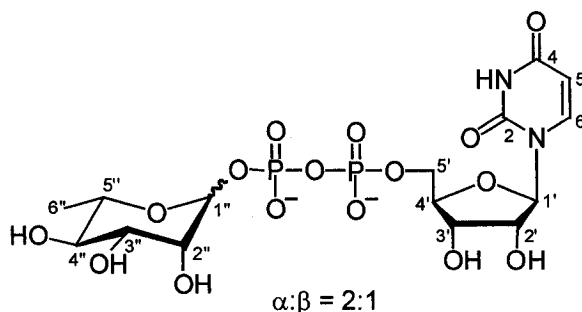
#### UDP- $\alpha$ -L-rhamnose (**153a**) (Method 2)



Following the procedure used for the preparation of UDP- $\beta$ -L-fucose (**151**) (Method 2), 2,3,4-tri-*O*-acetyl- $\alpha$ -L-rhamnopyranosyl bromide (**131**) (35 mg, 0.10 mmol) was coupled with uridine 5'-diphosphate (tetrabutylammonium salt (2.3 equiv by  $^1\text{H}$  NMR), 96 mg, 0.10 mmol) to prepare UDP- $\alpha$ -L-rhamnose (**153a**). After purification as described for **146**, UDP- $\alpha$ -L-rhamnose (**153a**, diammonium salt) was obtained as a white solid in 43% yield by UV spectroscopy ( $\lambda_{\text{max}}$  261 nm,  $\epsilon = 1.01 \times 10^4 \text{ M}^{-1}\text{cm}^{-1}$ ). Characterization data obtained for UDP- $\alpha$ -L-rhamnose (**153a**) prepared via Method 2 was

identical to that of **153a** prepared via Method 1, which was consistent with selected  $^1\text{H}$  NMR data reported by Barber and Behrman.<sup>250</sup>

#### UDP- $\alpha/\beta$ -L-rhamnose (**153b**)



This compound was prepared by an adaptation of a coupling procedure described by Uchiyama and Hindsgaul.<sup>143</sup> 1,2,3,4-Tetra-*O*-trimethylsilyl- $\alpha$ -L-rhamnopyranose (**156**) (45 mg, 0.10 mmol) was dissolved in anhydrous DCM (500  $\mu\text{L}$ ) in a round-bottomed flask under a nitrogen atmosphere. Trimethylsilyl iodide (15  $\mu\text{L}$ , 0.10 mmol) was added dropwise and the resulting reaction mixture was stirred for 1 h at rt. The quantitative formation of the desired glycosyl iodide (**157**) was confirmed by TLC (10:90 EtOAc:hexanes,  $R_f$  product = 0.80)<sup>n</sup> and  $^1\text{H}$  NMR ( $\delta$  6.69 (br s, 1 H, H-1)). In a second round-bottomed flask containing 3 Å molecular sieves (*ca.* 10), uridine 5'-diphosphate (tetrabutylammonium salt (2.3 equiv by  $^1\text{H}$  NMR), 96 mg, 0.10 mmol) was dissolved in anhydrous DCM (2.0 mL) under a nitrogen atmosphere. Anhydrous triethylamine (14  $\mu\text{L}$ , 0.10 mmol) was added and the resulting reaction mixture was stirred for 15 min at rt. The glycosyl iodide solution was subsequently transferred via cannula to the second round-bottomed flask containing UDP. After 2 h at rt, all glycosyl iodide had been

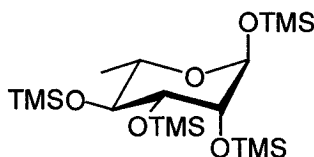
<sup>n</sup> Glycosyl iodide **157** degrades on silica gel TLC plates, presumably to the corresponding hemiacetals, which had an  $R_f$  of 0.22 in 10:90 EtOAc:hexanes.

consumed or hydrolyzed by TLC and  $^{31}\text{P}\{^1\text{H}\}$  NMR analysis of small aliquots of the reaction mixture (100  $\mu\text{L}$  quenched with  $\text{H}_2\text{O}$ ) taken after 1 and 2 h confirmed that the reaction had stopped progressing. Tetra-*n*-butylammonium fluoride (330  $\mu\text{L}$ , 0.33 mmol) was added and the reaction mixture was stirred for 1 h at rt. The reaction mixture was then filtered to remove molecular sieves and concentrated under reduced pressure. The resulting yellow syrup was re-dissolved in a minimal volume of HPLC-grade MeOH ( $\sim 1$  mL) and transferred to a centrifuge tube. A 0.05% w/v solution of NaI in acetone ( $\sim 5$  mL) was added<sup>273</sup> and the resulting heterogeneous mixture was vortexed and cooled for 15 min in a  $-20$  °C freezer. The mixture was centrifuged at  $4$  °C for 20 min. The pellet contained all  $^{31}\text{P}$ -containing compounds by  $^{31}\text{P}\{^1\text{H}\}$  NMR and less than 0.25 equiv of tetrabutylammonium counterions by  $^1\text{H}$  NMR. Analysis of the supernatant confirmed the absence of any  $^{31}\text{P}$ -containing compounds. The percentage conversion to UDP- $\alpha/\beta$ -L-rhamnose (**153b**) was determined via integration of  $^{31}\text{P}\{^1\text{H}\}$  NMR signals, while the  $\alpha:\beta$  ratio of the sugar nucleotide product was determined via integration of  $^1\text{H}$  NMR signals. Using these parameters, a 32% conversion to UDP- $\alpha/\beta$ -L-rhamnose (**153b**) in an  $\alpha:\beta$  ratio of 2:1 was obtained via the aforementioned reaction conditions. A repeat of the above reaction using MeCN as a solvent in lieu of DCM at rt resulted in a 27% conversion to **153b** and a similar  $\alpha:\beta$  ratio of 2:1. Lastly, repeating the aforementioned reaction at  $-40$  °C in DCM resulted in a 24% conversion to **173** and an  $\alpha:\beta$  ratio of 2:1. Purification attempts via automated anion exchange chromatography (12 mm x 15 cm column packed with SiliCycle™ Si-TMA chloride derivatized silica gel (200-400 mesh, 40-63  $\mu\text{M}$ ), solvent system =  $\text{H}_2\text{O}$  and 250 mM aqueous  $\text{NH}_4\text{OAc}$ , flow-rate = 10 mL/min, detection at 254 nm) were unsuccessful as lyophilization of potential sugar



nucleotide products resulted in their complete decomposition. This can possibly be attributed to the high ionic strength of lyophilized aqueous solutions as similar problems have previously been reported with other sugar nucleotides.<sup>258</sup>  $^1\text{H}$  and  $^{31}\text{P}\{^1\text{H}\}$  NMR data collected for the  $\alpha$  diastereomer of **153b** was consistent with data reported above for diastereomerically pure UDP- $\alpha$ -L-rhamnose (**153a**).  $^1\text{H}$  NMR (500 MHz,  $\text{D}_2\text{O}$ , pH 6):  $\delta$   $\beta$  diastereomer: 5.34 (dd,  $J_{1'',\text{P}} = 8.0$  Hz,  $J_{1'',2''} = 1.0$  Hz, 1 H, H-1'');  $^{31}\text{P}\{^1\text{H}\}$  NMR (202 MHz,  $\text{D}_2\text{O}$ , pH 6):  $\delta$  -11.4 (d,  $J_{\text{P,P}} = 20.2$  Hz, attached to D-ribose), -13.4 (d, attached to L-rhamnose). The reported  $^1\text{H}$  NMR data is consistent with selected data reported by Barber and Behrman.<sup>250</sup>

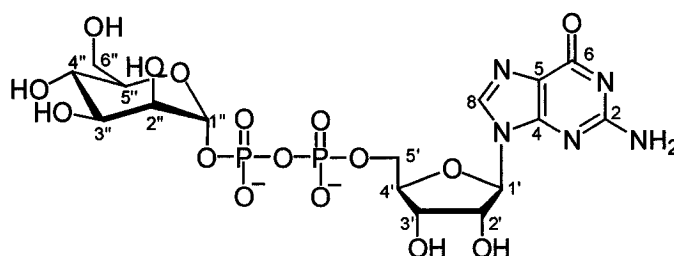
#### 1,2,3,4-Tetra-*O*-trimethylsilyl- $\alpha$ -L-rhamnopyranose (**156**)



This compound was prepared by an adaptation of a trimethylsilylation procedure described by Uchiyama and Hindsgaul.<sup>143</sup> L-Rhamnose monohydrate (500. mg, 2.74 mmol) was suspended in anhydrous pyridine (14 mL) in a round-bottomed flask under a nitrogen atmosphere and the resulting mixture was cooled to 0-5 °C in an ice-water bath. Trimethylsilyl chloride (2.1 mL, 16 mmol) was added and the reaction mixture was stirred for 1 h at 0-5 °C, after which time TLC analysis (10:90 EtOAc:hexanes,  $R_f$  product **156** = 0.56) revealed that the reaction was complete. The reaction mixture was diluted with hexanes (50 mL) and extracted with  $\text{H}_2\text{O}$  (5 x 25 mL). The organic layer was dried over  $\text{Na}_2\text{SO}_4$  and concentrated under reduced pressure to afford 1,2,3,4-tetra-*O*-trimethylsilyl- $\alpha$ -L-rhamnopyranose (**156**) as a colourless syrup (1.24 g, 2.74 mmol, 100%

yield).  $^1\text{H}$  NMR (500 MHz,  $\text{CDCl}_3$ ):  $\delta$  4.85 (d,  $J_{1,2} = 1.5$  Hz, 1 H, H-1), 3.80 (dd,  $J_{2,3} = 2.5$  Hz,  $J_{3,4} = 9.0$  Hz, 1 H, H-3), 3.70 (dq,  $J_{4,5} = 9.0$  Hz,  $J_{5,6} = 6.5$  Hz, 1 H, H-5), 3.64 (dd, 1 H, H-2), 3.59 (dd, 1 H, H-4), 1.19 (d, 3 H,  $\text{H}_3$ -6), 0.15 (s, 9 H,  $\text{Si}(\text{CH}_3)_3$ ), 0.14 (s, 9 H,  $\text{Si}(\text{CH}_3)_3$ ), 0.13 (s, 9 H,  $\text{Si}(\text{CH}_3)_3$ ), 0.12 (s, 9 H,  $\text{Si}(\text{CH}_3)_3$ );  $^{13}\text{C}$  NMR (126 MHz,  $\text{CDCl}_3$ ):  $\delta$  95.7 (C-1), 75.5 (C-2), 73.4 (C-4), 72.0 (C-3), 69.6 (C-5), 18.3 (C-6), 0.91 ( $\text{Si}(\text{CH}_3)_3$ ), 0.63 ( $\text{Si}(\text{CH}_3)_3$ ), 0.29 ( $\text{Si}(\text{CH}_3)_3$ ), -0.23 ( $\text{Si}(\text{CH}_3)_3$ ).

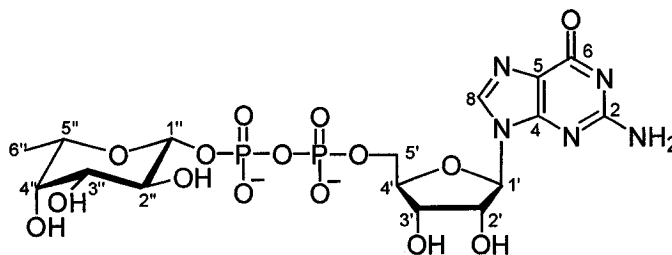
### GDP- $\alpha$ -D-mannose (**159**)



Following the procedure used for the preparation of UDP- $\beta$ -L-fucose (**151**) (Method 2), 2,3,4,6-tetra-*O*-acetyl- $\alpha$ -D-mannopyranosyl bromide (**161**) (41 mg, 0.10 mmol) was coupled with guanosine 5'-diphosphate (tetrabutylammonium salt (2.5 equiv by  $^1\text{H}$  NMR), 105 mg, 0.10 mmol) to prepare GDP- $\alpha$ -D-mannose (**159**). After purification as described for **151** (Method 2), GDP- $\alpha$ -D-mannose (**159**, diammonium salt) was obtained as a white solid (24 mg, 0.038 mmol, 38% yield by mass, 35% yield by UV spectroscopy at  $\lambda_{\text{max}}$  253 nm,  $\epsilon = 1.37 \times 10^4 \text{ M}^{-1}\text{cm}^{-1}$  over 2 steps).  $^1\text{H}$  NMR (500 MHz,  $\text{D}_2\text{O}$ , pH 6):  $\delta$  8.09 (s, 1 H, H-8), 5.92 (d,  $J_{1',2'} = 6.0$  Hz, 1 H, H-1'), 5.49 (br d,  $J_{1'',p} = 7.5$  Hz, 1 H, H-1''), 4.75 (dd,  $J_{2',3'} = 5.5$  Hz, 1 H, H-2'), 4.49 (dd,  $J_{3',4'} = 4.0$  Hz, 1 H, H-3'), 4.34 (m, 1 H, H-4'), 4.19 (m, 2 H, H-5a', H-5b'), 4.03 (br d,  $J_{2'',3''} = 3.3$  Hz, 1 H, H-2''), 3.90 (dd,  $J_{3'',4''} = 10.0$  Hz, 1 H, H-3''), 3.84 (m, 2 H, H-5'', H-6a''), 3.73 (dd,  $J_{5'',6b''} = 5.3$

Hz,  $J_{6a'',6b''} = 12.5$  Hz, 1 H, H-6b''), 3.66 (dd,  $J_{4'',5''} = 10.0$  Hz, 1 H, H-4'');  $^{13}\text{C}\{^1\text{H}\}$  NMR (126 MHz,  $\text{D}_2\text{O}$ , pH 6):  $\delta$  160.5 (C-6), 160.1 (C-2), 154.9 (C-4), 137.4 (C-8), 116.5 (C-5), 96.5 (C-1''), 86.8 (C-1'), 83.8 (C-4'), 73.7 (C-2'), 70.5 (C-3'), 70.3 (C-2''), 70.2 (C-3''), 69.9 (C-4''), 66.5 (C-5''), 65.3 (C-5'), 60.8 (C-6''); Coupled  $^{13}\text{C}$ - $^1\text{H}$  HSQC:  $^1J_{\text{C-1'',H-1''}} = 173$  Hz;  $^{31}\text{P}\{^1\text{H}\}$  NMR (202 MHz,  $\text{D}_2\text{O}$ , pH 6):  $\delta$  = -11.4 (d,  $J_{\text{P,P}} = 20.2$  Hz), -13.7 (d);  $t_{\text{R}}$  **159** = 5.26 min (Method A); LRMS (ESI $^-$ ) for  $\text{C}_{16}\text{H}_{25}\text{N}_5\text{O}_{16}\text{P}_2$  (free acid, 605.1 amu) =  $m/z$  604.1  $[\text{M-H}]^-$ . The reported  $^1\text{H}$  NMR data is consistent with that of Pallanca and Turner.<sup>257</sup>

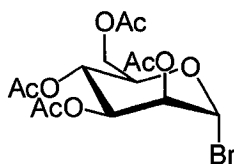
#### GDP- $\beta$ -L-fucose (160)



Following the procedure used for the preparation of UDP- $\beta$ -L-fucose (**151**) (Method 2), 2,3,4-tri-*O*-benzoyl- $\alpha$ -L-fucopyranosyl bromide (**124**) (56 mg, 0.10 mmol) was coupled with guanosine 5'-diphosphate (tetrabutylammonium salt (2.5 equiv by  $^1\text{H}$  NMR), 105 mg, 0.10 mmol) to prepare GDP- $\beta$ -L-fucose (**160**). After purification as described for **151** (Method 2), GDP- $\beta$ -L-fucose (**160**, diammonium salt) was obtained as a white solid (22 mg, 0.035 mmol, 35% yield by mass, 31% yield by UV spectroscopy at  $\lambda_{\text{max}}$  253 nm,  $\epsilon = 1.37 \times 10^4 \text{ M}^{-1}\text{cm}^{-1}$  over 2 steps).  $^1\text{H}$  NMR (500 MHz,  $\text{D}_2\text{O}$ , pH 6):  $\delta$  8.09 (s, 1 H, H-8), 5.92 (d,  $J_{1',2'} = 6.0$  Hz, 1 H, H-1'), 4.90 (dd,  $J_{1'',2''} = 8.0$  Hz,  $J_{1'',\text{P}} = 8.0$  Hz, 1 H, H-1''), 4.77 (dd,  $J_{2',3'} = 6.0$  Hz, 1 H, H-2'), 4.52 (dd,  $J_{3',4'} = 4.0$  Hz, 1 H, H-3'),

4.34 (m, 1 H, H-4'), 4.19 (m, 2 H, H-5a', H-5b'), 3.74 (br q,  $J_{5'',6''} = 6.5$  Hz, 1 H, H-5''), 3.69 (br d,  $J_{3'',4''} = 3.5$  Hz, 1 H, H-4''), 3.63 (dd,  $J_{2'',3''} = 10.0$  Hz, 1 H, H-3''), 3.54 (dd,  $J_{1'',2''} = 8.0$  Hz, 1 H, H-2''), 1.20 (d, 3 H, H<sub>3</sub>-6'');  $^{13}\text{C}\{^1\text{H}\}$  NMR (126 MHz, D<sub>2</sub>O, pH 6):  $\delta$  160.5 (C-6), 154.7 (C-2), 151.9 (C-4), 137.5 (C-8), 116.5 (C-5), 99.4 (C-1''), 86.7 (C-1'), 83.8 (C-4'), 73.6 (C-2'), 72.5 (C-3''), 71.5 (C-5''), 71.2 (C-4''), 71.1 (C-2''), 70.5 (C-3'), 65.3 (C-5'), 15.4 (C-6''); Coupled  $^{13}\text{C}$ - $^1\text{H}$  HSQC:  $^1J_{\text{C-1'',H-1''}} = 160$  Hz;  $^{31}\text{P}\{^1\text{H}\}$  NMR (202 MHz, D<sub>2</sub>O, pH 6):  $\delta$  -11.1 (d,  $J_{\text{P,P}} = 20.2$  Hz), -12.8 (d);  $t_{\text{R}}$  **160** = 5.29 min (Method A); LRMS (ESI<sup>+</sup>) for C<sub>16</sub>H<sub>25</sub>N<sub>5</sub>O<sub>15</sub>P<sub>2</sub> (free acid, 589.1 amu) =  $m/z$  588.1 [M-H]<sup>+</sup>. The reported  $^1\text{H}$ ,  $^{13}\text{C}\{^1\text{H}\}$ , and  $^{31}\text{P}\{^1\text{H}\}$  NMR data is consistent with that of Hindsgaul and coworkers<sup>258</sup> as well as that of Barker and coworkers.<sup>259</sup>

### 2,3,4,6-Tetra-*O*-acetyl- $\alpha$ -D-mannopyranosyl bromide (**161**)

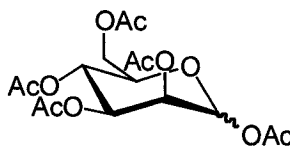


Following the procedure used for the preparation of glycosyl bromide **124**, 1,2,3,4,6-penta-*O*-acetyl- $\alpha/\beta$ -D-mannopyranose (**162**) (2.00 g, 5.12 mmol) was reacted with phosphorus tribromide (820  $\mu\text{L}$ , 8.7 mmol) and H<sub>2</sub>O (550  $\mu\text{L}$ , 31 mmol) in DCM (16 mL). The aforementioned protocol afforded 2,3,4,6-tetra-*O*-acetyl- $\alpha$ -D-mannopyranosyl bromide (**161**) (35:65 EtOAc:hexanes,  $R_f = 0.43$ )<sup>o</sup> as a pale orange syrup (1.78 g, 4.33 mmol, 85% yield).  $^1\text{H}$  NMR (500 MHz, CDCl<sub>3</sub>):  $\delta$  6.30 (d,  $J_{1,2} = 1.0$  Hz, 1 H, H-1), 5.72 (dd,  $J_{2,3} = 3.5$  Hz,  $J_{3,4} = 10.0$  Hz, 1 H, H-3), 5.45 (dd, 1 H, H-2), 5.37 (dd,

<sup>o</sup> Glycosyl bromide **161** degrades on silica gel TLC plates, presumably to the corresponding hemiacetals, which had an  $R_f$  of 0.11 in 35:65 EtOAc:hexanes.

$J_{4,5} = 10.0$  Hz, 1 H, H-4), 4.33 (dd,  $J_{5,6a} = 5.0$  Hz,  $J_{6a,6b} = 12.5$  Hz, 1 H, H-6a), 4.23 (ddd,  $J_{5,6b} = 2.5$  Hz, 1 H, H-5), 4.14 (dd, 1 H, H-6b), 2.18 (s, 3 H, C(O)CH<sub>3</sub>), 2.11 (s, 3 H, C(O)CH<sub>3</sub>), 2.08 (s, 3 H, C(O)CH<sub>3</sub>), 2.01 (s, 3 H, C(O)CH<sub>3</sub>); <sup>13</sup>C{<sup>1</sup>H} NMR (125 MHz, CDCl<sub>3</sub>): δ 170.5 (C(O)CH<sub>3</sub>), 169.7 (C(O)CH<sub>3</sub>), 169.6 (C(O)CH<sub>3</sub>), 169.5 (C(O)CH<sub>3</sub>), 83.1 (C-1), 72.9 (C-5), 72.2 (C-2), 68.0 (C-3), 65.4 (C-4), 61.5 (C-6), 20.74 (C(O)CH<sub>3</sub>), 20.66 (C(O)CH<sub>3</sub>), 20.63 (C(O)CH<sub>3</sub>), 20.55 (C(O)CH<sub>3</sub>).

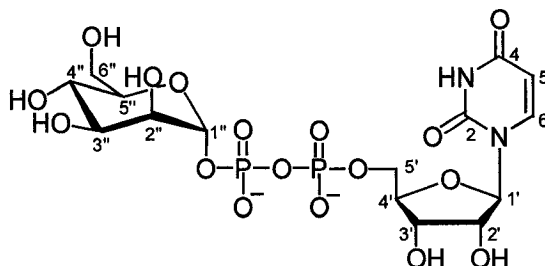
### 1,2,3,4,6-Penta-*O*-acetyl- $\alpha/\beta$ -D-mannopyranose (**162**)



Following the procedure used for the preparation of acetylated derivative **130**, D-Mannose (5.00 g, 27.8 mmol) was reacted with acetic anhydride (26 mL, 278 mmol) in pyridine (23 mL). The aforementioned protocol afforded 1,2,3,4,6-penta-*O*-acetyl- $\alpha/\beta$ -D-mannopyranose (**162**) (35:65 EtOAc:hexanes,  $R_f = 0.30$ ) as a colourless syrup in an  $\alpha/\beta$  ratio of 1:3 (10.12 g, 25.9 mmol, 93% yield). <sup>1</sup>H NMR (500 MHz, CDCl<sub>3</sub>): δ  $\alpha$  diastereomer: 5.87 (d,  $J_{1,2} = 1.0$  Hz, 1 H, H-1), 5.49 (dd,  $J_{2,3} = 3.0$  Hz, 1 H, H-2), 5.30 (dd,  $J_{3,4} = 10.0$  Hz,  $J_{4,5} = 10.0$  Hz, 1 H, H-4), 5.14 (dd, 1 H, H-3), 4.31 (dd,  $J_{5,6a} = 5.5$  Hz,  $J_{6a,6b} = 12.5$  Hz, 1 H, H-6a), 4.15 (dd,  $J_{5,6b} = 2.5$  Hz, 1 H, H-6b), 3.81 (ddd, 1 H, H-5), 2.22 (s, 3 H, C(O)CH<sub>3</sub>), 2.12 (s, 3 H, C(O)CH<sub>3</sub>), 2.10 (s, 3 H, C(O)CH<sub>3</sub>), 2.06 (s, 3 H, C(O)CH<sub>3</sub>), 2.01 (s, 3 H, C(O)CH<sub>3</sub>);  $\beta$  diastereomer: 6.09 (d,  $J_{1,2} = 2.0$  Hz, 1 H, H-1), 5.35 (m, 2 H, H-3, H-4), 5.26 (dd,  $J_{2,3} = 2.0$  Hz, 1 H, H-2), 4.28 (dd,  $J_{5,6a} = 5.0$  Hz,  $J_{6a,6b} = 12.5$  Hz, 1 H, H-6a), 4.11 (dd,  $J_{5,6b} = 2.5$  Hz, 1 H, H-6b), 4.06 (ddd, 1 H, H-5), 2.18 (s,

3 H, C(O)CH<sub>3</sub>), 2.17 (s, 3 H, C(O)CH<sub>3</sub>), 2.10 (s, 3 H, C(O)CH<sub>3</sub>), 2.06 (s, 3 H, C(O)CH<sub>3</sub>), 2.01 (s, 3 H, C(O)CH<sub>3</sub>).

### UDP- $\alpha$ -D-mannose (**163**)



Following the procedure used for the preparation of UDP- $\beta$ -L-fucose (**151**) (Method 2), 2,3,4,6-tetra-*O*-acetyl- $\alpha$ -D-mannopyranosyl bromide (**161**) (41 mg, 0.10 mmol) was coupled with uridine 5'-diphosphate (tetrabutylammonium salt (2.3 equiv by <sup>1</sup>H NMR), 96 mg, 0.10 mmol) to prepare UDP- $\alpha$ -D-mannose (**163**). After purification as described for **151** (Method 2), UDP- $\alpha$ -D-mannose (**163**, diammonium salt) was obtained as a white solid (20 mg, 0.033 mmol, 33% yield by mass, 29% yield by UV spectroscopy at  $\lambda_{\text{max}}$  261 nm,  $\epsilon = 1.01 \times 10^4 \text{ M}^{-1}\text{cm}^{-1}$  over 2 steps). <sup>1</sup>H NMR (500 MHz, D<sub>2</sub>O, pH 6):  $\delta$  7.93 (d,  $J_{5,6} = 8.0$  Hz, 1 H, H-6), 5.98 (d,  $J_{1',2'} = 3.5$  Hz, 1 H, H-1'), 5.95 (d, 1 H, H-5), 5.49 (br d,  $J_{1'',P} = 8.0$  Hz, 1 H, H-1''), 4.35 (m, 2 H, H-2', H-3'), 4.27 (m, 1 H, H-4'), 4.20 (m, 2 H, H-5a', H-5b'), 4.03 (br d,  $J_{2'',3''} = 3.5$  Hz, 1 H, H-2''), 3.90 (dd,  $J_{3'',4''} = 10.0$  Hz, 1 H, H-3''), 3.85 (m, 2 H, H-5'', H-6a''), 3.75 (dd,  $J_{5'',6b''} = 5.5$  Hz,  $J_{6a'',6b''} = 12.5$  Hz, 1 H, H-6b''), 3.66 (dd,  $J_{4'',5''} = 10.0$  Hz, 1 H, H-4''); <sup>13</sup>C{<sup>1</sup>H} NMR (126 MHz, D<sub>2</sub>O, pH 6):  $\delta$  167.5 (C-4), 152.8 (C-2), 141.5 (C-6), 102.8 (C-5), 96.5 (C-1''), 88.5 (C-1'), 83.2 (C-4'), 73.8 (C-2'), 73.7 (C-5''), 70.3 (C-2''), 69.9 (C-3'), 69.7 (C-3''), 66.5 (C-4''), 65.0 (C-5'), 60.8 (C-6''); Coupled <sup>13</sup>C-<sup>1</sup>H HSQC:  $J_{C-1'',H-1''} = 170$  Hz; <sup>31</sup>P{<sup>1</sup>H} NMR (202 MHz, D<sub>2</sub>O,

pH 6):  $\delta$  -11.6 (d,  $J_{P,P} = 20.2$  Hz), -13.9 (d);  $t_R$  **163** = 5.43 min (Method A); LRMS (ESI) for  $C_{15}H_{24}N_2O_{17}P_2$  (free acid, 566.1 amu) =  $m/z$  565.1  $[M-H]^-$ . The reported  $^1H$  and  $^{13}C\{^1H\}$  NMR data is consistent with that of Lee and coworkers.<sup>156</sup>

### 3.3. Nucleotidyltransferase Assay Conditions

The following nucleotidyltransferase assay conditions were adapted from reaction conditions previously described by Thorson and coworkers.<sup>155,157,158</sup> Enzymatic reactions containing 1.0 mM NTP, 2.0 mM sugar-1-phosphate, 2.2 mM  $MgCl_2$ , and 0.5 EU inorganic pyrophosphatase were initiated by the addition of 2 EU nucleotidyltransferase in Tris-HCl buffer (35 mM final buffer concentration, 50  $\mu$ L reaction volume). The enzymatic reactions were incubated for 30 min or 24 h at 37 °C, quenched with HPLC-grade MeOH (50  $\mu$ L), and centrifuged (5 min at 12,000 x g) to precipitate the denatured enzymes. The supernatants were subsequently subjected to HPLC analysis and sugar nucleotide product formation was confirmed by ESI-MS/MS. In the absence of nucleotidyltransferase, NTP, sugar-1-phosphate, or  $MgCl_2$ , no product formation was observed.

### 3.4. Characterization of Enzymatically Prepared Sugar Nucleotides

**Table 8.** Percentage conversions to sugar nucleotide products after 30 min incubations

enzyme	sugar-1-phosphate	NTP	% conversion	NDP-sugar retention time (min)
Cps2L	$\alpha$ -D-Glc-1-P	ATP	4	5.57
Cps2L	$\alpha$ -D-Glc-1-P	CTP	17	4.56
Cps2L	$\alpha$ -D-Glc-1-P	GTP	4	5.36
Cps2L	$\alpha$ -D-Glc-1-P	dTTP	87	5.66
Cps2L	$\alpha$ -D-Glc-1-P	UTP	95	5.32
Cps2L	$\alpha$ -D-GlcNH <sub>2</sub> -1-P	ATP	0	-
Cps2L	$\alpha$ -D-GlcNH <sub>2</sub> -1-P	CTP	0	-
Cps2L	$\alpha$ -D-GlcNH <sub>2</sub> -1-P	GTP	0	-
Cps2L	$\alpha$ -D-GlcNH <sub>2</sub> -1-P	dTTP	95	2.60
Cps2L	$\alpha$ -D-GlcNH <sub>2</sub> -1-P	UTP	96	2.36
Cps2L	$\alpha$ -D-GlcNAc-1-P	ATP	2	5.60
Cps2L	$\alpha$ -D-GlcNAc-1-P	CTP	0	-
Cps2L	$\alpha$ -D-GlcNAc-1-P	GTP	0	-
Cps2L	$\alpha$ -D-GlcNAc-1-P	dTTP	91	5.56
Cps2L	$\alpha$ -D-GlcNAc-1-P	UTP	4	5.51
Cps2L	$\alpha$ -D-Gal-1-P	ATP	0	-
Cps2L	$\alpha$ -D-Gal-1-P	CTP	0	-
Cps2L	$\alpha$ -D-Gal-1-P	GTP	0	-
Cps2L	$\alpha$ -D-Gal-1-P	dTTP	78	5.58
Cps2L	$\alpha$ -D-Gal-1-P	UTP	2	5.50
Cps2L	$\alpha$ -D-Man-1-P	ATP	0	-
Cps2L	$\alpha$ -D-Man-1-P	CTP	0	-
Cps2L	$\alpha$ -D-Man-1-P	GTP	0	-
Cps2L	$\alpha$ -D-Man-1-P	dTTP	64	5.70
Cps2L	$\alpha$ -D-Man-1-P	UTP	7	5.45
Cps2L	$\beta$ -L-Fuc-1-P	ATP	0	-
Cps2L	$\beta$ -L-Fuc-1-P	CTP	0	-
Cps2L	$\beta$ -L-Fuc-1-P	GTP	0	-
Cps2L	$\beta$ -L-Fuc-1-P	dTTP	10	5.80
Cps2L	$\beta$ -L-Fuc-1-P	UTP	0	-



enzyme	sugar-1-phosphate	NTP	% conversion	NDP-sugar retention time (min)
RmlA	$\alpha$ -D-Glc-1-P	ATP	0	-
RmlA	$\alpha$ -D-Glc-1-P	CTP	0	-
RmlA	$\alpha$ -D-Glc-1-P	GTP	5	5.42
RmlA	$\alpha$ -D-Glc-1-P	dTTP	100	5.65
RmlA	$\alpha$ -D-Glc-1-P	UTP	97	5.44
RmlA	$\alpha$ -D-GlcNH <sub>2</sub> -1-P	ATP	0	-
RmlA	$\alpha$ -D-GlcNH <sub>2</sub> -1-P	CTP	0	-
RmlA	$\alpha$ -D-GlcNH <sub>2</sub> -1-P	GTP	0	-
RmlA	$\alpha$ -D-GlcNH <sub>2</sub> -1-P	dTTP	94	2.60
RmlA	$\alpha$ -D-GlcNH <sub>2</sub> -1-P	UTP	92	2.35
RmlA	$\alpha$ -D-GlcNAc-1-P	ATP	0	-
RmlA	$\alpha$ -D-GlcNAc-1-P	CTP	0	-
RmlA	$\alpha$ -D-GlcNAc-1-P	GTP	0	-
RmlA	$\alpha$ -D-GlcNAc-1-P	dTTP	57	5.65
RmlA	$\alpha$ -D-GlcNAc-1-P	UTP	15	5.50
RmlA	$\alpha$ -D-Gal-1-P	ATP	0	-
RmlA	$\alpha$ -D-Gal-1-P	CTP	0	-
RmlA	$\alpha$ -D-Gal-1-P	GTP	0	-
RmlA	$\alpha$ -D-Gal-1-P	dTTP	92	5.61
RmlA	$\alpha$ -D-Gal-1-P	UTP	5	5.64
RmlA	$\alpha$ -D-Man-1-P	ATP	0	-
RmlA	$\alpha$ -D-Man-1-P	CTP	0	-
RmlA	$\alpha$ -D-Man-1-P	GTP	0	-
RmlA	$\alpha$ -D-Man-1-P	dTTP	92	5.60
RmlA	$\alpha$ -D-Man-1-P	UTP	20	5.45
RmlA	$\beta$ -L-Fuc-1-P	ATP	0	-
RmlA	$\beta$ -L-Fuc-1-P	CTP	0	-
RmlA	$\beta$ -L-Fuc-1-P	GTP	0	-
RmlA	$\beta$ -L-Fuc-1-P	dTTP	3	5.79
RmlA	$\beta$ -L-Fuc-1-P	UTP	0	-
RmlA3	$\alpha$ -D-Glc-1-P	ATP	6	5.58
RmlA3	$\alpha$ -D-Glc-1-P	CTP	18	4.52
RmlA3	$\alpha$ -D-Glc-1-P	GTP	8	5.35
RmlA3	$\alpha$ -D-Glc-1-P	dTTP	100	5.69
RmlA3	$\alpha$ -D-Glc-1-P	UTP	96	5.49
RmlA3	$\alpha$ -D-GlcNH <sub>2</sub> -1-P	ATP	0	-

enzyme	sugar-1-phosphate	NTP	% conversion	NDP-sugar retention time (min)
RmlA3	$\alpha$ -D-GlcNH <sub>2</sub> -1-P	CTP	0	-
RmlA3	$\alpha$ -D-GlcNH <sub>2</sub> -1-P	GTP	0	-
RmlA3	$\alpha$ -D-GlcNH <sub>2</sub> -1-P	dTTP	77	2.67
RmlA3	$\alpha$ -D-GlcNH <sub>2</sub> -1-P	UTP	94	2.37
RmlA3	$\alpha$ -D-GlcNAc-1-P	ATP	0	-
RmlA3	$\alpha$ -D-GlcNAc-1-P	CTP	0	-
RmlA3	$\alpha$ -D-GlcNAc-1-P	GTP	0	-
RmlA3	$\alpha$ -D-GlcNAc-1-P	dTTP	29	5.72
RmlA3	$\alpha$ -D-GlcNAc-1-P	UTP	19	5.51
RmlA3	$\alpha$ -D-Gal-1-P	ATP	0	-
RmlA3	$\alpha$ -D-Gal-1-P	CTP	0	-
RmlA3	$\alpha$ -D-Gal-1-P	GTP	0	-
RmlA3	$\alpha$ -D-Gal-1-P	dTTP	77	5.72
RmlA3	$\alpha$ -D-Gal-1-P	UTP	3	5.48
RmlA3	$\alpha$ -D-Man-1-P	ATP	0	-
RmlA3	$\alpha$ -D-Man-1-P	CTP	0	-
RmlA3	$\alpha$ -D-Man-1-P	GTP	0	-
RmlA3	$\alpha$ -D-Man-1-P	dTTP	66	5.67
RmlA3	$\alpha$ -D-Man-1-P	UTP	15	5.43
RmlA3	$\beta$ -L-Fuc-1-P	ATP	0	-
RmlA3	$\beta$ -L-Fuc-1-P	CTP	0	-
RmlA3	$\beta$ -L-Fuc-1-P	GTP	0	-
RmlA3	$\beta$ -L-Fuc-1-P	dTTP	7	5.78
RmlA3	$\beta$ -L-Fuc-1-P	UTP	0	-

\* Percentage conversion = [NDP-sugar / (NDP-sugar + NTP)] x 100 where NDP-sugar is equal to the product peak integration and NTP is equal to the NTP peak integration

**Table 9.** HPLC retention times of NTP and NDP standards

standard	retention time (min)
ATP	7.46
CTP	7.26
GTP	7.34
dTTP	7.54
UTP	7.47
ADP	5.88
CDP	4.92
GDP	5.64
dTDP	6.02
UDP	5.82

**Table 10.** Comparison of percentage conversions to sugar nucleotide products after 30 min and 24 h incubations

enzyme	sugar-1-phosphate	NTP	% conversion * after 30 min	% conversion * after 24 h
Cps2L	$\alpha$ -D-Glc-1-P	ATP	4	69
Cps2L	$\alpha$ -D-Glc-1-P	CTP	17	69
Cps2L	$\alpha$ -D-Glc-1-P	GTP	4	82
Cps2L	$\alpha$ -D-GlcNAc-1-P	ATP	2	32
Cps2L	$\alpha$ -D-GlcNAc-1-P	UTP	4	97
Cps2L	$\alpha$ -D-Gal-1-P	UTP	2	28
Cps2L	$\alpha$ -D-Man-1-P	UTP	7	95
Cps2L	$\beta$ -L-Fuc-1-P	dTTP	10	96
RmlA	$\alpha$ -D-Glc-1-P	GTP	5	20
RmlA	$\alpha$ -D-GlcNAc-1-P	UTP	15	86
RmlA	$\alpha$ -D-Gal-1-P	UTP	5	14
RmlA	$\alpha$ -D-Man-1-P	UTP	20	24
RmlA	$\beta$ -L-Fuc-1-P	dTTP	3	72
RmlA3	$\alpha$ -D-Glc-1-P	ATP	6	94
RmlA3	$\alpha$ -D-Glc-1-P	CTP	18	96
RmlA3	$\alpha$ -D-Glc-1-P	GTP	8	99
RmlA3	$\alpha$ -D-GlcNAc-1-P	dTTP	29	97
RmlA3	$\alpha$ -D-GlcNAc-1-P	UTP	19	98
RmlA3	$\alpha$ -D-Gal-1-P	UTP	3	90
RmlA3	$\alpha$ -D-Man-1-P	UTP	15	98
RmlA3	$\beta$ -L-Fuc-1-P	dTTP	7	98

\* Percentage conversion = [NDP-sugar / (NDP-sugar + NTP)] x 100 where NDP-sugar is equal to the product peak integration and NTP is equal to the NTP peak integration

**Table 11.** Sugar nucleotide ESI-MS/MS data

sugar nucleotide product	molecular formula (free acid)	molecular mass	[M-H] <sup>-</sup> (m/z)	EPI fragments (m/z)
ADP- $\alpha$ -D-Glc	C <sub>16</sub> H <sub>25</sub> N <sub>5</sub> O <sub>15</sub> P <sub>2</sub>	589.1	587.6	346.0, 241.0, 158.9, 133.9, 97.0, 78.8
CDP- $\alpha$ -D-Glc	C <sub>15</sub> H <sub>25</sub> N <sub>3</sub> O <sub>16</sub> P <sub>2</sub>	565.1	563.8	374.8, 260.8, 133.8, 92.9, 78.8
GDP- $\alpha$ -D-Glc	C <sub>16</sub> H <sub>25</sub> N <sub>5</sub> O <sub>16</sub> P <sub>2</sub>	605.1	603.8	361.8, 240.8, 158.9, 97.0, 78.8
dTDP- $\alpha$ -D-Glc	C <sub>16</sub> H <sub>26</sub> N <sub>2</sub> O <sub>16</sub> P <sub>2</sub>	564.1	562.8	320.9, 241.0, 194.9, 158.9, 97.0, 78.8
UDP- $\alpha$ -D-Glc	C <sub>15</sub> H <sub>24</sub> N <sub>2</sub> O <sub>17</sub> P <sub>2</sub>	566.1	564.7	322.9, 241.0, 158.9, 97.0, 78.8
dTDP- $\alpha$ -D-GlcNH <sub>2</sub>	C <sub>16</sub> H <sub>27</sub> N <sub>3</sub> O <sub>15</sub> P <sub>2</sub>	563.1	561.7	382.8, 256.92, 176.9, 158.9, 96.8, 78.8
UDP- $\alpha$ -D-GlcNH <sub>2</sub>	C <sub>15</sub> H <sub>25</sub> N <sub>3</sub> O <sub>16</sub> P <sub>2</sub>	565.1	563.8	384.7, 272.9, 176.9, 158.9, 96.8, 79.0
ADP- $\alpha$ -D-GlcNAc	C <sub>18</sub> H <sub>28</sub> N <sub>6</sub> O <sub>15</sub> P <sub>2</sub>	630.1	628.8	407.9, 282.0, 272.9, 158.9, 134.0, 79.0
dTDP- $\alpha$ -D-GlcNH <sub>2</sub>	C <sub>18</sub> H <sub>29</sub> N <sub>3</sub> O <sub>16</sub> P <sub>2</sub>	605.1	603.8	382.8, 282.0, 256.9, 176.9, 158.9, 79.0
UDP- $\alpha$ -D-GlcNH <sub>2</sub>	C <sub>17</sub> H <sub>27</sub> N <sub>3</sub> O <sub>17</sub> P <sub>2</sub>	607.1	605.8	385.0, 282.0, 272.9, 176.9, 158.9, 78.8
dTDP- $\alpha$ -D-Gal	C <sub>16</sub> H <sub>26</sub> N <sub>2</sub> O <sub>16</sub> P <sub>2</sub>	564.1	562.8	382.9, 321.0, 256.9, 241.0, 176.9, 158.9, 97.0, 79.0
UDP- $\alpha$ -D-Gal	C <sub>15</sub> H <sub>24</sub> N <sub>2</sub> O <sub>17</sub> P <sub>2</sub>	566.1	564.8	384.8, 322.9, 272.9, 211.0, 158.9, 97.0, 79.0
dTDP- $\alpha$ -D-Man	C <sub>16</sub> H <sub>26</sub> N <sub>2</sub> O <sub>16</sub> P <sub>2</sub>	564.1	562.8	382.8, 320.9, 256.9, 176.9, 158.9, 96.8, 78.8
UDP- $\alpha$ -D-Man	C <sub>15</sub> H <sub>24</sub> N <sub>2</sub> O <sub>17</sub> P <sub>2</sub>	566.1	564.7	384.8, 322.9, 272.9, 158.9, 96.8, 79.0
dTDP- $\beta$ -L-Fuc	C <sub>16</sub> H <sub>26</sub> N <sub>2</sub> O <sub>15</sub> P <sub>2</sub>	548.1	546.8	382.8, 256.9, 176.9, 158.9, 97.0, 78.8

## Chapter 4. Conclusions

---

Several advances in the preparation of sugar nucleotides via chemical and enzymatic approaches for use as glycosyltransferase enzyme substrates have been described.

With respect to chemical synthesis, a novel methodology was developed to efficiently access the 2,6-dideoxysugar L-digitoxose, which was subsequently coupled with uridine 5'-diphosphate to prepare a novel 2,6-dideoxysugar nucleotide. Numerous approaches were also explored to prepare structurally related sugar nucleotides, resulting in the synthesis and purification of eleven compounds with varied carbohydrate residues and nucleoside bases. Of the methodologies investigated, the coupling of sugar-1-phosphates with nucleoside 5'-monophosphate-*N*-methylimidazolidine donors was found to be a fast and reliable method for preparing sugar nucleotides in moderate yield, although purification from dinucleoside diphosphate byproducts was sometimes difficult. Direct coupling approaches involving iodosugar donors were also effective and purification could be greatly simplified through the use of alkaline phosphatase to degrade unreacted nucleoside 5'-diphosphates; however, anomeric stereoselectivity was difficult to control. Interestingly, the coupling of acylated glycosyl bromides with nucleoside 5'-diphosphates provided efficient access to a series of D-manno- and L-fuco-linked sugar nucleotides of exclusively  $\alpha$  and  $\beta$  anomeric stereochemistry, respectively, using the well-established concept of neighbouring group participation. This represents the first report of a stereoselective direct coupling procedure for preparing these biologically relevant enzyme substrates.

Enzymatic approaches to prepare sugar nucleotides were also investigated by exploring the substrate promiscuity of three thymidyltransferases from bacterial sources. After incubation of enzymes with a variety of sugar-1-phosphates and nucleoside 5'-triphosphates for 24 h in lieu of the usual 0.5 h assay time, a series of fifteen structurally diverse sugar nucleotides were prepared in good yield, demonstrating a high level of thymidyltransferase substrate promiscuity. These results also illustrated a lack of substrate and product inhibition occurring at these millimolar concentrations. Future work will focus on scaling up these enzymatic reactions and purifying sugar nucleotide products to further investigate the synthetic potential of these biocatalysts.

Sugar nucleotides prepared via chemical and enzymatic approaches will be used as possible substrates for the JadS glycosyltransferase in the quest to probe the substrate promiscuity of this enzyme and potentially prepare differentially glycosylated analogues of jadomycin B in due course.

## References

---

- (1) Newman, D. J.; Cragg, G. M.; Snader, K. M. *Nat. Prod. Rep.* **2000**, *17*, 215-234.
- (2) Fleming, A. *Br. J. Exp. Pathol.* **1929**, *10*, 226-236.
- (3) Chain, E.; Florey, H. W.; Gardner, A. D.; Heatley, N. G.; Jennings, M. A.; Orr-Ewing, J.; Sanders, A. G. *Lancet* **1940**, *2*, 226-228.
- (4) Ohno, M.; Otsuka, M.; Yagisawa, M.; Kondo, S.; Öppinger, H.; Hoffmann, H.; Sukatsch, D.; Hepner, L. L.; Male, C. L. In *Pharmaceuticals: Classes, Therapeutic Agents, Areas of Application*; McGuire, J. L.; Ed.; Wiley-VCH: Toronto, ON, 2000; Vol. 3, pp 951-1106.
- (5) Butler, M. S. *J. Nat. Prod.* **2004**, *67*, 2141-2153.
- (6) Newman, D. J.; Cragg, G. M.; Snader, K. M. *J. Nat. Prod.* **2003**, *66*, 1022-1037.
- (7) Vining, L. C. In *Genetics and Biochemistry of Antibiotic Production*; Vining, L. C.; Stuttard, C.; Eds.; Butterworth-Heinemann: Newton, MA, 1995; pp 1-7.
- (8) Cragg, G. M.; Newman, D. J. *Trends Pharmacol. Sci.* **2002**, *23*, 404-405.
- (9) Knight, V.; Sanglier, J.-J.; DiTullio, D.; Braccili, S.; Bonner, P.; Waters, J.; Hughes, D.; Zhang, L. *Appl. Microbiol. Biotechnol.* **2003**, *62*, 446-458.
- (10) Ohno, M.; Otsuka, M.; Yagisawa, M. In *Pharmaceuticals: Classes, Therapeutic Agents, Areas of Application*; McGuire, J. L.; Ed.; Wiley-VCH: Toronto, ON, 2000; Vol. 3, pp 819-824.
- (11) Krohn, K.; Rohr, J. *Top. Curr. Chem.* **1997**, *188*, 127-195.
- (12) Rohr, J.; Thiericke, R. *Nat. Prod. Rep.* **1992**, *9*, 103-137.
- (13) Dann, M.; Lefemine, D. V.; Barbatschi, F.; Shu, P.; Kunstmann, M. P.; Mitscher, L. A.; Bohonos, N. *Antimicrob. Agents Chemother.* **1965**, *5*, 832-835.
- (14) Kunstmann, M. P.; Mitscher, L. A. *J. Org. Chem.* **1966**, *31*, 2920-2925.
- (15) Drautz, H.; Zähler, H.; Rohr, J.; Zeeck, A. *J. Antibiot.* **1986**, *39*, 1657-1669.



- (16) Baig, I.; Kharel, M.; Kobylansky, A.; Zhu, L.; Rebets, Y.; Ostash, B.; Luzhetskyy, A.; Bechthold, A.; Fedorenko, V. A.; Rohr, J. *Angew. Chem. Int. Ed.* **2006**, *45*, 7842-7846.
- (17) Bililign, T.; Griffith, B. R.; Thorson, J. S. *Nat. Prod. Rep.* **2005**, *22*, 742-760.
- (18) Trefzer, A.; Hoffmeister, D.; Künzel, E.; Stockert, S.; Weitnauer, G.; Westrich, L.; Rix, U.; Fuchser, J.; Bindseil, K. U.; Rohr, J.; Bechthold, A. *Chem. Biol.* **2000**, *7*, 133-142.
- (19) Künzel, E.; Faust, B.; Oelkers, C.; Weissbach, U.; Bearden, D. W.; Weitnauer, G.; Westrich, L.; Bechthold, A.; Rohr, J. *J. Am. Chem. Soc.* **1999**, *121*, 11058-11062.
- (20) Rohr, J.; Beale, J. M.; Floss, H. G. *J. Antibiot.* **1989**, *42*, 1151-1157.
- (21) Okazaki, T.; Kitahara, T.; Okami, Y. *J. Antibiot.* **1975**, *28*, 176-184.
- (22) Waksman, S. A. *The Actinomycetes: A Summary of Current Knowledge*; The Ronald Press Company: New York, NY, 1967; pp 3-6.
- (23) Okami, Y.; Hotta, K. In *Actinomycetes in Biotechnology*; Goodfellow, M.; Williams, S. T.; Mordarski, M.; Eds.; Academic Press: San Diego, CA, 1988; pp 33-67.
- (24) Zheng, J.-T.; Rix, U.; Zhao, L.; Mattingly, C.; Adams, V.; Chen, Q.; Rohr, J.; Yang, K.-Q. *J. Antibiot.* **2005**, *58*, 405-408.
- (25) Ayer, S. W.; McInnes, A. G.; Thibault, P.; Walter, J. A.; Doull, J. L.; Parnell, T.; Vining, L. C. *Tetrahedron Lett.* **1991**, 6301-6304.
- (26) Doull, J. L.; Ayer, S. W.; Singh, A. K.; Thibault, P. *J. Antibiot.* **1993**, *46*, 869-871.
- (27) Doull, J. L.; Singh, A. K.; Hoare, M.; Ayer, S. W. *J. Ind. Microbiol.* **1994**, *13*, 120-125.
- (28) Rix, U.; Zheng, J.; Rix, L. L. R.; Greenwell, L.; Yang, K.; Rohr, J. *J. Am. Chem. Soc.* **2004**, *126*, 4496-4497.
- (29) Syvitski, R. T.; Borissow, C. N.; Graham, C. L.; Jakeman, D. L. *Org. Lett.* **2006**, *8*, 697-700.
- (30) Jakeman, D. L.; Graham, C. L.; Reid, T. R. *Bioorg. Med. Chem. Lett.* **2005**, *15*, 5280-5283.
- (31) Jakeman, D. L.; Farrell, S.; Young, W.; Doucet, R. J.; Timmons, S. C. *Bioorg. Med. Chem. Lett.* **2005**, *15*, 1447-1449.

- (32) Richard, C.; Blay, J.; Jakeman, D. L. *unpublished data*.
- (33) Lowary, T. L. *Carbohydr. Res.* **2006**, *341*, 1207-1207.
- (34) Křen, V.; Martínková, L. *Curr. Med. Chem.* **2001**, *8*, 1303-1328.
- (35) Thorson, J. S.; Hosted, T. J., Jr.; Jiang, J.; Biggins, J. B.; Ahlert, J. *Curr. Org. Chem.* **2001**, *5*, 139-167.
- (36) Weymouth-Wilson, A. C. *Nat. Prod. Rep.* **1997**, *14*, 99-110.
- (37) Le, G. T.; Abbenante, G.; Becker, B.; Grathwohl, M.; Halliday, J.; Tometzki, G.; Zuegg, J.; Meutermans, W. *Drug Discov. Today* **2003**, *8*, 701-709.
- (38) Champney, W. S.; Tober, C. L. *Curr. Microbiol.* **2000**, *41*, 126-135.
- (39) Mazzei, T.; Mini, E.; Novelli, A.; Periti, P. *J. Antimicrob. Chemother.* **1993**, *31*, 1-9.
- (40) Jones, P. H.; Rowley, E. K. *J. Org. Chem.* **1968**, *33*, 665-670.
- (41) Flynn, E. H.; Murphy, H. W.; McMahon, R. E. *J. Am. Chem. Soc.* **1955**, *77*, 3104-3106.
- (42) Flynn, E. H.; Sigal, M. V.; Wiley, P. E.; Gerzon, K. *J. Am. Chem. Soc.* **1954**, *76*, 3121-3131.
- (43) Gladue, R. P.; Bright, G. M.; Isaacson, R. E.; Newborg, M. F. *J. Antimicrob. Chemother.* **1989**, *33*, 277-282.
- (44) McGuire, J. M.; Bunch, R. L.; Anderson, R. C.; Boaz, H. E.; Flynn, E. H.; Powell, M.; Smith, J. W. *Antibiot. Chemother.* **1952**, *2*, 281-283.
- (45) Weinstein, M. J.; Wagman, G. H.; Marquez, J. A.; Testa, R. T.; Oden, E.; Waitz, J. A. *J. Antibiot.* **1969**, *22*, 253-258.
- (46) Marquez, J.; Murawski, A.; Wagman, G. H.; Jaret, R. S.; Reimann, H. *J. Antibiot.* **1969**, *22*, 259-264.
- (47) Volchegursky, Y.; Hu, J.; Katz, L.; McDaniel, R. *Mol. Microbiol.* **2000**, *37*, 752-762.
- (48) Lee, M. D.; Dunne, T. S.; Siegel, M. M.; Chang, C. C.; Morton, G. O.; Borders, D. B. *J. Am. Chem. Soc.* **1987**, *109*, 3464-3466.

- (49) Lee, M. D.; Dunne, T. S.; Chang, C. C.; Ellestad, G. A.; Siegel, M. M.; Morton, G. O.; McGahren, W. J.; Borders, D. B. *J. Am. Chem. Soc.* **1987**, *109*, 3466-3468.
- (50) Jones, R. R.; Bergman, R. G. *J. Am. Chem. Soc.* **1972**, *94*, 660-661.
- (51) Christner, D. F.; Frank, B. L.; Kozarich, J. W.; Stubbe, J. A.; Golik, J.; Doyle, T. W.; Rosenberg, I. E.; Krishnan, B. J. *J. Am. Chem. Soc.* **1992**, *114*, 8763-8767.
- (52) Kumar, R. A.; Ikemoto, N.; Patel, D. J. *J. Mol. Biol.* **1997**, *265*, 187-201.
- (53) Ikemoto, N.; Kumar, R. A.; Ling, R. A.; Ling, T. T.; Ellestad, G. A.; Danishefsky, S. J.; Patel, D. J. *Proc. Natl. Acad. Sci.* **1995**, *92*, 10506-10510.
- (54) Zunino, F.; Pratesi, G.; Perego, P. *Biochem. Pharmacol.* **2001**, *61*, 933-938.
- (55) Arcamone, F.; Animati, F.; Bigioni, M.; Capranico, G.; Caserini, C.; Cipollone, A.; De Cesare, M.; Ettorre, A.; Guano, F.; Manzini, S.; Monteagudo, E.; Pratesi, G.; Salvatore, C.; Supino, R.; Zunino, F. *Biochem. Pharmacol.* **1999**, *57*, 1133-1139.
- (56) Findlay, B. P.; Walker-Dilks, C. *Cancer Prev. Control* **1998**, *2*, 140-146.
- (57) Takagi, Y.; Kobayashi, N.; Chang, M. S.; Lim, G.-J.; Tsuchiya, T. *Carbohydr. Res.* **1998**, *307*, 217-232.
- (58) Baer, H. H.; Siemsen, L. *Can. J. Chem.* **1988**, *66*, 187-190.
- (59) Ahmed, A.; Peters, N. R.; Fitzgerald, M. K.; Watson, J. A. Jr.; Hoffmann, F. M.; Thorson, J. S. *J. Am. Chem. Soc.* **2006**, *128*, 14224-14225.
- (60) Haas, L. F. *J. Neurol. Neurosurg. Psychiatry* **1996**, *60*, 427-427.
- (61) Pelletier, P. S.; Caventou, J. *Ann. Chim. Phys.* **1820**, *14*, 69-83.
- (62) Kirschning, A.; Chen, G.-w.; Dräger, G.; Schuberth, I.; Tietze, L. F. *Bioorg. Med. Chem.* **2000**, *8*, 2347-2354.
- (63) Sezaki, M.; Kondo, S.; Maeda, K.; Umezawa, H.; Ohno, M. *Tetrahedron* **1970**, *26*, 5171-5190.
- (64) Toshima, K. *Carbohydr. Res.* **2006**, *341*, 1282-1297.
- (65) Lin, H.; Walsh, C. T. *J. Am. Chem. Soc.* **2004**, *126*, 13998-14003.

- (66) Rostovtsev, V. V.; Green, L. G.; Fokin, V. V.; Sharpless, K. B. *Angew. Chem. Int. Ed.* **2002**, *41*, 2596-2599.
- (67) Langenhan, J. M.; Peters, N. R.; Guzei, I. A.; Hoffmann, F. M.; Thorson, J. S. *Proc. Natl. Acad. Sci.* **2005**, *102*, 12305-12310.
- (68) Langenhan, J. M.; Griffith, B. R.; Thorson, J. S. *J. Nat. Prod.* **2005**, *68*, 1696-1711.
- (69) Griffith, B. R.; Langenhan, J. M.; Thorson, J. S. *Curr. Opin. Biotechnol.* **2005**, *16*, 622-630.
- (70) Thorson, J. S.; Barton, W. A.; Hoffmeister, D.; Albermann, C.; Nikolov, D. B. *ChemBioChem* **2004**, *5*, 16-25.
- (71) Sánchez, C.; Zhu, L.; Braña, A. F.; Salas, A. P.; Rohr, J.; Méndez, C.; Salas, J. A. *Proc. Natl. Acad. Sci.* **2005**, *102*, 461-466.
- (72) Jakeman, D. L.; Borissow, C. N.; Graham, C. L.; Timmons, S. C.; Reid, T. R.; Syvitski, R. T. *Chem. Commun.* **2006**, 3738-3740.
- (73) Barton, W. A.; Lesniak, J.; Biggins, J. B.; Jeffrey, P. D.; Jiang, J.; Rajashankar, K. R.; Thorson, J. S.; Nikolov, D. B. *Nat. Struct. Biol.* **2001**, *8*, 545-552.
- (74) Yang, J.; Liu, L.; Thorson, J. S. *ChemBioChem* **2004**, *5*, 992-996.
- (75) Hoffmeister, D.; Thorson, J. S. *ChemBioChem* **2004**, *5*, 989-992.
- (76) Hoffmeister, D.; Yang, J.; Liu, L.; Thorson, J. S. *Proc. Natl. Acad. Sci.* **2003**, *100*, 13184-13189.
- (77) Yang, J.; Fu, X.; Jia, Q.; Shen, J.; Biggins, J. B.; Jiang, J.; Zhao, J.; Schmidt, J. J.; Wang, P. G.; Thorson, J. S. *Org. Lett.* **2003**, *5*, 2223-2226.
- (78) Yang, J.; Hoffmeister, D.; Liu, L.; Fu, X.; Thorson, J. S. *Bioorg. Med. Chem.* **2004**, *12*, 1577-1584.
- (79) Blanchard, S.; Thorson, J. S. *Curr. Opin. Chem. Biol.* **2006**, *10*, 263-271.
- (80) Fu, X.; Albermann, C.; Jiang, J.; Liao, J.; Zhang, C.; Thorson, J. S. *Nat. Biotechnol.* **2003**, *21*, 1467-1469.
- (81) Fu, X.; Albermann, C.; Zhang, C.; Thorson, J. S. *Org. Lett.* **2005**, *7*, 1513-1515.

- (82) Zhang, C.; Griffith, B. R.; Fu, Q.; Albermann, C.; Fu, X.; Lee, I.-K.; Li, L.; Thorson, J. S. *Science* **2006**, *313*, 1291-1294.
- (83) Glaser, L.; Brown, D. H. *J. Biol. Chem.* **1957**, *228*, 729-742.
- (84) Cardini, C. E.; Leloir, L. F.; Chiriboga, J. *J. Biol. Chem.* **1955**, *214*, 149-155.
- (85) Minami, A.; Kakinuma, K.; Eguchi, T. *Tetrahedron Lett.* **2005**, 6187-6190.
- (86) Zhang, C.; Albermann, C.; Fu, X.; Thorson, J. S. *J. Am. Chem. Soc.* **2006**, *128*, 16420-16421.
- (87) Hu, Y.; Walker, S. *Chem. Biol.* **2002**, *9*, 1287-1296.
- (88) Leloir, L. F. *Science* **1971**, *172*, 1299-1303.
- (89) *Les Prix Nobel in 1970*; Odelberg, W., Ed.; Nobel Foundation: Stockholm, 1971.
- (90) Augé, C.; David, S.; Mathieu, C.; Gautheron, C. *Tetrahedron Lett.* **1984**, 1467-1470.
- (91) Wong, C.-H.; Haynie, S. L.; Whitesides, G. M. *J. Org. Chem.* **1982**, *47*, 5416-5418.
- (92) Coutinho, P. M.; Deleury, E.; Davies, G. J.; Henrissat, B. *J. Mol. Biol.* **2003**, *328*, 307-317.
- (93) Breton, C.; Snajdrova, L.; Jeanneau, C.; Koča, J.; Imberty, A. *Glycobiology* **2006**, *16*, 29R-37R.
- (94) Davies, G. J.; Henrissat, B. *Biochem. Soc. Trans.* **2002**, *30*, 291-297.
- (95) Campbell, J. A.; Davies, G. J.; Bulone, V.; Henrissat, B. *Biochem. J.* **1997**, *326*, 929-939.
- (96) Henrissat, B. *Biochem. J.* **1991**, *280*, 309-316.
- (97) Campbell, J. A.; Davies, G. J.; Bulone, V.; Henrissat, B. *Biochem. J.* **1998**, *329*, 719-719.
- (98) Coutinho, P. M.; Henrissat, B. In *Recent Advances in Carbohydrate Bioengineering*; Gilbert, H. J.; Davies, G.; Henrissat, B.; Svensson, B.; Eds.; The Royal Society of Chemistry: Cambridge, UK, 1999; pp 3-12.
- (99) Bourne, Y.; Henrissat, B. *Curr. Opin. Struct. Biol.* **2001**, *11*, 593-600.

- (100) Ünlügil, U. M.; Rini, J. M. *Curr. Opin. Struct. Biol.* **2000**, *10*, 510-517.
- (101) Chiu, C. P. C.; Watts, A. G.; Lairson, L. L.; Gilbert, M.; Lim, D.; Wakarchuk, W. W.; Withers, S. G.; Strynadka, N. C. J. *Nat. Struct. Mol. Biol.* **2004**, *11*, 163-170.
- (102) Lovering, A. L.; de Castro, L. H.; Lim, D.; Strynadka, N. C. J. *Science* **2007**, *315*, 1402-1405.
- (103) Wrabl, J. O.; Grishin, N. V. *J. Mol. Biol.* **2001**, *314*, 365-374.
- (104) Zechel, D. L.; Withers, S. G. *Acc. Chem. Res.* **2000**, *33*, 11-18.
- (105) McCarter, J. D.; Withers, S. G. *Curr. Opin. Struct. Biol.* **1994**, *4*, 885-892.
- (106) Sinnott, M. L. *Chem. Rev.* **1990**, *90*, 1171-1202.
- (107) Rix, U.; Fischer, C.; Remsing, L. L.; Rohr, J. *Nat. Prod. Rep.* **2002**, *19*, 542-580.
- (108) Lairson, L. L.; Withers, S. G. *Chem. Commun.* **2004**, 2243-2248.
- (109) Murray, B. W.; Takayama, S.; Schultz, J.; Wong, C.-H. *Biochemistry* **1996**, *35*, 11183-11195.
- (110) Kozmon, S.; Tvaroška, I. *J. Am. Chem. Soc.* **2006**, *128*, 16921-16927.
- (111) Ramakrishnan, B.; Boeggeman, E.; Ramasamy, V.; Qasba, P. K. *Curr. Opin. Struct. Biol.* **2004**, *14*, 593-600.
- (112) Quirós, L. M.; Carbajo, R. J.; Braña, A. F.; Salas, J. A. *J. Biol. Chem.* **2000**, *275*, 11713-11720.
- (113) Mulichak, A. M.; Losey, H. C.; Walsh, C. T.; Garavito, R. M. *Structure* **2001**, *9*, 547-557.
- (114) Stick, R. V.; Watts, A. G. *Monatsh. Chem.* **2002**, *133*, 541-554.
- (115) Persson, K.; Ly, H. D.; Dieckelmann, M.; Wakarchuk, W. W.; Withers, S. G.; Strynadka, N. C. J. *Nat. Struct. Biol.* **2001**, *8*, 166-175.
- (116) Sinnott, M. L.; Jencks, W. P. *J. Am. Chem. Soc.* **1980**, *102*, 2026-2032.
- (117) Tvaroška, I. *Carbohydr. Res.* **2004**, *339*, 1007-1014.

- (118) Gibson, R. P.; Tarling, C. A.; Roberts, S.; Withers, S. G.; Davies, G. J. *J. Biol. Chem.* **2004**, *279*, 1950-1955.
- (119) Pedersen, L. C.; Dong, J.; Taniguchi, F.; Kitagawa, H.; Krahm, J. M.; Pedersen, L. G.; Sugahara, K.; Negish, M. *J. Biol. Chem.* **2003**, *278*, 14420-14428.
- (120) Gibson, R. P.; Turkenburg, J. P.; Charnock, S. J.; Lloyd, R.; Davies, G. J. *Chem. Biol.* **2002**, *9*, 1337-1346.
- (121) Gastinel, L. N.; Bignon, C.; Misra, A. K.; Hindsgaul, O.; Shaper, J. H.; Joziassse, D. H. **2001**, *20*, 638-649.
- (122) Lairson, L. L.; Chiu, C. P. C.; Ly, H. D.; He, S.; Wakarchuk, W. W.; Strynadka, N. C. J.; Withers, S. G. *J. Biol. Chem.* **2004**, *279*, 28339-28344.
- (123) Bornscheuer, U. T.; Kazlauskas, R. J. *Angew. Chem. Int. Ed.* **2004**, *43*, 6032-6040.
- (124) Oberthür, M.; Leimkuhler, C.; Kruger, R. G.; Lu, W.; Walsh, C. T.; Kahne, D. *J. Am. Chem. Soc.* **2005**, *127*, 10747-10752.
- (125) Albermann, C.; Soriano, A.; Jiang, J.; Vollmer, H.; Biggins, J. B.; Barton, W. A.; Lesniak, J.; Nikolov, D. B.; Thorson, J. S. *Org. Lett.* **2003**, *5*, 933-936.
- (126) Mulichak, A. M.; Lu, W.; Losey, H. C.; Walsh, C. T.; Garavito, R. M. *Biochemistry* **2004**, *43*, 5170-5180.
- (127) Fischer, C.; Rodríguez, L.; Patallo, E. P.; Lipata, F.; Braña, A. F.; Méndez, C.; Salas, J. A.; Rohr, J. *J. Nat. Prod.* **2002**, *65*, 1685-1689.
- (128) Freel Meyers, C. L.; Oberthür, M.; Anderson, J. W.; Kahne, D.; Walsh, C. T. *Biochemistry* **2003**, *42*, 4179-4189.
- (129) Minami, A.; Uchida, R.; Eguchi, T.; Kakinuma, K. *J. Am. Chem. Soc.* **2005**, *127*, 6148-6149.
- (130) Hancock, S. M.; Vaughan, M. D.; Withers, S. G. *Curr. Opin. Chem. Biol.* **2006**, *10*, 509-519.
- (131) Aharoni, A.; Thieme, K.; Chiu, C. P. C.; Buchini, S.; Lairson, L. L.; Chen, H.; Strynadka, N. C. J.; Wakarchuk, W. W.; Withers, S. G. *Nat. Methods* **2006**, *3*, 609-614.
- (132) Wang, L.; White, R. L.; Vining, L. C. *Microbiology* **2002**, *148*, 1091-1103.

- (133) Jakeman, D. L. *unpublished data*.
- (134) Elhalabi, J. M.; Rice, K. G. *Curr. Med. Chem.* **1999**, *6*, 93-116.
- (135) Moffatt, J. G. *Methods Enzymol.* **1966**, *8*, 136-142.
- (136) Moffatt, J. G.; Khorana, H. G. *J. Am. Chem. Soc.* **1961**, *83*, 649-658.
- (137) Morais, L. L.; Yuasa, H.; Bennis, K.; Ripoche, I.; Auzanneau, F.-I. *Can. J. Chem.* **2006**, *84*, 587-596.
- (138) Zhao, Y.; Thorson, J. S. *J. Org. Chem.* **1998**, *63*, 7568-7572.
- (139) Wittmann, V.; Wong, C.-H. *J. Org. Chem.* **1997**, *62*, 2144-2147.
- (140) Chang, C.-W. T.; Liu, H.-w. *Bioorg. Med. Chem. Lett.* **2002**, *12*, 1493-1496.
- (141) Zhang, Q.; Liu, H.-w. *Bioorg. Med. Chem. Lett.* **2001**, *11*, 145-149.
- (142) Arlt, M.; Hindsgaul, O. *J. Org. Chem.* **1995**, *60*, 14-15.
- (143) Uchiyama, T.; Hindsgaul, O. *J. Carbohydr. Chem.* **1998**, *17*, 1181-1190.
- (144) Hanessian, S.; Lu, P.-P.; Ishida, H. *J. Am. Chem. Soc.* **1998**, *120*, 13296-13300.
- (145) Ernst, C.; Klaffke, W. *J. Org. Chem.* **2003**, *68*, 5780-5783.
- (146) Ernst, C.; Klaffke, W. *Tetrahedron Lett.* **2001**, 2973-2975.
- (147) Lindquist, L.; Kaiser, R.; Reeves, P. R.; Lindberg, A. A. *Eur. J. Biochem.* **1993**, *211*, 763-770.
- (148) Sheu, K.-F. R.; Richard, J. P.; Frey, P. A. *Biochemistry* **1979**, *18*, 5548-5556.
- (149) Tsuboi, K. K.; Fukunaga, K.; Petricciani, J. C. *J. Biol. Chem.* **1969**, *244*, 1008-1015.
- (150) Melo, A.; Glaser, L. *J. Biol. Chem.* **1965**, *240*, 398-405.
- (151) Mizanur, R. M.; Zea, C. J.; Pohl, N. L. *J. Am. Chem. Soc.* **2004**, *126*, 15993-15998.
- (152) Barton, W. A.; Lesniak, J.; Biggins, J. B.; Jeffrey, P. D.; Jiang, J.; Rajashankar, K. R.; Thorson, J. S.; Nikolov, D. B. *Nat. Struct. Biol.* **2001**, *8*, 545-552.



- (153) Blankenfeldt, W.; Asuncion, M.; Lam, J. S.; Naismith, J. H. *EMBO J.* **2000**, *19*, 6652-6663.
- (154) Brown, K.; Pompeo, F.; Dixon, S.; Mengin-Lecreulx, D.; Cambillau, C.; Bourne, Y. *EMBO J.* **1999**, *18*, 4096-4107.
- (155) Jiang, J.; Biggins, J. B.; Thorson, J. S. *J. Am. Chem. Soc.* **2000**, *122*, 6803-6804.
- (156) Bae, J.; Kim, K.-H.; Kim, D.; Choi, Y.; Kim, J. S.; Koh, S.; Hong, S.-I.; Lee, D.-S. *ChemBioChem* **2005**, *6*, 1963-1966.
- (157) Jiang, J.; Albermann, C.; Thorson, J. S. *ChemBioChem* **2003**, *4*, 443-446.
- (158) Jiang, J.; Biggins, J. B.; Thorson, J. S. *Angew. Chem. Int. Ed.* **2001**, *40*, 1502-1505.
- (159) Yang, J.; Fu, X.; Liao, J.; Liu, L.; Thorson, J. S. *Chem. Biol.* **2005**, *12*, 657-664.
- (160) Barton, W. A.; Biggins, J. B.; Jiang, J.; Thorson, J. S.; Nikolov, D. B. *Proc. Natl. Acad. Sci.* **2002**, *99*, 13397-13402.
- (161) Zea, C. J.; Pohl, N. L. *Anal. Biochem.* **2004**, *328*, 196-202.
- (162) Mallams, A. K.; Puar, M. S.; Rossman, R. R. *J. Am. Chem. Soc.* **1981**, *103*, 3938-3940.
- (163) Tomita, F.; Tamaoki, T.; Shirahata, K.; Kasai, M.; Morimoto, M.; Ohkubo, S.; Mineura, K.; Ishii, S. *J. Antibiot.* **1980**, *33*, 668-670.
- (164) Zielinski, J.; Jereczek, E.; Sowinski, P.; Falkowski, L.; Rudowski, A.; Borowski, E. *J. Antibiot.* **1979**, *32*, 565-568.
- (165) Reichstein, T.; Weiss, E. *Adv. Carbohydr. Chem.* **1962**, *17*, 65-120.
- (166) Huan, V. D.; Ohtani, K.; Kasai, R.; Yamasaki, K.; Tuu, N. V. *Chem. Pharm. Bull.* **2001**, *49*, 453-460.
- (167) Abe, F.; Mori, Y.; Okabe, H.; Yamauchi, T. *Chem. Pharm. Bull.* **1994**, *42*, 1777-1783.
- (168) Rupprath, C.; Schumacher, T.; Elling, L. *Curr. Med. Chem.* **2005**, *12*, 1637-1675.
- (169) Andreana, P. R.; McLellan, J. S.; Chen, Y.; Wang, P. G. *Org. Lett.* **2002**, *4*, 3875-3878.

- (170) Braun, M.; Moritz, J. *Synlett* **1991**, 10, 750-752.
- (171) Fronza, G.; Fuganti, C.; Grasselli, P.; Pedrocchi-Fantoni, G.; Zirotti, C. *Tetrahedron Lett.* **1982**, 4143-4146.
- (172) Toshima, K.; Yoshida, T.; Mukaiyama, S.; Tatsuta, K. *Carbohydr. Res.* **1991**, 222, 173-188.
- (173) Bock, K.; Lundt, I.; Pedersen, C. *Acta Chem. Scand.* **1984**, B38, 555-561.
- (174) Brimacombe, J. S.; Hanna, R.; Saeed, M. S.; Tucker, L. C. N. *J. Chem. Soc. Perkin Trans. 1* **1982**, 2583-2587.
- (175) Klemer, A.; Rodemeyer, G. *Chem. Ber.* **1974**, 107, 2612-2614.
- (176) Clode, D. M.; Horton, D.; Weckerle, W. *Carbohydr. Res.* **1976**, 49, 305-314.
- (177) Brimacombe, J. S. *Methods Carbohydr. Chem.* **1972**, 6, 376-378.
- (178) Horton, D.; Weckerle, W. *Carbohydr. Res.* **1988**, 174, 305-312.
- (179) Horton, D.; Weckerle, W. *Carbohydr. Res.* **1975**, 44, 227-240.
- (180) Cheung, T.-M.; Horton, D.; Sorenson, R. J.; Weckerle, W. *Carbohydr. Res.* **1978**, 63, 77-89.
- (181) Pu, L.; Grubbs, R. H. *J. Org. Chem.* **1994**, 59, 1351-1353.
- (182) Ceré, V.; Guenzi, A.; Pollicino, S.; Sandri, E.; Fava, A. *J. Org. Chem.* **1980**, 45, 261-264.
- (183) Berlin, K. D.; Rathore, B. S.; Peterson, M. *J. Org. Chem.* **1965**, 30, 226-228.
- (184) Wharton, P. S.; Hiegel, G. A.; Ramaswami, S. *J. Org. Chem.* **1964**, 29, 2441-2442.
- (185) Morin, C. *Chem. Lett.* **1986**, 1055-1056.
- (186) Winkle, M. R.; Lansinger, J. M.; Ronald, R. C. *J. Chem. Soc. Chem. Commun.* **1980**, 87-88.
- (187) Harangi, J.; Lipták, A.; Szurmai, Z.; Nánasi, P. *Carbohydr. Res.* **1985**, 136, 241-248.
- (188) Lemieux, R. U.; Nagabhushan, T. I.; Paul, B. *Can. J. Chem.* **1972**, 50, 773-776.

- (189) Lipták, A.; Imre, J.; Nánási, P. *Carbohydr. Res.* **1981**, *92*, 154-156.
- (190) Klemer, A.; Balkau, D. *J. Chem. Res.* **1978**, (S), 303-303; (M), 3823-3830.
- (191) Hodgson, R.; Nelson, A. *Org. Biomol. Chem.* **2004**, *2*, 373-386.
- (192) Köpper, S.; Thiem, J. *J. Carbohydr. Chem.* **1987**, *6*, 57-85.
- (193) Coxon, B. *J. Carbohydr. Chem.* **1984**, *3*, 525-543.
- (194) Shull, B. K.; Wu, Z.; Koreeda, M. *J. Carbohydr. Chem.* **1996**, *15*, 955-964.
- (195) Dixon, J. T.; van Heerden, F. R.; Holzapfel, C. W. *Tetrahedron: Asymmetry* **2005**, *16*, 393-401.
- (196) Czernecki, S.; Vijayakumaran, K.; Ville, G. *J. Org. Chem.* **1986**, *51*, 5472-5475.
- (197) Luche, J.-L. *J. Am. Chem. Soc.* **1978**, *100*, 2226-2227.
- (198) Cousins, R. P. C.; Pritchard, R. G.; Raynor, C. M.; Smith, M.; Stoodley, R. J. *Tetrahedron Lett.* **2002**, 489-492.
- (199) Larson, E. R.; Danishefsky, S. *J. Am. Chem. Soc.* **1983**, *105*, 6715-6716.
- (200) Bartoli, G.; Bartolacci, M.; Giuliani, A.; Marcantoni, E.; Massaccesi, M. *Eur. J. Org. Chem.* **2005**, *14*, 2867-2879.
- (201) Corey, E. J.; Venkateswarlu, A. *J. Am. Chem. Soc.* **1972**, *94*, 6190-6191.
- (202) Corey, E. J.; Snider, B. B. *J. Am. Chem. Soc.* **1972**, *94*, 2549-2550.
- (203) Miethchen, R. *J. Fluorine Chem.* **2004**, *125*, 895-901.
- (204) Thomas, S. O.; Singleton, V. L.; Lowery, J. A.; Sharpe, R. W.; Preuss, L. M.; Porter, J. N.; Mowat, J. H.; Bohonos, N. *Antibiotics Ann.* **1956**, 716-721.
- (205) Morton, G. O.; Lancaster, J. E.; Van Lear, G. E.; Fulmor, W.; Meyer, W. E. *J. Am. Chem. Soc.* **1969**, *91*, 1535-1537.
- (206) O'Hagan, D.; Schaffrath, C.; Cobb, S. L.; Hamilton, J. T. G.; Murphy, C. D. *Nature* **2002**, *416*, 279-279.
- (207) Nyffeler, P. T.; Gonzalez Durón, S.; Burkart, M. D.; Vincent, S. P.; Wong, C.-H. *Angew. Chem. Int. Ed.* **2005**, *44*, 192-212.

- (208) Toshima, K. *Carbohydr. Res.* **2000**, 327, 15-26 and references cited therein.
- (209) Withers, S. G.; Aebersold, R. *Protein Sci.* **1995**, 4, 361-372.
- (210) Braun, C.; Brayer, G. D.; Withers, S. G. *J. Biol. Chem.* **1995**, 270, 26778-26781.
- (211) Street, I. P.; Kempton, J. B.; Withers, S. G. *Biochemistry* **1992**, 31, 9970-9978.
- (212) Hayashi, T.; Murray, B. W.; Wang, R.; Wong, C.-H. *Bioorg. Med. Chem.* **1997**, 5, 497-500.
- (213) Banks, R. E. *J. Fluorine Chem.* **1998**, 87, 1-17.
- (214) Barton, D. H. R.; Godinho, L. S.; Hesse, R. H.; Pechet, M. M. *Chem. Commun.* **1968**, 804-806.
- (215) Schack, C. J.; Christe, K. O. *Inorg. Chem.* **1979**, 18, 2619-2620.
- (216) Barton, D. H. R.; Ganguly, A. K.; Hesse, R. H.; Loo, S. N.; Pechet, M. M. *Chem. Commun.* **1968**, 806-808.
- (217) Tius, M. A. *Tetrahedron* **1995**, 51, 6605-6634.
- (218) Burkart, M. D.; Zhang, Z.; Hung, S.-C.; Wong, C.-H. *J. Am. Chem. Soc.* **1997**, 119, 11743-11746.
- (219) Butchard, G. C.; Kent, P. W. *Tetrahedron* **1979**, 35, 2439-2443.
- (220) Lam, S. N.; Gervay-Hague, J. *Org. Lett.* **2003**, 5, 4219-4222.
- (221) Veyrières, A. In *Carbohydrates in Chemistry and Biology*; Ernst, B.; Hart, G. W.; Sinaÿ, P., Eds.; Wiley-VCH Verlag GmbH: Weinheim, DE, 2000; Vol. 1, pp 367-405.
- (222) Withers, S. G.; Percival, M. D.; Street, I. P. *Carbohydr. Res.* **1989**, 187, 43-66.
- (223) Oberthür, M.; Leimkuhler, C.; Kahne, D. *Org. Lett.* **2004**, 6, 2873-2876.
- (224) Losey, H. C.; Peczu, M. W.; Chen, Z.; Eggert, U. S.; Dong, S. D.; Pelczer, I.; Kahne, D.; Walsh, C. T. *Biochemistry* **2001**, 40, 4745-4755.
- (225) Greene, T. W.; Wuts, P. G. M. *Protective Groups in Organic Synthesis*, 2nd ed.; John Wiley & Sons, Inc.: New York, NY, 1991; pp 68-73, 77-83.

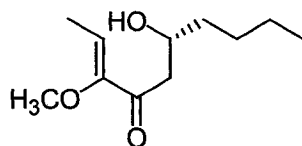
- (226) Thiem, J.; Meyer, B. *Chem. Ber.* **1980**, *113*, 3075-3085.
- (227) Kováč, P. In *Modern Methods in Carbohydrate Synthesis*; Khan, S. H.; O'Neill, R. A., Eds.; Frontiers in Natural Product Research; Harwood: Foster City, CA, 1996; Vol. 1, pp 55-81.
- (228) Perdomo, G. R.; Krepinsky, J. J. *Tetrahedron Lett.* **1987**, 5595-5598.
- (229) Grynkiewicz, G.; Konopka, M. *Polish J. Chem.* **1987**, *61*, 149-153.
- (230) Bock, K.; Meldal, M. *Acta Chem. Scand.* **1984**, *B38*, 255-266.
- (231) Binkley, R. W.; Koholic, D. J. *J. Org. Chem.* **1989**, *54*, 3577-3581.
- (232) Higashi, K.; Nakayama, K.; Shioya, E.; Kusama, T. *Chem. Pharm. Bull.* **1991**, *39*, 2502-2504.
- (233) Classon, B.; Garegg, P. J.; Norberg, T. *Acta Chem. Scand.* **1984**, *B38*, 195-201.
- (234) Monneret, C.; Martin, A.; Pais, M. *J. Carbohydr. Chem.* **1988**, *7*, 417-434.
- (235) Thiem, J.; Köpper, S. *J. Carbohydr. Chem.* **1983**, *2*, 75-97.
- (236) Thiem, J.; Meyer, B. *Chem. Ber.* **1980**, *113*, 3058-3066.
- (237) Mohamady, S.; Jakeman, D. L. *J. Org. Chem.* **2005**, *70*, 10588-10591.
- (238) Marlow, A. L.; Kiessling, L. L. *Org. Lett.* **2001**, *3*, 2517-2519.
- (239) Freel Meyers, C. L.; Borch, R. F. *Org. Lett.* **2001**, *3*, 3765-3768.
- (240) Bogachev, V. S. *Russ. J. Bioorg. Chem.* **1996**, *22*, 599-604.
- (241) Upreti, M.; Vishwakarma, R. A. *Tetrahedron Lett.* **1999**, 2619-2622.
- (242) Knerr, L.; Pannecoucke, X.; Luu, B. *Tetrahedron Lett.* **1998**, 273-274.
- (243) Ichikawa, Y.; Sim, M. M.; Wong, C.-H. *J. Org. Chem.* **1992**, *57*, 2943-2946.
- (244) Liang, H. Ph. D. Thesis, Dalhousie University, 2005.
- (245) Bock, K.; Pedersen, C. *J. Chem. Soc. Perkin Trans. 2* **1974**, 293-297.
- (246) Bock, K.; Lundt, I.; Pedersen, C. *Tetrahedron Lett.* **1973**, 1037-1040.

- (247) Duus, J. Ø.; Gotfredsen, C. H.; Bock, K. *Chem. Rev.* **2000**, *100*, 4589-4614.
- (248) Graninger, M.; Kneidinger, B.; Bruno, K.; Scheberl, A.; Messner, P. *Appl. Environ. Microbiol.* **2002**, *68*, 3708-3715.
- (249) Sabesan, S.; Neira, S. *Carbohydr. Res.* **1992**, *223*, 169-185.
- (250) Barber, G. A.; Behrman, E. J. *Arch. Biochem. Biophys.* **1991**, *288*, 239-242.
- (251) Prihar, H. S.; Behrman, E. J. *Biochemistry* **1973**, *12*, 997-1002.
- (252) Lucas, S.; Timmons, S. C.; Jakeman, D. L. *unpublished data*.
- (253) Dinev, Z.; Wardak, A. Z.; Brownlee, R. T. C.; Williams, S. J. *Carbohydr. Res.* **2006**, *341*, 1743-1747.
- (254) Wu, Q.; Liu, Y.-n.; Chen, H.; Molitor, E. J.; Liu, H.-w. *Biochemistry* **2007**, *46*, 3759-3767.
- (255) Palcic, M. M. *Methods Enzymol.* **1994**, *230*, 300-316.
- (256) Koeller, K. M.; Wong, C.-H. *Glycobiology* **2000**, *10*, 1157-1169.
- (257) Pallanca, J. E.; Turner, N. J. *J. Chem. Soc. Perkin Trans. 1* **1993**, 3017-3022.
- (258) Gokhale, U. B.; Hindsgaul, O.; Palcic, M. M. *Can. J. Chem.* **1990**, *68*, 1063-1071.
- (259) Nunez, H. A.; O'Connor, J. V.; Rosevear, P. R.; Barker, R. *Can. J. Chem.* **1981**, *59*, 2086-2095.
- (260) Timmons, S. C.; Jakeman, D. L. *Org. Lett.* **2007**, *9*, 1227-1230.
- (261) Collier, A.; Wagner, G. *Org. Biomol. Chem.* **2006**, *4*, 4526-4532.
- (262) Zhang, Z.; Tsujimura, M.; Akutsu, J.; Sasaki, M.; Tajima, H.; Kawarabayashi, Y. *J. Biol. Chem.* **2005**, *280*, 9698-9705.
- (263) Bonofiglio, L.; García, E.; Mollerach, M. *Curr. Microbiol.* **2005**, *51*, 217-221.
- (264) Kudo, F.; Kawabe, K.; Kuriki, H.; Eguchi, T.; Kakinuma, K. *J. Am. Chem. Soc.* **2005**, *127*, 1711-1718.
- (265) Murrell, J. M.; Liu, W.; Shen, B. *J. Nat. Prod.* **2004**, *67*, 206-213.

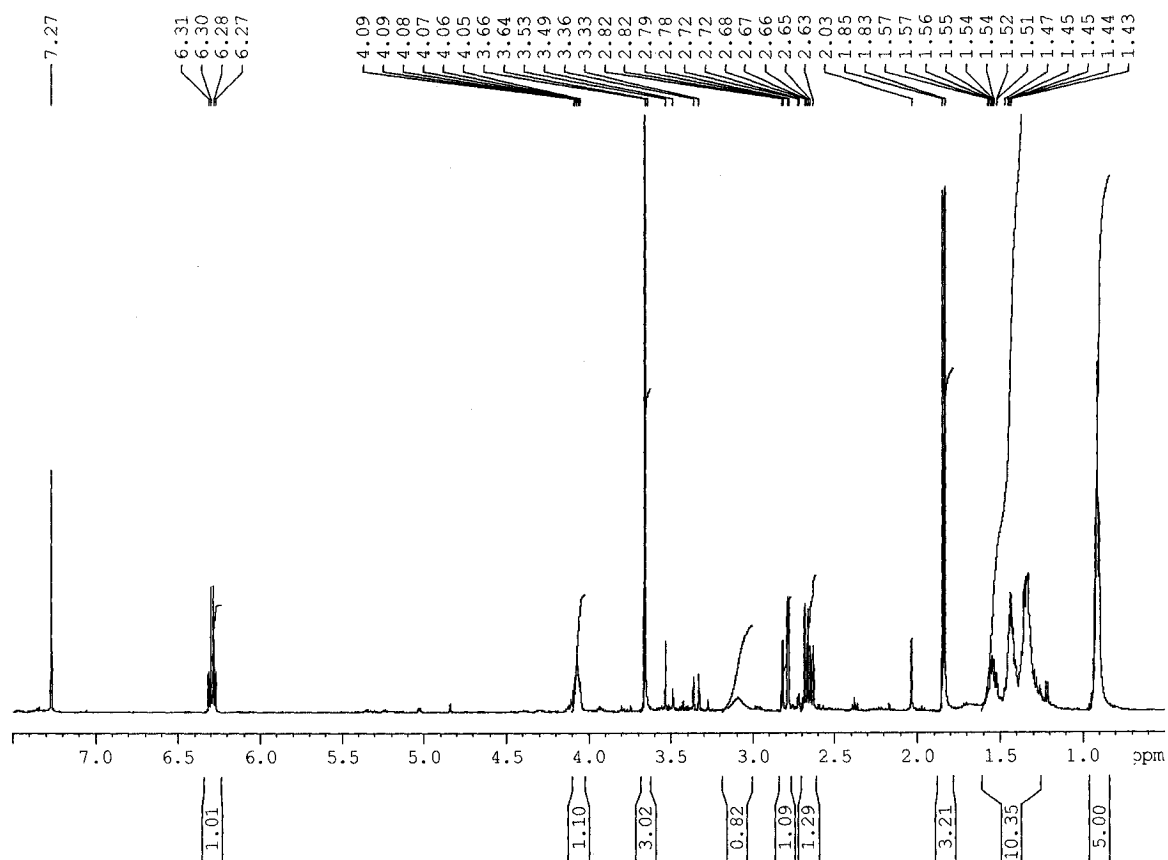
- (266) Truman, A. W.; Huang, F.; Llewellyn, N. M.; Spencer, J. B. *Angew. Chem. Int. Ed.* **2007**, *46*, 1462-1464.
- (267) Timmons, S. C.; Mosher, R. H.; Knowles, S. A.; Jakeman, D. L. *Org. Lett.* **2007**, *9*, 857-860.
- (268) McNally, D. J.; Hui, J. P. M.; Aubry, A. J.; Mui, K. K. K.; Guerry, P.; Brisson, J.-R.; Logan, S. M.; Soo, E. C. *J. Biol. Chem.* **2006**, *281*, 18489-18498.
- (269) Paulsen, H.; Bünsch, H. *Chem. Ber.* **1978**, *111*, 3484-3496.
- (270) Bols, M.; Lundt, I.; Ottosen, E. R. *Carbohydr. Res.* **1991**, *222*, 141-149.
- (271) Zhao, Y.; Biggins, J. B.; Thorson, J. S. *J. Am. Chem. Soc.* **1998**, *120*, 12986-12987.
- (272) Khaled, A.; Ivannikova, T.; Augé, C. *Carbohydr. Res.* **2004**, *339*, 2641-2649.
- (273) Liu, X.; Adams, H.; Blackburn, G. M. *Chem. Commun.* **1998**, 2619-2620.

## Appendix 1. NMR Spectra of Representative Compounds

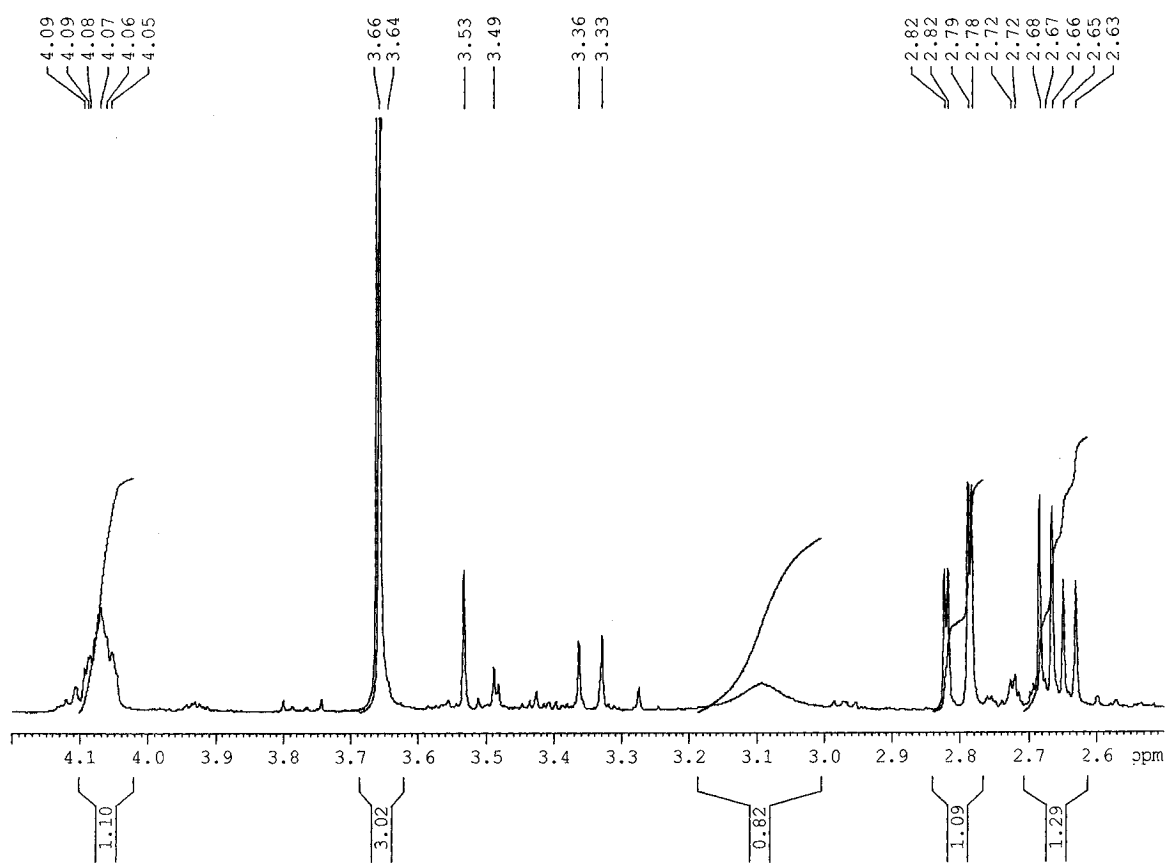
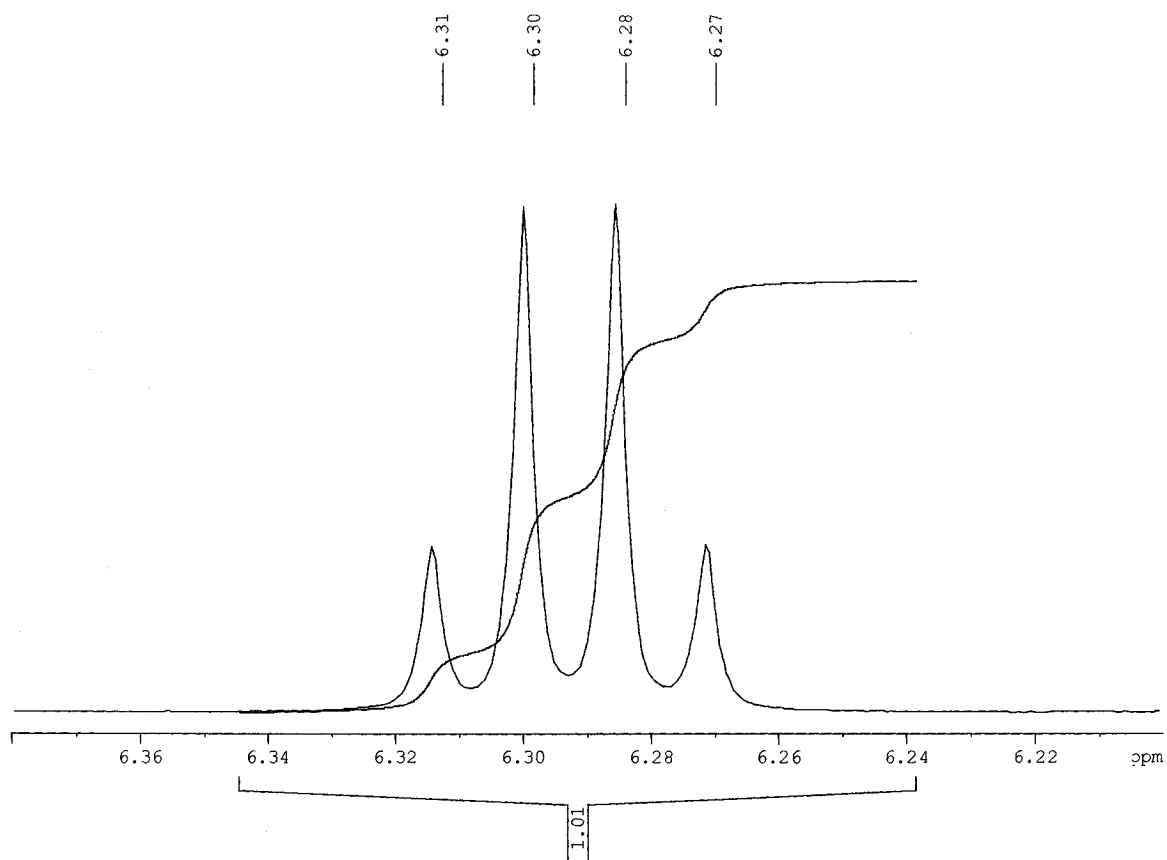
Figure 80. NMR spectra of (6*R*)-6-hydroxy-3-methoxy-dec-2-en-4-one (**77**)

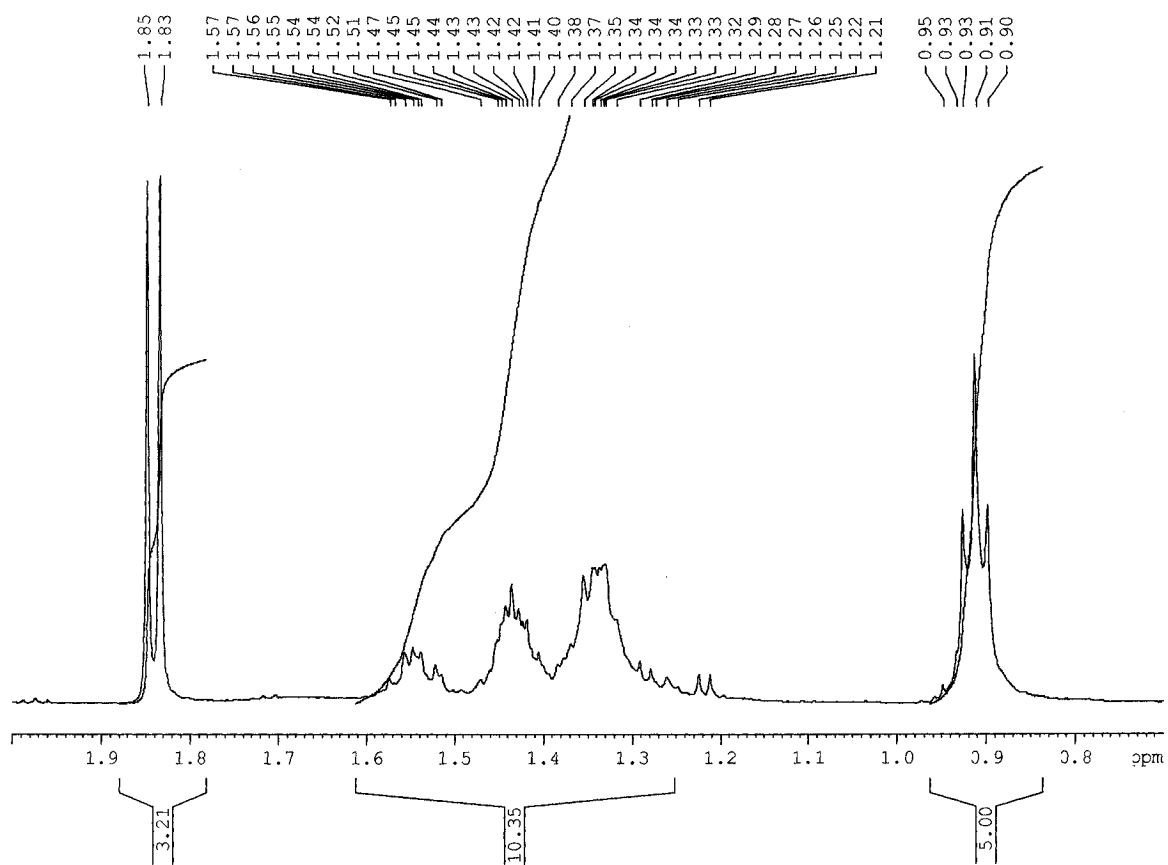


a) Full  $^1\text{H}$  NMR spectrum of **77** and expansions

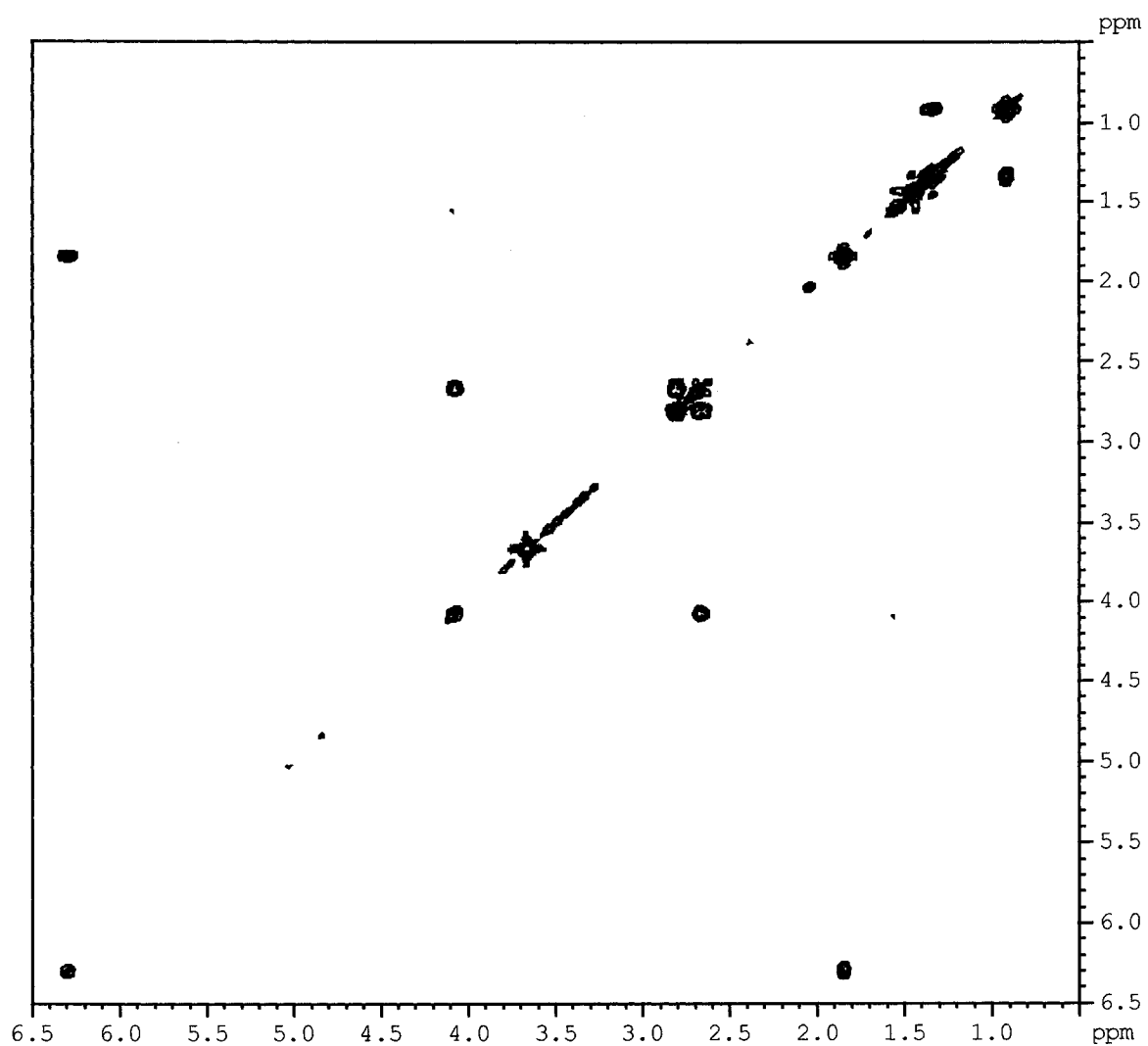




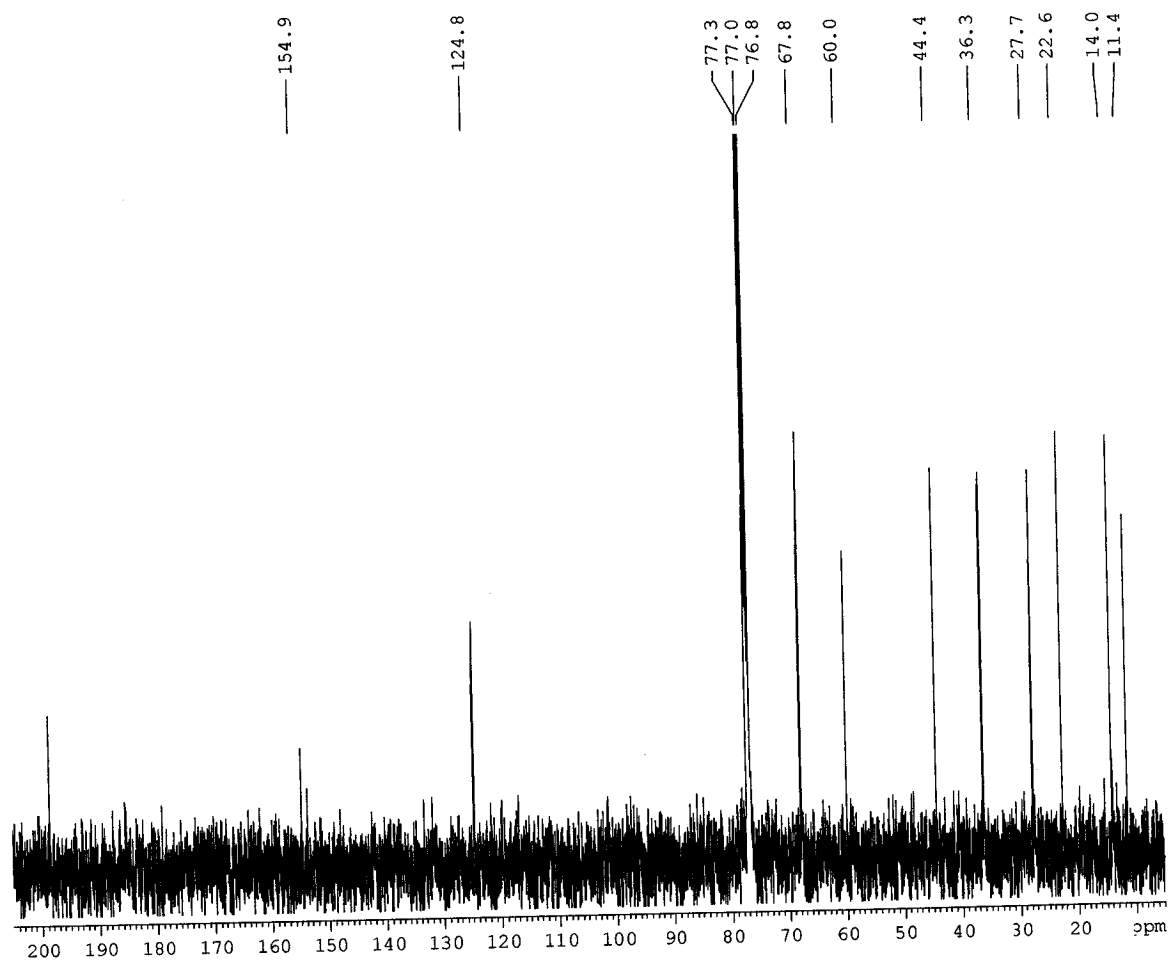




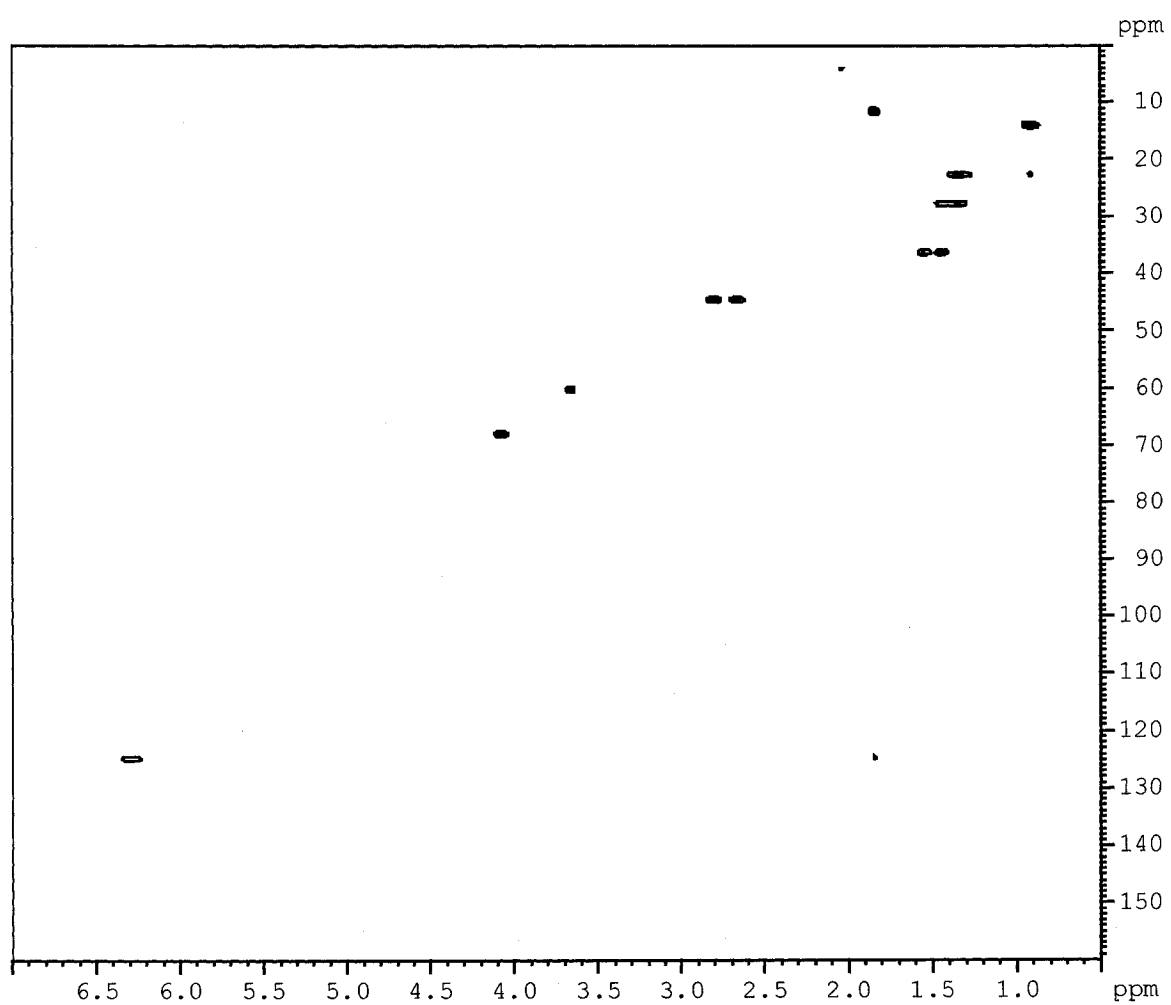
b) COSY NMR spectrum of 77



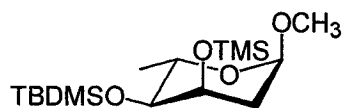
c)  $^{13}\text{C}\{^1\text{H}\}$  NMR spectrum of **77**



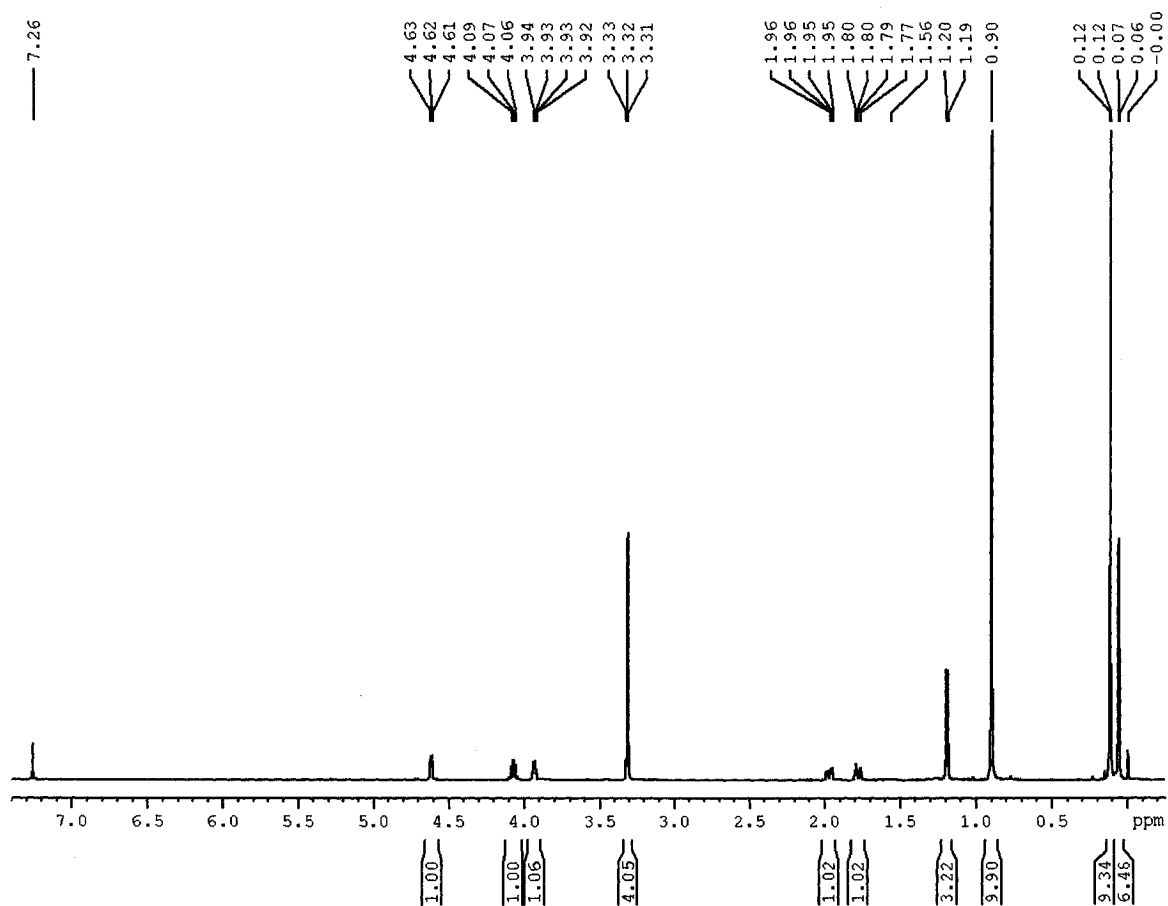
d)  $^{13}\text{C}$ - $^1\text{H}$  HSQC NMR spectrum of **77**

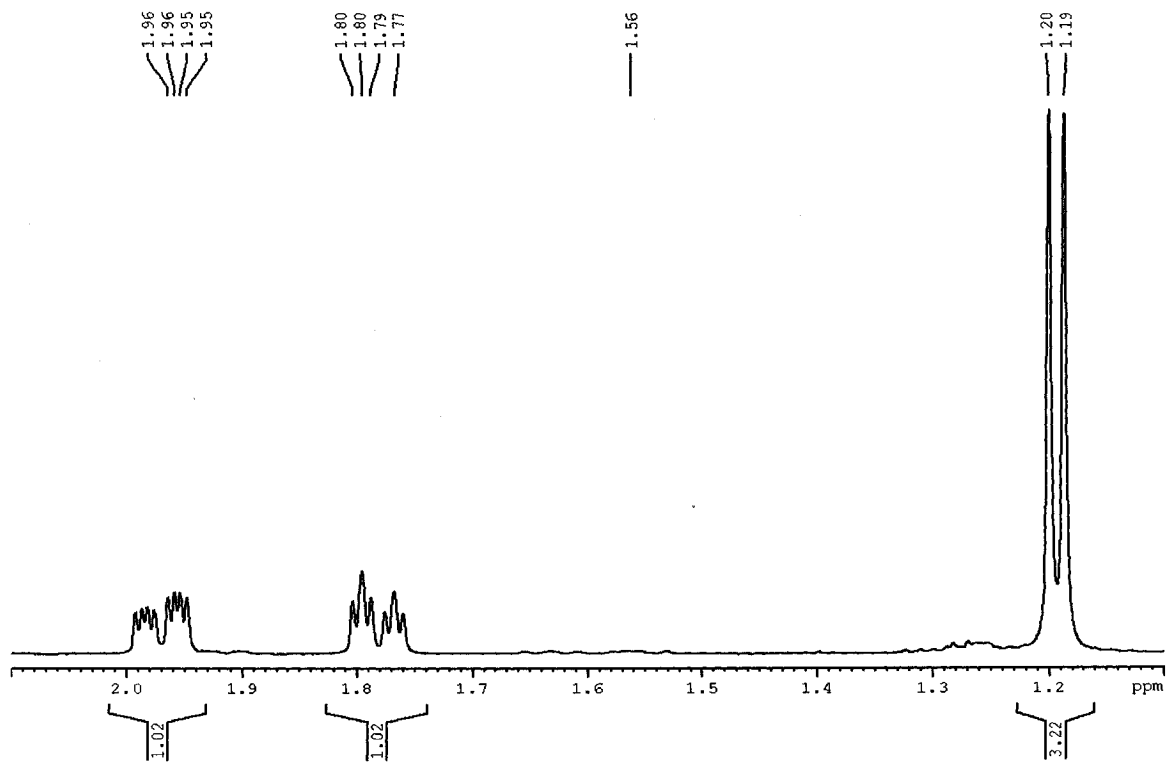
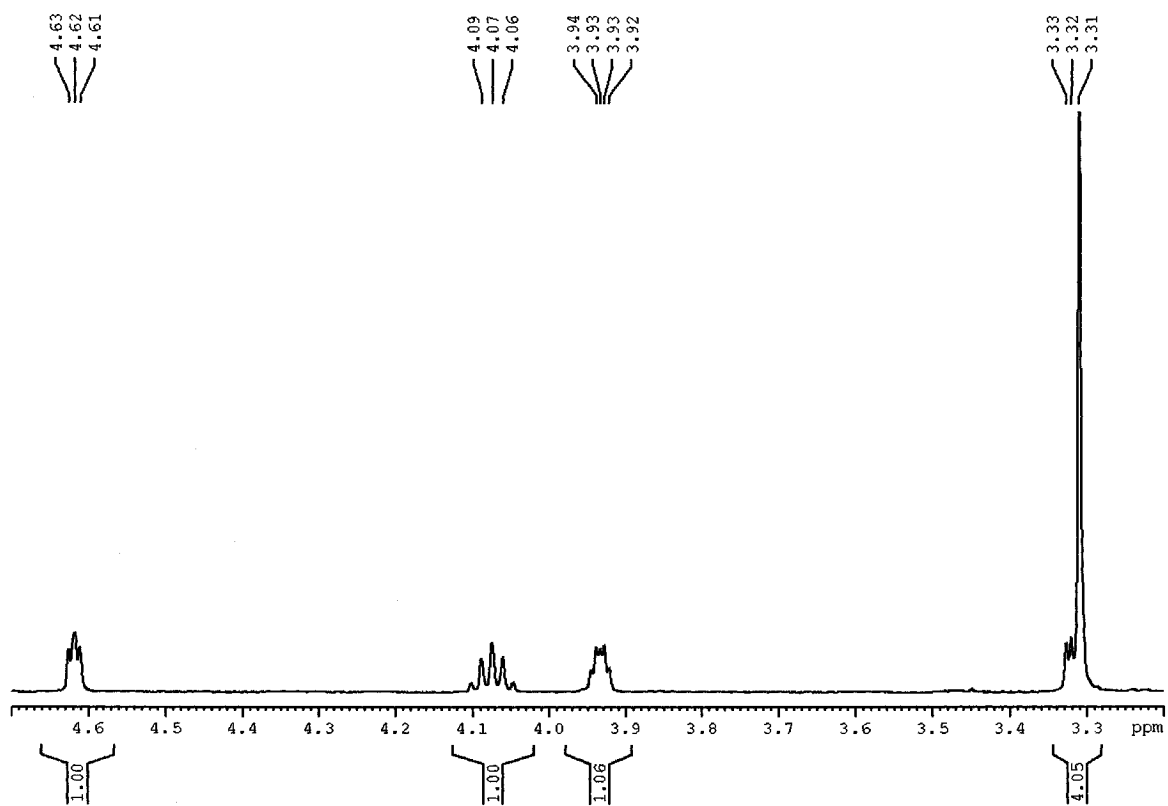


**Figure 81.** NMR spectra of methyl 4-*O*-(*tert*-butyldimethylsilyl)-2,6-dideoxy-3-*O*-(trimethylsilyl)- $\alpha$ -L-*ribo*-hexopyranoside (**90**)



a) Full  $^1\text{H}$  NMR spectrum of **90** and expansions





b)  $^{13}\text{C}\{^1\text{H}\}$  NMR Spectrum of **90**

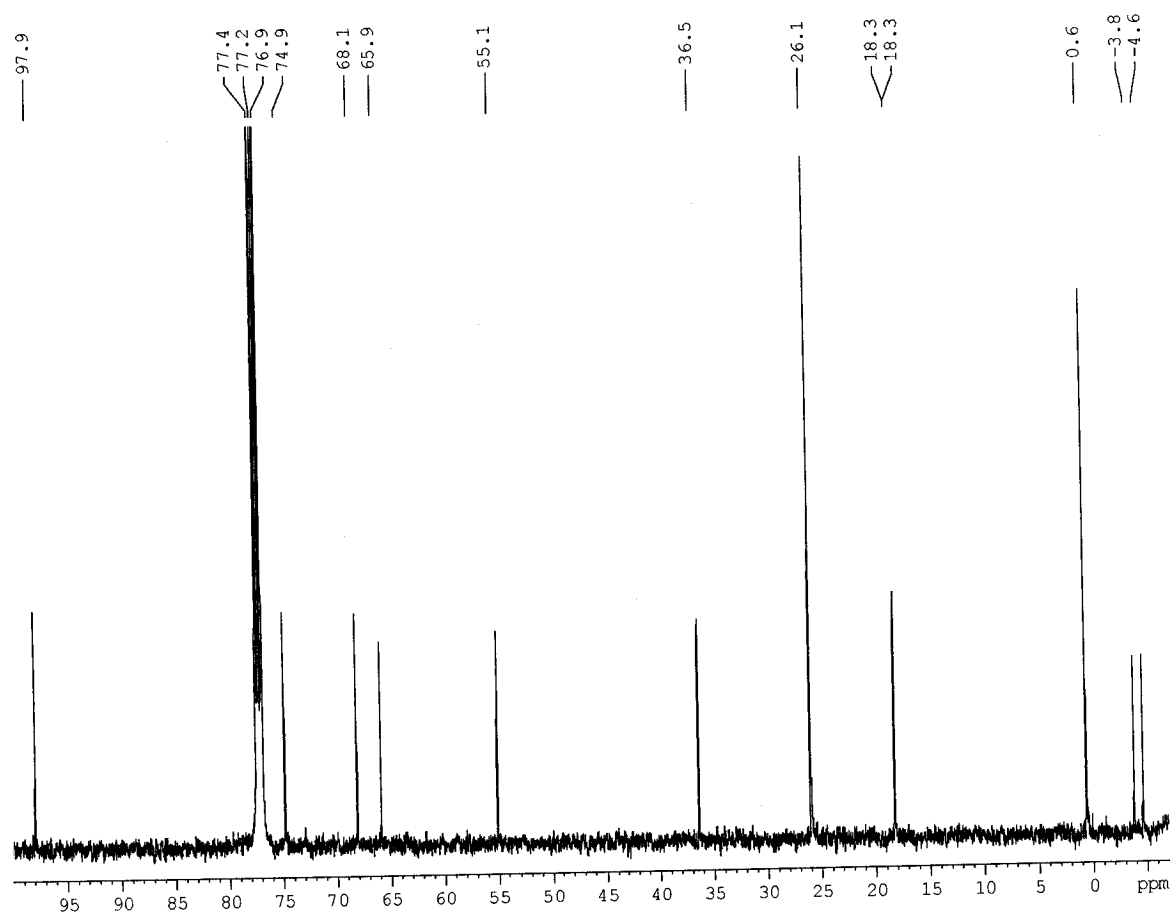
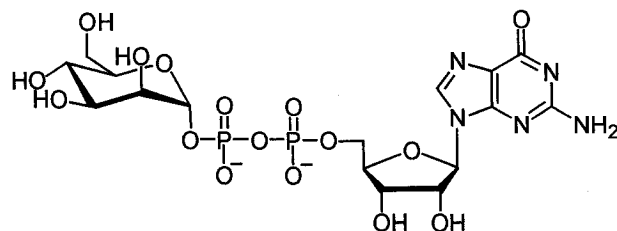
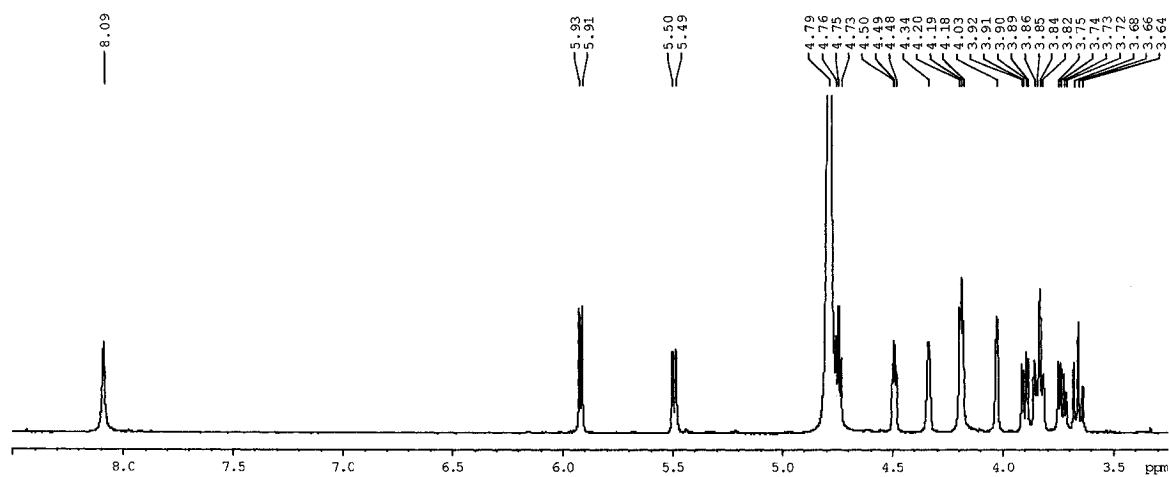




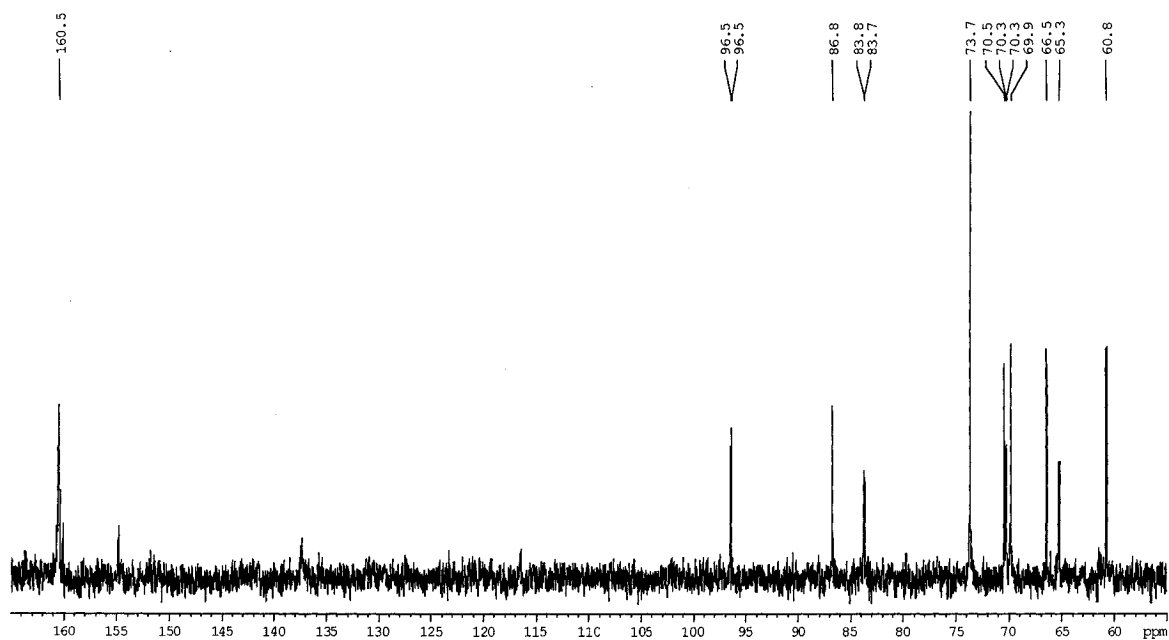
**Figure 82.** NMR spectra of GDP- $\alpha$ -D-mannose (**159**)



a)  $^1\text{H}$  NMR spectrum of **159**



b)  $^{13}\text{C}\{^1\text{H}\}$  NMR spectrum of **159**



c)  $^{31}\text{P}\{^1\text{H}\}$  NMR spectrum of **159** and expansion

